

Integrated Thermal Design and Optimization Study for Active Integrated Power Electronic Modules (IPEMs)

By

Ying-Feng Pang

Thesis submitted to the Faculty of the
Virginia Polytechnic Institute and State University
in partial fulfillment of the requirements for the degree of
Master of Science
In
Mechanical Engineering

APPROVED:

Elaine P. Scott, Co-Advisor

Karen A. Thole, Co-Advisor

Jan Helge Bøhn, Committee Member

August 26, 2002

Blacksburg, Virginia

Keywords: Power Electronics Cooling, Thermal Management, Integrated Design Optimizations

Integrated Thermal Layout Design and Optimization Study for Active Integrated Power Electronic Modules (IPEMs)

Ying-Feng Pang

(Abstract)

Thermal management is one of many critical tasks in the design of power electronic systems. It has become increasingly important as a result of the introduction of high power density and integrated modules. It has also been realized that higher temperatures do affect reliability due to a variety of physical failure mechanisms that involve thermal stresses and material degradation. Therefore, it is important to consider temperature as design parameter in developing power electronic modules.

The NSF Center for Power Electronics System (CPES) at Virginia Tech previously developed a first generation (Gen-I) active Integrated Power Electronics Module (IPEM). This module represents CPES's approach to design a standard power electronic module with low labor and material costs and improved reliability compared to industrial Intelligent Power Modules (IPM). A preliminary Generation II (Gen-II.A) active IPEM was built using embedded power technology, which removes the wire bonds from the Gen-I IPEM. In this module, the three primary heat-generating devices are placed on a direct bonded copper substrate in a multi-chip module format.

The overall goal of this research effort was to optimize the thermal performance of this Gen-II.A IPEM. To achieve this goal, a detailed three-dimensional active IPEM was modeled using the thermal-fluid analysis program ESC in I-DEAS to study the thermal performance of the Gen-II.A IPEM. Several design variables including the ceramic material, the ceramic thickness, and the thickness of the heat spreader were modeled to optimize IPEM geometric design and to improve the thermal performance while reducing the footprint. Input variables such as power loss and interface material thicknesses were studied in a sensitivity and uncertainty analysis. Other design constraints such as electrical design and packaging technology were also considered in the thermal optimization of the design.

A new active IPEM design named Gen-II.C was achieved with reduced-size and improved thermal and electrical performance. The success of the new design will enable the replacement of discrete components in a front-end DC/DC converter by this standard module with the best thermal and electrical performance. Future improvements can be achieved by replacing the current silicon chip with a higher thermal-conductivity material, such as silicon carbide, as the power density increases, and by, exploring other possible cooling techniques.

Acknowledgments

I would like to express my deepest gratitude to my academic and research advisor Dr. Elaine Scott for her guidance and constant support in helping me to conduct and complete this work. I would also like to thank Dr. Karen Thole for her constant encouragement and her expertise. In addition, I want to thank Dr. Jan Helge Bøhn for serving on my advisory committee, as well as for his generous advice. I am indebted to the National Science Foundation and CPES for funding this work and for providing research facilities. I want to thank Jonah, Yingxiang, Dr. Zhenxian Liang, and Dr. Dushan Boroyevich in the Electrical and Computer Engineering Department for their active participation in this research.

Many thanks to all the people I have come to know in Virginia Tech and Blacksburg, whose friendship and companionship I will always enjoy. I owe my sincere appreciation to my family and relatives who have supported and encouraged me over the years. I especially want to thank Ming Luo for his inspiration and continuous encouragement during my studies. Finally, I want to extend my profound appreciation to my beloved parents for their love, affection, and invaluable support during my life and studies.

This work was funded under award number EEC-9731677.

I-DEAS is a registered trademark of EDS.

ICEPAK is a registered trademark of Fluent Inc.

Maxwell Q3D is a registered trademark of Ansoft Corporation.

Table of Contents

| | |
|---|-------|
| Abstract | .ii |
| Acknowledgments | .iv |
| Table of Contents | .v |
| Nomenclature | .vii |
| Acronyms | .viii |
| List of Figures | .xi |
| Lists of Tables | .xii |
| 1 Introduction | 1 |
| 1.1 Background and Motivation | 1 |
| 1.2 Overview of Power Electronics | 6 |
| 1.3 Research Goals and Approach | 10 |
| 1.4 Thesis Outline | 11 |
| 2 Literature Review | 13 |
| 2.1 Active Cooling Technologies | 13 |
| 2.2 Passive Cooling Technologies | 18 |
| 2.3 Overview of Thermal Modeling in Electronic Systems | 21 |
| 2.4 Uncertainty Analysis | 24 |
| 2.5 Summary | 26 |
| 3 Validation of Modeling Technique Using Discrete Components | 27 |
| 3.1 General Modeling Characteristics | 27 |
| 3.2 Computational Modeling of MOSFETs | 28 |
| 3.3 Sensitivity and Uncertainty Analysis in Thermal Modeling of MOSFETs .. | 33 |
| 3.4 Experimental Setup | 34 |
| 3.5 Experimental Procedures | 36 |
| 3.6 Results and Discussions | 39 |
| 4 Thermal Design of Active Integrated Power Electronics Modules (IPEMs) | 49 |
| 4.1 Electrical and Packaging Constraints | 50 |
| 4.2 Design Strategy | 54 |
| 4.3 Thermal Modeling of Active IPEM | 55 |

| | | |
|-----|---|-----|
| 4.4 | Parametric Analysis | 59 |
| 4.5 | Sensitivity and Uncertainty Analysis | 60 |
| 5 | Results and Discussions | 62 |
| 5.1 | Parametric Study | 62 |
| 5.2 | Sensitivity and Uncertainty Analysis..... | 71 |
| 5.3 | Solution and Results Convergence | 75 |
| 6 | Conclusions and Recommendations | 76 |
| | References | 79 |
| | Appendix A: Thermal Couplings | 85 |
| A.1 | Modeling of MOSFET | 86 |
| A.2 | Modeling of IPEM | 87 |
| | Appendix B: Simulation Data | 90 |
| B.1 | Thermal Simulations of MOSFETs | 90 |
| B.2 | Thermal Simulations of IPEMs | 105 |
| | Appendix C: Data Sheets for Experiment Equipments | 146 |
| | Appendix D: Quotation for DBC Ceramic | 151 |
| | Vita | 154 |

Nomenclature

| | | | |
|----------------|--|----------------|-------------------------|
| A | Area, m ² | R | Resistance, °C/W |
| I | Current, A | t | Time, s |
| K | Thermal Conductivity, W/m-K | T | Temperature, °C |
| L | Thickness, m | V | Voltage, Volt |
| N _p | Total number of critical input parameters | X ⁺ | Sensitivity Coefficient |
| Q | Power Loss, W | β | Model parameter |
| | | σ | Uncertainty, °C |

Subscripts

| | |
|---|--|
| M | Measured |
| N | Nominal |
| P | Predicted |
| S | Perturbed (for sensitivity calculations) |
| β | Model input parameter |
| ∞ | Ambient |

Acronyms

| | |
|--------|---|
| AC | Alternative Current |
| CFD | Computational Fluid Dynamics |
| CPES | Center for Power Electronic Systems |
| DBC | Direct-Bonded Copper |
| DC | Direct Current |
| ESC | Electronic System Cooling |
| GTO | Gate Turn-Off Thyristor |
| IGBT | Insulated Gate Bipolar Transistor |
| IPEM | Integrated Power Electronic Module |
| IPM | Intelligent Power Module |
| MOSFET | Metal Oxide Semiconductor Field Effect Transistor |

List of Figures

| | |
|--|----|
| Figure 1.1: Timeline Plot of Transistor Counts on Intel Processors Superimposed on Moore's Prediction..... | 2 |
| Figure 1.2: Time-line Plot of Intel Microprocessor Power Dissipation | 3 |
| Figure 1.3: Power Dissipation Trend in Telecommunications and Computing System | 4 |
| Figure 1.4: Failure in Electronics Components..... | 5 |
| Figure 1.5: Power Electronics Trends and Applications | 7 |
| Figure 1.6: Current Industry Intelligent Power Module | 10 |
| Figure 2.1: Schematic of Typical Thermoelectric Cooler | 15 |
| Figure 2.2: Schematic of Refrigeration Cycle | 16 |
| Figure 2.3: Cool Chips are based off of a technology called a Thermionic Converter... 17 | 17 |
| Figure 2.4: Schematic on How the Cool Chips Work | 17 |
| Figure 3.1: An Overview for Electronics System Cooling Simulation | 29 |
| Figure 3.2: Typical Commercial Package MOSFET: (a) N-Channel Enhancement Mode MOSFET Cross-section, and (b) Schematic of MOSFET | 30 |
| Figure 3.3: An Exploded View of MOSFET Modeled for Thermal Analysis | 31 |
| Figure 3.4: Discrete MOSFET Model: (a) Boundary Conditions, and (b) Position of MOSFETs on the Heat Sink. (All Dimensions in mm.) | 32 |
| Figure 3.5: Flow Channel Used in the Experiment: (a) Insulated Flow Channel, and (b) MOSFETs on the Heat Sink | 35 |
| Figure 3.6: Experiment Set Up | 36 |
| Figure 3.7: Location of Thermocouples: (a) at the inlet airflow, and (b) on the MOSFET and Heat Sink | 37 |
| Figure 3.8: Circuit Diagram of the Experiment | 38 |
| Figure 3.9: Calibration Data of the Infrared Camera Using Thermocouples | 40 |
| Figure 3.10: Location of Output Variable 1 (at the top of MOSFET) and Output Variable 2 (at the top of silicon) | 41 |

| | |
|---|----|
| Figure 3.11: Surface Temperature Distribution of MOSFETs: (a) Predicted Temperature Distribution from Computational Result, and (b) Temperature Distribution Result from Experiment | 43 |
| Figure 3.12: Equivalent Thermal Resistance Network for a MOSFET | 44 |
| Figure 3.13: Margin Errors for Experimental Data and Simulation Result of Junction Temperature (Output Variable 2) | 45 |
| Figure 3.14: Margin Errors for Experimental Data and Simulation Result of Output Variable 1 | 46 |
| Figure 3.15: Margin Errors for Experimental Data and Simulation Result of Output Variable 3 | 47 |
| Figure 3.16: Sensitivity Uncertainties for Each Critical Input Parameter on Output Variable 3 | 48 |
| Figure 4.1: Schematic of IPEM | 51 |
| Figure 4.2: Conceptual Structure of Embedded Power Module | 52 |
| Figure 4.3: Process Flow Chart of Embedded Power Technology | 53 |
| Figure 4.4: Process of Integrated Design Strategy | 54 |
| Figure 4.5: Boundary Conditions | 57 |
| Figure 4.6: IPEM Model for the Thermal Analysis: (a) Details of the IPEM Model, and (b) Positioning of Components on Heat Sink | 58 |
| Figure 4.7: Location of Interest in IPEM for Sensitivity and Uncertainty Study | 61 |
| Figure 5.1: Steady-state Temperature Distributions for: (a) Gen-II.A, and (b) Gen-II.B | 64 |
| Figure 5.2: Trade-offs Between Electrical and Thermal Performance for Different DBC Ceramic Thicknesses | 65 |
| Figure 5.3: Trade-offs Between Cost and Electrical Performance for Different DBC Ceramic Thicknesses | 66 |
| Figure 5.4: Comparison of Cost for Different DBC Ceramic Materials at Different Thicknesses | 67 |
| Figure 5.5: Effect of Heat Spreader Thickness on Maximum Temperature of Gen-II IPEM | 68 |

| | |
|--|----|
| Figure 5.6: Steady-state Temperature Distributions on the Heat Spreaders for: | |
| (a) Case 6 and, (b) Case 8 | 70 |
| Figure 5.7: Steady-state Temperature Distributions for: (a) Case 6, and (b) Case 8 | 71 |
| Figure 5.8: Sensitivity Coefficients for Each Critical Parameter on Each of the | |
| Critical Output Variables | 73 |
| Figure 5.9: Measured Uncertainty for Each Critical Input Parameter | 73 |
| Figure 5.10: Sensitivity-uncertainty for Each Critical Parameter on Each of the Critical | |
| Output Variables | 74 |
| Figure 5.11: Overall Uncertainty for Each Critical Output Variables | 74 |

List of Tables

| | | |
|-------------|--|-----|
| Table 2.1: | Limitations and Capabilities for Compressor-based Cooling, Thermoelectric Coolers, and Passive Cooling | 21 |
| Table 3.1: | The Thermal Conductivity and Thermal Resistance Values for Materials Used in Thermal MOSFET Model | 33 |
| Table 3.2: | Nominal Values and Uncertainty of Parameters Used in Sensitivity and Uncertainty Analysis | 41 |
| Table 3.3: | Overall Uncertainty for Each Critical Output Variables | 42 |
| Table 3.4: | Thermal Resistance Value Required for Equation 3.11 | 44 |
| Table 4.1: | Components Used in IPEM Module | 56 |
| Table 4.2: | Equivalent Thermal Resistance Value for All Relevant Interface Conditions in IPEM Model | 58 |
| Table 4.3: | Thermal Conductivity Values for Materials Used in IPEM Model | 59 |
| Table 4.4: | Variables Used in Parametric Study | 60 |
| Table 4.5: | Nominal Values and Measurement Uncertainty of Parameters Used in Sensitivity and Uncertainty Analysis | 61 |
| Table 5.1: | Summary of the Thermal Simulation and the Parametric Study | 63 |
| Table 5.2: | Specifications for Gen-II.C IPEM | 71 |
| Table A.1: | Thermal Coupling Properties | 85 |
| Table B1.1: | Thermal Analysis of MOSFETs | 90 |
| Table B1.2: | Sensitivity Analysis on Power Loss | 103 |
| Table B1.3: | Sensitivity Analysis on Solder | 103 |
| Table B1.4: | Sensitivity Analysis on Thermal Pad | 104 |
| Table B1.5: | Sensitivity Analysis on Contact Resistance (Screw) | 104 |
| Table B2.1: | Thermal Analysis of Gen-II.A IPEM | 105 |
| Table B2.2: | Thermal Analysis of Gen-II.B IPEM | 114 |
| Table B2.3: | Thermal Analysis of Modified Gen-II.B IPEM (Case 8) | 128 |
| Table B2.4: | Sensitivity Analysis on Power Loss A | 142 |
| Table B2.5: | Sensitivity Analysis on Power Loss B | 142 |
| Table B2.6: | Sensitivity Analysis on Epoxy A | 142 |

| | |
|--|-----|
| Table B2.7: Sensitivity Analysis on Epoxy B | 143 |
| Table B2.8: Sensitivity Analysis on Solder A | 143 |
| Table B2.9: Sensitivity Analysis on Solder B | 144 |
| Table B2.10:Sensitivity Analysis on Grease | 145 |
| Table C1: Data Sheet for TO247 Package | 146 |
| Table C2: Data Sheet for Papst-Motoren Axial Fan | 150 |

Chapter 1

Introduction

Thermal control of electronic components has been one of the primary areas of application of advanced heat transfer techniques. One significant area where thermal management has played a crucial role is in the area of power electronics. Devices of this type are usually used on a large scale where the heat flux levels are much greater than microelectronics. In many cases, catastrophic failure is a result of steep temperature gradient in the localized temperature distribution. The local heat transfer characteristics are complex, as the heat dissipated in the chip is conducted into the substrate and then transferred by some combination of thermal conduction, convection and radiation to the outer surface through numerous components. This detailed distribution is commonly simplified by identifying a junction to case resistance; however, the variation over the complex surface could yield surface heat flux values ranging from 0.1 to 0.3 W/m² or more.

1.1 Background and Motivation

Heat removal from the chips now ranks among the major technical problems that need to be solved to achieve higher power density. For years, the chip industry has been trying to maintain the pace of Moore's prediction, the projection that the number of transistors on integrated circuits would double every eighteen months or so. Figure 1.1 [25] shows this prediction of the growth of semiconductor transistor density by Intel founder Dr. Gordon Moore, who originally made these observations. This remarkable rate of advancement has resulted in smaller feature sizes, and improved manufacturing techniques, which allow for more efficient circuit designs and materials, that result in better circuit performance. Thus, the heat issue becomes a serious threat to the continual achievement of Moore's prediction.

As semiconductors become more complex and new milestones in transistor size and performance are achieved, power consumption and heat have recently emerged as limiting factors to the continued pace of new chip designs and manufacturing techniques.

Imagine in a processor where there are hundreds of millions, and even billions of smaller and faster transistors which are packed on to a single piece of silicon the size of a thumbnail. The power consumption and the dissipation of heat generated in the processor core becomes a significant technical challenge. Thus, power and heat have become the biggest issue of the decade while semiconductor industry continues to strive to improve transistor speed and power efficiency.

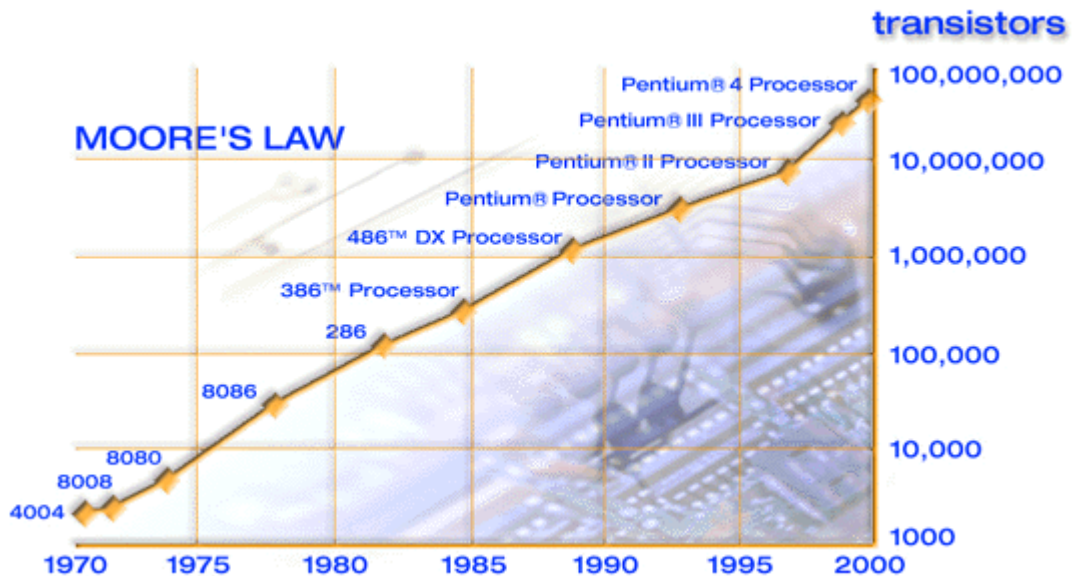


Figure 1.1 Timeline Plot of Transistor Counts on Intel Processors Based on Moore's Prediction [25]

With the current device and manufacturing technologies, the electronics industry aim for continued significant increases in power with time. With the conversion of transistor densities into power dissipation, Figure 1.2 [4] shows the increase of microprocessor power dissipation for Intel Corporation with time. With the significant increase in transistor count required to achieve the peak performance target, the power consumption has grown exponentially with time.

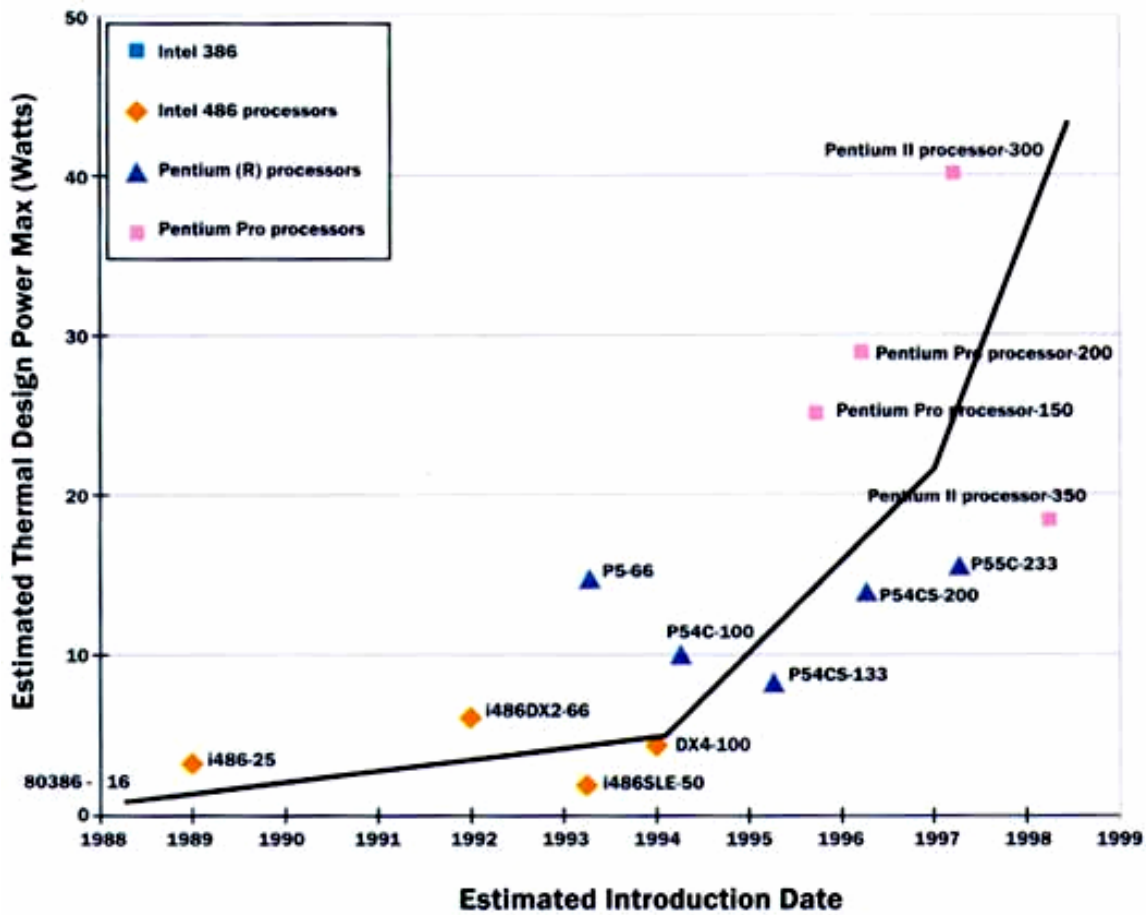


Figure 1.2 Time-line Plot of Intel Microprocessor Power Dissipation [4]

Over the years, there has been a great amount of effort to reduce the size of the devices. With the increase in power dissipation and reduction in the size, the growth in power density defines the limits of performance, functionality and reliability of electronics system. Figure 1.3 indicates the power dissipation trend in telecommunications and computing systems. With all points indicating the continuous increase in power densities, the thermal management solutions play an increasingly important role in determining the future semiconductor device technology.

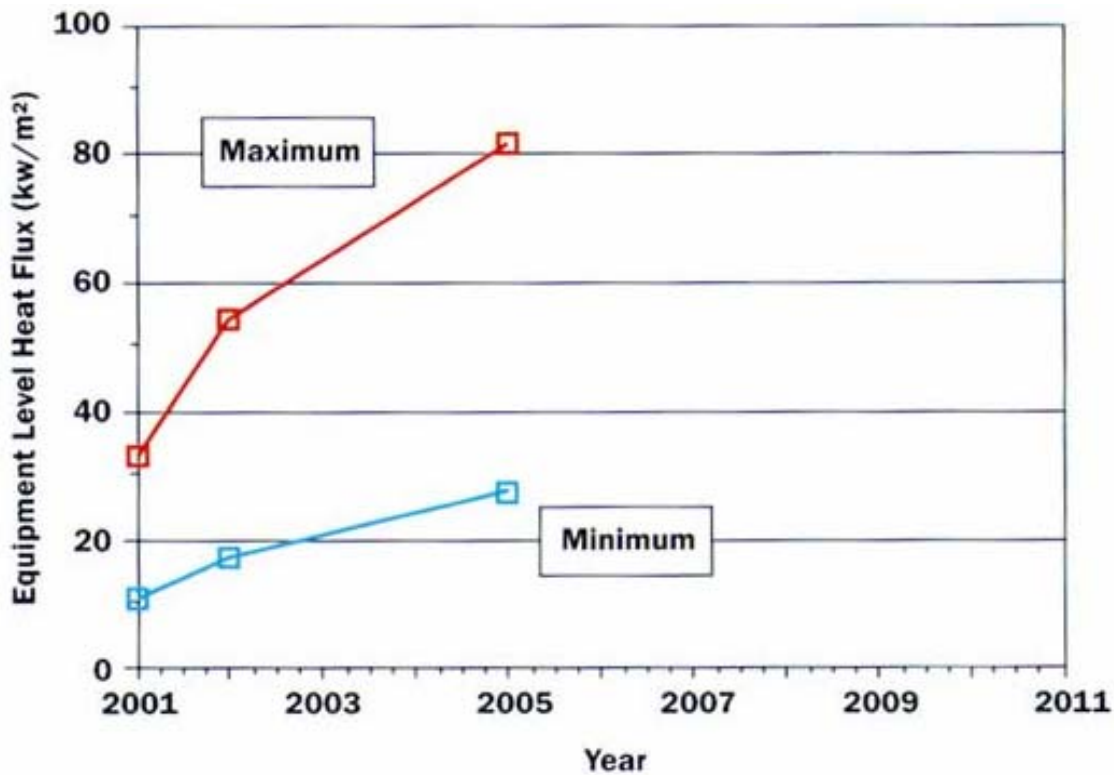


Figure 1.3 Power Dissipation Trend in Telecommunications and Computing System [5]

Thermal failures such as mechanical stresses, thermal de-bonding and thermal fracture become many of the possible breakdowns of electronics components. Mismatch of the thermal coefficient expansion between two different materials, especially at the interface conditions, could result in the separation of interfaces and bonds between different parts in a module at higher temperature. In addition, fatigue in the solder connections and cracking in substrate are common failure in electronics components when operating at off-limit temperatures. Figure 1.4 shows that the failure in electronics during operation due to temperature is as high as 55%.

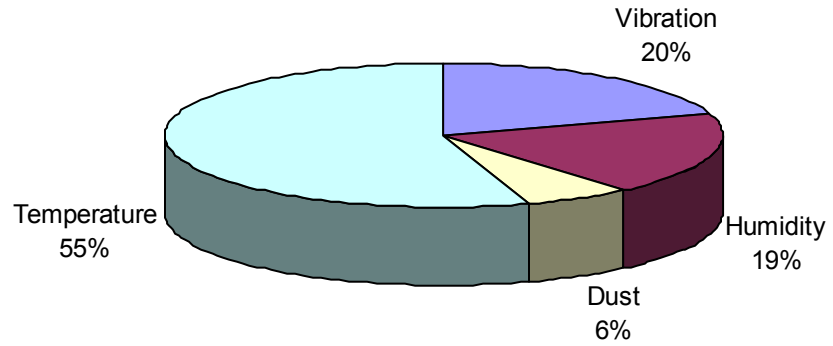


Figure 1.4 Failure in Electronics Components [29]

There are many other reasons why thermal management is of ever increasing importance. Lasance [31] mentioned three typical reasons. Firstly, at the component level, designers try to minimize package dimensions while increasing power density, which makes the problem of minimizing the thermal resistance from junction to case a crucial part of the package design. Secondly, in most of the electronic industries, thermal design tends to be an afterthought of the design process only if the prototype raises any thermal issues. Thus, it results in a longer and ineffective design time. So, thermal management should be an important and necessary part of any concurrent design environment, and must be accepted by all the people involved. Thirdly, the limit of pushing the use of air-cooling with a heat sink and fan is expected to be reached in the coming years. As a consequence of such a physical limit, design rules become very important in achieving reliable temperature predictions and better thermal solutions without costly redesign or over design.

1.2 Overview of Power Electronics

Power electronics refers to control and conversion of electrical power by semiconductor devices wherein these devices operate as switches [31]. It is an enabling technology and widely used in computers, automobiles, telecommunications, space systems and satellites, motors, lighting and alternative energy. Power electronics is essential for the development of extremely dynamic, low-voltage applications such as high performance microprocessor computer systems and it is increasingly important to the automotive industry. For instance, power electronics is an enabling technology for the development of cleaner and more efficient vehicles. As a result, reliability, durability and cost become very crucial issues.

Thyristor, silicon transistor and the Gate Turn-Off Thyristor (GTO) were the first power electronics modules introduced in the 1960s. In the past few years, the power electronics device technology has made tremendous progress. High power bipolar transistors have become mature products and have been used for many applications such as motor drives. Diodes and transistors such as Gate Turn-Off Thyristor (GTO), Metal Oxide Semiconductor Field Effect Transistor (MOSFET) and Insulated Gate Bipolar

Transistors (IGBT) have made a tremendous impact on the power electronics industry as well as its applications. Figure 1.5 shows power electronics trends and their applications.

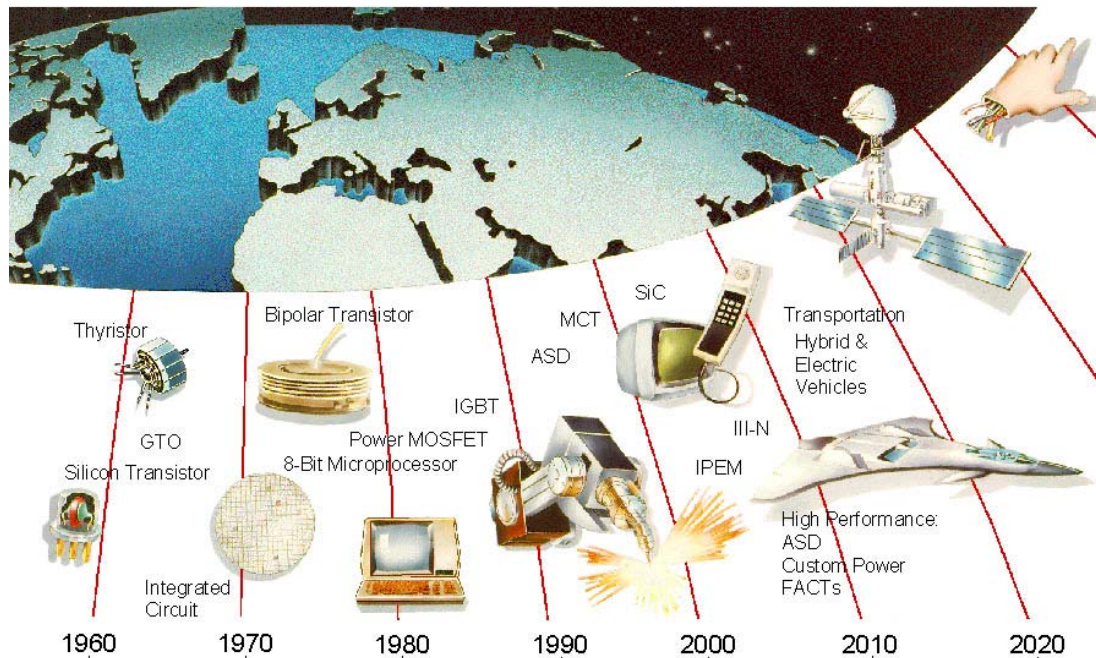


Figure 1.5 Power Electronics Trends and Applications [15]

In the US, electric motors dominate the major energy use. With the invention of the IGBT, three-phase inverters for high power motor applications became practical. The main task of power electronics is to control and convert electrical power from one form to another. The four main forms of conversion are:

- Rectification referring to conversion of AC voltage to DC voltage,
- DC-to-AC conversion,
- DC-to DC conversion and
- AC-to-AC conversion.

Power electronics also play an important role in energy efficiency and the renewable energy area as the renewable energy sources are heavily dependent on power electronics and power electronics packaging. With the tremendous increased in global energy consumption to enhance human living standards, renewable energy sources and high energy-efficient motor drives systems become a new and economically viable solution to reduce the global energy consumption.

Typical design constraints in power electronics include the following factors that affect the cost of the power electronics packages [16]:

- i. Miniaturization of part count,
- ii. Minimization of mass,
- iii. Minimization of footprint and/or form factor (volume),
- iv. Minimization of radiated and conductive electrical noise,
- v. Minimization of acoustical noise,
- vi. Maximization of input/output efficiency,
- vii. Maximization of circuit reliability,
- viii. Maximization of manufacturability,
- ix. Maximization of power density,
- x. Production of a light, compact, inexpensive, reliable, and efficient product, and
- xi. Production of an environmentally safe product.

With all the design constraints of power electronics stated above, there are some issues with the power electronics technology. It usually requires a long design cycle, which leads to high cost. Most of the power electronics packages contain non-standard circuits and parts. This makes the manufacturing automation often impractical due to its labor intensiveness. As a consequence, the industry has produced new concepts involving a standard module, such as the Intelligent Power Module (IPM), which would ideally have sufficient intelligence to establish their operating parameters for specific applications, allowing the power interface to specify the application's characteristics.

The standardization of power electronics module design holds the key to large cost reductions and performance enhancements. It replaces complex power electronic circuits with a single part, reduces development and design costs for complex power circuits, and simplifies development and design of large electric power systems. Other key market-driving-forces for pushing a standard module include better reliability, smaller footprints and easier system integration. With the potential of standard power electronics modules in the market, Semikron introduced their intelligent integrated module, SkiiP, as shown in Figure 1.6a. SkiiP is a standardized and compact design of an IGBT module with integrated drivers and current sensors, and optimal thermal management. Other companies such as Toshiba, Fuji and Infineon have also introduced their standard IPM (Figure 1.6).



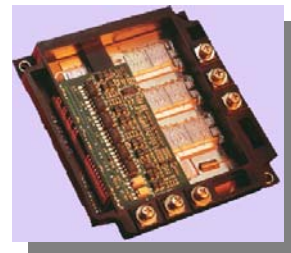
(a) Semikron [48]



(b) Fuji [21]



(c) Eupec / Infineon [17]



(d) Toshiba [55]

Figure 1.6 Current Industry Intelligent Power Modules

1.3 Research Goals and Approach

This thesis presents an integrated thermal design and optimization of an active Integrated Power Electronics Module (IPEM). This prototype is a preliminary design for Generation II IPEM built at the Center for Power Electronics (CPES) at Virginia Tech. The module was packaged using embedded power technology, which is similar to the power-over-layer technology developed at General Electric Corporation [41]. This new packaging technology eliminates wire bonds from the Generation I IPEM.

To fully utilize the capabilities of such a module, there is a need to develop integrated electrical, structural and thermal design strategies. Thermal design of IPEM requires a concurrent approach to insure that multidisciplinary design goals are achieved without creating long design cycle times inherent to sequential design approaches. With this basis, the objectives of this research effort include the following goals:

1. To develop and implement an integrated electro-thermal design strategy for the next generation of the Gen-II IPEM,

2. To optimize thermal performance of the active IPEM with the considerations of electrical and packaging limitations, and
3. To reduce the geometric footprint while maintaining all other design specifications.

To achieve these goals, four steps were applied. First, a modeling method using the numerical code Electronics System Cooling (ESC) in I-DEAS was used to model two discrete power electronic components. The simulation results were then validated by experiment results. Next, the validated modeling method was applied to model a detailed three-dimensional IPEM. Finite element thermal analyses were conducted on each of the proposed electrical layouts. Thirdly, a parametric study was conducted to further optimize the design layout. The parametric study involved the study of the effects of the heat spreader thickness, the DBC ceramic thickness, and the DBC ceramic material type on the thermal performance of the chosen layout. Then, sensitivity and uncertainty analyses were performed to determine the predictive uncertainty of various temperatures in the model.

1.4 Thesis Outline

This thesis consists of seven chapters including necessary background, motivation and the objectives of the research effort in Chapter 1. Chapter 2 provides some related information and previous research done by other researchers in the same area. It includes a review of recent literature of heat transfer in electronics. A valid and reasonable modeling method for discrete power electronics components is presented in Chapter 3. An experiment set up and results from experiments are also discussed and compared to the simulation results in order to validate the modeling method on power electronics components.

Chapter 4 covers the thermal modeling of Generation II IPEM using the modeling method developed in Chapter 3. A computational methodology and detailed description of model development for optimizing IPEM design including boundary conditions are also covered in this chapter. Development of sensitivity study is also discussed in Chapter 4. Chapter 5 presents the results from the optimization and sensitivity studies of

the IPEM design. Finally, Chapter 6 provides conclusions and summary of the research effort as well as the recommendations for future research interest.

Chapter 2

Literature Review

The present trend in power electronics design is towards high power density with larger heat dissipations despite a more compact package. Consequently, a powerful and effective thermal design must be applied to help sustain the trend of increased miniaturization of power electronics devices. Nevertheless, power electronics miniaturization and packaging is a new technical specialization area of power electronics. It is a combination of many technical areas of study. As thermal management is one of these areas, good thermal design is an extremely important component in the development of reliable power electronics products.

Since power input to the electronics is converted to heat in several different forms, thermal science is playing an increasingly important role in the advancement of electronics technology. Examples of the different forms of heat losses are switching losses in semiconductors, dielectric losses, magnetic losses, and ohmic losses in conductors and resistors.

Thermal analysis deserves and must receive special attention because the thermal management strategy for a power electronic product has a large impact on the cost, reliability, operating environment, and performance of electronics systems. The numbers of articles published and research efforts on various aspects of heat transfer in power electronic systems over the past ten years have far exceeded that in previous decades. The concentration of this chapter will be on some of the recent proposed techniques in electronics cooling and design methodology.

2.1 Active Cooling Technologies

Thermal management can be categorized into active cooling techniques and passive cooling techniques. Mechanically assisted cooling subsystems are said to provide active cooling since they require energy. Active cooling techniques offer high cooling capacity. Most importantly, they allow temperature control that can cool below ambient temperatures. Active cooling methods also require less air-cooling, or even eliminate the

use of cooling fan. Air/liquid jet impingement, forced liquid convection, thermoelectric coolers, and refrigeration systems are examples of active cooling techniques.

Mechanically assisted cooling subsystems reduce the heat sink surface temperature to below ambient air temperature. A heat sink that operates at below ambient temperatures is referred as a cold plate. The most common cold plate technologies for high performance cooling are vapor compression refrigeration, thermoelectric devices, and chilled fluid loops.

Unlike a simple heat sink, a thermoelectric cooler permits lowering the temperature of a module below ambient as well as stabilizing the temperature of modules which are subject to widely varying ambient conditions. Thermoelectric cooling is a solid-state method of heat transfer through dissimilar semiconductor materials. It has much in common with conventional refrigeration methods; only the actual system for cooling is different. The main working parts in a conventional refrigeration system are the evaporator, condenser, and compressor. However, in thermoelectric refrigeration, the three main working parts are replaced with a cold junction, a heat sink, and a DC power supply (Figure 2.1).

The refrigerant in both liquid and vapor form is replaced by two dissimilar conductors. The cold junction, which replaces the evaporator, becomes cold through absorption of energy by the electrons as they pass from one semiconductor to another. Due to the energy absorption by the refrigerant, the refrigerant changes from liquid to vapor. The compressor is replaced by a DC power source that pumps the electrons from one semiconductor to another. A heat sink replaces the conventional condenser fins, discharging the accumulated heat energy from the system [52]. While both systems function according to the same thermodynamic principles, thermoelectric coolers are small, lightweight devices with no moving parts to wear out. Thus they can often be included within the equipment or even become an integral part of cooled components. Figure 2.1 shows a schematic of a typical thermoelectric cooler.

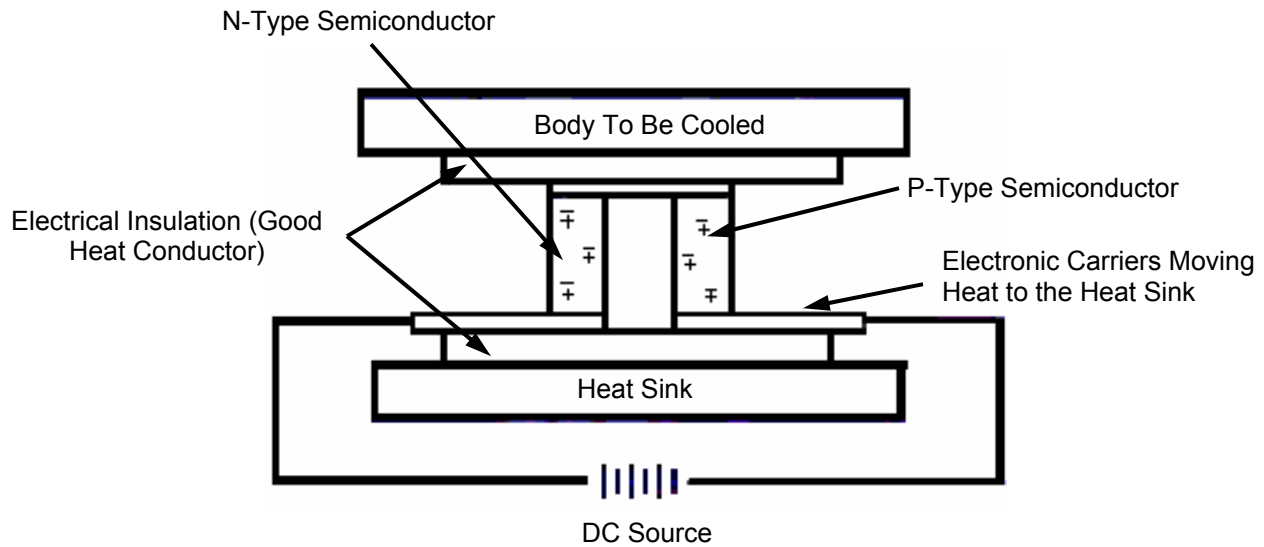


Figure 2.1 Schematic of Typical Thermoelectric Cooler [53]

While a thermoelectric system has a Carnot efficiency of 5-8%, a conventional refrigeration cycle can operate at a maximum Carnot efficiency of about 50%. Because of its better efficiency, Peeples [44] presented the use of vapor compression refrigeration in cooling high performance applications especially in computing and telecommunications. He mentioned that vapor compression refrigeration offered several important advantages. These included low mass flow rate, high coefficient of performance (COP), low cold plate temperatures and the ability to transport heat away from its source. Figure 2.2 shows the schematic for a conventional refrigeration cycle.

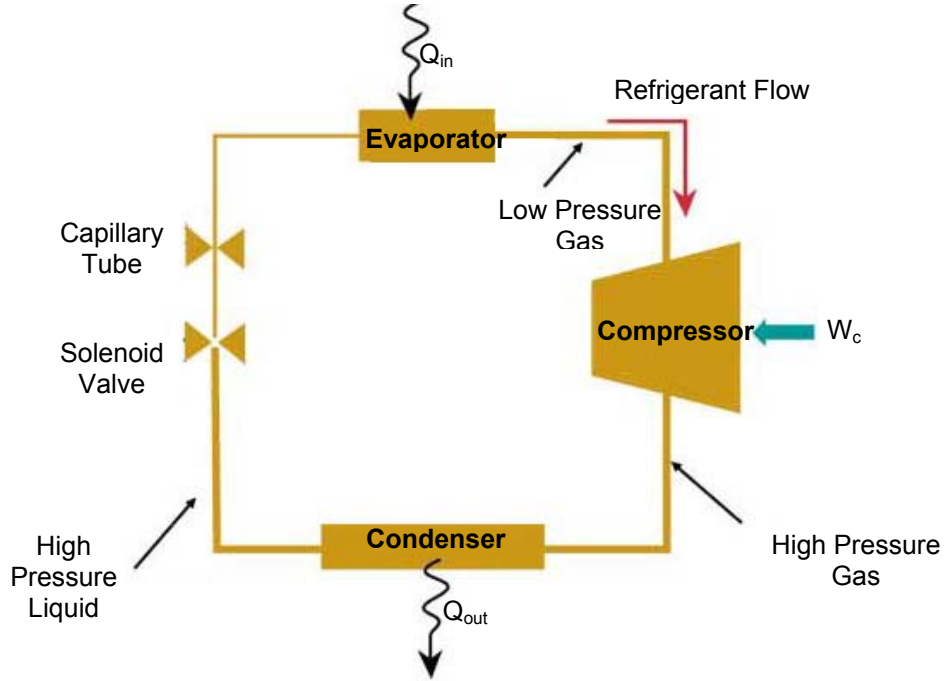


Figure 2.2 Schematic of Refrigeration Cycle [44]

While the conventional refrigeration systems perform better than the thermoelectric cycles, Borealis Exploration Limited [9] introduced a better and more efficient technology—Cool Chips Thermal Management Technology. Using a revolutionary new thermionic technology, Cool Chips can deliver up to 70-80% of the maximum (Carnot) theoretical efficiency. Cool Chips are a form of vacuum diode that pumps heat from one side of the chip to the other to provide localized cooling and refrigeration (Figure 2.3). Figure 2.4 shows the heat path in a Cool Chips. Because they are smaller and lighter than competing technologies with greater efficiency, Cool Chips have potential applications for thermal management in aircraft and spacecraft, where size, weight and power requirements are at a premium.

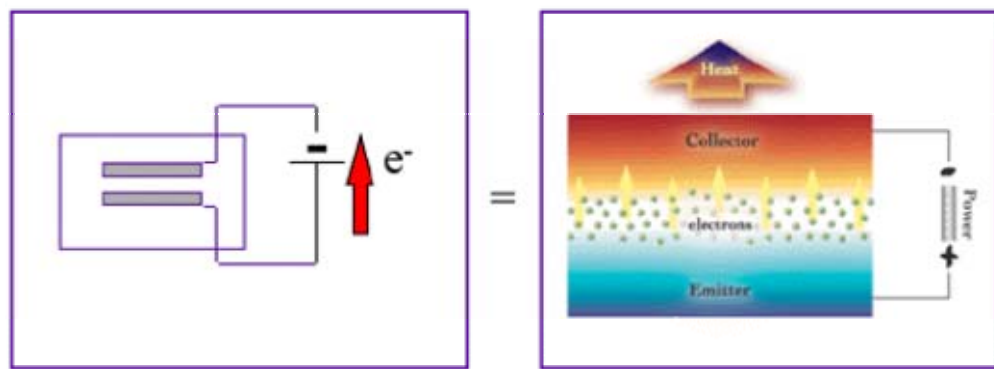


Figure 2.3 Cool Chips are based off of a technology called a Thermionic Converter [9]

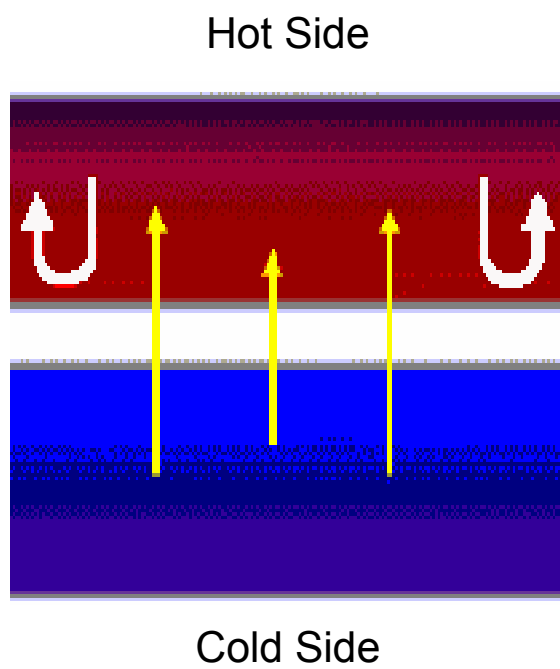


Figure 2.4 Schematic on How the Cool Chips Work [8]

Other than the refrigeration systems, the thermoelectric systems, and the thermionic technology discussed above, some other researches have also worked on improving the heat transfer performance by increasing the heat transfer coefficient. One of the cooling methods that has drawn varied interest in this area is the jet impingement method. To investigate the effect of jet impingement on heat transfer coefficient, Pais et al. [42] conducted experiments with a circular jet for different levels of submersion, different Reynolds numbers, and different jet diameters. Their results showed that the heat transfer coefficient could be enhanced by as much as 25% if the jet was submerged as opposed to being free from submersion. Wadsworth et al. [57] also performed experiments to investigate the single-phase heat transfer performance of the jets. They concluded that increasing jet velocity could increase the chip's cooling rate. In addition, cooling via rectangular jets maintained nearly isothermal chip surface conditions.

2.2 Passive Cooling Technologies

Passive cooling becomes equally important as active cooling especially in module level thermal management although passive cooling is limited to what it can achieve. With spatial limitations in module design, passive cooling is often more practical than active cooling. Typical passive cooling techniques apply high conductivity adhesives, silicone gel and epoxy to replace low conductivity interface materials. A good design layout of a module can also help in achieving an effective passive cooling. Other passive cooling methods include applying effective heat spreaders and heat sinks to the electronics package. Recent technologies such as integration of the heat pipes to the electronics package and phase change techniques are commonly used in order to dissipate the maximum amount of heat from the module during operation.

Yovanovich [61] mentioned the importance of contact and convection thermal resistances that occur at the numerous interfaces and at the air-cooled interfaces in associated with electronics packaging. The material, spreading, and constriction resistances can be predicted quite accurately by means of the numerous thermal

resistance models and solution methods described over the past and many of which are presented in the chapters of Yovanovich and Antonetti [62].

While interface materials play an important role in determining the thermal performance of an electronic system, many research efforts have also been performed on optimizing the structure within the electronic package. Recently Ohbu et al. [40] at Toshiba Corporation studied the difference in the temperature rise as a function of changing thickness of the heat spreader and distance between chips in package structure optimization. Evaluation of reduced ceramic substrate thickness on maximum junction temperature revealed that there is relatively no improvement with aluminum nitride, however a more notable improvement with aluminum oxide [22].

In addition, Welch [58] pointed out that adding a heat spreader to the electronics module could improve the heat dissipation capability of the module since the spreader increases heat transfer by efficiently distributing the applied energy over an increased surface area. The performance of a heat spreader depends on many variables such as its dimensions, its material thermal conductivity, etc. He also introduced a numerical approach to optimal sizing of rectangular isotropic thermal spreaders.

Other than using heat spreader, researchers also believed that the optimization of the heat sink also help in improving the thermal performance of an electronic package. An efficient heat sink would help in lower the junction temperature as the power density in power modules continues to increase. Therefore, Ferdowsi et al. [18] reviewed thermal performances of several different types of heat sinks based on natural convection and forced convection, a number of parameters such as fin spacing, base thickness and fin dimensions.

Many efforts have been focused on convective cooling, and the thermo-structural behavior of plastics and adhesives used. Especially high power electronic packages, they require more vigorous methods of thermal control. Direct immersion liquid cooling with phase change has been proven to be one of the most effective heat transfer processes. It also offers an alternative for cooling high-density power electronics packages. As a result, Yoo et al. [60] considered solid liquid phase change materials (PCM) based hybrid thermal management methods as an alternative passive cooling. As the PCM starts melting, the temperature increase rate of the heated component drops significantly. PCM

can be mounted under the heat sink base, or incorporated between every channel of a heat sink. However, the major drawback of this method is the high thermal resistance between the component and the heat sink [23].

Similarly, Yang et al. [59] addressed several different aspects of thermal dynamics of two-phase flow in a narrow channel. They applied a Computational Fluids Dynamic (CFD) method for two-phase flow in order to simulate the hydrodynamics of Taylor bubbles in a narrow channel. They also experimentally studied the condensation heat transfer inside a square channel. Their results showed that the wave structure of the interface of two-phase flow could enhance significantly the heat transfer between the liquid film and heated wall. Normington et al. [38] also presented experimental results related to the use of mixtures of dielectric liquids to control temperatures and overshoot while handling high heat fluxes.

With all the limitations and capabilities of certain cooling techniques, the thermal designer should be careful in choosing the right methods. A summary of limitations and capabilities of certain cooling methods is shown in Table 2.1.

Table 2.1 Limitations and Capabilities for Compressor-based Cooling, Thermoelectric Coolers, and Passive Cooling [54]

| | Compressor-Based Cooling | Thermoelectric Coolers | Passive Cooling |
|-----------------------------|--|---|--|
| Performance & Maintenance | <ul style="list-style-type: none"> – Offers near or below ambient temperatures. – Requires excess maintenance. | <ul style="list-style-type: none"> – Performs the same cooling function as Freon-based refrigerators. – Virtually maintenance-free. | <ul style="list-style-type: none"> – Performance based upon total surface area of heat transfer, amount of airflow and ambient temperatures. – Virtually maintenance-free. |
| Efficiency & Operating Cost | <ul style="list-style-type: none"> – Requiring 100% active cooling for effectiveness. – Average power consumption is high, costing more to operate. | <ul style="list-style-type: none"> – Requiring 100% active cooling for effectiveness. – Average power consumption is high, costing more to operate. | <ul style="list-style-type: none"> – Only requires power consumption to run fans. |
| Reliability | <ul style="list-style-type: none"> – Requires repair or replacement of valves, coils, and moving parts. | <ul style="list-style-type: none"> – No moving parts other than fans. – Provides years of reliability. | <ul style="list-style-type: none"> – No moving parts other than fans. – Provides years of reliability. |
| Power Density & Weight | <ul style="list-style-type: none"> – Gives excellent heat dissipation in an air-conditioner system. – Weight of a unit depends on the rated BTU/hr or Watt capacity. | <ul style="list-style-type: none"> – Gives average heat dissipation – Weight is determined by the size and effectiveness of attached heat sinks. | <ul style="list-style-type: none"> – Low heat dissipation. – Large volumes are required for adequate heat transfer. |

2.3 Overview of Thermal Modeling in Electronics Systems

Thermal analysis can be performed by a variety of methods. Simulation using numerical modeling is inherently a computationally intensive process, since there are many equations to be solved iteratively. Computer aided design (CAD) systems are used to describe geometrical models, to manipulate data, and to display final results. Therefore, CAD systems with thermal analysis and computational fluid dynamics (CFD) modules become very powerful tools to investigate the thermal distribution within the electronics package. Yet, thermal modeling is difficult due to the many uncertainties in the input parameters.

Sridhar [50] evaluated the commercial software Icepak as a thermal design tool for electronics. Using a three-chip Multi-Chip Module (MCM) as a case study, he modeled the module such that the heat dissipated by the power chips was conducted through the substrate. In this case, the heat dissipated is then transferred to the air on the other side by natural convection. Icepak allowed him to mesh the module and the substrate with finer grids while meshing other parts with coarser grids. Comparing his numerical solution with some experimental data, Sridhar concluded that CFD could be used in predicting the flow and temperature distribution in complex configurations, both at the module as well as the system level. This prediction capability would allow the designers to evaluate variations in material properties, geometry and component layouts, and the effect of these design variables on the operating junction temperatures.

Other than Icepak, Free et al. [20] developed another commercial algorithm called Electronic System Cooling (ESC) by coupling the CFD technology and heat transfer equations. ESC is a new analysis technology using a finite difference approach. To reduce the product life cycles in the competitive marketplace, ESC was integrated into a feature based mechanical design system, I-DEAS. ESC also ensured modeling flexibility from insensitive to element mesh spacing and distortion. In addition, Agonafer et al. [2] presented a numerical model of an entire thermal conduction module in ESC using a thermal coupling methodology. This thermal coupling technology created heat paths between elements that were not geometrically connected and allowed heat transfer process to be more accurately modeled. This powerful technique conveniently couples dissimilar fluids and thermal models by introducing a thermal couplings methodology to the thermal network.

There are quite a few commercial software available in the market today. Still, researchers continue to work on designing new and better programs for thermal analysis. For example, Cullimore et al. [14] presented new simulation techniques for designing air-cooled electronics. They described a new approach using multidimensional heat transfer modeling in combination with quasi-multidimensional flow solutions for fast and easily modified models. In this approach, one-dimensional flow circuits were connected directly to two- or three-dimensional thermal models derived from CAD or FEM models. Without stand-alone CFD codes, this approach was much faster to generate and to solve.

For the same reason, this approach was more suitable for parametric and sensitivity analyses.

As mentioned earlier, simulations using numerical modeling is a very computational intensive process. A complicated numerical model could take days for a program to solve the many equations iteratively. Therefore, researchers have tried to minimize the computational processing time by simplifying their numerical models without distorting the accuracy of the results. Nelson et al. [37] examined the effect of removing a layer in multi-layer microelectronics devices when modeling a three-dimensional thermal model in order to obtain accurate results with lower processing times. To speed up the thermal analysis process, their results showed the possibility of neglecting some layers when modeling multi-layer electronics packages.

Similarly, Linton et al. [33] performed several simulations and experiments to investigate the trade-off between using coarse-meshed and fine-meshed grids in the modeling of heat sinks. They created a coarse-meshed model and a fine-meshed model to represent the heat sink in the simulations, and compared these two models to the experiment results. Linton et al. concluded that it was acceptable to model heat sinks using a coarse mesh in the thermal modeling of electronic systems. Using coarse meshes in the thermal modeling of heat sinks would help in reducing the processing time and costs.

With the conveniences of using commercial software, Rizzo [45] addressed the possible misuse of such powerful tools. To properly use the commercial software, the user has to understand the nature of the calculations of the software. Finite element solutions could be wrong because of some serious modeling mistakes such as the misunderstanding of actual physics. After all, finite element modeling is only an approximated representation of the actual physics.

2.4 Uncertainty Analysis

Lack of accurate values for heat transfer coefficients, thermal resistances of components, input parameters (such as physical properties and air resistance coefficients), and temperature-reliability relationships are also critical problems in obtaining accurate simulation results. Cullimore [13] presented both current and future methods of dealing with uncertainties such as a combination of testing and statistical evaluations. He classified the uncertainty into three categories:

1. Uncertainties in performance parameters (contact conductance, film coefficients, dissipation levels, etc.)
2. Environment or usage uncertainties (ambient temperature and humidity, duty cycle, etc.)
3. Manufacturing variations (bonding, fan performance, filter resistance, etc.)

Cullimore [13] also suggested several techniques to test the reliability of the thermal design simulations in a given thermal or fluid model with random variables and defined failure limits. To do so, he presented a Monte Carlo sampling method, a descriptive sampling method, and a gradient method. The Monte Carlo sampling selected the values of uncertain variables randomly according to their probability distribution functions. The Monte Carlo method required many samples, but it yielded the most information. In descriptive sampling method, the user specified the number of samples to be made, based on the cost the user could afford. The specified number became the resolution with which the distributions in the random variables were subdivided. Only one value from each subdivision was sampled after the distributions of the random variables had been subdivided. The gradient method required only $N+1$ samples, where N is the number of random variables. This method estimated reliability by measuring gradients in the responses with respect to the random variables.

In addition to Cullimore's concern, Lasance [30] also presented possible uncertainties in numerical model and experimental data. First, he mentioned several possible factors of influencing the accuracy in numerical modeling as well as the experimental accuracy. The influence of the algorithms and approximation used by the numerical code, the influence of the mesh size, the radiation heat transfer approximations, and the complexity of the physical phenomena were some critical factors

in achieving accurate numerical results. Lasance further mentioned temperature measurements, velocity measurements, and heat flux sensors as the most common inherent errors in all experiments. To have a fair comparison between experimental and numerical results, he then distinguished the insufficiently well-known physical properties (thermal conductivities, emmisivities, temperature-dependent physical properties) and input parameters (thermal data of components, air resistance coefficients, contact and interface resistances, surface roughness) as the major issues in achieving the agreement between experimental and numerical results. He concluded that a maximum of 30% error was acceptable in a comparison between numerical solutions and experiments.

With all the uncertainties discussed above, researchers tried to find a way to present experimental results with describing the uncertainties involved. Thus, Moffat [35] presented a way to describe the uncertainties in experimental results. First, he identified the sources of errors in engineering measurements and the relationship between the error and uncertainty. From there, the intended true value of a measurement was identified through the quantitative estimation of the individual errors. Moffat also presented a technique for numerical executing analyses when computerized data interpretation is involved.

2.5 Summary

Miniaturization, increased integration, and higher demands to quality have made it necessary to take thermal management and temperature related failures seriously. Good thermal design is often required to achieve high reliability, low manufacturing cost (to avoid expensive cooling solutions), small size, and a predictable development time (to avoid redesigns and reduce time-to-market). With the available of powerful computational tools, the design cycle time and the cost of designing new power electronics can be greatly reduced. In addition, the efforts of improving current computational tools as design tools have proved the future potential of computational analysis in various heat transfer analysis.

Chapter 3

Validation of Modeling Techniques Using Discrete Components

Current commercial software provides a very powerful method for carrying out thermal and flow simulations. However, it is very important that the users be aware of the mathematical foundation behind the software. Conservation of energy, conservation of mass and momentum, heat transfer coefficients, and calculation of pressure drop and flow resistance of flow field are the foundational concepts of heat transfer behind the software. In addition, it is also important to know how reliable the simulation results are. Therefore, verification by measurements is desired whenever possible. This chapter presents a modeling method for power electronics systems with the validation of results from experimental data. To validate the thermal modeling method for modeling a generic power electronics component, two discrete power electronics components were modeled using the Electronics System Cooling (ESC) program provided in I-DEAS release 8.

The validation approach is to perform a comparison of simulation results to experimental data such as thermocouple measurements and infrared images. Since the physical models in the computational simulations contain uncertainties due to a lack of complete understanding of the physical process, sensitivity and uncertainty analysis were performed to identify and quantify error and uncertainty in the models. The accuracy required in the validation is dependent on the application. Therefore, the validation should be flexible to allow various levels of accuracy.

3.1 General Modeling Characteristics

ESC is an available commercial thermal and computational fluid dynamics (CFD) program developed by the Maya Heat Transfer Technology Corporation. In ESC, the CFD solver technology uses an element-based method, allowing users to model turbulent flow as well as three-dimensional fluid velocity, temperature, and pressure distributions. The flow solver computes a solution to the nonlinear, coupled, partial differential

equations for the conservation of mass, energy and momentum of the three-dimensional geometry. On the other hand, the thermal solver technology uses finite difference based methods and provides thermal coupling technology to create heat paths between discontinuous meshes [51].

Typical computational process includes modeling, meshing, defining boundary conditions and analysis options, solving, post processing and evaluation. Figure 3.1 presents an overview for ESC simulation.

3.2 Computational Modeling of MOSFETs

A discrete power electronics module such as a MOSFET consists of four elements: the gate, source, drain, and the substrate (Figure 3.2a). The basic functioning principle of the MOSFET is the control of a current flowing between two semiconductor electrodes. The drain and the source are placed on the same element, with a third electrode, the gate, between the drain and the source. Both the drain and the source are n-type semiconductor, and are isolated from the p-type substrate by reversed-biased p-n diodes. The voltage applied to the gate controls the flow of electrons from the source to the drain.

A commercial package of MOSFET is an assembly of parts bonded together by solder, adhesive, molding compound, and mechanical parts such as bolts and springs. In this study, two commercial packages TO247 mounted on a heat sink were used and modeled in simulation. Three major physical parts of MOSFET (a copper base plate, a silicon device and a plastic injected molded cover) were modeled to form a simple computational model of TO247 package. Because the heat transfer to the three terminals extending from the package was ignored, the terminals were not modeled. Figure 3.2b shows the physical parts of a commercial MOSFET.

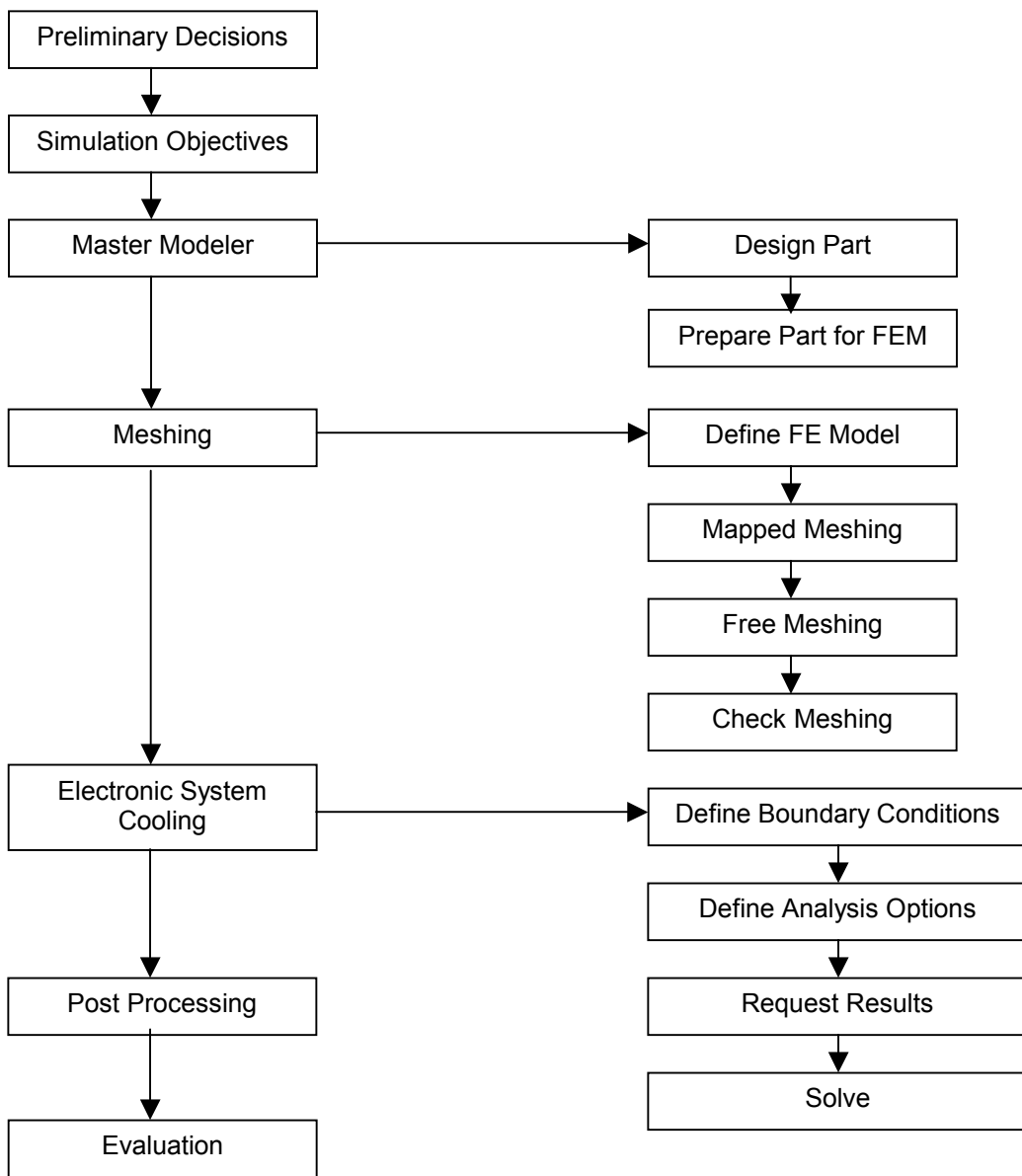


Figure 3.1 An Overview for Electronics System Cooling Simulation [51]

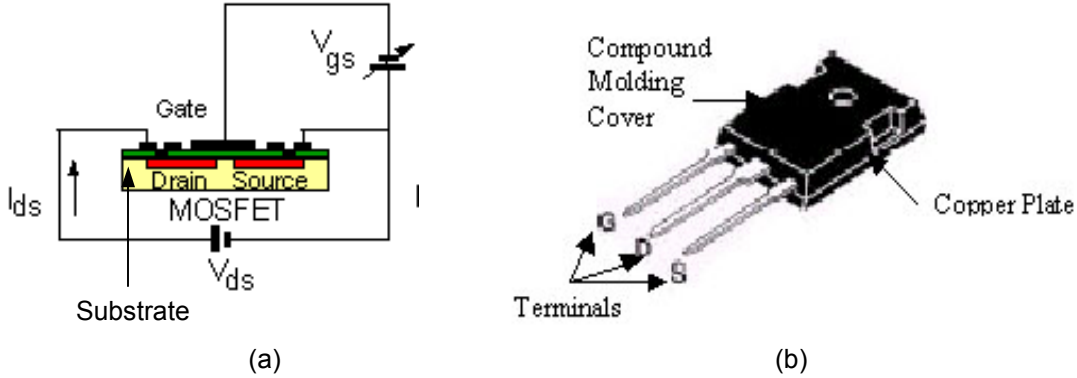


Figure 3.2 Typical Commercial Package MOSFET: (a) N-Channel Enhancement Mode MOSFET Cross-section [49], and (b) Schematic of MOSFET [26]

The silicon device was assumed to have perfect contact with the compound molding cover. The soldered and thermal pad interfaces between various components were represented by equivalent thermal resistance values. These interfaces were the interface between the copper plate and the heat sink, and the soldered interface between the silicon device and the copper plate. Figure 3.3 illustrates the exploded view of the numerical model in I-DEAS.

A heat sink was used to increase the heat dissipation to the air. To provide airflow over the model, a flow channel was included in the simulation. Applying an inlet fan at one end of the channel, the other end of the channel was vented to an experimental measured ambient temperature of 23.5°C. The inlet fan provided a constant volumetric flow rate of 0.05 m³/s. With the fixed channel area, the outlet velocity was 2.22 m/s. Figure 3.4a shows the boundary conditions of the numerical model. The dimensions of the heat sink and the position of the MOSFETs on the heat sink are shown in Figure 3.4b (note that the dimensions are in the unit of millimeter).

The power loss from each MOSFET was determined from the experiment as discussed in Section 3.5.2. The power loss was assumed to be uniform across the top surface of silicon devices. In the modeling, finer grids were applied for the heat-dissipating surfaces. Within the MOSFET, there was a conduction path from the silicon device to the copper plate and the compound molding cover, from the copper plate to the heat sink, and convection from both the heat sink and the MOSFET to the ambient air. The thermal conductivities and thermal resistance values for all of the materials used in

the models are listed in Table 3.1. These values were used to calculate relevant thermal coupling values in the simulations.

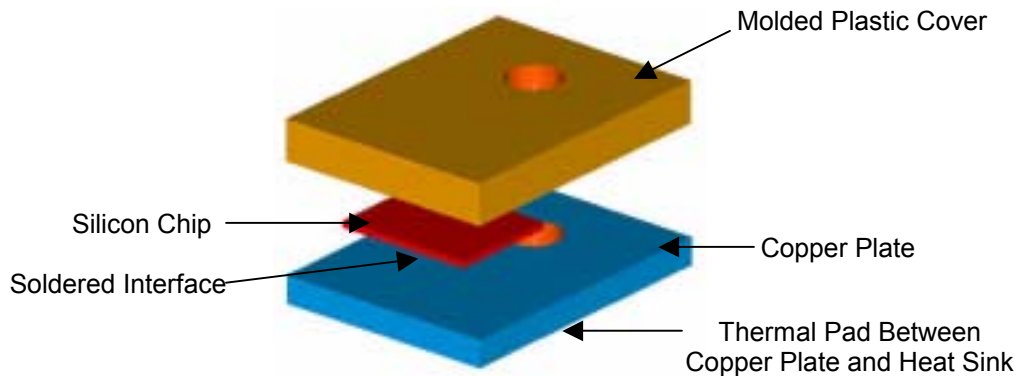
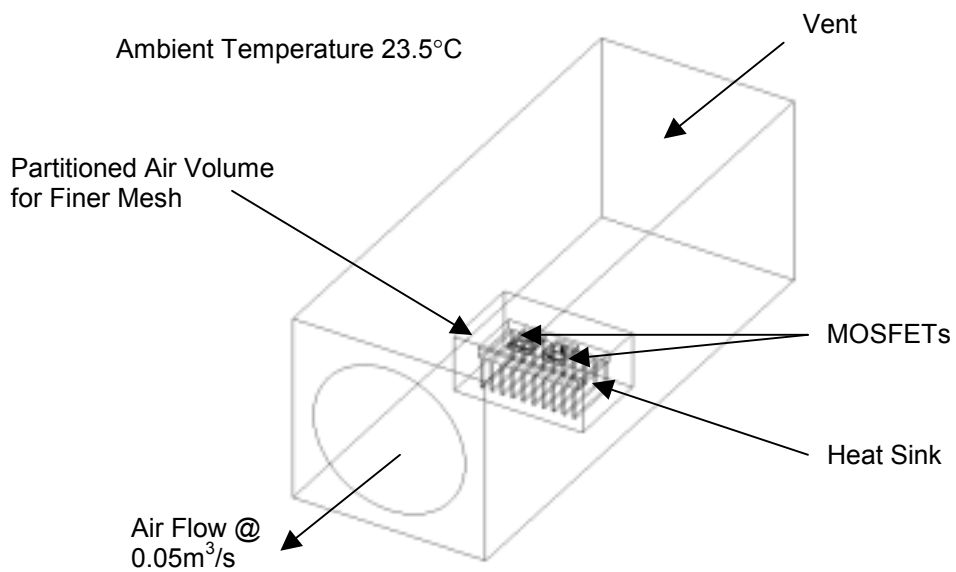
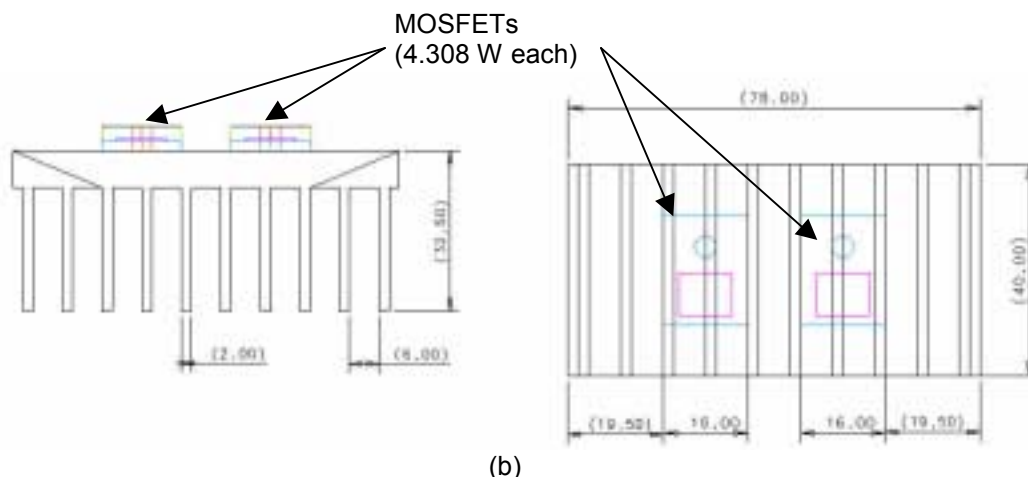


Figure 3.3 An Exploded View of MOSFET Modeled for Thermal Analysis



(a)



(b)

Figure 3.4 Discrete MOSFET Model: (a) Boundary Conditions, and (b) Position of MOSFETs on the Heat Sink. (All Dimensions in mm.)

Table 3.1 The Thermal Conductivity and Thermal Resistance Values for Materials Used in Thermal MOSFET Model [34]

| Material | Thermal Conductivity (W/mK) | Thickness (mm) |
|------------------|--------------------------------|-------------------|
| Compound Molding | 1 | 3 |
| Silicon | 117.5 | 0.5 |
| Copper | 395 | 2 |
| Aluminum | 164 | NA |
| Solder | 51 | 0.127 |
| Thermal Pad | 0.067 | 0.254 |
| Stainless Steel | 26 | NA |

3.3 Sensitivity and Uncertainty Analysis in Thermal Modeling of MOSFETs

A sensitivity analysis provides information on how the model depends upon the input parameters to the model. As a whole, sensitivity analyses are used to increase the confidence in the model and its prediction, by providing an understanding of how the model response variables respond to changes in the inputs. Therefore, it is related to uncertainty analyses. An uncertainty analysis aims to quantify the overall uncertainty associated with the results as a result of the individual uncertainties of the inputs to the model.

In the uncertainty analysis implemented here, a four-step analysis strategy was employed. First, we identified important sensitive parameters in the modeling. The second step involved the determination of the uncertainty for each of these parameters. The third step involved the determination of the sensitivity of each input parameter. Finally, the overall uncertainties on the critical output parameters were determined. The sensitivity coefficient is defined as the change in the nominal temperature with respect to the change in the input parameter values. For each parameter, the sensitivity coefficient was defined as a dimensionless term, X_i^+ :

$$X_i^+ = \frac{\partial T^+}{\partial \beta^+} \cong \frac{\Delta T^+}{\Delta (\beta_S)_i^+}. \quad (3.1)$$

The non-dimensional temperature, ΔT^+ , is defined by

$$\Delta T^+ = \left| \frac{T_N(\beta_{N_i}) - T_s(\beta_{S_i})}{T_N(\beta_{N_i}) - T_\infty} \right| , \quad (3.2)$$

where T_∞ is the ambient temperature, and $T_N(\beta_{N_i})$ and $T_s(\beta_{S_i})$ are the respective predicted temperatures for each parameter using β_{N_i} and β_{S_i} . β_{N_i} is the nominal value of sensitivity parameter, and β_{S_i} is defined by

$$\beta_{S_i} = \beta_{N_i} + 0.01 \cdot \beta_{N_i} . \quad (3.3)$$

In addition, $T_N(\beta_{N_i})$ is also referred as the nominal temperature. Finally, the non-dimensional sensitivity difference, $\Delta(\beta_s)_i^+$, is defined by

$$\Delta(\beta_s)_i^+ = \left| \frac{\Delta(\beta_s)_i}{\beta_{N_i}} \right| , \quad (3.4)$$

where $\Delta(\beta_s)_i$ is the one percent variation of the nominal value β_{N_i} . Uncertainty of each parameter, σ_i , is defined by

$$\sigma_i = X_i^+ \cdot \sigma_{\beta_i} , \quad (3.5)$$

where X_i^+ is the sensitivity coefficient defined in Equation 3.1, and σ_{β_i} is the measurement uncertainties. The overall uncertainty for the j^{th} output variable, σ_j , was then defined as

$$\sigma_j = \sqrt{\sum_{i=1}^{N_p} (X_i^+ \cdot \sigma_{\beta_i})^2} , \quad (3.6)$$

where N_p is the number of critical parameters.

3.4 Experimental Setup

There is always a question of how accurate numerical simulations are when compared to experiments. Although there is a significant increase in the use of computational codes to predict the thermal behavior of electronic systems, numerical models should always be validated by experiments. To validate the thermal model discussed in Section 3.2, a well-designed experiment was conducted. This experiment consisted of two commercially-packaged MOSFETs, a heat sink, a fan, a flow channel, and two pieces of honey combs.

A wooden box as shown in Figure 3.5a was constructed as a flow channel. With two commercially-packaged MOSFETs (TO247) attached to a heat sink, the MOSFETs and the heat sink were placed at the center of the flow channel (Figure 3.5b). By painting the heat sink and the inner surface of the box with black paint of emissivity of 0.85, the emissivity of the surfaces could be maximized. To allow the infrared camera to be able to see through the wooden box, an infrared window was fitted into the top of the wooden box. One AC fan unit model 4600Z from PAPST-MOTOREN with volume flow rate capacity of $180 \text{ m}^3/\text{hr}$ was mounted at the outlet of the box. Also two sheets of honeycomb were placed at the two ends of the box to straighten the flow. Figure 3.6 shows the experiment set up.

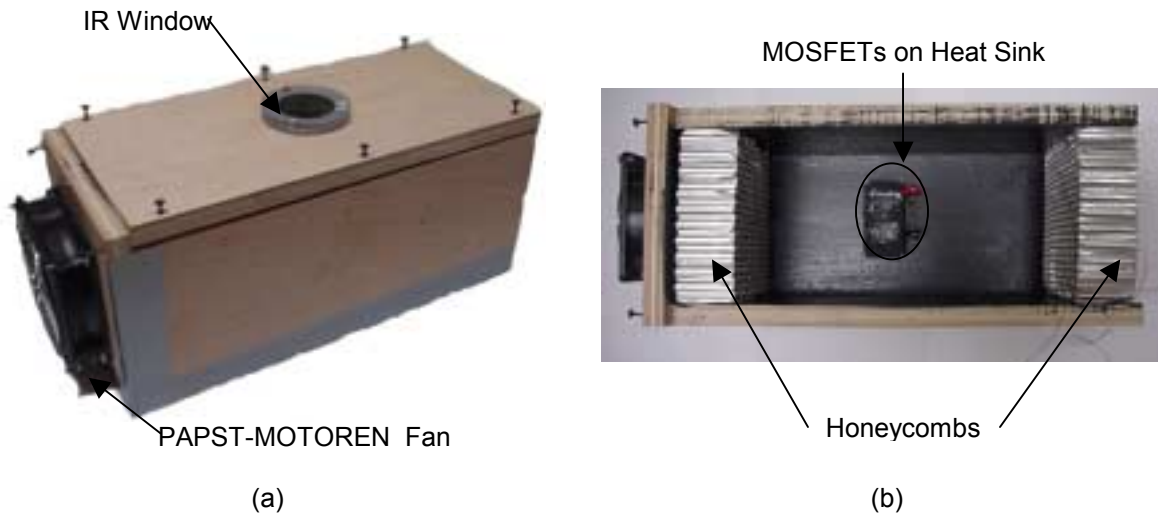


Figure 3.5 Flow Channel Used in the Experiment: (a) Insulated Flow Channel, and (b) MOSFETs on the Heat Sink

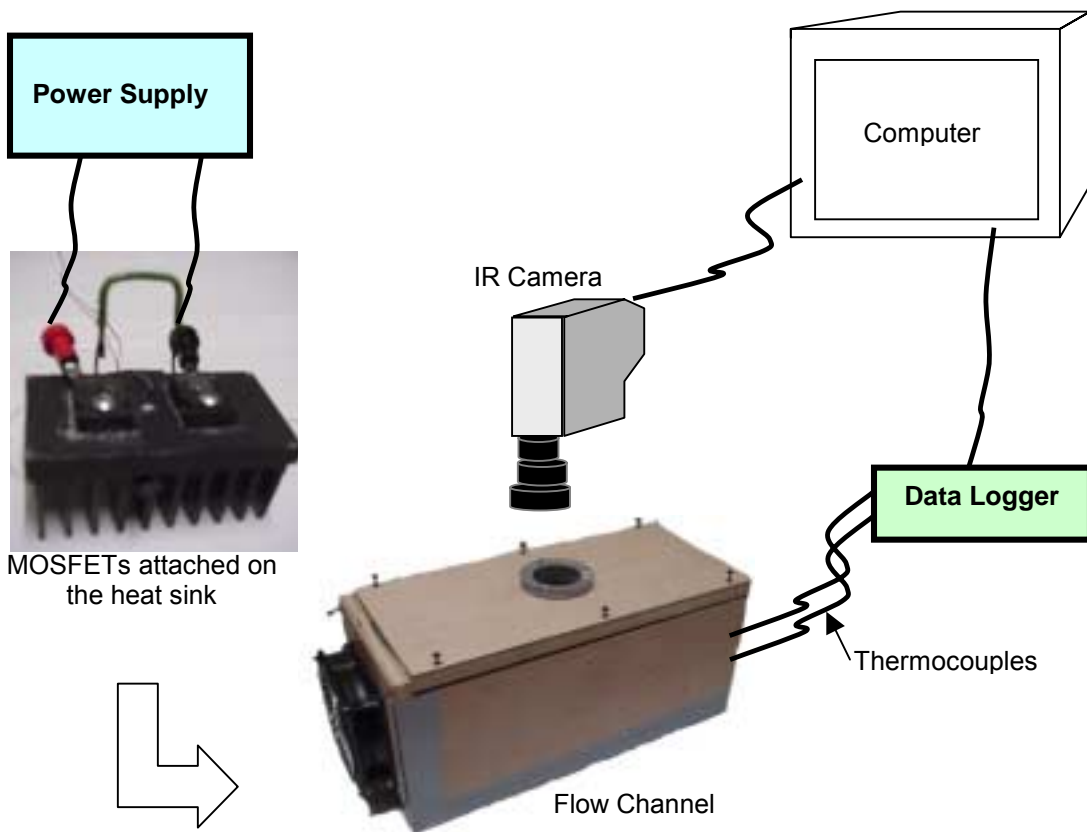


Figure 3.6 Experiment Set Up

3.5 Experimental Procedures

3.5.1 Calibration Step

The measurement procedure consisted of two distinct steps: a calibration step and a power step. In calibration step, a thermocouple was used to calibrate the infrared camera. An infrared camera PM290 with Thermogram, the data acquisition software, was used to record and capture thermal images. At the same time, three thermocouples were placed at the inlet of the flow (Figure 3.7a), on the heat sink as well as the bottom of TO247 (Figure 3.7b).

The thermocouple located at the inlet of the flow monitored the inlet airflow temperature throughout the experiment. At the same time, the thermocouple attached on the top surface of the heat sink (Thermocouple 2) was used to calibrate the infrared

camera, before and during the experiment. Calibration was done such that the temperature displayed from the thermal image was as close as the temperature shown from Thermocouple 2. In this experiment, the infrared camera was calibrated to a difference of 0.1°C over a temperature rise of 5°C . To calibrate the infrared camera, emissivity and the background temperature in the infrared camera were adjusted to 0.91 and 22°C to achieve the desired calibration. Measurements from thermocouples were processed using a data acquisition system, Personal DAQ Model 55 and Personal DAQView. Full field thermal images and data from the infrared camera were saved in Thermogram.

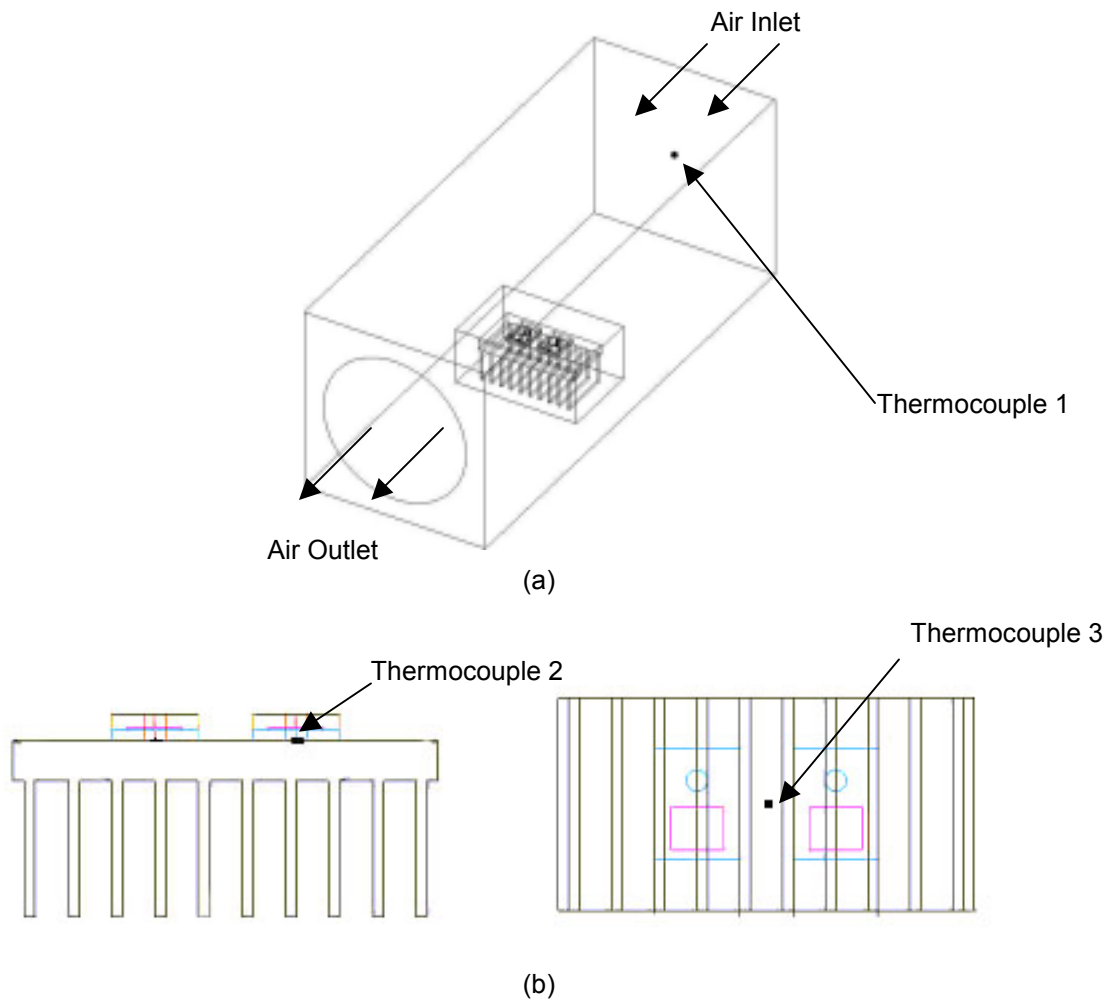


Figure 3.7 Location of Thermocouples: (a) at the inlet airflow, and (b) on the MOSFET and Heat Sink

3.5.2 Power Step

To determine the power loss from the MOSFETs, a power supply with two amperes was supplied to the discrete modules. Two voltage/current multi-meters were used to measure the voltage and current across the MOSFETs. The circuit diagram is shown in Figure 3.8. Then, the power loss, Q_{loss} , could be calculated using Equation 3.7:

$$Q_{loss} = V \cdot I, \quad (3.7)$$

where V is the measured voltage and I is the measured current. The voltage and current associated with the power loss that established across the silicon chips was then measured and the power loss was calculated to be 8.62 W using Equation 3.7. In this experiment, the modules were allowed to achieve steady state.

It was also critical to know how accurate the measured power loss was because any uncertainty in the measured power loss could result in the difference between simulation result and experiment result. The most important feature in the MOSFET was the resistance across the MOSFET when the device was operating. Power consumption and incidental heat generation increased with this resistance. By using reverse bias to deplete the current carriers in the channel with direct current, the power loss could be measured accurately within 0.5%.

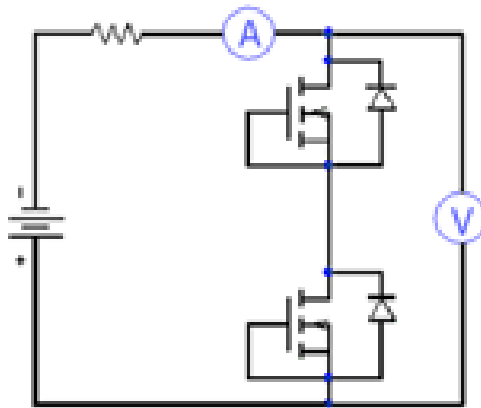


Figure 3.8 Circuit Diagram for the Experiment

3.6 Results and Discussions

3.6.1 Calibration of the Infrared Camera

Measurements from the thermocouples were processed using a data acquisition system—Personal DAQ Model 55 and Personal DAQView. The measured surface temperature contours from the infrared camera were compared with the predicted temperature distributions from simulations. Figure 3.9 shows calibration curve for the infrared camera using thermocouple with 8.616 W of power loss from both MOSFETs. In this experiment, the step resolution for the infrared camera was 0.1°C while the step resolution for data acquisition system was 0.01°C. At the calibration point (Thermocouple 3 in Figure 3.7b), both the temperature from the infrared camera and the thermocouple showed about 31.6°C during steady-state condition. With the most deviation of 0.43°C between the infrared camera and the thermocouple over the temperature rise of 13.3°C, the infrared camera was considered well calibrated. Therefore, the temperature image from the infrared camera could represent an actual temperature field within the same percent of errors as the thermocouples.

Located at the bottom of the MOSFET, the thermocouple (Thermocouple 2 in Figure 3.7b) showed a maximum of 37.3°C at steady-state condition. The airflow temperature was at an average of 23.5°C throughout the experiment. In addition, the infrared camera showed that the highest temperature on the top surface of the molded plastic cover was 36°C.

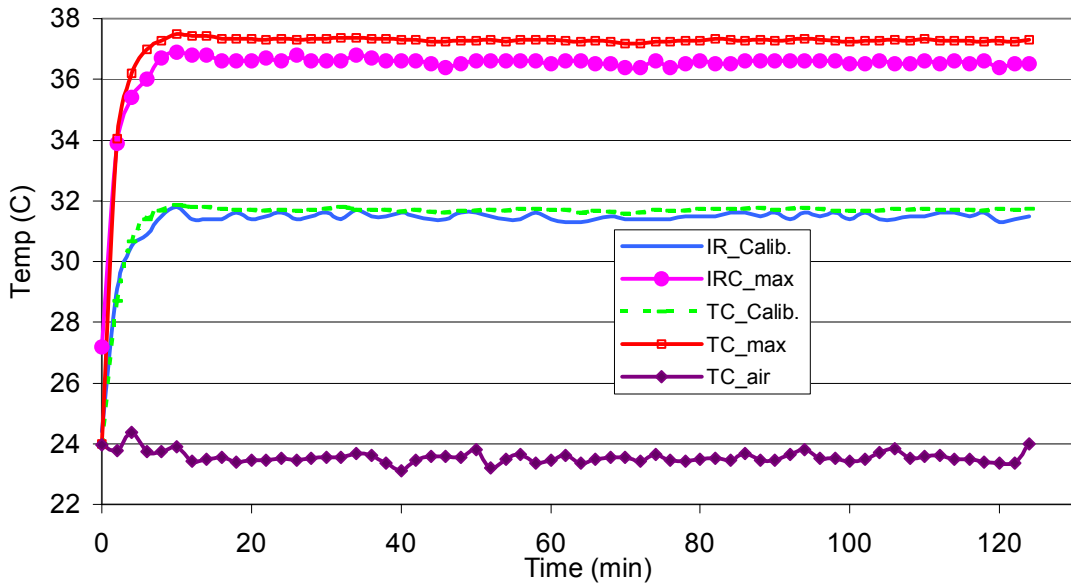


Figure 3.9 Calibration Data of the Infrared Camera Using Thermocouples

3.6.2 Sensitivity and Uncertainties in Numerical Model

As mentioned in Section 3.3, uncertainty analyses involve identifying critical input parameters and critical output variables. The critical input parameters are the inputs to the numerical models such as the power losses, the interface conditions, and the boundary conditions. On the other hand, the critical output variables are the output results that we are interested at. These critical output variables can be the temperature at certain locations in the numerical model. In this case, we were able to identify five critical input parameters in the model. Table 3.2 lists these five input parameters with the nominal values used in the modeling as well as the uncertainty for each of these parameters. Solder resistance and thermal pad resistance are illustrated in Figure 3.3. Besides the power loss, the uncertainties for the other four parameters were rough estimates due to the lack of physical knowledge. The uncertainties for the solder resistance and the thermal pad resistance were estimated as 80% of the nominal values. The contact resistance was estimated as 200% error while the air flow rate was estimated as 50% error. On the other hand, direct current (DC) was supplied to power up the MOSFETs so that power loss was able to be determined within 0.5% of error.

Three critical output variables were selected to study the uncertainty in the numerical model. One is the temperature at the top surface of the MOSFET. The second critical output variable is the temperature at the top surface of the silicon and the third critical output variable is the temperature on the heat sink located between the two MOSFETs as shown in Figure 3.10. The overall uncertainties for these three output variables were calculated using Equation 3.6 described in Section 3.3 and results were listed in Table 3.3.

Table 3.2 Nominal Values and Uncertainty of Input Parameters Used in Sensitivity and Uncertainty Analysis

| Parameter | Sensitivity Parameter, β_i | Nominal Value, β_{Ni} | Uncertainty, σ_{β_i} |
|-----------|--|-----------------------------|---------------------------------|
| 1 | Power Loss (W) | 8.62 | 0.043 |
| 2 | Solder Resistance ($^{\circ}\text{C}/\text{W}$) | 0.062 | 0.05 |
| 3 | Thermal Pad Resistance ($^{\circ}\text{C}/\text{W}$) | 0.13 | 0.1 |
| 4 | Contact Resistance—Screw ($^{\circ}\text{C}/\text{W}$) | 5 | 10 |
| 5 | Air Flow Rate (m^3/s) | 0.05 | 0.025 |

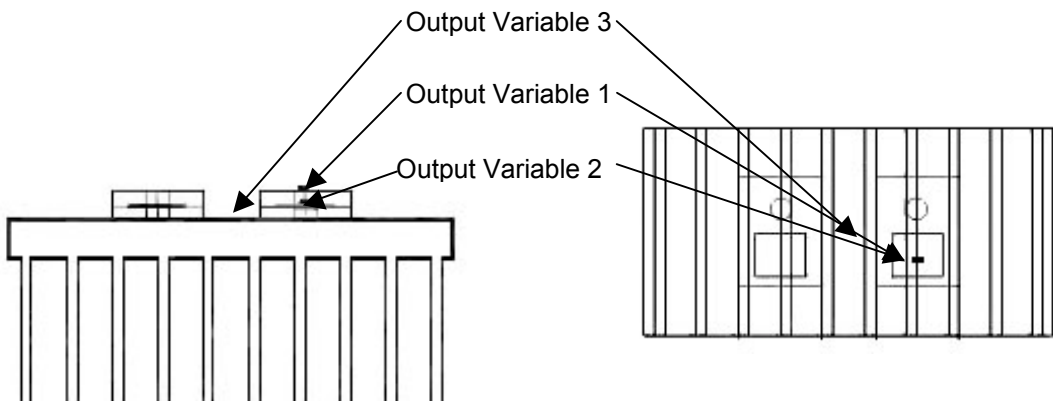


Figure 3.10 Location of Output Variable 1 (at the top of MOSFET), Output Variable 2 (at the top of silicon), Output 3 (on the heat sink)

Table 3.3 Overall Uncertainty for Each Critical Output Variables

| Critical Output Variables | Nominal Temperature (°C) | Uncertainty (°C) |
|---------------------------|--------------------------|------------------|
| Output Variable 1 | 36.18 | ±0.12 |
| Output Variable 2 | 38.31 | ±0.05 |
| Output Variable 3 | 36.75 | ±5.3 |

3.6.3 Comparison between Experiment and Simulation

The numerical model of MOSFETs agreed with the experimental results within 2°C, shown in Figures 3.11a and b. The temperature field on the MOSFETs of the numerical model corresponds well with the image from the experiment. However, the temperature field on the heat sink in the numerical model is 4.2°C higher than the experiment result. Further study on this difference is addressed by looking at the margin error for the simulation result and the experimental data. With the known temperatures on the top surface of the molded plastic cover and at the bottom of the MOSFET, the junction temperature located on the top surface of the silicon can be calculated.

An equivalent thermal resistance is illustrated in Figure 3.12. A power loss of 4.31 W was dissipated from the top surface of the silicon. From there, the heat flowed to the top and the bottom of the MOSFET (Figure 3.11). The total heat dissipation was divided into the heat dissipated to the top of the MOSFET and the heat dissipated to the bottom of the MOSFET:

$$Q_{in} = Q_{top} + Q_{bottom}, \quad (3.8)$$

where Q_{top} can be calculated using:

$$Q_{top} = \frac{T_{junction} - T_{surface}}{R_{molded}}, \quad (3.9)$$

where $T_{junction}$ is the junction temperature, $T_{surface}$ is the temperature on the top of the MOSFET, and R_{molded} is the thermal resistance of the molded plastic cover.

Q_{bottom} can be calculated as

$$Q_{bottom} = \frac{T_{junction} - T_{bottom}}{R_{equivalent}}, \quad (3.10)$$

where T_{bottom} is the temperature at the bottom of the MOSFET and $R_{\text{equivalent}}$ is the equivalent resistance from the silicon to the bottom of the MOSFET and can be calculated using:

$$R_{\text{equivalent}} = R_{\text{silicon}} + R_{\text{solder}} + R_{\text{copper}}, \quad (3.11)$$

where R_{silicon} is the resistance of the silicon, R_{solder} is the resistance of the solder, and R_{copper} is the resistance of the copper plate.

The resistance values required for calculating $R_{\text{equivalent}}$ in Equation 3.11 are listed in Table 3.4. With the known T_{surface} and T_{bottom} from the experiment as 36°C and 37.3°C, the T_{junction} was calculated as 37.9°C. On the other hand, the simulation results showed the T_{junction} as 38.4°C. The difference between the simulation result and the calculated junction temperature from the experimental data is less than 1°C.

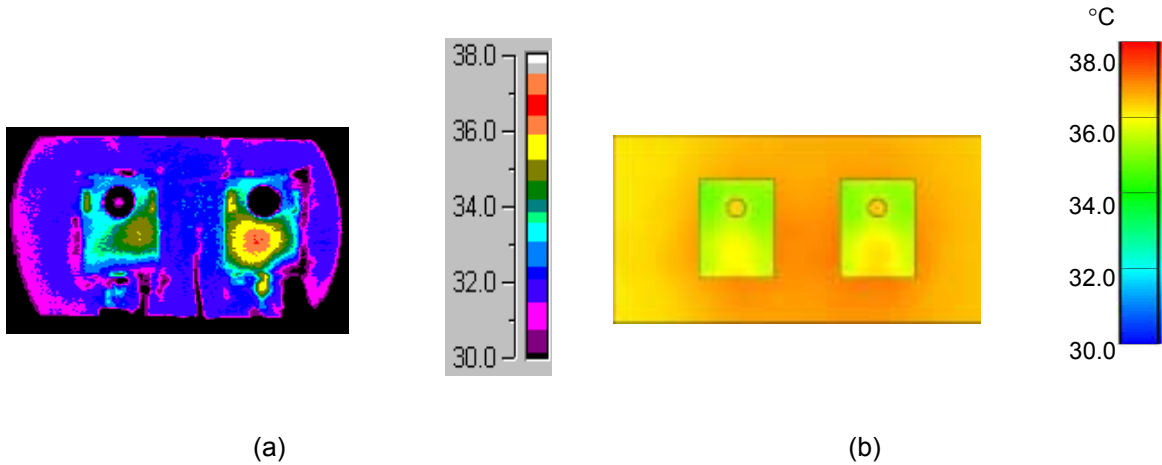


Figure 3.11 Surface Temperature Distribution of MOSFETs: (a) Temperature Distribution Result from Experiment, and (b) Predicted Temperature Distribution from Computational Result (Note Color Scales are Different.)

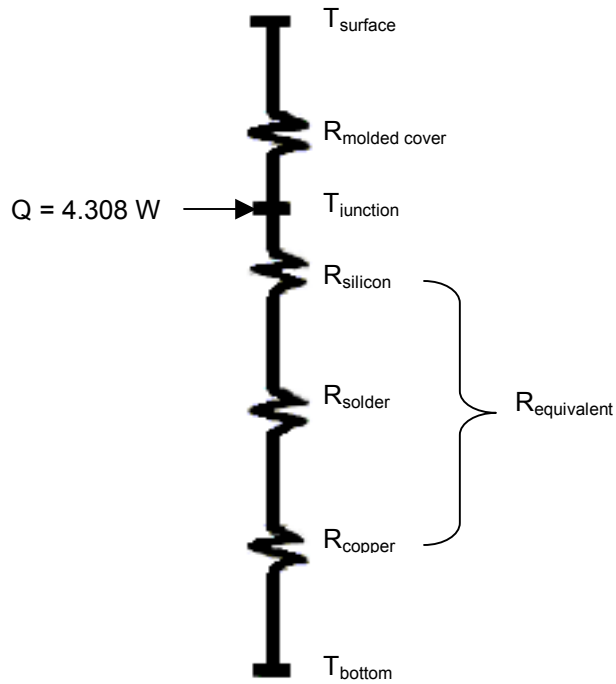


Figure 3.12 Equivalent Thermal Resistance Network for a MOSFET

Table 3.4 Thermal Resistance Value Required for Equation 3.11

| Part | Resistance Value ($^{\circ}\text{C}/\text{W}$) |
|---------|--|
| Silicon | 0.053 |
| Solder | 0.0622 |
| Copper | 0.015 |

With an uncertainty in the experimental measurement of about $\pm 0.5^{\circ}\text{C}$, the calculated junction temperature from the experimental data was calculated to be $37.9 \pm 0.5^{\circ}\text{C}$. Similarly, with the calculated uncertainty in the junction temperature of $\pm 0.05^{\circ}\text{C}$, the junction temperature in the numerical model is $38.4 \pm 0.05^{\circ}\text{C}$. The margin errors for both the experimental data and the simulation result for junction temperature are illustrated in Figure 3.13. Although the margin error for the simulation result is small, it crosses the margin error of the experimental data. Therefore, we can say that the

junction temperature in the simulation result has a good agreement with the experimental result.

The experimental uncertainty for the Output Variable 1 in Figure 3.9 is $36 \pm 0.5^\circ\text{C}$ while the uncertainty in the numerical model is $36.2 \pm 0.12^\circ\text{C}$. The margin errors for the experimental data and the simulation are shown in Figure 3.14. Both the upper and lower margin errors of the simulation results fall between the margin errors of the experimental result. Hence, the temperature from the simulation at Output Variable 1 is said to have good agreement with the experiment result.

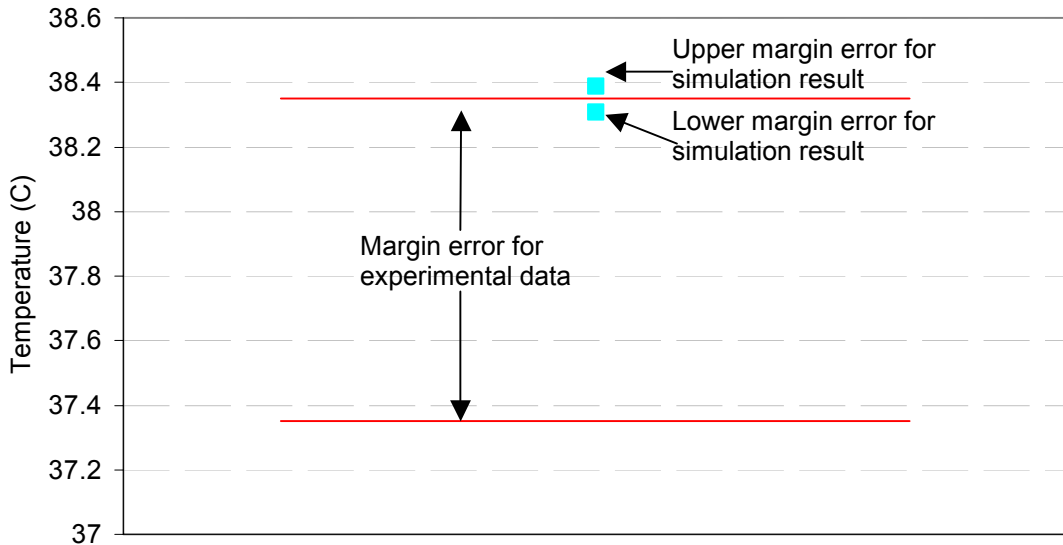


Figure 3.13 Margin Errors for Experimental Data and Simulation Result of Junction Temperature (Output Variable 2)

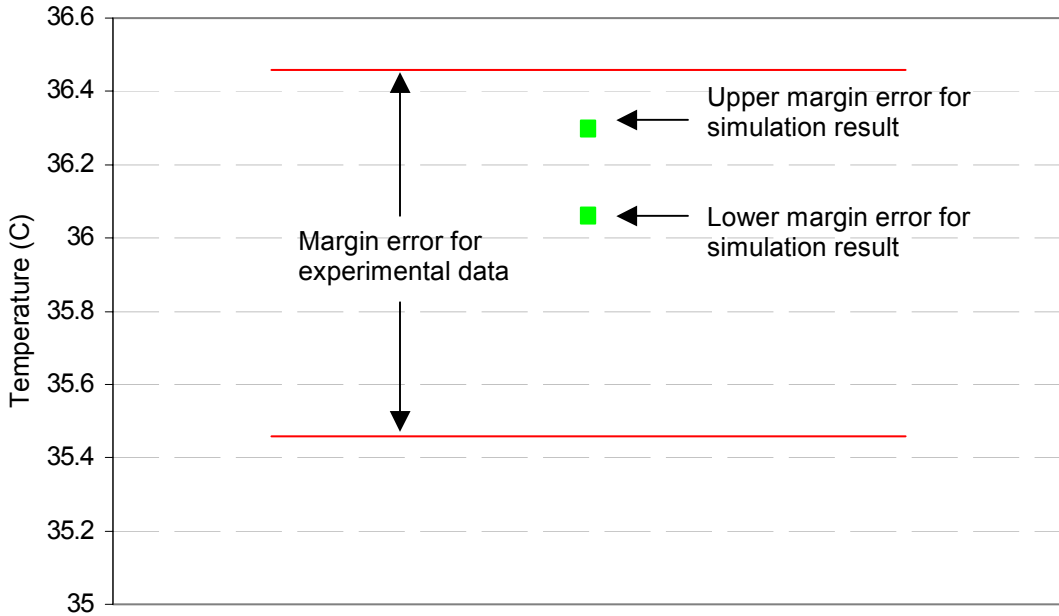


Figure 3.14 Margin Errors for Experimental Data and Simulation Result of Output Variable 1

Figure 3.15 shows the comparison between the experimental data and the simulation result for Output Variable 3. The experimental uncertainty for the Output Variable 3 is $32.5 \pm 0.5^\circ\text{C}$ while the uncertainty in the numerical model is $36.8 \pm 4.5^\circ\text{C}$. The margin error for the simulation result is much larger than the margin error for the experimental data. However, the margin error for the experimental data falls in the margin error for the simulation result. To further study the 4.2°C between the experimental data and the simulation result, the contribution of uncertainties from each of the critical input on Output Variable 3 was studied. Figure 3.16 compares the sensitivity uncertainty for each critical input parameter to the Output Variable 3 in which the dimensionless sensitivity uncertainty, σ^+ , is defined by

$$\sigma^+ = \frac{\sigma_i}{\beta_{N_i}}, \quad (3.12)$$

where σ_i is the sensitivity uncertainty of each input parameter and β_{N_i} is the nominal value of sensitivity input parameter. Figure 3.16 shows that contact resistance contributes the most uncertainty followed by the solder resistance and the thermal pad

resistance. Thus, the uncertainty in contact resistance will need to be improved in order to achieve a more accurate simulation result on Output Variable 3.

Although the uncertainties in the numerical model were rough estimations, still, the margin error of the simulation results fell within the margin error of the experiment results. This indicated a good agreement between the simulation results and experimental data. This also indicated the close estimation of the numerical model to the real world observations. Finally, a thermal analysis technique using ESC was developed and validated by experimental system. The technique can be applied to achieve reliable predicted temperature distribution for future power electronics modules. As for now, the technique will be used in the study of Integrated Power Modules (IPEMs) that will be discussed in Chapter 4.

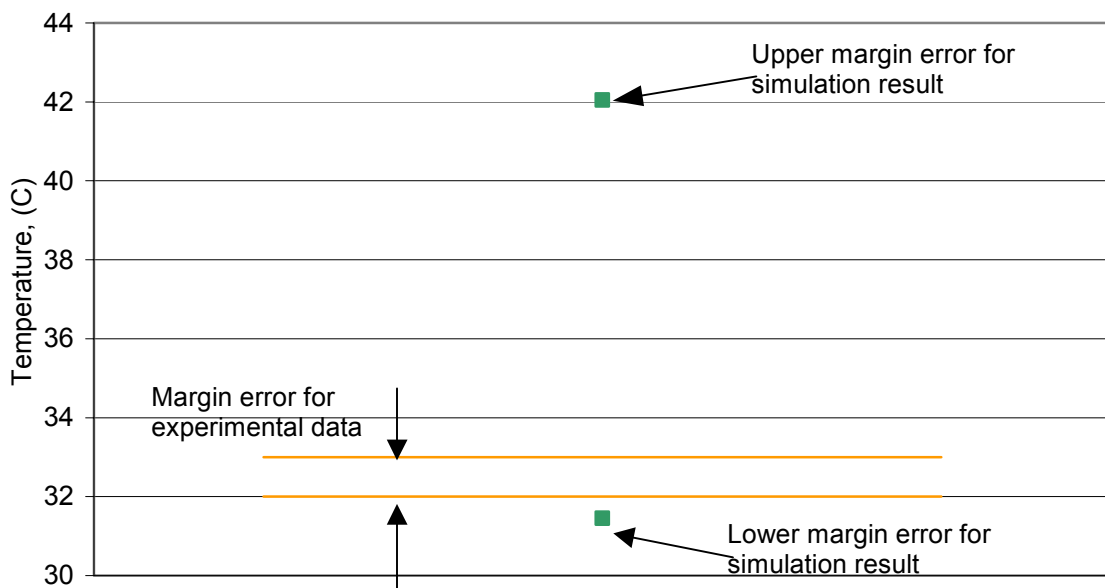


Figure 3.15 Margin Errors for Experimental Data and Simulation Result of Output Variable 3

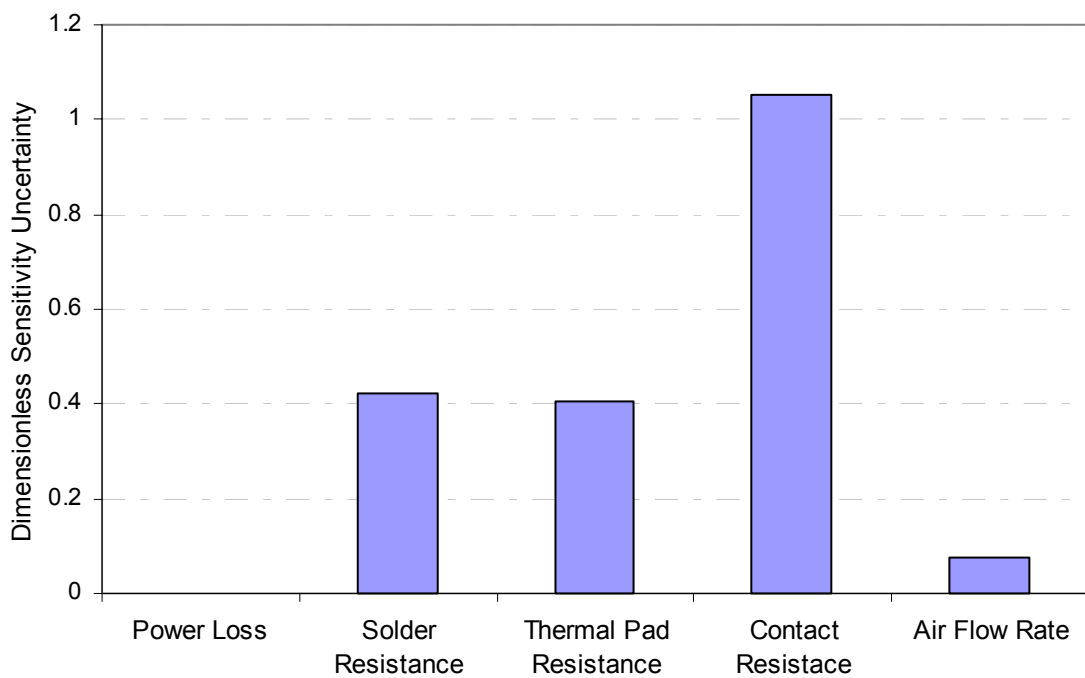


Figure 3.16 Dimensionless Sensitivity Uncertainty, σ^+ , for Each Critical Input Parameter on Output Variable 3

Chapter 4

Thermal Design of Active Integrated Power Electronics Modules (IPEMs)

The cooling of electronics is often the least understood and most often ignored part of electronics design. All power electronics modules have a maximum junction temperature that cannot be exceeded. As for the IPEMs, the maximum junction temperature is set to be 125°C. This maximum junction temperature is directly related to the maximum power dissipation. Device longevity is, in many cases, attributed to keeping its junction temperature within these limits [32]. Therefore, thermal design optimization of power electronics modules is important in increasing the device longevity.

In power electronics, it is believed that the next level of improvement can be achieved by developing Integrated Power Electronics Modules (IPEMs) [32]. IPEMs enable greater integration and standardization within power electronics systems and the end-use applications. Nevertheless, current manufacturing technology uses wire bonds for interconnection of power chips. The resistance, noise and fatigue failure of the wire bonds tend to reduce the electrical and mechanical performance of the modules. As a result, advanced interconnect technologies to replace wire bonds are being developed. To package the IPEMs, CPES uses a deposited metallization based integration technology that is named embedded power technology [32]. Embedded power technology allows high-density capabilities in the structure as well as flexible 3-D interconnections.

This chapter presents the electrical and packaging constraints in optimizing the thermal performance of the IPEMs. This chapter also presents the design strategy applied for optimizing the design layout, the thermal modeling of IPEMs, the parametric analysis for achieving an optimized design layout, sensitivity and uncertainty analysis for determining the predictive uncertainty of various temperatures in the model.

4.1 Electrical and Packaging Constraints

Understanding the thermal characteristics of power electronics modules such as IPEMs is important for two primary reasons. The first is that maximizing the electrical performance of IPEMs can adversely affect the thermal performance. In electrical analysis, we want to minimize the parasitic inductance in the module. Parasitic inductance stores energy when the devices are turned on. However, this energy is released as a spike when the devices are turned off. As a function of current rate and inductance, the voltage spike increases as the current rate and parasitic inductance increase. With high parasitic inductance and high current flow rate, the high voltage spike can damage the module easily. To improve long-term reliability, we have to reduce the parasitic inductance in the module. One way to reduce the parasitic inductance is to reduce the etched copper area in the module as shown in Figure 4.1. Nevertheless, reducing etched copper area decreases the heat spreading area on the copper trace. As a consequence, the heat loss from the devices cannot be dissipated effectively. Continuous heating without effective dissipation from the devices can damage the devices. This over-heating will result in reliability failure.

The second reason for understanding the thermal characteristics of IPEMs is to predict reliability of the module from the thermal performance. Thermal modeling is required to accurately identify hot spots and temperature distributions in the module. Commonly, the peak temperature at the device is referred to as the junction temperature. For IPEMs, the junction temperature is the peak temperature of the devices. The thermal analysis of IPEMs is primarily a conduction problem. Radiation and convection are usually present when considering the use of a heat sink in the system. Nonetheless, the radiation effect is ignored in this optimization study. Conduction is dominant at the module level, and is the focus of this study.

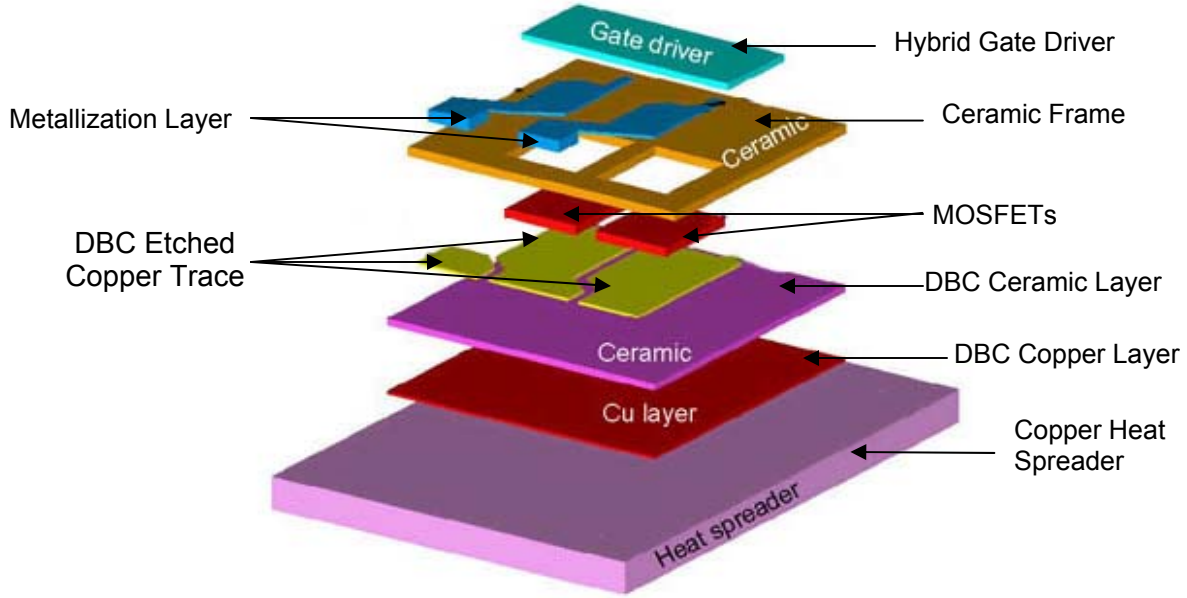


Figure 4.1 Schematic of IPEM

In addition to the electrical constraints as discussed above, the packaging method also restricts the thermal performance of the IPEMs. Using low thermal conductivity materials as interface materials can reduce the thermal performance of the IPEMs. With the current packaging method employed by CPES, there is also a limitation in the size of the IPEM that the research center can package. Therefore, a good understanding of the packaging method and its constraints will also help in maximizing the thermal performance of the IPEM.

Liang et al. [32] presented the conceptual structures of packaged IPEMs using embedded power technology as shown in Figure 4.2. An IPEM is composed of three parts: the power stage, the electronics circuitry, and the base substrate. Included in the power stage structure were the ceramic frame, the power chips (silicon), the dielectrics, and the metallization circuit. The base substrate provided electrical interconnection and thermal path of power chips. The electronics circuitry included a hybrid gate driver and control components. The IPEMs were constructed using embedded power technology. Four steps were used in the process, as shown in Figure 4.3. First, the ceramic was cut to allow for power devices to be embedded in the frame. Next, two MOSFET dies were embedded in the ceramic frame. In step three, the MOSFET dies were covered by

dielectrics with holes in the aluminum pads of the chips. Finally, the metal deposition method was employed in step four.

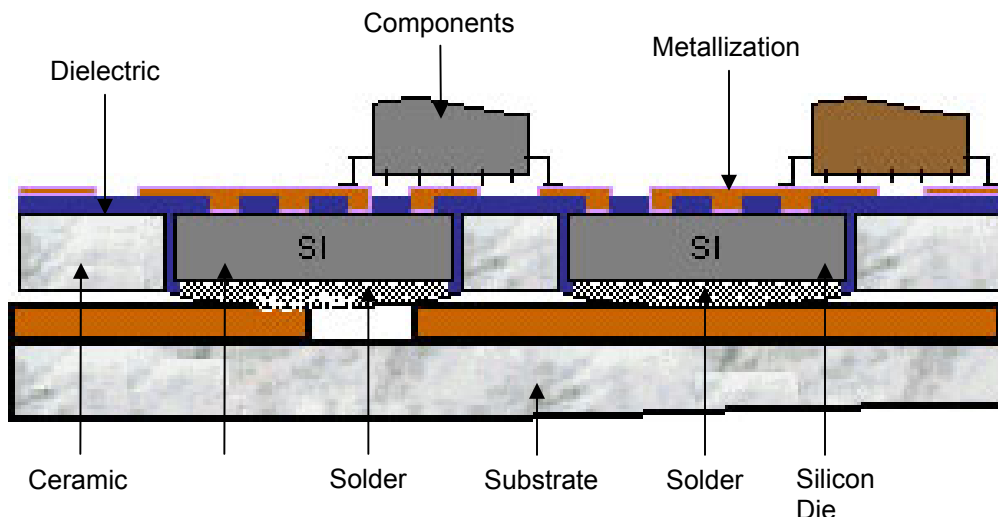


Figure 4.2 Conceptual Structure of Embedded Power Module [32]



Step 1: Ceramic Cutting



Step 2: Device Mounting



Step 3: Dielectric Pattern



Step 4: Metallization Pattern

Figure 4.3 Process Flow Chart of Embedded Power Technology [32]

4.2 Design Strategy

A two-step integrated design strategy was employed to optimize the thermal and electrical performance of the IPEM. First the parasitic inductance and capacitance of the existing IPEM (identified as Gen-II.A) were analyzed using Maxwell Q3D Extractor [3]. To reduce the geometric footprint of the module, a limited number of electrically feasible improvements to the layout were proposed. The best layout was then selected and named Generation II-B (Gen-II.B). The second step involved a detailed parametric study of the Gen-II.B layout to further refine the design, which is discussed in Section 4.4. The parametric study resulted in the final design—Gen-II.C. Figure 4.4 shows the process of the integrated design strategy.

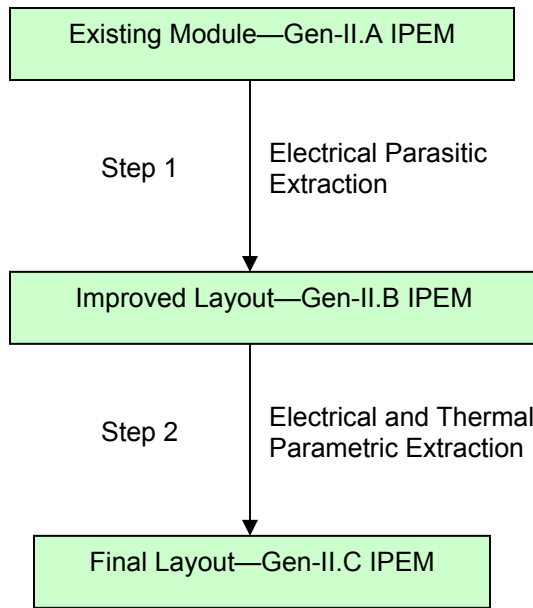


Figure 4.4 Process of Integrated Design Strategy

4.3 Thermal Modeling of Active IPEMs

Accurate thermal model predictions of the IPEMs temperature can be very challenging. Any thermal characterization must consider the details within the module. Various methods for predicting temperature fields in the IPEMs are available, ranging from scaling known results from similar modules to full-scale numerical modeling. The choice of methods depends on the required accuracy. The most commonly used scaling parameter is to express the thermal resistance from the junction to some location under the IPEM. However, some lateral effect of heat spreading cannot be properly represented in the scaling.

The thermal modeling techniques employed for analytical evaluations included I-DEAS Design Modeler and ESC. The Design Modeler was used to model individual parts. The main parts in the model were the copper layer, the ceramic layer, the etched copper layer, the metallization layer, the silicon devices, the ceramic frame, and the gate driver. To simplify the high-density circuitry in the gate driver, the gate driver was modeled as a homogenous ceramic block.

Understanding the physical structure of the IPEM was the first step in the modeling process. As shown in Figure 4.1, the copper layer, the ceramic layer, and the etched copper layer in the thermal model were physically a direct bonded copper (DBC) layer. These layers were manufactured such that they were essentially in perfect contact. The metallization layer was a layer of copper attached on the etched copper layer. Soldered on the etched copper layer were two silicon devices. The metallization layer was in contact with the top surface of the silicon devices. To improve the contact between the silicon devices and the ceramic frame, epoxy filled the gap between the silicon devices and the ceramic frame. The hybrid gate driver shown in Figure 4.1 was a separate-packaged module. It was attached to the top surface of the ceramic frame using epoxy. Epoxy was also used to fill the gap between the ceramic frame and the etched copper layer. The components used in the model are summarized in Table 4.1.

Table 4.1 Components Used in IPEM Module

| Part | Part Number/Thickness | Description |
|---|-----------------------|---------------------|
| Silicon chips—MOSFET | IXFD21N50 | 500V/20A |
| Etched Copper Trace | 12 mil | Top Layer of DBC |
| Ceramic Layer—Alumina (Al_2O_3) | 25 mil | Middle Layer of DBC |
| Copper Layer | 12 mil | Bottom Layer of DBC |
| Ceramic Frame—Alumina (Al_2O_3) | 35 mil | Surrounding Layer |
| Copper | 10 mil | Metallization Layer |

Three-dimensional geometric numerical models were used for all components in the physical structure. To improve the accuracy of the results, all available details were included in the model. Each model was mounted on an aluminum heat sink. To provide airflow over the model, a flow channel was included, with a constant volume flow rate of $0.0094 \text{ m}^3/\text{s}$ at one end of the channel. The other end of the channel was vented to an ambient temperature of 50°C , as shown in Figure 4.5. With the fixed channel area, the outlet airflow rate was 1.1 m/s . The top of the module was assumed to be adiabatic since the actual physical module was encapsulated.

Each module had three heat sources: two silicon devices (MOSFETs) and a gate driver. To a thermal engineer, the dissipated power always is the parameter of interest. As discussed in previous chapter, a MOSFET consists of four elements: the gate, the source, the drain, and the substrate. The voltage applied to the gate controls the flow of electrons from the source to the drain. Current flow between the source and drain results in resistive heating. An exact description of where heat is generated is complicated. However, it is usually sufficient to assume that heat is generated uniformly across the top surface of the silicon die. Similarly, the power loss is assumed to be generated uniformly across the top surface of the gate driver.

The power loss for each of the heat sources was measured and provided by researchers in the Direct Power Supply (DPS) group at Virginia Tech. The two silicon devices dissipated a total of 19 W : 7 W for the innermost one and 12 W for the outside one. The gate driver dissipated only 1 W as shown in Figure 4.6a. The positions of components are illustrated in Figure 4.6b. In addition, all interface conditions were represented by the equivalent thermal resistance values shown in Table 4.2. These

equivalent thermal resistance values were resistant of the particular layer at that particular interface. The thermal conductivities for all of the materials used in the models are listed in Table 4.3.

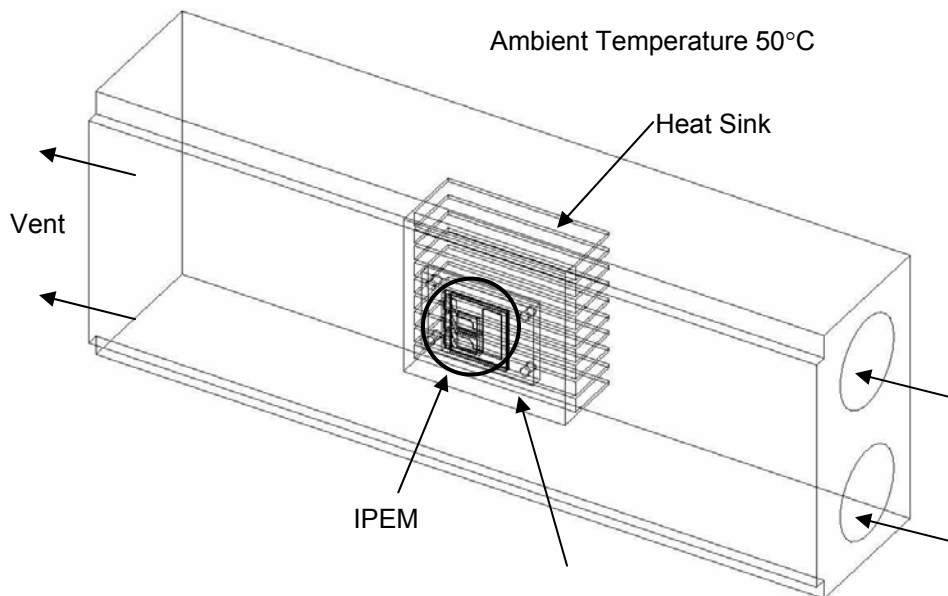


Figure 4.5 Boundary Conditions

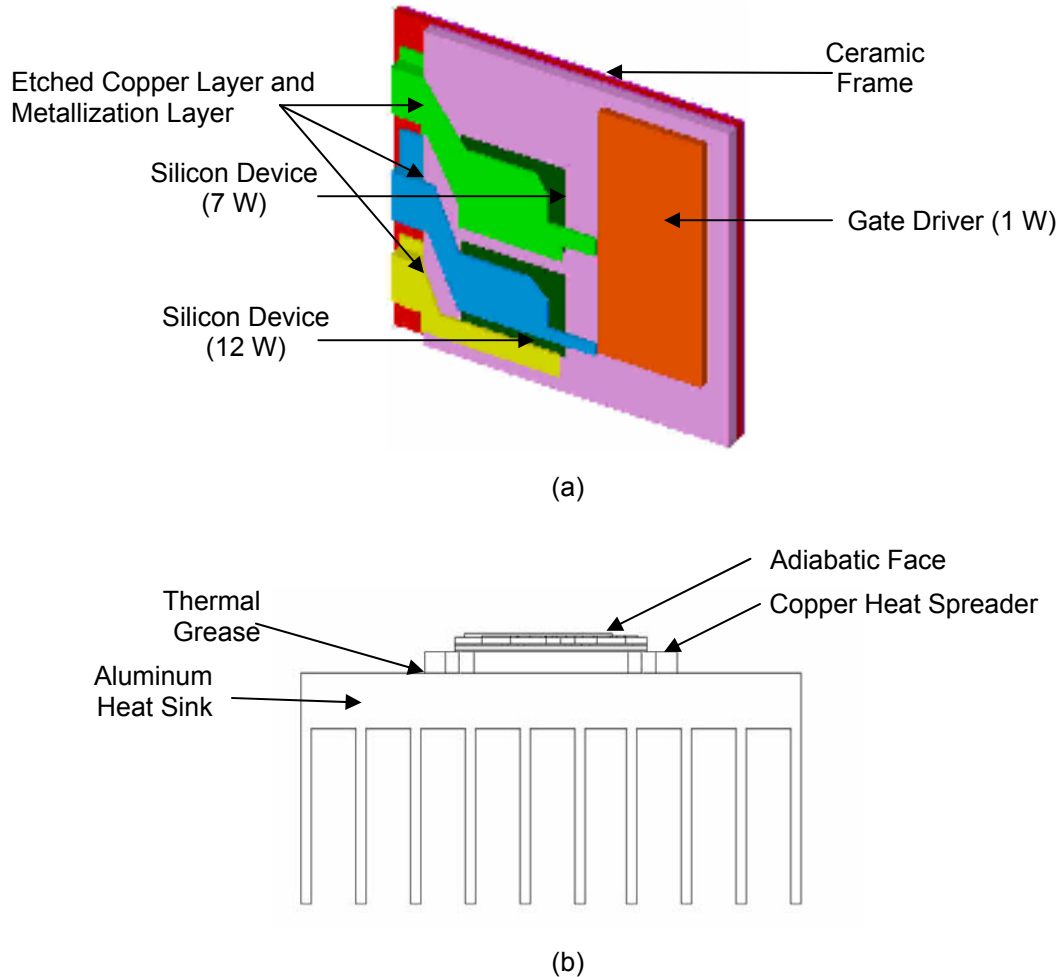


Figure 4.6 IPEM Model for the Thermal Analysis: (a) Details of the IPEM Model, and (b) Positioning of Components on Heat Sink

Table 4.2 Equivalent Thermal Resistance Value for All Relevant Interface Conditions in IPEM Model

| Interface Location | Equivalent Thermal Resistance Value (°C/W) |
|-----------------------------------|--|
| Silicon and Copper Trace | 0.04 |
| Silicon and Ceramic Frame | 25.70 |
| Gate Driver and Ceramic Frame | 0.50 |
| DBC Copper Base and Heat Spreader | 0.03 |
| DBC Copper Base and Heat Sink | 0.03 |
| Heat Spreader and Heat Sink | 0.07 |

Table 4.3 Thermal Conductivity Values for Materials Used in IPEM Model

| Material | Thermal Conductivity (W/m-K) |
|---|------------------------------|
| Copper | 395 |
| Aluminum | 164 |
| Ceramic—Aluminum Nitride (AlN) | 150 |
| Ceramic—Alumina (Al ₂ O ₃) | 26 |
| Solder | 51 |
| Thermal Grease | 1 |
| Silicone Gel | 0.2 |
| Epoxy | 1.4 |

4.4 Parametric Analysis

The purpose of the parametric analysis was to study the effects of the type of material and the thickness of certain layers on the thermal performance of the IPEM. Specifically the material used for the DBC ceramic layer was studied at different thicknesses, and the effects of changing the thickness of the heat spreader was investigated. Table 4.4 shows the parameters used in this study. All of the simulations in the parametric study were performed using ESC.

Each model was modeled with an optional heat spreader. It was assumed that there was a conduction path from the two heat sources to the copper trace to the DBC ceramic layer, and from the ceramic layer to the bottom copper layer (Figure 4.1). From there, it was assumed that the major heat flow paths involved conduction from the IPEM module to the heat spreader, conduction from the heat spreader to the heat sink, and convection from both the heat spreader and heat sink to the ambient air. Another heat path was from the gate driver to the ceramic frame, from the ceramic frame to a layer of gel, and from the gel to the DBC layer.

Table 4.4 Variables Used in Parametric Study

| Variable | Value | | | |
|-------------------------|--------------------------------|--------|--------|------|
| DBC Ceramic Material | Al ₂ O ₃ | AlN | | |
| DBC Ceramic Thickness | 15 mil | 25 mil | 40 mil | |
| Heat Spreader Thickness | 0 mm (none) | 1 mm | 3 mm | 5 mm |

4.5 Sensitivity and Uncertainty Analysis

Models and uncertainty go hand in hand. To determine the predictive uncertainty of various temperatures in the model, sensitivity and uncertainty studies were performed. As mentioned in Section 3.3, sensitivity analyses help increase the confidence in the model predictions and uncertainty analyses quantify the overall uncertainty in the model.

In this uncertainty analysis for the IPEM, we were able to identify several critical variables as shown in Figure 4.8. Power losses of both MOSFETs and all of the interface conditions were the critical input parameters. The interface conditions included the epoxy, solder, and the thermal grease. On the other hand, junction temperature, gate temperature, average temperature of the module, and the minimum heat sink temperature were the critical output parameters. In addition, we were also able to determine the uncertainty for each of these parameters. These uncertainties were based on the estimated measurement errors, listed in Table 4.4.

To determine the sensitivity of each input parameter, simulations based on one percent variation of the nominal were performed. Sensitivity coefficients for each of these parameters were calculated using Equations 3.1, 3.2, 3.3, and 3.4. Uncertainties for each parameter were calculated using Equation 3.5. Finally, the overall uncertainties on the critical output parameters were determined using Equation 3.6, and are shown in Table 4.5.

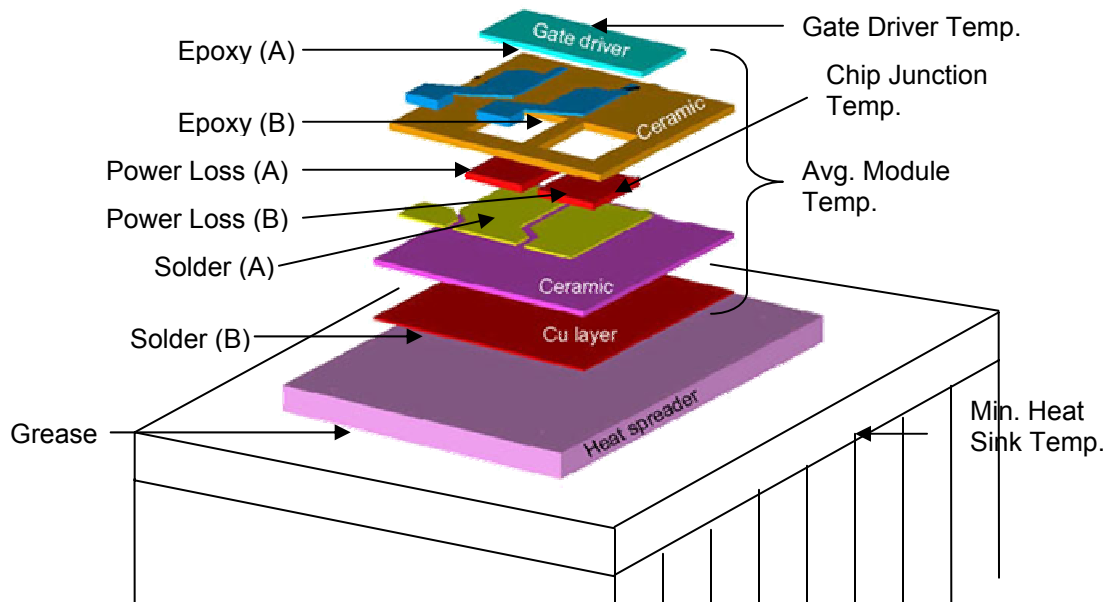


Figure 4.7 Location of Interest in IPEM for Sensitivity and Uncertainty Study

Table 4.5 Nominal Values and Measurement Uncertainty of Parameters Used in Sensitivity and Uncertainty Analysis

| Sensitivity Parameter, β_i | Nominal Value, β_{Ni} | Uncertainty, $\sigma_{\beta i}$ |
|---|-----------------------------|---------------------------------|
| Power Loss (A) | 7 W | +3 W |
| Power Loss (B) | 12 W | +3 W |
| Gate – Ceramic Frame, Epoxy (A) | 5 mil | ± 1 mil |
| MOSFETs – Ceramic frame, Epoxy (B) | 20 mil | ± 1 mil |
| MOSFETs – DBC Etched Copper Trace, Solder (A) | 5 mil | ± 1 mil |
| DBC Copper Layer – Heat Spreader, Solder (B) | 5 mil | ± 2 mil |
| Heat Spreader – Heat Sink, Grease | 5 mil | ± 1 mil |

Chapter 5

Results and Discussions

It is instructive to consider the thermal impact of various IPEMs designs since temperatures have always been the limiting factor in minimizing the size and optimizing the thermal performance of the IPEMs. Both the parametric, sensitivity and uncertainty studies discussed in Chapter 4 can give us insight on the thermal characteristics of the IPEMs. The results from these three studies are discussed and presented in this chapter. Based on these results, the most feasible electrical and thermal IPEM layout was determined. Finally, a discussion on solution convergence is also presented in this chapter.

5.1 Parametric Study

Ten cases were studied based on ten different possible layouts with the variation in the size of the IPEM, two different materials and three thicknesses of the DBC ceramic, and the option of using heat spreader with three different thicknesses. These variations are listed in Table 4.4. First, the thermal performance of the Gen-II.A and Gen-II.B IPEMs were compared. With the reduction of four percent in size and thirty percent reduction in the copper trace area from Gen-II.A to Gen-II.B, the Gen-II.B design resulted in a maximum temperature increase of almost 4°C. The Gen-II.B design also resulted in an overall average increase of almost 3°C over the Gen-II.A design as shown in Table 5.1. Figure 5.1 illustrates the steady-state temperature distributions of the Gen-II.A and Gen-II.B IPEMs.

The second phase of the thermal analysis involved a parametric study to identify the critical factors affecting the thermal performance of Gen-II.B IPEM. Based on the variables identified in Table 4.4, we were able to study eight different cases. With Gen-II.B set as the base model, each of these cases is modification of the Gen-II.B IPEM. The results from these cases are also shown in Table 5.1. The maximum temperatures in the

MOSFETs, the gate driver, and the overall module average temperature are provided for each case. These temperatures are referred to as the “critical temperatures” in the following discussion.

Table 5.1 Summary of the Thermal Simulation and the Parametric Study

| IPEM Model | IPEM Size (mm ²) | Ceramic Materials | DBC Ceramic Thickness (mm) | Heat Spreader (HS) Thickness (mm) | Max. MOSFET Temp. (°C) | Max. Gate Temp. (°C) | Avg. Module Temp. (°C) |
|-------------------------------------|------------------------------|--------------------------------|----------------------------|-----------------------------------|------------------------|----------------------|------------------------|
| Base Models | | | | | | | |
| Gen-II.A | x ¹ | Al ₂ O ₃ | 0.635 (25 mil) | NA | 92.2 | 87.4 | 88.1 |
| Gen-II.B | y ² | Al ₂ O ₃ | 0.635 (25 mil) | NA | 95.9 | 93.2 | 90.7 |
| Gen-II.B Modifications | | | | | | | |
| Case 1 (AIN) | y ² | AlN | 0.635 (25 mil) | NA | 94.4 | 92.2 | 90.1 |
| Case 2 (15 mil DBC) | y ² | Al ₂ O ₃ | 0.381 (15 mil) | NA | 95.9 | 93.1 | 90.6 |
| Case 3 (40 mil DBC) | y ² | Al ₂ O ₃ | 1.016 (40 mil) | NA | 96.0 | 93.3 | 90.8 |
| Case 4 (1 mm HS) | y ² | Al ₂ O ₃ | 0.635 (25 mil) | 1 | 88.7 | 87.7 | 84.2 |
| Case 5 (3 mm HS) | y ² | Al ₂ O ₃ | 0.635 (25 mil) | 3 | 89.3 | 88.7 | 85.8 |
| Case 6 (5 mm HS) | y ² | Al ₂ O ₃ | 0.635 (25 mil) | 5 | 89.7 | 89.6 | 86.2 |
| Case 7 (AlN ₃ + 5 mm HS) | y ² | AlN | 0.635 (25 mil) | 5 | 88.3 | 88.4 | 85.6 |
| Case 8 (5 mm HS +Centered) | y ² | Al ₂ O ₃ | 0.635 (25 mil) | 5 | 89.7 | 89.8 | 86.5 |
| ¹ x = 26.9 mm × 30.0 mm; | | | | | | | |
| ² y = 28.5 mm × 27.3 mm | | | | | | | |

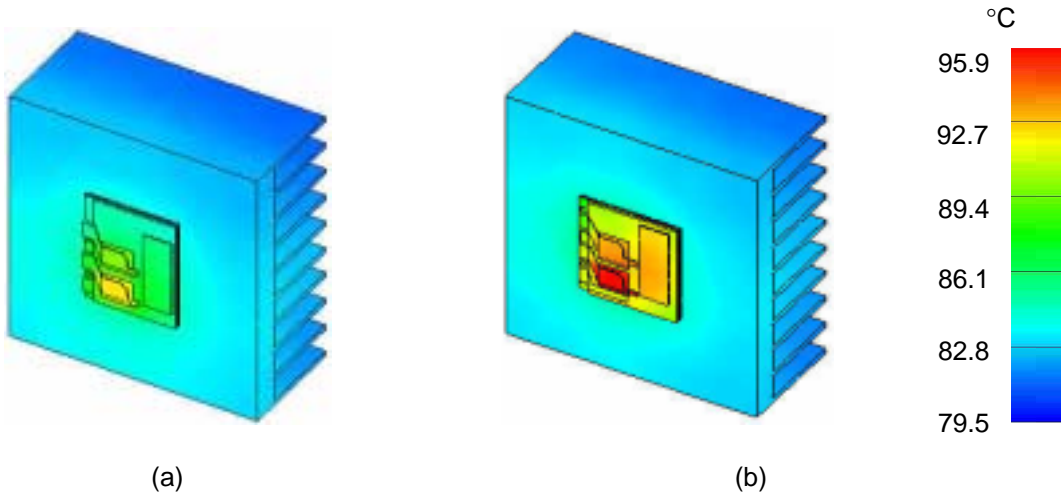


Figure 5.1 Steady-state Temperature Distributions for: (a) Gen-II.A, and (b) Gen-II.B

In Case 1, instead of aluminum oxide, aluminum nitride was used as the DBC ceramic material. The critical temperatures improved up to 1.5°C compared to those from the Gen-II.B IPEM. Although the thermal conductivity of aluminum nitride is at least six times higher than aluminum nitride, the improvement in the thermal performance of the IPEM was relatively small. This was because the reduction in the etched copper trace area reduced the total heat transfer area from the etched copper trace to the DBC ceramic layer. This ultimately reduced the effectiveness of heat spreading in the DBC ceramic layer.

To compare the thermal performance of IPEM using different thicknesses of DBC ceramic layer, Case 2 and 3 were presented. Results from a 15-mil (0.381 mm) layer thick (Case 2) and a 40-mil (1.016 mm) layer thick (Case 3) were compared to the 25-mil (0.635 mm) layer of the Gen-II.B case. Theoretically, the thinner the layer is, the smaller the thermal resistance across the layer. Nevertheless, the simulation results show that increasing the DBC ceramic thickness decreases the performance only minimally. Therefore, reliability issues and cost factors became the guidelines of selecting the desired thickness. Case 3 was not chosen as the desired thickness due to cost factors associated with the increase in the thickness. Since a 15-mil (0.381 mm) layer thick DBC

ceramic provided a less reliable structure than a 25-mil (0.635 mm) DBC ceramic, Case 2 was also eliminated.

To achieve the best design, we realize that there are trade-offs between the electrical, thermal, and practical considerations. Results of the electrical analyses are described in [10]. In the electrical analyses, both the reducing the trace area and increasing the ceramic layer thickness were found to substantially increase electrical performance. On the other hand, the choice of material (Al_2O_3 or AlN) had only a moderate effect on the electrical performance as shown in Figure 5.2. When using aluminum oxide as DBC ceramic material, electrical performance increases as the thickness of the DBC ceramic increases. On the other hand, the thermal performance decreases as the thickness of the DBC ceramic increases, all be it only slightly. Since the thickness of the DBC ceramic does not influence the thermal performance dramatically, we then compared the costs and the electrical performances of different thicknesses of the DBC ceramic.

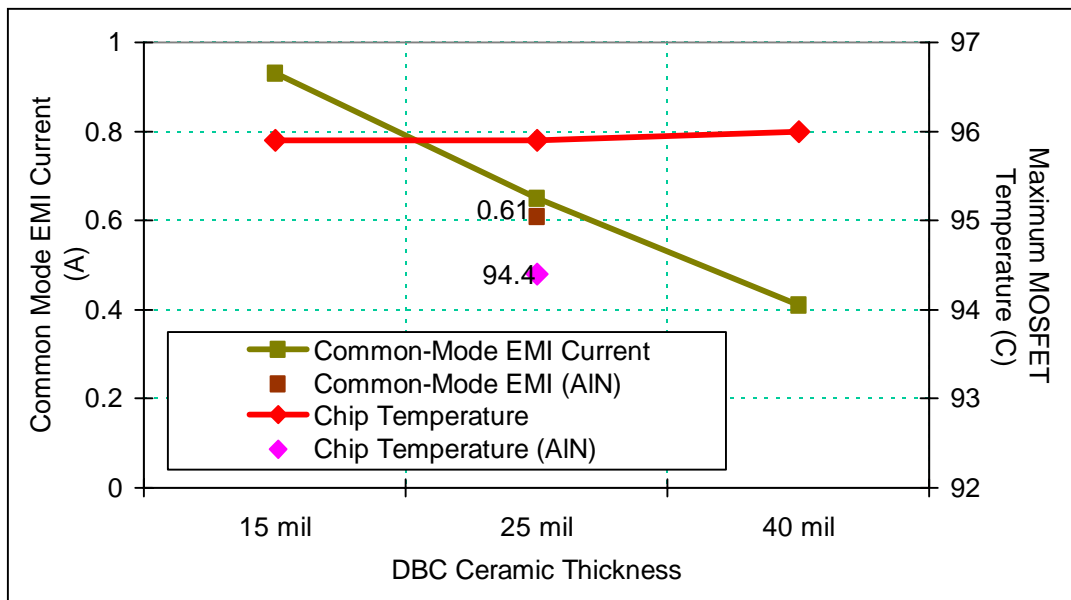


Figure 5.2 Trade-offs Between Electrical and Thermal Performance for Different DBC Ceramic Thicknesses

Figure 5.3 shows the costs and the electrical performances of three different DBC ceramic thicknesses. The cost of the DBC ceramic drops from 15-mil to 25-mil and increases from 25-mil to 40-mil DBC ceramic. Meanwhile, the electrical performance increases as the thickness of the DBC ceramic increases. With the fact that the change in the costs is more significant than the improvement in the electrical performance, we chose 25-mil (0.635 mm) as the DBC ceramic thickness.

Also shown in Figure 5.2 are the common mode current and the maximum MOSFET temperature for the case where 25-mil (0.635 mm) aluminum nitride DBC ceramic was used in electrical and thermal simulations. The aluminum nitride ceramic material proved to be more beneficial in both electrical and thermal performance, although this improvement was relatively small. In addition, the high-cost of the aluminum nitride material illustrated in Figure 5.4 makes the selection of aluminum nitride as the ceramic material impractical at this moment since our goal is to achieve a low cost and reliable IPEM. The costs shown in Figure 5.4 is based on the order volume of 50 pieces of DBC ceramic.

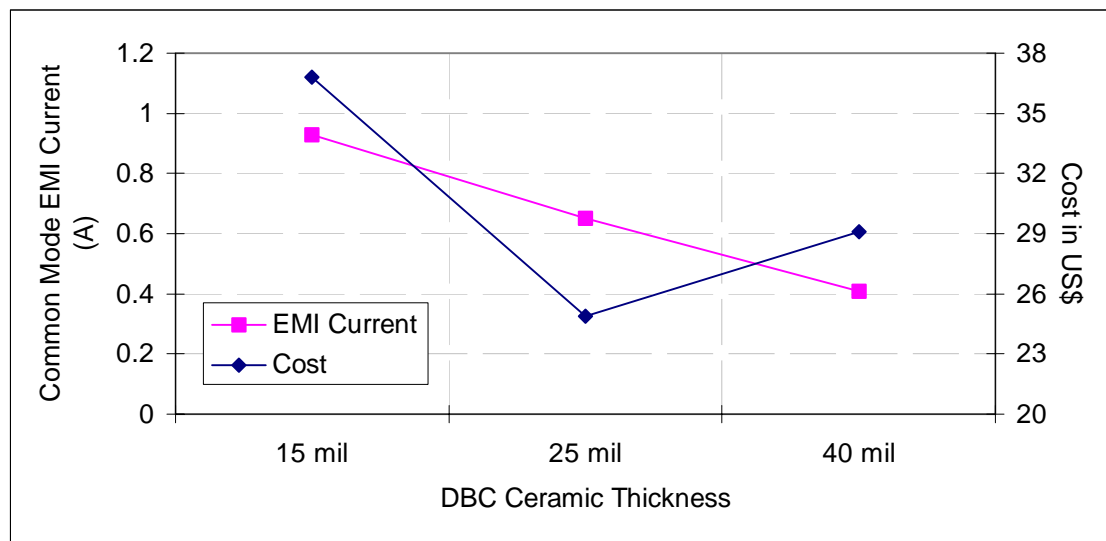


Figure 5.3 Trade-offs Between Cost and Electrical Performance for Different DBC Ceramic Thicknesses

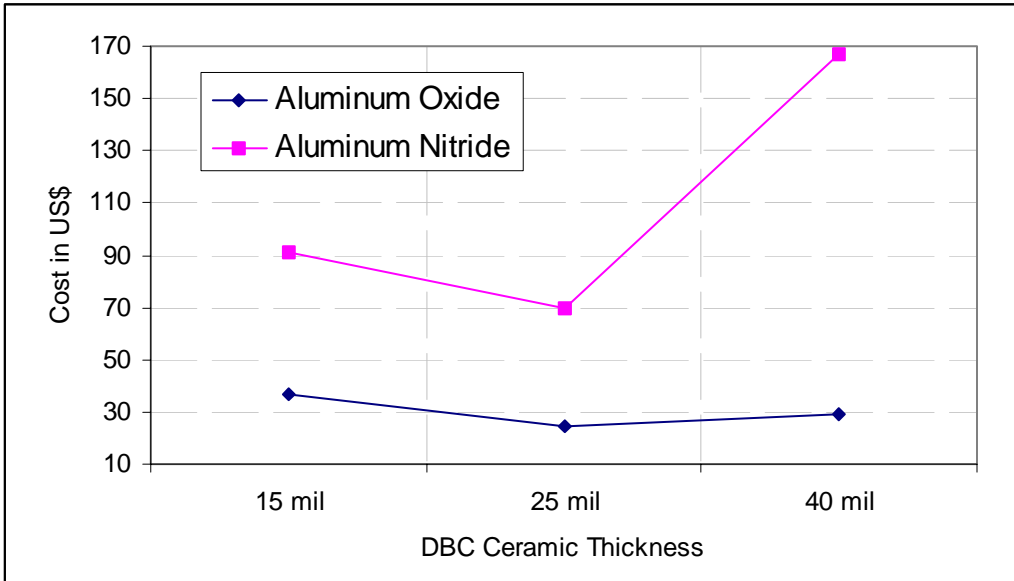


Figure 5.4 Comparison of Cost for Different DBC Ceramic Materials at Different Thicknesses [56]

Based on the previous discussion, a 25-mil (0.635 mm) aluminum oxide DBC ceramic was chosen for the design. To further study other possibilities for improving the Gen-II.B design, a heat spreader was added to the design. The results for Cases 4-8 in Table 5.1 show that the use of a heat spreader greatly improved the thermal performance of the IPEM. Without heat spreader, the maximum temperature of the MOSFET was between 94°C and 96°C. With heat spreader, all of the critical temperatures in the IPEM dropped below 90°C. Thus, we recommended adding the copper heat spreader to the module.

Cases 4-6 listed in Table 5.1 are the results for a 1 mm, 3 mm, and 5 mm thick copper heat spreader. These results show that the critical temperatures increase with the increase in the thickness of the heat spreader. Figure 5.5 shows that the maximum MOSFET temperature increases as the heat spreader thickness increases. However, the

effect is relatively small. The maximum MOSFET temperatures in these three cases changed within 1°C although the thickness of the heat spreader increased from 1 mm to 5 mm. The temperature rise here is small since the material is copper. As a result, the heat spreader hindered the heat transfer slightly due to the added resistance layer. On the other hand, the addition of the heat spreader was significant as it promoted heat transfer by providing a large conductive surface to dissipate heat.

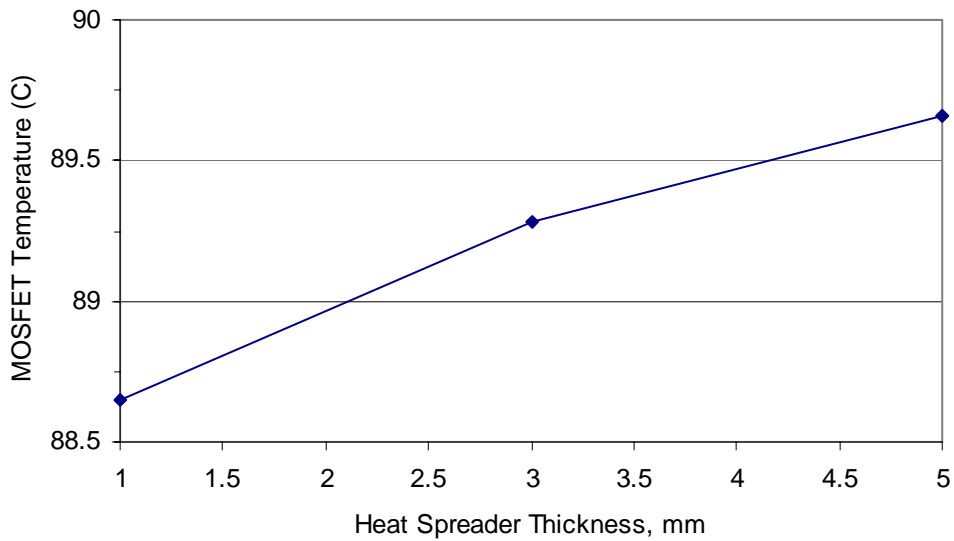


Figure 5.5 Effect of Heat Spreader Thickness on Maximum Temperature of Gen-II IPEM

Again, reliability issues and cost factors became the guidelines of selecting the desired thickness of the copper heat spreader. We believed that a 1 mm thick heat spreader provided a less reliable structure than a 3 mm thick or a 5 mm thick heat spreader. Therefore, the 1 mm heat spreader was not selected as the desired thickness for the heat spreader. On the other hand, we believed that a 3 mm thick heat spreader could provide a better structural stability with less deformation during the period of operation. The 5 mm thick heat spreader also did not show a significant improvement in thermal performance compared to the 3 mm thick heat spreader. Hence, the 5 mm thick heat spreader also was not chosen as the desired thickness due to the cost factors associated with the increase in the thickness.

Listed in Table 5.1, Case 7 was the modification of Case 6 by changing the DBC ceramic material from aluminum oxide to aluminum nitride. In this case, the results show that the critical temperatures were improved to about 1°C compared to Case 4-6. Although Case 7 performed better among these four cases (Case 4-7), Case 7 was not selected as the best design since the cost of aluminum nitride is about five times higher than aluminum oxide which was not warranted with the slight improvement in thermal performance. Thus, a 3 mm thick heat spreader (Case 5) was selected as the desired heat spreader thickness for the IPEM.

In looking at the temperature distribution on the heat spreader for Case 6 (Figure 5.6a), it was evident that the heat flow was asymmetric. This prompted a modification to increase the effectiveness of the heat spreader. To investigate an additional possible layout, the heat sources in Case 6 were placed at the center of the heat spreader. This modification in Case 6 was then listed as Case 8 in Table 5.1. Figure 5.7 shows the steady-state temperature distributions for Case 6 and Case 8. It was surprising to see that Case 8 did not show any improvement in thermal performance over Case 6. Although the resulting temperature distribution is more symmetrical, the MOSFET temperature was unchanged and the gate driver temperature slightly increased (Table 5.1). The effect of centering the heat sources at the heat spreader can be seen in Figure 5.6b. However, both cases still showed better thermal performance over the base model—Gen-II.B design.

Although the simulation results revealed that the heat was being effectively distributed from the MOSFETs by using heat spreader, the heat distribution from the gate driver appeared to be poor. Therefore, the gate driver became the limiting factor in the thermal analysis although it has only 1 W of power loss. Thus, there is a need for future detailed analyses of the gate driver.

Finally, we achieved a final design layout identified as Generation II.C (Gen-II.C), which is also Case 5 listed in Table 5.1. The specifications for the Gen-II.C IPEM are listed in Table 5.2. Gen-II.C has a 4% smaller footprint than Gen-II.A, and a 30% smaller etched copper trace area. In addition, it has a significantly lower junction temperature and gate temperature than the Gen-II.B IPEM.

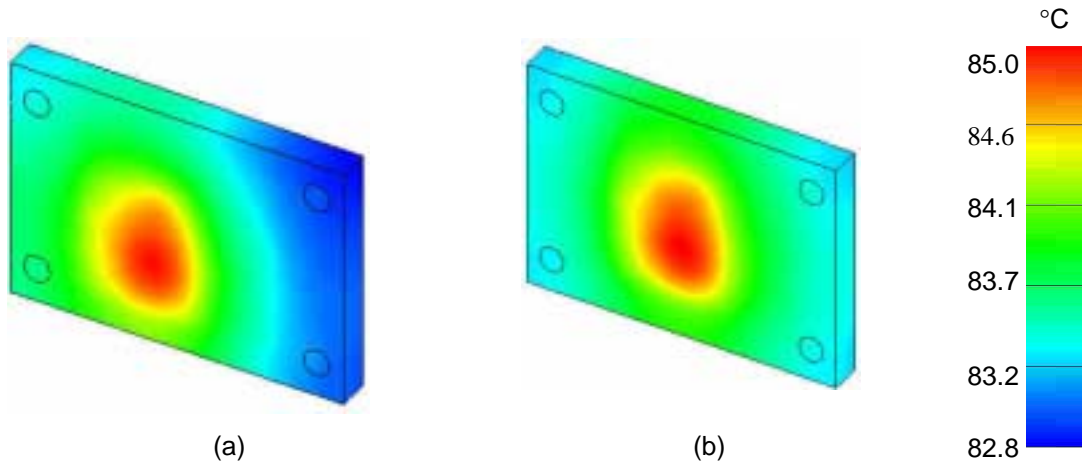


Figure 5.6 Steady-state Temperature Distributions on the Heat Spreaders for: (a) Case 6 and, (b) Case 8

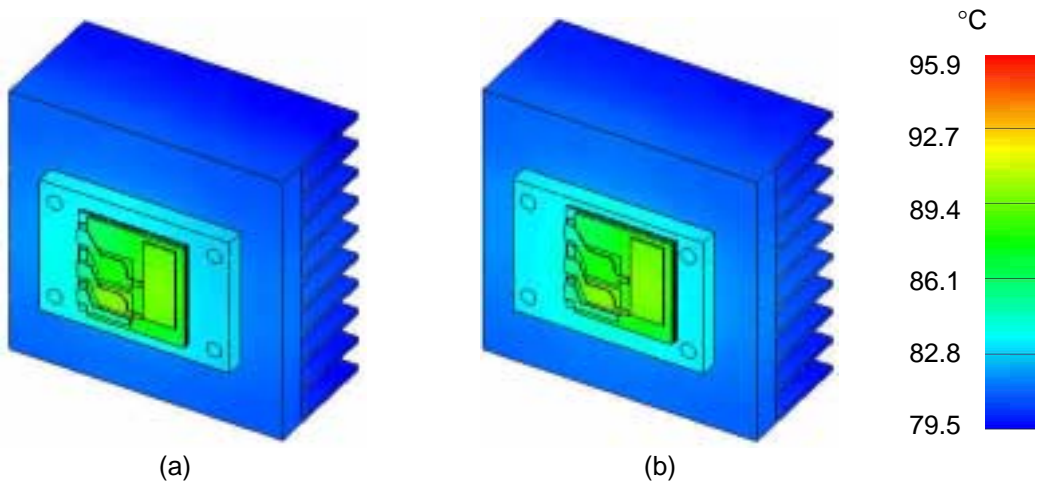


Figure 5.7 Steady-state Temperature Distributions for: (a) Case 6, and (b) Case 8

Table 5.2 Specifications for Gen-II.C IPEM

| | |
|--------------------------------|---|
| IPEM Size | 28.5 mm x 27.3 mm (778.05 mm ²) |
| DBC Ceramic Material | Aluminum Oxide (Al_2O_3) |
| DBC Ceramic Thickness | 25 mil (0.635 mm) |
| Copper Heat Spreader Thickness | 3 mm |

5.2 Sensitivity and Uncertainty Analysis

Following the analysis method discussed in Section 4.5, the Gen-II.B IPEM with a 5 mm thick heat spreader (Case 6) was chosen as the model for all of the uncertainty analyses. Sensitivity coefficients based on each of the critical input parameters were calculated using Equation 3.1. Figure 5.8 shows the sensitivity coefficients calculated for each of the critical output variables. The critical output variables are the gate driver temperature, the chip junction temperature, the average module temperature, and the minimum heat sink temperature. In addition, the critical input parameters are Epoxy A, Epoxy B, Power Loss A, Power Loss B, Solder A, Solder B, and Grease. Since this study focused only on the module itself without concerning the effect of the convection from

the heat sink, the fluid flow and convection heat transfer parameters were not considered as the sensitivity parameters. The most sensitive input parameter is the thickness of Solder B illustrated in Figure 4.7. The sensitivity of the Solder B is well over three times higher than that of the other parameters. Power Loss B, 12 W heat dissipation at the outermost MOSFET, is ranked as the second most sensitive parameter, followed by Power Loss A. The variation in the other parameters is considered to be insignificant in all cases.

Using the sensitivities in Figure 5.8 and the measurement uncertainties shown in Figure 5.9, the predicted uncertainty of each parameter was calculated as shown in Figure 5.10. The results show that the thickness of Solder B contributed the highest uncertainty in the IPEM model followed by Power Loss B and Power Loss A. Again, the uncertainty in the other parameters is considered to be insignificant in all cases. Figure 5.11 shows the overall uncertainty for each of the critical output variables. The results were calculated using Equation 3.6. Based on the results obtained, the overall uncertainty associated with the thermal model can be characterized using Equation 3.6 at Section 3.3. The MOSFET temperature has the highest uncertainty of 8°C followed by the average temperature of IPEM. The minimum heat sink temperature has the least uncertainty among the four investigated temperatures.

This analysis indicates the importance of developing methodologies to accurately estimate power losses and interface conditions. With the improvements in estimating these critical input variables, the simulation results are expected to lie within the true results with smaller error margins.

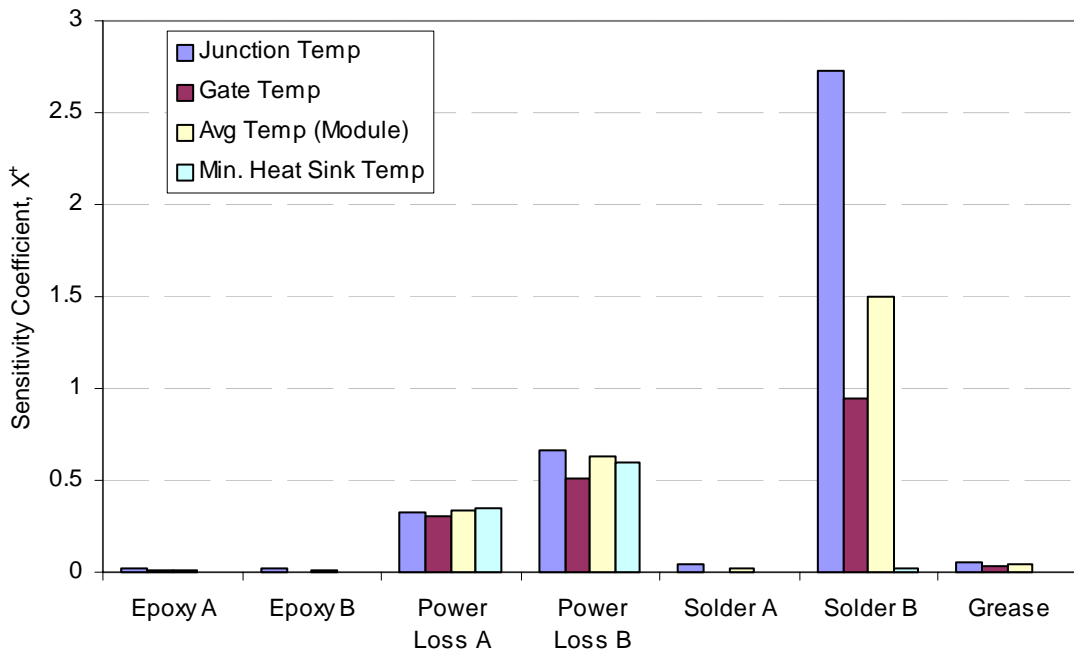


Figure 5.8 Sensitivity Coefficients for Each Critical Input Parameter on Each of the Critical Output Variable

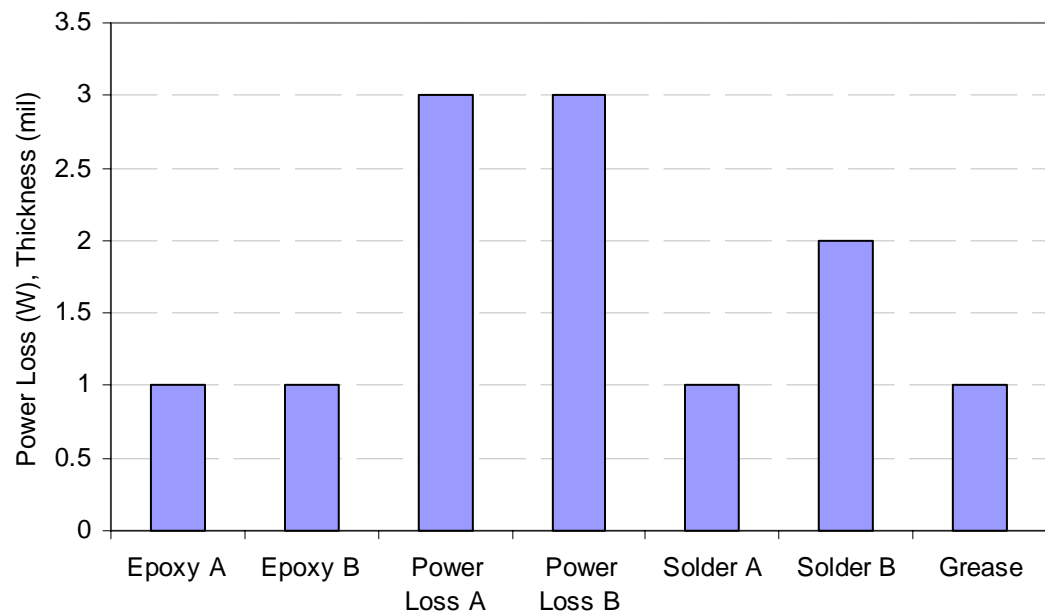


Figure 5.9 Measured Uncertainty for Each Critical Input Parameter

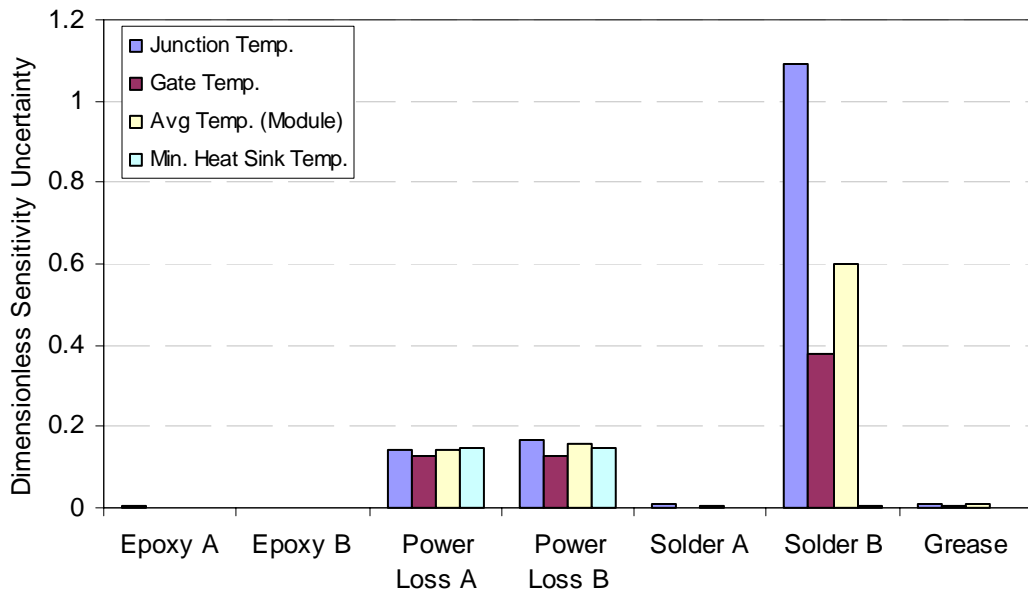


Figure 5.10 Dimensionless Sensitivity Uncertainty, σ^+ , for Each Critical Input Parameter on Each of the Critical Output Variable

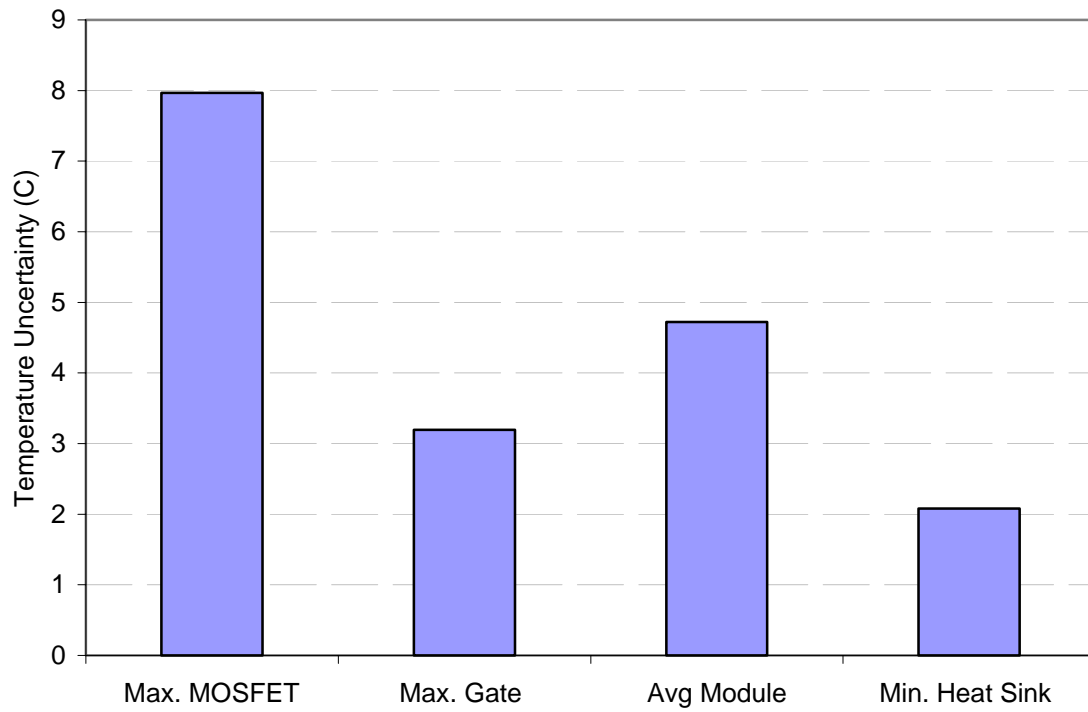


Figure 5.11 Overall Uncertainty for Each Critical Output Variable

5.3 Solution and Results Convergence

In order to perform a confident numerical analysis, one has to understand how the solvers and convergence work in the numerical code. There are usually two types of convergence: solution convergence and results convergence. Solution convergence is the convergence of the mathematical model that was sent to the solver. Convergence differs by type of solution, but generally is when a change between subsequent iterations is within a tolerance. In general, the mesh size can have some effect. The greater the local gradient, the more problems there can be with convergence. More elements will assist the solver to achieve quicker convergence as far as number of iterations. This concept is very solver dependent.

Results convergence is the convergence of the solution to the FEM when compared to reality. When an FE model is built, the solid model is discretized into many connected elements each representing a local polynomial representing the local volume. An infinite number of elements will give a precise solution. By reducing the elements from infinity to a realistic number, some accuracy will be lost. It is up to the analyst to determine what difference between an infinite solution and the realistic solution is acceptable [19]. In addition, the analyst should be aware of the type of solution being performed, either h-element method or p-element method.

There is no universal guide for mesh sizes. It is more of a learned art form than some standard rules. In practical terms, the model is first meshed with a coarse mesh, then with a finer mesh. The analyst will have to solve the FE models, compare the results, refine the mesh and solve the model again. This process continues until the solution does not change. With experience and knowledge of the part, an analyst may eliminate the above and start with a sufficiently refined mesh.

Chapter 6

Conclusions and Recommendations

The most reliable and well-designed electronic device can malfunction or fail if it overheats. Good thermal design is often paramount in achieving high reliability, low manufacturing cost, small size and a predictable development time. The thermal design must be able to dissipate the maximum amount of power required to maintain operating T_{junction} within limit. Thus, thermal design is an important aspect in the overall production design process to achieve the desired operational and reliability objectives for the product. In this research, we managed to achieve a few goals discussed in Section 1.3. The contributions of this thesis are discussed in the following.

Validation of thermal modeling method. Numerical modeling is always the fastest and easiest way of analyzing the thermal performance of electronic systems. However, it is always advisable to validate the method of modeling in order to have certain confidence in the numerical results. To validate the method of performing thermal analysis using I-DEAS, both numerical analysis and experimental work were performed using two discrete power electronics components. Results of adequately meshed numerical models were compared to experiment results. Both the numerical and the experimental results showed a good agreement of within 1.5°C in the temperature distribution. In addition, the margin errors of simulation results were within the margin errors of experimental data.

Achievement in new IPEM design layout. With the achievements in performing thermal analysis using discrete components, a technique to predict the temperature field within the IPEMs was presented to assist the future power electronics research in module level thermal analysis. In early stage of IPEM design, thermal issues were recognized and were brought to the designer's attention. The thermal analyses allowed thermally optimized IPEM to be utilized in non-optimized systems. A two-step integrated design strategy was employed to improve the thermal and electrical performance of an IPEM design. The analyses involved parametric study to achieve a new design, which was identified as Gen-II.C. Having a 4% and 30 % reduction in the overall size and copper trace area, Gen-II.C IPEM is an improved thermal and electrical model from Gen-II.A

IPEM. In summary, we implemented the two-step integrated design strategy successfully to redesign the existing Gen-II.A IPEM. The final design, Gen-II.C IPEM, provided a 3°C reduction in the maximum temperature over Gen-II.A, thus providing an increase in the overall thermal performance.

Cost and reliability factors in choosing DBC ceramic layer. The thermal analysis demonstrated that the choice of material and thickness of the DBC ceramic layer had only a moderate effect on the thermal performance. However, aluminum nitride would be a better choice than aluminum oxide if the costs could be justified.

Effect of additional heat spreader. The thermal analysis also showed that the addition of the copper heat spreader had a significant improvement on the thermal performance. In addition, it was found that the heat dissipation from the gate driver is poor. Hence, it is recommended that the design of the gate driver be revised to help improving the thermal performance of the IPEM in the future.

Importance of accurate input parameters in thermal modeling. The sensitivity analysis demonstrated the importance of accurate input parameters. To accurately perform numerical analysis, it is important to know the most sensitivity parameter in the model. This study shows that more accurate methodologies are needed to estimate the interface conditions and the power loss in particular. Solder B, which is the interface between the DBC copper layer and the copper heat spreader, was the most sensitive input parameter among the seven input parameters. In addition, the MOSFET temperature shows an uncertainty of 8°C.

Future power dissipation trend in IPEMs. In all the cases we have studied in Chapter 4, the maximum temperatures of IPEMs do not exceed the limit of the specified junction temperature, 125°C. However, with the continual achievement of Moore's prediction and the continuous increase in power densities of the future semiconductor devices as discussed in Section 1.1, the power density of IPEMs can also increase from 26 KW/m² to 75 KW/m² over the years where the junction temperature of the IPEMs could be over 125°C. Therefore, other possible methods of improving the thermal performance of the IPEM should be investigated in the future. These include using better thermal conductivity materials for the silicon die and the interface materials,

implementing different cooling strategies such as improved heat sink design and active cooling techniques.

References

- [1] Agonafer, D. and Free, J. A., “Conjugate Model of a Pin-Fin Heat Sink Using a Hybrid Conductance and CFD Model Within an Integrated MCAE Tool,” <http://www.mayahtt.com/expertise/papers/index.asp> (Leuren, Belgium: EUTHERM, 1995).
- [2] Agonafer, D. and Free, J. A., “Numerical Modeling of an Entire Thermal Conduction Module using a Thermal Coupling Methodology,” <http://www.mayahtt.com/expertise/papers/index.asp> (San Francisco, CA: ASME International Mechanical Engineering Congress, 1995).
- [3] Ansoft Corporation, “Maxwell 3D,” <http://www.ansoft.com/products/em/max3d/> (Pittsburg, PA: Ansoft Corporation).
- [4] Azar, K., “The History of Power Dissipation,” http://www.electronics-cooling.com/html/2000_jan_a2.html (Southborough, MA: Electronics Cooling, 2000).
- [5] Azar, K., “Managing Power Requirements in the Electronics Industry,” http://www.electronics-cooling.com/html/2000_dec_a1.html (Southborough, MA: Electronics Cooling, 2000).
- [6] Bar-Cohen A., and Kraus A.D., *Advances in Thermal Modeling of Electronic Components and Systems*, Vol. 3 (New York: ASME Press and IEEE Press, 1993).
- [7] Bejan, A., *Convection Heat Transfer*, 2nd edition (New York: Wiley, 1995).
- [8] Borealis Exploration Limited, “The Science Behind Cool Chips,” <http://www.coolchips.gi/technology/overview.shtml> (Gibraltar: Borealis Exploration Limited).
- [9] Borealis Exploration Limited, “Cool Chips Technical Description—Technology Introduction,” <http://www.coolchips.gi/slides/tech/frame03.html> (Gibraltar: Borealis Exploration Limited).
- [10] Chen, J., Pang, Y. F., Boroyevich, B., Scott, E. P., and Thole, K. A., “Electrical Layout Design Considerations for Power Electronics Modules,” to be presented at the 37th Annual IAS Meeting, Pittsburg, PA, Oct. 13-18, 2002.
- [11] Chu, R. C. and Chrysler, G. M., “Recent Development of Cooling Technology and Thermal Design for Leading-Edge Electronic Products,” *International Journal of Transport Phenomena*, Vol. 1, 1998, pp. 31-40.

- [12] Culham, J. R., Lemczyk, T. F., Lee, S., and Yovanovich, M. M., Meta – “A Conjugate Heat Transfer Model For Air Cooling of Circuit Boards With Arbitrarily Located Heat Sources,” *1991 ASME National Heat Transfer Conference, Heat Transfer In Electronic Equipment*, HTD-Vol. 171, pp. 117.
- [13] Cullimore, B. A., “Dealing with Uncertainties and Variations in Thermal Design,” *Proceedings of IPACK’01 ASME International Electronic Packaging Technical Conference and Exhibition*, Vol. 2, 2001, pp. 639-646.
- [14] Cullimore, B. A., Johnson, D. A. and Welch, M. J., “Novel Simulation Techniques for Design of Air-cooled Electronics,” *Proceedings of IPACK’01 ASME International Electronic Packaging Technical Conference and Exhibition*, Vol. 2, 2001, pp. 647-652.
- [15] Electric Power Institute, “Power Electronics Reference Guide,” <http://www.epri.com> (Palo Alto, CA: EPRI).
- [16] Elshabini, A., “Low Cost Power Electronics Packaging,” http://www.imaps.org/adv_micro/2001jul_aug/1.html (Washington, D.C.: IMAPS, 2001).
- [17] Eupec Inc., “Econopack+—A New IGBT Module for Optimized Inverter Solutions,” http://www.eupec.com/p/e/pdf/ed_pcim_2000_bostonf.pdf (Nurembug, Germany: Eupec Inc.)
- [18] Ferdowsi, A. and Viskanta, R., “Analysis of Conjugate Heat Transfer in a Three-dimensional Microchannel Heat Sink for Cooling of Electronic Components,” *International Journal of Heat and Mass Transfer*, Vol. 3, 1999, pp. 89-97.
- [19] Florence, J., Senior Customer Applications Engineer of I-DEAS and FEMAP CAE Team (Milford, OH: 25 April 2002), email to Ying-Feng Pang.
- [20] Free, J. A., Russell, R. and Louie J., “Recent Advances in Thermal/Flow Simulation: Integrating Thermal Analysis into the Mechanical Design Process,” *Proceedings of 11th Semiconductor Thermal Measurement and Management Symposium*, 1995, pp. 136-145.
- [21] Fuji Semiconductor, Inc., “Power Module IPM,” http://www.fujielectric.co.jp/eng/denshi/scd/prod_pm.html (Saddle Brook, NJ: Fuji Semiconductor, Inc.).
- [22] Fusaro J. M., Romero G. L., Rodriguez P. and Martinez, J. L. Jr., “Thermal Characterization of DBC and MMC Stacks for Power Modules,” *31st Industry Applications Conference Proceeding*, Vol. 3, 1996, pp. 1411-1417.

- [23] Gauche, P. and Xu, W., “Modeling Phase Change Material in Electronics Using CFD-A Case Study,” *Proceedings of 2000 International Conference on High-Density Interconnect and Systems Packaging, Denver, Colorado*, 2000, pp. 402-407.
- [24] Incropera, F. P. and DeWitt D. P., *Fundamentals of Heat and Mass Transfer*, 4th edition (New York: Wiley, 1995).
- [25] Intel Corporation, “Moore’s Law,”
<http://www.intel.com/research/silicon/mooreslaw.htm> (Santa Clara, CA: Intel Corporation).
- [26] IXYS Corporation, “Discrete MOSFETs—Standard N-Channel Types,”
<http://www.ixys.com/Appasp/pdmfet01.asp> (Santa Clara, CA: IXYS Corporation).
- [27] Kim, S. J. and Lee, S. W., *Air Cooling Technology for Electronic Equipment*, (New York: CRC Press, 1996).
- [28] Kreith, F. and Bohn, M. S., *Principles of Heat Transfer*, 6th edition (California: Brooks/Cole, 2001).
- [29] Kristiansen, H., “Thermal Management in Electronics,”
http://www.ppd.chalmers.se/edu/mpr235/mpr235_thermgmnt.pdf (Göteborg, Sweden: Chalmers University of Technology, 2001).
- [30] Lasance, C. J. M., “The Conceivable Accuracy of Experimental and Numerical Thermal Analyses of Electronic Systems,” *17th IEEE SEMI-THERM Symposium*, 2001, pp. 180-198.
- [31] Lasance, C. J. M., “The Need For A Change In Thermal Design Philosophy,” Electronics Cooling, October 1995, http://www.electronics-cooling.com/Resources/EC_Articles/OCT95/oct95_04.htm (Southborough, MA: Electronics Cooling, 1995).
- [32] Liang, Z. X. and Lee, F., “Embedded Power Technology for IPMs Packaging Applications,” *16th Applied Power Electronics Conference and Exposition (APEC)*, 2001, Vol. 2, 2001, pp. 1057-1061.
- [33] Linton, R. L. and Agonafer, D., “Coarse & Detailed CFD Modeling of a Finned Heat Sink,” *Proceedings of 1994 Intersociety Conference on Thermal Phenomena in Electronic Systems*, 1994, pp. 156-161.
- [34] MatWeb, “MatWeb, Your Source for Materials Information,”
<http://www.matweb.com> (Christiansburg, VA: MatWeb).

- [35] Moffat, R. J., "Describing the Uncertainties in Experimental Results," *Experimental Thermal and Fluid Science*, Vol. 1, 1988, pp. 3-17.
- [36] Moffat, R. J., "Using Uncertainty Analysis in the Planning of an Experiment," *ASME Journal of Fluids Engineering*, Vol. 107, 1985, pp. 173-178.
- [37] Nelson, D. J. and Creel, K. E., "Criteria for Approximating a Layer in Three-Dimensional Thermal Models of Multilayer Microelectronics," *Proceedings of 1994 Intersociety Conference on Thermal Phenomena in Electronic Systems*, 1994, pp. 207-213.
- [38] Normington, P. J. C., Mahalingam, M. and Lee, T. Y., "Thermal Management Control Without Overshoot Using Combinations if Boiling Liquids," *1992 Intersociety Conference on Thermal and Thermomechanical Phenomena in Electronic Systems Proceeding*, 1992, pp. 49-58.
- [39] Ogiso, Ken, "Estimation of An Overall Cooling Performance In Electronics Thermal Design (The Case of Forced Convection)," *Advances in Electronic Packaging* 1997, Vol. 2, 1997, pp. 1989-1994.
- [40] Ohbu, T., Kodani, K., Tada, N., Matsumoto, T., Kijima, K. and Saito, S, Toshiba Corporation, "Study of Power Module Package Structures," *International Workshop Integrated Power Packaging*, 2000, pp. 46-50.
- [41] Ozmat, B., Korman, C. S., McConnelee, P., Kheraluwala, M., Delgado, E. and Fillion, R., "A New Power Module Packaging Technology For Enhanced Thermal Performance," *2000 Intersociety Conference on Thermal and Thermomechanical Phenomena in Electronic Systems Proceeding*, Vol. 2, 2000, pp. 287-296.
- [42] Pais, M. R., Leland, J. E., Chang, W. S., "Single-Phase Heat Transfer Characteristics of Submerged Jet Impingement Cooling Using JP-5," *1994 Intersociety Conference on Thermal and Thermomechanical Phenomena in Electronic Systems Proceeding*, 1994, pp. 178-183.
- [43] Pak, B. C., Chun, W. C., Baek, B. J. and Copeland, D., "Forced Air Cooling By Using Manifold Microchannel Heat Sinks," *Advances in Electronic Packaging* 1997, Vol. 2, 1997, pp. 1837-1842.
- [44] Peeples, J. W., "Vapor Compression Refrigeration for High Performance Applications," http://www.electronics-cooling.com/html/2001_august_a1.html (Southborough, MA: Electronics Cooling, August 2001).
- [45] Rizzo, T., "Safety Tips and Techniques for FEA in Modeling Solids," http://www.electronics-cooling.com/Resources/EC_Articles/JUN95/jun95_02.htm (Southborough, MA: Electronics Cooling, June 1995).

- [46] Sarno, C. and Moulin, G., “Thermal Management of Highly Integrated Electronic Packages-in Avionics Applications,” <http://www.electronics-cooling.com> (Southborough, MA: Electronics Cooling, August 2001).
- [47] Schmidt, R. R., “Thermal Management of Office Data Processing Centers,” *Advances in Electronic Packaging* 1997, Vol. 2, 1997, pp. 1995-2010.
- [48] Semikron International, “Integrated Intelligent Power Electronics,” <http://www.semikron.com/products/skip.html> (Nürnberg, Germany: Semikron International).
- [49] Sentron CMT, “General Information About ISFET Technology,” <http://www.sentron.nl/info/isfetgrn.htm> (Enschede, The Netherlands: Sentron).
- [50] Sridhar, S., “Evaluation of Thermal Design Tool for Electronics—A Three Chip MCM as a Case Study,” *Proceedings of Electronic Components and Technology Conference*, 1995, pp. 876-878.
- [51] Structural Dynamics Research Corporation, *Electronics System Cooling (ESC) Course Manual* (Milford, OH: Structural Dynamics Research Corporation, 1999).
- [52] Teca Corporation, “Thermoelectric Technology,” <http://www.thermoelectric.com> (Chicago, IL: Teca Corporation).
- [53] TE Technology Inc., “Thermoelectric Modules,” <http://www.tetech.com/modules/description.html> (Traverse City, MI: TE Technology Inc.).
- [54] ThermoTek, Inc., <http://www.thermotekusa.com/smart.html> (Dallas, TX: ThermoTek).
- [55] Toshiba America Electronic Components, Inc., “Six-In-One Package Offers Low-Cost IGBT Solution for Industrial Drive Market,” <http://www.toshiba.com/taec/press/to-727.htm> (Irvine, CA: TAEC, 1997).
- [56] Utz-Kistner, A., Area Sales Manager America (Addison, Tx: 11 July 2002), email to Ying-Feng Pang.
- [57] Wadsworth, D. C. and Mudawar, I., “Cooling of a Multichip Electronic Module by means of Confined Two-Dimensional Jets of Dielectric Liquid,” *1989 National Heat Transfer Conference, Heat Transfer in Electronics*, Vol. 111, 1989, pp. 79-87.
- [58] Welch, J. W., “Numerical Approach To Optimal Sizing of Rectangular Isotropic Thermal Spreaders,” *Proceedings of IPACK'01 ASME International Electronic Packaging Technical Conference and Exhibition*, Vol. 2, 2001, pp. 609-615.

- [59] Yang, S. L., Palm, B., Kazachkov, I. and Sehgal, B. R., "On Mechanism of Enhancement of Two-Phase Flow Heat Transfer In A Narrow Channel," *2000 Intersociety Conference on Thermal and Thermomechanical Phenomena in Electronic Systems Proceeding*, Vol. 2, 2000, pp. 48-55.
- [60] Yoo, D. W. and Joshi, Y. K., "Smart Thermal Management Systems Based on Solid Liquid Phase Change Materials (PCM)," *Proceedings of IPACK'01 ASME International Electronic Packaging Technical Conference and Exhibition*, Vol. 2, 2001, pp. 601-607.
- [61] Yovanovich, M. M., "Heat Transfer In Electronic Packaging," *10th International Heat Transfer Conference*, Vol. 1, 1994, pp. 93.
- [62] Yovanovich, M. M. and Antonetti, V. W., *Application of Thermal Contact Resistance Theory to Electronic Packages*, Chapter 2, *Advances in Thermal Modeling of Electronic Components and Systems*, Vol. 1, (eds), Bar-Cohen, A. and Kraus, A. D. (New York: Hemisphere Publishing Corporation, 1988).

Appendix A

Thermal Couplings

Thermal couplings provide conductance between unconnected elements with dissimilar meshes. It also provides an additional heat path through which the heat may flow. In Electronic System Cooling (ESC), a conductance value was calculated based on the area of elements and a user specified parameter. There are seven types of thermal coupling a user can specify. Based on the best information a user knows about the model, the user can select any of the thermal coupling type listed in Table A.1 as the input parameter. If the parts created in I-DEAS were meshed individually and later assembled into one finite element model, the required thermal couplings for the simulation are the interfaces between two solid bodies.

Table A.1 Thermal Coupling Properties [51]

| Thermal Coupling Type | Coupling Value | Typical Unit (SI) |
|-----------------------|------------------------------------|----------------------|
| Absolute | Conductance | W/°C |
| Conductive | Thermal Conductivity | W/m·°C |
| Constant Coefficient | Heat Transfer Coefficient | W/m ² ·°C |
| Radiative | View-Factor | Unitless |
| Interface | Heat Transfer Coefficient | W/m ² ·°C |
| Resistant | Resistance | °C/W |
| Edge | Heat Transfer Coefficient / Length | W/m ² ·°C |

A1. Modeling of MOSFET

In the modeling of discrete MOSFET, there were three main parts: the heat sink, the copper plate, and the compound molded cover with silicon (Figures 3.3 and 3.4). From Figure 3.10, we can see the needs of applying thermal couplings between the heat sink and the copper plate, the copper plate and the silicon, and the copper plate and the compound molded cover. Resistant type thermal coupling was used in all the simulations presented in this thesis. Since the interface materials were known most of the time, the resistance values can be calculated easily. However, the resistant between the copper plate and the compound molded cover was a rough estimation. With the assumption of perfect contact at this interface, a very small resistance of $0.0002^{\circ}\text{C}/\text{W}$ was used as the thermal coupling value. The coupling between the copper plate and the silicon, R_{solder} , was calculated using Equation A.1,

$$\begin{aligned} R_{\text{solder}} &= \frac{L_{\text{solder}}}{k_{\text{solder}} \cdot A_{\text{solder}}} \\ &= \frac{0.000254\text{m}}{51\text{W/m}\cdot\text{K} \cdot 0.008\text{m} \cdot 0.01\text{m}}, \\ &= 0.062\text{ }^{\circ}\text{C/W} \end{aligned} \quad (\text{A.1})$$

where L_{solder} is the thickness of the solder between the silicon and the copper plate, k_{solder} is the thermal conductivity of the solder, and A_{solder} is the silicon area. The silicon area was calculated by

$$A_{\text{solder}} = \text{Length(solder)} \cdot \text{Width(solder)}. \quad (\text{A.2})$$

The thermal coupling between the copper plate and the heat sink, $R_{\text{thermalpad}}$, was calculated using Equation A.3,

$$\begin{aligned} R_{\text{thermalpad}} &= R'_{\text{thermalpad}} \cdot A_{\text{copper}} \\ &= 0.25\text{ }^{\circ}\text{C/W} \cdot \text{in}^2 \cdot \frac{16}{25.4}\text{in} \cdot \frac{21}{25.4}\text{in}, \\ &= 0.1302\text{ }^{\circ}\text{C/W} \end{aligned} \quad (\text{A.3})$$

where $R'_{\text{thermalpad}}$ is the thermal resistance of the thermal pad in the unit of $^{\circ}\text{C}/\text{W}\cdot\text{in}^2$ and A_{copper} is the copper area.

A.2 Modeling of IPEM

Resistant type of thermal coupling was also used in the modeling of IPEMs. A total of five major thermal couplings were used in the IPEM model at the interfaces illustrated in Figure 4.8. At the interface between the gate driver and the ceramic frame, the resistance of the epoxy A, R_{epoxy_A} , is calculated using Equation A.4,

$$\begin{aligned} R_{\text{epoxy}_A} &= \frac{L_{\text{epoxy}_A}}{k_{\text{epoxy}} \cdot A_{\text{gate}}} \\ &= \frac{0.000127\text{m}}{1.43\text{ W/m}\cdot\text{K} \cdot 0.021\text{m} \cdot 0.009\text{m}} , \\ &= 0.496\text{ }^{\circ}\text{C/W} \end{aligned} \quad (\text{A.4})$$

where L_{epoxy_A} is the measured thickness of the epoxy, k_{epoxy} is the thermal conductivity of the epoxy, and A_{gate} is the bottom area of the gate driver.

In Figure 4.8, Epoxy B is the interface between the silicon and the ceramic frame. This interface was modeled as the resistance of the epoxy, R_{epoxy_B} , and is calculated using Equation A.5,

$$\begin{aligned} R_{\text{epoxy}_B} &= \frac{L_{\text{epoxy}_B}}{k_{\text{epoxy}} \cdot A_{\text{si-ceramic}}} \\ &= \frac{0.000508\text{m}}{1.43\text{ W/m}\cdot\text{K} \cdot 1.53\times 10^{-5}\text{m} \cdot 1.24\times 10^{-5}\text{m}} , \\ &= 12.845\text{ }^{\circ}\text{C/W} \end{aligned} \quad (\text{A.5})$$

where $A_{\text{si-ceramic}}$ is the contact area between the silicon and the ceramic frame. Note that Equation A.5 calculates the resistant between one MOSFET and the ceramic frame. Since there are two MOSFET in the IPEM model, the input value for the R_{epoxy_B} was doubled in the simulations.

The third interface in the IPEM model is the soldered interface between the MOSFET and the etched copper trace. The resistance of the solder, R_{solder_A} , is calculated using Equation A.6,

$$\begin{aligned} R_{\text{solder}_A} &= \frac{L_{\text{solder}_A}}{k_{\text{solder}} \cdot A_{\text{MOSFET}}} \\ &= \frac{0.127 \times 10^{-3} \text{m}}{51 \text{W/m}\cdot\text{K} \cdot 0.0072 \text{m} \cdot 0.0088 \text{m}} , \\ &= 0.0392 \text{ }^{\circ}\text{C/W} \end{aligned} \quad (\text{A.6})$$

where A_{MOSFET} is the bottom area of the MOSFET. Another soldered interface in the IPEM model is the interface between the DBC copper layer and the heat spreader. The resistant at this interface, R_{solder_B} , is calculated using Equation A.7,

$$\begin{aligned} R_{\text{solder}_B} &= \frac{L_{\text{solder}_B}}{k_{\text{solder}} \cdot A_{\text{DBCcopper}}} \\ &= \frac{0.127 \times 10^{-3} \text{m}}{51 \text{W/m}\cdot\text{K} \cdot 0.0285 \text{m} \cdot 0.0273 \text{m}} , \\ &= 0.0032 \text{ }^{\circ}\text{C/W} \end{aligned} \quad (\text{A.7})$$

where $A_{\text{DBCcopper}}$ is the contact area between the DBC copper layer and the heat spreader. In addition to the soldered interface, the greased interface between the heat spreader and the heat sink is calculated using Equation A.8,

$$\begin{aligned} R_{\text{grease}} &= \frac{L_{\text{grease}}}{k_{\text{grease}} \cdot A_{\text{grease}}} \\ &= \frac{0.127 \times 10^{-3} \text{m}}{1 \text{W/m}\cdot\text{K} \cdot 0.05 \text{m} \cdot 0.036 \text{m}} , \\ &= 0.07 \text{ }^{\circ}\text{C/W} \end{aligned} \quad (\text{A.8})$$

where A_{grease} is the greased area.

Other than the five major thermal couplings discussed above, five other thermal couplings were also input to the simulation to provide an additional heat path through which the heat may be flow. These five thermal couplings include the interfaces between: (1) the silicon and the metallization layer, (2) the DBC etched copper trace and the DBC ceramic layer, (3) the DBC ceramic layer and the DBC copper layer, (4) the ceramic frame and the gel, and (5) the gel and the DBC ceramic layer. These interfaces did not have a physical interface material, and thus the values for these thermal couplings

were rough estimations. An essentially perfect contact was assumed at all of these interfaces. Therefore, a very small resistant value was used for each of the interface conditions.

Appendix B

Simulation Data

The ESC simulation message file, escmsg.dat, provides the information about the model specified for the ESC analysis. The simulation message file shows mesh size, the solver options, the boundary conditions summary, and the flow conditions summary. There are also flow solver messages, thermal solver messages, and solution summary messages in the simulation message file. The flow solver messages provide detailed information about the iterative flow solver process. Similarly, the thermal solver messages provide detailed information about the iterative thermal solver and coupled solution process. Finally, the solution summary messages provide detailed information about the solution and solver convergence. This appendix presents the simulation message files generated from different cases studied in this research. Since the only difference in the thermal simulation of sensitivity and uncertainty was the thermal coupling values, only one complete simulation message file is shown for thermal simulation of MOSFET and thermal simulation of IPEM. In other sensitivity cases, only the coupling values are included here.

B.1 Thermal Simulations of MOSFETs

This section lists the ESC simulation files for the thermal analysis and the sensitivity analysis of the MOSFETs.

Table B1.1 Thermal Analysis of MOSFETs

```
I-DEAS Electronics System Cooling
=====
Thermal/Flow Solver Software Copyright (c) 1994
MAYA Heat Transfer Technologies Ltd.

Run directory specified for ESC/TMG analysis:
/home/ypangideas/IDEAS/5-28-pad/

TMG/ESC Version 8.0.0 April 3 12:00:00 EST 2000
=====
ID2ESC - Thermal/flow model file builder
=====
Time: Tue May 28 12:18:47 2002
```

```

+-----+
|           Model Builder           |
+-----+

Reading model file...
...model file read.

+-----+
|           Model Summary           |
+-----+

Finite Element Model
-----

Model File: /home/ypangideas/IDEAS/TO247-new.mfl

Current FE Study: DEFAULT FE STUDY

Number of nodes in thermal model:          2815
Number of elements in thermal model:        9129

Number of nodes in flow model:              18198
Number of elements in flow model:           86387

Solution Options
-----
Steady-State Analysis
Solution Method:                           Concurrent
Communication Frequency:                  5
Solving Flow
Solving Thermal

Ambient Temperature:                      2.350E+01 C
Ambient Pressure:                         1.014E+05 Pa

Fluid buoyancy:                           Off
Gravity Acceleration:                    9.810E+00 m/s^2
Gravity Vector:   X: 0.000E+00 Y: 0.000E+00 Z:-1.000E+00

Flow laminar/turbulent model:             Fixed viscosity

Flow solver iteration limit:              1000
Flow converged when RMS residual less than: 2.000E-04
Flow solver physical time step:          2.000E+00 s
Flow solver heat imbalance:              2.000E-02

Thermal Boundary Conditions
-----
Number of thermal boundary conditions:     1

Thermal Boundary Condition      Type      Value      FSF TCP
-----
1 - THERMAL BOUNDARY CONDIT  Heat Load    8.616E+00 W      No  No
-----
```

Thermal Couplings

Number of thermal couplings: 8

| Thermal Coupling | Type | Value |
|------------------|------|-------|
| | | |

| | | |
|--|------------|-----------|
| 1 - THERMAL COUPLING LSI_SOLDER | Resistance | 6.220E-02 |
| Primary Area: 8.000E-05 m ² | | |
| Secndry Area: 3.247E-04 m ² | | |
| 2 - THERMAL COUPLING RSI_SOLDER | Resistance | 6.220E-02 |
| Primary Area: 8.000E-05 m ² | | |
| Secndry Area: 3.247E-04 m ² | | |
| 3 - THERMAL COUPLING LCU_SINK | Resistance | 1.302E-01 |
| Primary Area: 3.247E-04 m ² | | |
| Secndry Area: 3.120E-03 m ² | | |
| 4 - THERMAL COUPLING RCU_SINK | Resistance | 1.302E-01 |
| Primary Area: 3.247E-04 m ² | | |
| Secndry Area: 3.120E-03 m ² | | |
| 5 - THERMAL COUPLING LCU_LCOMP | Resistance | 2.434E-04 |
| Primary Area: 3.247E-04 m ² | | |
| Secndry Area: 2.456E-04 m ² | | |
| 6 - THERMAL COUPLING RCU_RCOMP | Resistance | 2.434E-04 |
| Primary Area: 3.247E-04 m ² | | |
| Secndry Area: 2.456E-04 m ² | | |
| 7 - THERMAL COUPLING LPIN | Resistance | 5.000E+00 |
| Primary Area: 3.663E-05 m ² | | |
| Secndry Area: 6.257E-05 m ² | | |
| 8 - THERMAL COUPLING RPIN | Resistance | 5.000E+00 |
| Primary Area: 3.663E-05 m ² | | |
| Secndry Area: 6.257E-05 m ² | | |

Flow Surfaces

Number of flow surfaces: 2

| Flow Surface | Surface +ve side | Properties e side | Elements Surf/c Atchd |
|--------------|------------------|-------------------|-----------------------|
|--------------|------------------|-------------------|-----------------------|

| | | | |
|---|-----------------------|-----|-----|
| 1 - FLOW SURFACE SINK Area: 3.120E-03 m ² | SURFACE PR SURFACE PR | 116 | 188 |
| 2 - FLOW SURFACE PIN Area: 2.463E-05 m ² | SURFACE PR SURFACE PR | 108 | 0 |

Flow Blockages

Number of flow blockages: 2

| Flow Blockage | Type | Loss Coeff |
|--|--------------|---------------|
| 1 - FLOW BLOCKAGE SINK Volume: 4.340E-05 m ³ | Auto-convect | 0.000E+00 1/m |
| 2 - FLOW BLOCKAGE COMPOUND Volume: 1.870E-06 m ³ | Auto-convect | 0.000E+00 1/m |

Fans

Number of fans: 1

| Fan | Type | Value |
|--|-----------|-----------------------------|
| 1 - Outlet - FAN 1 Area: 1.091E-02 m ² | Vol. Flow | 5.000E-02 m ³ /s |

```

Vents
-----
Number of vents: 1

Vent           Type
-----
1 - VENT 1      Ambient
  Area: 2.102E-02 m^2
-----

Performing mesh checks...

- interior and warping angle
  checks on fluid elements...
  ...angle checks on fluid
  elements completed.

- interior and warping angle
  checks on thermal elements...
  ...angle checks on thermal
  elements completed.

- coincident node check
  on fluid model...
  ...node check on fluid
  model completed.

- coincident node check
  on thermal model...

+-----+
| ID2ESC - WARNING 1214           GRP001 |
+-----+
| Coincident thermal nodes found. If the air mesh was generated
| with the PEX Mesher, you can probably ignore this message. If not
| perform a coincident node check on the model.

Pairs of coincident node labels:
  692,      973 /      696,      972 /      1118,      1233
  1117,     1235 /      699,     19701 /     1232,     19966
  777,      974 /      773,      1002 /     1119,      1314
  1147,     1310 /      768,     19675 /     1273,     19940
  693,      971 /      698,      970 /     1116,      1234
  1115,     1236 /
| Number of coincident nodes found: 32
+-----+

...node check on thermal
model completed.

...mesh checks completed.

Building free face list...
...found 14724 free faces.

Processing flow blockages...
...Blockage 1 done,
...Blockage 2 done.

Processing fans...
- Building entity face list...
  ...found 537 entity faces.
...Fan 1 done.

Processing vents...
- Building entity face list...
  ...found 950 entity faces.
...Vent 1 done.

```

```

Processing flow surfaces...

- Building entity face list...
  ...found      112 entity faces.
- Computing sand-grain roughness
  due to obstruction elements...
  ...computation of sand-grain
  roughness completed.

+-----+
| ID2ESC - WARNING 1144
+-----+
| Flow Surface 1 - FLOW SURFACE SINK
| More than 21.5% of the flow surface is not in contact with the
| fluid. This may be caused by a mis-alignment of the flow surface
| with the fluid nodes, or by other entities which are overlapping
| the present flow surface.
+-----+

...Flow Surface 1 done,

- Building entity face list...
  ...found      0 entity faces.

+-----+
| ID2ESC - WARNING 1144
+-----+
| Flow Surface 2 - FLOW SURFACE PIN
| More than 99.9% of the flow surface is not in contact with the
| fluid. This may be caused by a mis-alignment of the flow surface
| with the fluid nodes, or by other entities which are overlapping
| the present flow surface.
+-----+

...Flow Surface 2 done,

- Processing flow surfaces
  due to convective blockage...
  ...done.

Flow Model Conditions:
-----
Total Fluid Volume available for Flow: 8.9532E-03 m^3

Estimated Characteristic Velocity: 2.3062E+00 m/s
Estimated Characteristic Length: 2.0757E-01 m

Approximate Reynolds number: 3.1231E+04
Approximate Mach number: 6.7248E-03
Approximate Grashof number: 1.2734E+06

Number of Flow Sub-domains: 1

Writing flow model files...
...done.

Writing thermal model files...
...done.

Executing Coupled Thermal/Flow Solver

COUPLED - Coupled Flow/Thermal analysis
=====
Time: Tue May 28 12:19:52 2002

```

```

+-----+
| Preparing Thermal Model - Elapsed Time: 01 min 11 sec |
+-----+

Cpu time=      0.0      MAIN Module
Cpu time=      2.5      DATACH Module
Cpu time=     25.4      ECHOS Module
Cpu time=     33.4      COND Module
Cpu time=     51.0      VUFAC Module
Cpu time=    82.2      MEREL Module
Cpu time=   147.6      ANP Module

+-----+
| Solving ESC Model - Elapsed Time: 04 min 27 sec |
+-----+

+-----+
| Initialization Information |
+-----+

Pressure-Gradients array not found in FLI file.
Zero initial values will be used.

+-----+
| Average Scale Information |
+-----+

Global Length Scale      :      2.076E-01
Density Scale            :      1.190E+00
Dynamic Viscosity Scale :      1.850E-05
Velocity Scale           :      0.000E+00
Prandtl Number           :      7.085E-01
Cp Scale                 :      1.007E+03
Conductivity Scale       :      2.630E-02

+-----+
| Convergence History |
+-----+

TIME STEP =      1      SIMULATION TIME = 2.00E+00      CPU SECONDS = 2.40E+01
+-----+
| Equation | Rate | RMS Res | Max Res | Location | Linear Solution |
+-----+-----+-----+-----+-----+-----+
| U - Mom | 0.00 | 0.0E+00 | 0.0E+00 | 0 | 0.0E+00 OK
| V - Mom | 0.00 | 0.0E+00 | 0.0E+00 | 0 | 0.0E+00 OK
| W - Mom | 0.00 | 0.0E+00 | 0.0E+00 | 0 | 0.0E+00 OK
| P - Mass | 0.00 | 3.1E-04 | 4.8E-03 | 3402 | 15.9 7.2E-02 OK
+-----+-----+-----+-----+-----+-----+
| H-Energy | 0.00 | 0.0E+00 | 0.0E+00 | 0 | 5.5 0.0E+00 OK
+-----+-----+-----+-----+-----+-----+

Flow solver - Mass Imbalance          = 0.0000E+00%
Flow solver - X Momentum Imbalance   = 0.0000E+00%
Flow solver - Y Momentum Imbalance   = 0.0000E+00%
Flow solver - Z Momentum Imbalance   = 0.0000E+00%
Flow solver - Energy Imbalance        = 0.0000E+00%

TIME STEP =      2      SIMULATION TIME = 4.00E+00      CPU SECONDS = 7.41E+01
+-----+
| Equation | Rate | RMS Res | Max Res | Location | Linear Solution |
+-----+-----+-----+-----+-----+-----+
| U - Mom | 0.00 | 6.6E-03 | 9.2E-02 | 11581 | 1.4E-02 OK
| V - Mom | 0.00 | 7.0E-03 | 1.0E-01 | 10931 | 1.6E-02 OK
| W - Mom | 0.00 | 4.4E-02 | 1.5E-01 | 6085 | 9.7E-03 OK
| P - Mass | 99.99 | 3.3E-02 | 5.5E-01 | 3334 | 8.5 2.6E-02 OK
+-----+-----+-----+-----+-----+-----+
| H-Energy | 0.00 | 0.0E+00 | 0.0E+00 | 0 | 5.4 0.0E+00 OK
+-----+-----+-----+-----+-----+-----+

```

```

+-----+-----+-----+-----+-----+
Flow solver - Mass Imbalance = -7.6602E+00%
Flow solver - X Momentum Imbalance = 4.4621E-02%
Flow solver - Y Momentum Imbalance = -1.2132E-01%
Flow solver - Z Momentum Imbalance = -6.6040E+01%
Flow solver - Energy Imbalance = 0.0000E+00%

TIME STEP = 3 SIMULATION TIME = 6.00E+00 CPU SECONDS = 1.14E+02
-----
| Equation | Rate | RMS Res | Max Res | Location | Linear Solution |
+-----+-----+-----+-----+-----+
| U - Mom | 0.36 | 2.4E-03 | 3.0E-02 | 15359 | 3.2E-02 OK
| V - Mom | 0.36 | 2.5E-03 | 2.7E-02 | 4296 | 2.7E-02 OK
| W - Mom | 0.32 | 1.4E-02 | 9.2E-02 | 3374 | 1.3E-02 OK
| P - Mass | 0.32 | 1.1E-02 | 1.6E-01 | 3274 | 8.5 1.8E-02 OK
+-----+-----+-----+-----+
| H-Energy | 0.00 | 1.5E-02 | 4.7E-01 | 1618 | 18.8 5.3E-03 OK
+-----+-----+-----+-----+

Flow solver - Mass Imbalance = -1.9159E+00%
Flow solver - X Momentum Imbalance = -1.6195E-02%
Flow solver - Y Momentum Imbalance = 1.7755E-02%
Flow solver - Z Momentum Imbalance = 2.1375E+01%
Flow solver - Energy Imbalance = 0.0000E+00%

Heat Convected to the Fluid = 8.61598E+00 ( 8.61598E+00)
Heat Convected from the Fluid = 0.00000E+00 ( 0.00000E+00)
Convective Heat Residual = 3.32060E-07
Maximum Solid Temperature Change = 3.75887E+01

+-----+-----+-----+-----+-----+
| CSOLVER | Minimum | Location | Maximum | Location | Average Convg |
+-----+-----+-----+-----+-----+
| y+ | 2.22E+00 | 96740 | 1.90E+01 | 95817 | 1.29E+01 ok
| htc | 2.82E+00 | 96704 | 1.93E+02 | 3201 | 2.10E+01
| T-Solid | 3.47E+01 | 3747 | 3.88E+01 | 3008 | 3.70E+01 OK
+-----+-----+-----+-----+

```

TIME STEP = 4 SIMULATION TIME = 8.00E+00 CPU SECONDS = 1.61E+02

```

-----
| Equation | Rate | RMS Res | Max Res | Location | Linear Solution |
+-----+-----+-----+-----+-----+
| U - Mom | 0.46 | 1.1E-03 | 2.3E-02 | 4306 | 3.2E-02 OK
| V - Mom | 0.44 | 1.1E-03 | 2.3E-02 | 4424 | 3.2E-02 OK
| W - Mom | 0.38 | 5.3E-03 | 4.1E-02 | 3414 | 1.3E-02 OK
| P - Mass | 0.27 | 2.8E-03 | 4.1E-02 | 3432 | 8.5 2.1E-02 OK
+-----+-----+-----+-----+
| H-Energy | 0.19 | 3.0E-03 | 9.1E-02 | 1618 | 18.8 4.7E-03 OK
+-----+-----+-----+-----+-----+
```

```

Flow solver - Mass Imbalance = -4.8173E-01%
Flow solver - X Momentum Imbalance = 2.0318E-03%
Flow solver - Y Momentum Imbalance = -2.3983E-02%
Flow solver - Z Momentum Imbalance = 8.2140E+00%
Flow solver - Energy Imbalance = 2.6552E+01%
```

TIME STEP = 5 SIMULATION TIME = 1.00E+01 CPU SECONDS = 2.07E+02

```

-----
| Equation | Rate | RMS Res | Max Res | Location | Linear Solution |
+-----+-----+-----+-----+-----+
| U - Mom | 0.57 | 6.1E-04 | 1.3E-02 | 4306 | 2.2E-02 OK
| V - Mom | 0.55 | 6.2E-04 | 1.4E-02 | 4424 | 2.2E-02 OK
| W - Mom | 0.39 | 2.1E-03 | 1.6E-02 | 3414 | 1.0E-02 OK
| P - Mass | 0.34 | 9.6E-04 | 1.5E-02 | 3464 | 8.5 2.2E-02 OK
+-----+-----+-----+-----+-----+
```

| |
|---|
| H-Energy 0.21 6.3E-04 1.7E-02 1618 18.8 5.5E-03 OK |
| Flow solver - Mass Imbalance = -1.4257E-01% |
| Flow solver - X Momentum Imbalance = -2.6731E-03% |
| Flow solver - Y Momentum Imbalance = -2.2435E-02% |
| Flow solver - Z Momentum Imbalance = 2.6777E+00% |
| Flow solver - Energy Imbalance = 6.0616E+00% |
| TIME STEP = 6 SIMULATION TIME = 1.20E+01 CPU SECONDS = 2.52E+02 |
| +-----+-----+-----+-----+-----+-----+ |
| Equation Rate RMS Res Max Res Location Linear Solution |
| +-----+-----+-----+-----+-----+-----+ |
| U - Mom 0.53 3.3E-04 7.0E-03 4306 1.6E-02 OK |
| V - Mom 0.53 3.3E-04 7.1E-03 4424 1.7E-02 OK |
| W - Mom 0.41 8.6E-04 7.9E-03 3176 7.8E-03 OK |
| P - Mass 0.46 4.4E-04 7.0E-03 3464 8.5 2.1E-02 OK |
| +-----+-----+-----+-----+-----+-----+ |
| H-Energy 0.25 1.6E-04 2.7E-03 2143 18.8 5.3E-03 OK |
| +-----+-----+-----+-----+-----+-----+ |
| Flow solver - Mass Imbalance = -3.3557E-02% |
| Flow solver - X Momentum Imbalance = 9.6429E-05% |
| Flow solver - Y Momentum Imbalance = -8.7394E-03% |
| Flow solver - Z Momentum Imbalance = 5.4839E-01% |
| Flow solver - Energy Imbalance = 1.5053E+00% |
| TIME STEP = 7 SIMULATION TIME = 1.40E+01 CPU SECONDS = 2.98E+02 |
| +-----+-----+-----+-----+-----+-----+ |
| Equation Rate RMS Res Max Res Location Linear Solution |
| +-----+-----+-----+-----+-----+-----+ |
| U - Mom 0.51 1.7E-04 3.4E-03 4306 1.4E-02 OK |
| V - Mom 0.51 1.7E-04 3.4E-03 4424 1.7E-02 OK |
| W - Mom 0.41 3.5E-04 3.8E-03 3176 6.6E-03 OK |
| P - Mass 0.48 2.1E-04 3.3E-03 3136 8.5 2.0E-02 OK |
| +-----+-----+-----+-----+-----+-----+ |
| H-Energy 0.43 6.8E-05 1.6E-03 1616 18.8 4.6E-03 OK |
| +-----+-----+-----+-----+-----+-----+ |
| Flow solver - Mass Imbalance = -7.9782E-03% |
| Flow solver - X Momentum Imbalance = 2.3022E-03% |
| Flow solver - Y Momentum Imbalance = -1.7088E-03% |
| Flow solver - Z Momentum Imbalance = 7.7257E-02% |
| Flow solver - Energy Imbalance = 4.3194E-01% |
| TIME STEP = 8 SIMULATION TIME = 1.60E+01 CPU SECONDS = 3.45E+02 |
| +-----+-----+-----+-----+-----+-----+ |
| Equation Rate RMS Res Max Res Location Linear Solution |
| +-----+-----+-----+-----+-----+-----+ |
| U - Mom 0.50 8.4E-05 1.6E-03 4306 1.5E-02 OK |
| V - Mom 0.50 8.4E-05 1.6E-03 4383 1.5E-02 OK |
| W - Mom 0.44 1.6E-04 1.8E-03 3176 7.9E-03 OK |
| P - Mass 0.46 9.8E-05 1.7E-03 3136 8.5 1.9E-02 OK |
| +-----+-----+-----+-----+-----+-----+ |
| H-Energy 7.14 4.8E-04 9.3E-03 2125 18.8 4.8E-03 OK |
| +-----+-----+-----+-----+-----+-----+ |
| Flow solver - Mass Imbalance = -2.2044E-03% |
| Flow solver - X Momentum Imbalance = 6.8629E-04% |
| Flow solver - Y Momentum Imbalance = -1.7147E-04% |
| Flow solver - Z Momentum Imbalance = -3.1505E-02% |
| Flow solver - Energy Imbalance = 5.1717E+00% |
| Heat Convected to the Fluid = 8.61599E+00 (8.61367E+00) |
| Heat Convected from the Fluid = 0.00000E+00 (0.00000E+00) |
| Convective Heat Residual = 2.69447E-04 |
| Maximum Solid Temperature Change = 3.62083E-01 |
| +-----+-----+-----+-----+-----+-----+ |
| CSOLVER Minimum Location Maximum Location Average Convg |
| +-----+-----+-----+-----+-----+-----+ |

| | | | | | | | |
|--|----------|----------|---------|----------|----------|-----------------|----|
| | y+ | 1.93E+00 | 96739 | 2.58E+01 | 95817 | 1.68E+01 | ok |
| | htc | 2.81E+00 | 96704 | 1.94E+02 | 3201 | 2.28E+01 | |
| | T-Solid | 3.45E+01 | 3747 | 3.85E+01 | 3008 | 3.67E+01 | OK |
| +-----+-----+-----+-----+-----+-----+-----+-----+ | | | | | | | |
| TIME STEP = 9 SIMULATION TIME = 1.80E+01 CPU SECONDS = 3.91E+02 | | | | | | | |
| +-----+-----+-----+-----+-----+-----+-----+-----+ | Equation | Rate | RMS Res | Max Res | Location | Linear Solution | |
| | U - Mom | 0.50 | 4.2E-05 | 7.6E-04 | 4306 | 1.5E-02 | OK |
| | V - Mom | 0.49 | 4.1E-05 | 7.8E-04 | 4383 | 1.6E-02 | OK |
| | W - Mom | 0.47 | 7.4E-05 | 1.0E-03 | 7945 | 1.2E-02 | OK |
| | P - Mass | 0.45 | 4.4E-05 | 7.8E-04 | 3136 | 8.5 1.9E-02 | OK |
| +-----+-----+-----+-----+-----+-----+-----+-----+ | | | | | | | |
| | H-Energy | 0.26 | 1.2E-04 | 2.3E-03 | 2125 | 18.8 4.9E-03 | OK |
| +-----+-----+-----+-----+-----+-----+-----+-----+ | | | | | | | |
| Flow solver - Mass Imbalance = -5.4484E-04% | | | | | | | |
| Flow solver - X Momentum Imbalance = -1.8868E-06% | | | | | | | |
| Flow solver - Y Momentum Imbalance = 1.3517E-04% | | | | | | | |
| Flow solver - Z Momentum Imbalance = -3.3265E-02% | | | | | | | |
| Flow solver - Energy Imbalance = 1.3126E+00% | | | | | | | |
| TIME STEP = 10 SIMULATION TIME = 2.00E+01 CPU SECONDS = 4.37E+02 | | | | | | | |
| +-----+-----+-----+-----+-----+-----+-----+-----+ | Equation | Rate | RMS Res | Max Res | Location | Linear Solution | |
| | U - Mom | 0.49 | 2.0E-05 | 3.5E-04 | 4314 | 1.6E-02 | OK |
| | V - Mom | 0.49 | 2.0E-05 | 3.7E-04 | 4383 | 1.6E-02 | OK |
| | W - Mom | 0.49 | 3.6E-05 | 6.2E-04 | 7945 | 1.5E-02 | OK |
| | P - Mass | 0.44 | 1.9E-05 | 3.4E-04 | 3134 | 8.5 1.8E-02 | OK |
| +-----+-----+-----+-----+-----+-----+-----+-----+ | | | | | | | |
| | H-Energy | 0.26 | 3.2E-05 | 5.8E-04 | 2125 | 18.8 4.9E-03 | OK |
| +-----+-----+-----+-----+-----+-----+-----+-----+ | | | | | | | |
| Flow solver - Mass Imbalance = -1.3965E-03% | | | | | | | |
| Flow solver - X Momentum Imbalance = -1.5559E-04% | | | | | | | |
| Flow solver - Y Momentum Imbalance = 9.8796E-05% | | | | | | | |
| Flow solver - Z Momentum Imbalance = -2.0787E-02% | | | | | | | |
| Flow solver - Energy Imbalance = 3.2547E-01% | | | | | | | |
| TIME STEP = 11 SIMULATION TIME = 2.20E+01 CPU SECONDS = 4.82E+02 | | | | | | | |
| +-----+-----+-----+-----+-----+-----+-----+-----+ | Equation | Rate | RMS Res | Max Res | Location | Linear Solution | |
| | U - Mom | 0.49 | 9.9E-06 | 1.5E-04 | 4314 | 1.6E-02 | OK |
| | V - Mom | 0.49 | 9.9E-06 | 1.7E-04 | 4383 | 1.6E-02 | OK |
| | W - Mom | 0.50 | 1.8E-05 | 3.5E-04 | 7945 | 1.8E-02 | OK |
| | P - Mass | 0.44 | 8.5E-06 | 1.5E-04 | 3134 | 8.5 1.7E-02 | OK |
| +-----+-----+-----+-----+-----+-----+-----+-----+ | | | | | | | |
| | H-Energy | 0.26 | 8.4E-06 | 1.4E-04 | 2125 | 18.8 5.1E-03 | OK |
| +-----+-----+-----+-----+-----+-----+-----+-----+ | | | | | | | |
| Flow solver - Mass Imbalance = -6.8889E-05% | | | | | | | |
| Flow solver - X Momentum Imbalance = -1.3588E-04% | | | | | | | |
| Flow solver - Y Momentum Imbalance = 2.5323E-04% | | | | | | | |
| Flow solver - Z Momentum Imbalance = -1.0614E-02% | | | | | | | |
| Flow solver - Energy Imbalance = 8.1650E-02% | | | | | | | |
| TIME STEP = 12 SIMULATION TIME = 2.40E+01 CPU SECONDS = 5.28E+02 | | | | | | | |
| +-----+-----+-----+-----+-----+-----+-----+-----+ | Equation | Rate | RMS Res | Max Res | Location | Linear Solution | |
| | U - Mom | 0.49 | 4.8E-06 | 8.2E-05 | 3946 | 1.7E-02 | OK |
| | V - Mom | 0.49 | 4.8E-06 | 7.6E-05 | 3907 | 1.6E-02 | OK |
| | W - Mom | 0.51 | 9.1E-06 | 2.0E-04 | 7945 | 2.1E-02 | OK |
| | P - Mass | 0.44 | 3.8E-06 | 6.3E-05 | 3134 | 8.5 1.7E-02 | OK |
| +-----+-----+-----+-----+-----+-----+-----+-----+ | | | | | | | |
| | H-Energy | 0.26 | 2.2E-06 | 3.5E-05 | 2125 | 18.8 4.9E-03 | OK |
| +-----+-----+-----+-----+-----+-----+-----+-----+ | | | | | | | |

```

Flow solver - Mass Imbalance = 1.0647E-04%
Flow solver - X Momentum Imbalance = -8.3014E-05%
Flow solver - Y Momentum Imbalance = 1.3767E-04%
Flow solver - Z Momentum Imbalance = -5.2027E-03%
Flow solver - Energy Imbalance = 2.0646E-02%

TIME STEP = 13 SIMULATION TIME = 2.60E+01 CPU SECONDS = 5.73E+02
+-----+
| Equation | Rate | RMS Res | Max Res | Location | Linear Solution |
+-----+-----+-----+-----+-----+-----+
| U - Mom | 0.49 | 2.3E-06 | 4.7E-05 | 3946 | 1.8E-02 OK
| V - Mom | 0.49 | 2.4E-06 | 4.3E-05 | 3907 | 1.6E-02 OK
| W - Mom | 0.51 | 4.6E-06 | 1.1E-04 | 7945 | 2.3E-02 OK
| P - Mass | 0.45 | 1.7E-06 | 3.1E-05 | 3907 | 8.5 1.6E-02 OK
+-----+-----+-----+-----+-----+
| H-Energy | 12.36 | 2.7E-05 | 6.2E-04 | 1618 | 18.8 5.0E-03 OK
+-----+-----+-----+-----+
Flow solver - Mass Imbalance = 1.9414E-04%
Flow solver - X Momentum Imbalance = -4.0818E-05%
Flow solver - Y Momentum Imbalance = 5.6102E-05%
Flow solver - Z Momentum Imbalance = -2.4599E-03%
Flow solver - Energy Imbalance = 2.8888E-01

Heat Convected to the Fluid = 8.61598E+00 ( 8.61592E+00 )
Heat Convected from the Fluid = 0.00000E+00 ( 0.00000E+00 )
Convective Heat Residual = 7.85878E-06
Maximum Solid Temperature Change = 2.28386E-02

```

```

+-----+-----+-----+-----+-----+
| CSOLVER | Minimum | Location| Maximum | Location| Average Convg|
+-----+-----+-----+-----+-----+
| y+      | 1.87E+00 | 96739 | 2.60E+01 | 95817 | 1.68E+01 ok
| htc     | 2.80E+00 | 96704 | 1.94E+02 | 3201  | 2.28E+01
| T-Solid | 3.45E+01 | 3747  | 3.85E+01 | 3008  | 3.67E+01 OK
+-----+-----+-----+-----+

```

Execution terminating:
all RMS residual AND global imbalance
are below their target criteria.

```

+-----+
| Computed Model Constants |
+-----+
Turbulence length scale (Turbulence model 1) = 2.9664E-02
Turbulence velocity scale (Turbulence model 1) = 4.6638E+00
Turbulence viscosity (Turbulence Model 1) = 1.6463E-03

+-----+
| Boundary Mass Flow and Total Source Term Summary |
+-----+
ADIABATIC FACES 0.0000E+00
CONVECTING FACES 0.0000E+00
OUTLET_FAN 1_FAN 1 -5.9484E-02
VENT 1_VENT 1 5.9484E-02
OPEN_TETRAHEDRAL_ELEMENTS 0.0000E+00
-----
Global Mass Balance: 1.1548E-07
Global Imbalance, in %: 0.0002 %

+-----+
| Boundary Momentum Flow and Total Source Term Summary |
+-----+

```

| | X-Comp. | Y-Comp. | Z-Comp. |
|---------------------------|-------------|-------------|-------------|
| ADIABATIC FACES | 3.5198E-05 | 7.9248E-05 | 5.6421E-03 |
| CONVECTING FACES | 9.4977E-07 | -9.3771E-04 | -5.8115E-03 |
| OUTLET_FAN 1_FAN 1 | -3.3827E-05 | 8.5811E-04 | -7.1204E-02 |
| VENT 1_VENT 1 | -2.4014E-06 | 4.6248E-07 | 7.1368E-02 |
| OPEN_TETRAHEDRAL_ELEMENTS | 0.0000E+00 | 0.0000E+00 | 0.0000E+00 |
| Global Momentum Balance: | -8.0731E-08 | 1.1096E-07 | -4.8652E-06 |
| Global Imbalance, in %: | 0.0000 % | 0.0001 % | -0.0025 % |

| Boundary Energy Flow and Total Source Term Summary | | |
|--|-------------|--|
| ADIABATIC FACES | 0.0000E+00 | |
| CONVECTING FACES | 8.6159E+00 | |
| OUTLET_FAN 1_FAN 1 | -8.5910E+00 | |
| VENT 1_VENT 1 | 0.0000E+00 | |
| OPEN_TETRAHEDRAL_ELEMENTS | 0.0000E+00 | |
| Global Energy Balance: | 2.4890E-02 | |
| Global Imbalance, in %: | 0.2889 % | |

| Locations of maximum residuals | | | | | |
|--------------------------------|--------|------------|------------|------------|--|
| Equation | Node # | X | Y | Z | |
| U - Mom | 3946 | 7.500E-02 | 6.786E-02 | 2.000E-01 | |
| V - Mom | 3907 | 6.786E-02 | 7.500E-02 | 2.000E-01 | |
| W - Mom | 7945 | 6.838E-02 | -7.500E-02 | 1.904E-01 | |
| P - Mass | 3907 | 6.786E-02 | 7.500E-02 | 2.000E-01 | |
| H-Energy | 1618 | -9.000E-03 | 2.500E-03 | -3.500E-03 | |

| Peak Values of residuals | | | |
|--------------------------|----------------------|---------------|----------------|
| Equation | Peak occur at loop # | Peak Residual | Final Residual |
| U - Mom | 2 | 6.64560E-03 | 2.34361E-06 |
| V - Mom | 2 | 7.00612E-03 | 2.36248E-06 |
| W - Mom | 2 | 4.41615E-02 | 4.63234E-06 |
| P - Mass | 2 | 3.29934E-02 | 1.69313E-06 |
| H-Energy | 3 | 1.54829E-02 | 2.68159E-05 |

| Average Scale Information | | |
|---------------------------|-----------|--|
| Global Length Scale : | 2.076E-01 | |
| Density Scale : | 1.190E+00 | |
| Dynamic Viscosity Scale : | 1.850E-05 | |
| Advection Time Scale : | 9.176E-02 | |
| Reynolds Number : | 3.022E+04 | |
| Velocity Scale : | 2.263E+00 | |
| Prandtl Number : | 7.085E-01 | |
| Temperature Range : | 2.298E+00 | |
| Cp Scale : | 1.007E+03 | |
| Conductivity Scale : | 2.630E-02 | |

```

+-----+
|           y+ information (min, max, average)          |
+-----+
|   Face set name      |  min y+  |  max y+  |  ave y+  |
+-----+
|ADIABATIC FACES      |  2.71E+00 |  3.02E+01 |  1.96E+01 |
|CONVECTING FACES     |  1.87E+00 |  2.60E+01 |  1.68E+01 |
+-----+



+-----+
|           CPU Requirements of Numerical Solution      |
+-----+



Equation Type      Discretization      Linear Solution
(secs. %total)      (secs. %total)

-----
Momentum-Mass      2.76E+02  46.8 %      1.15E+02  19.5 %
Scalars            9.13E+01  15.5 %      1.07E+02  18.1 %



+-----+
|           Memory Usage Information                   |
+-----+
|   Peak Memory Use:      36784 Kb
|   Shared Workspace:    4019248 words
+-----+



+-----+
| Coupled Solution Summary                         |
+-----+



Maximum Temperature:      38.543 at Element      3008
Minimum Temperature:      34.519 at Element      3747
Average Temperature:      36.677

Maximum Heat Transfer Coefficient:      0.194E+03
Minimum Heat Transfer Coefficient:      0.280E+01
Average Heat Transfer Coefficient:      0.228E+02

Maximum Y+ Value:          0.260E+02
Minimum Y+ Value:          0.187E+01
Average Y+ Value:          0.168E+02
Percent of faces with Y+ < 30:      100.0
Percent of faces with Y+ < 11.5:      19.6

-----  

ESC WARNING: Y+ Values
-----  

Mesh correction is ON. The solver will compensate where Y+ values are less than 30. ( Although mesh correction is ON, it is recommended to make sure that the mesh is not too fine or that the turbulent model selected is appropriate for the flow regime.)  

Heat flow into temperature B.C.s:      0.954E-06
Heat flow from temperature B.C.s:      0.000E+00
Heat convected to fluid:              0.862E+01
Heat convected from fluid:             0.000E+00
Total heat load on non-fluid elements: 0.862E+01
Total Heat Imbalance:                -0.477E-05
Percent Heat Imbalance:               -0.553E-04 %

Total Number Of Iterations          13
Maximum Temperature Change:        0.228E-01 at Element      96503

Maximum Temperature Change in Coupled Solution:      0.228E-01
Normalized Convective Heat Imbalance in Coupled Solution:  0.786E-05

```

```
Coupled Solve complete. Maximum boundary condition change  
between iterations is less than target.
```

```
Cpu time= 903.0 RSLTPOST Module
```

```
ESCRR - Converting analysis results
```

```
=====
```

```
Time: Tue May 28 12:37:19 2002
```

```
+-----+  
| Results Recovery |  
+-----+
```

```
Recovering Velocity  
Recovering Temperature  
Recovering Heat Flux
```

```
Reading fluid flow results...
```

```
Reading thermal results...
```

```
Writing results data to escrra.dat...
```

```
+-----+  
| Solution Summary |  
+-----+
```

| Results Summary | Maximum | Minimum | Average |
|-------------------|------------|------------|-------------------|
| Fluid Temperature | 2.580E+01 | 2.350E+01 | 2.358E+01 C |
| Fluid Velocity | 4.664E+00 | 5.225E-02 | 2.216E+00 m/s |
| Fluid Pressure | -8.539E-01 | -1.778E+01 | -3.685E+00 Pa |
| Solid Temperature | 3.854E+01 | 3.452E+01 | 3.668E+01 C |
| Y+ | 2.597E+01 | 1.868E+00 | 1.684E+01 |
| Heat Trans. Coef. | 1.943E+02 | 2.798E+00 | 2.279E+01 W/m^2-C |

| Volume/Mass Flow Summary (Values < 0 are outflow) | Volume Flow | Mass Flow |
|--|------------------|-----------------|
| FAN 1 | -5.000E-02 m^3/s | -5.948E-02 kg/s |
| VENT 1 | 4.997E-02 m^3/s | 5.948E-02 kg/s |

```
Flow Solver:
```

| Heat Convected To/From Fluid (Values < 0 are outflows) | Positive Side | Negative Side |
|---|---------------|---------------|
| FLOW SURFACE SINK | 1.529E+00 W | 0.000E+00 W |
| FLOW SURFACE PIN | 6.809E+00 W | 0.000E+00 W |
| FLOW BLOCKAGE SINK | 2.773E-01 W | 0.000E+00 W |
| Total Heat Convected to Fluid | 8.616E+00 W | |

```
Thermal Solver: Heat Flow
```

| | |
|---------------------------------------|--------------|
| Total heat load on non-fluid elements | 8.616E+00 W |
| Heat flow from temperature B.C.s | 0.000E+00 W |
| Heat flow into temperature B.C.s | -9.537E-07 W |
| Heat convected to fluid | 8.616E+00 W |
| Heat convected from fluid | 0.000E+00 W |
| Total Heat Imbalance | -4.768E-06 W |

```
Solver Convergence
```

| | |
|---|------------------|
| Thermal solver - Maximum temperature change | 2.284E-02 C |
| Flow solver - Momentum imbalance | -0.00246 Percent |
| Flow solver - Mass imbalance | 0.00019 Percent |
| Flow solver - Energy imbalance | 0.28888 Percent |
| Coupled solution - Maximum temperature change | 2.284E-02 C |
| Coupled solution - Normalized Heat Imbalance | 7.859E-06 |

```
+-----+  
|          END  
+-----+
```

Solution elapsed time: 19 min 30 sec

Table B1.2 Sensitivity Analysis on Power Loss

| | |
|--|-----------|
| Number of thermal boundary conditions: | 1 |
| Thermal Boundary Condition | Type |
| 1 - THERMAL BOUNDARY CONDIT | Heat Load |

Table B1.3 Sensitivity Analysis on Solder

| | |
|------------------------------|------------|
| Number of thermal couplings: | 8 |
| Thermal Coupling | Type |
| 1 - LSI_SOLDER | Resistance |
| Primary Area: 8.000E-05 m^2 | 6.282E-02 |
| Secndry Area: 3.247E-04 m^2 | |
| 2 - RSI_SOLDER | Resistance |
| Primary Area: 8.000E-05 m^2 | 6.282E-02 |
| Secndry Area: 3.247E-04 m^2 | |
| 3 - LCU_SINK | Resistance |
| Primary Area: 3.247E-04 m^2 | 1.302E-01 |
| Secndry Area: 3.120E-03 m^2 | |
| 4 - RCU_SINK | Resistance |
| Primary Area: 3.247E-04 m^2 | 1.302E-01 |
| Secndry Area: 3.120E-03 m^2 | |
| 5 - LCU_LCOMP | Resistance |
| Primary Area: 3.247E-04 m^2 | 2.434E-04 |
| Secndry Area: 2.456E-04 m^2 | |
| 6 - RCU_RCOMP | Resistance |
| Primary Area: 3.247E-04 m^2 | 2.434E-04 |
| Secndry Area: 2.456E-04 m^2 | |
| 7 - LPIN | Resistance |
| Primary Area: 3.663E-05 m^2 | 5.000E+00 |
| Secndry Area: 6.257E-05 m^2 | |
| 8 - RPIN | Resistance |
| Primary Area: 3.663E-05 m^2 | 5.000E+00 |
| Secndry Area: 6.257E-05 m^2 | |

Table B1.4 Sensitivity Analysis on Thermal Pad

| Number of thermal couplings: | | | 8 |
|------------------------------|------------|-----------|---|
| Thermal Coupling | Type | Value | |
| 1 - LSI_SOLDER | Resistance | 6.220E-02 | |
| Primary Area: 8.000E-05 m^2 | | | |
| Secndry Area: 3.247E-04 m^2 | | | |
| 2 - RSI_SOLDER | Resistance | 6.220E-02 | |
| Primary Area: 8.000E-05 m^2 | | | |
| Secndry Area: 3.247E-04 m^2 | | | |
| 3 - LCU_SINK | Resistance | 1.315E-01 | |
| Primary Area: 3.247E-04 m^2 | | | |
| Secndry Area: 3.120E-03 m^2 | | | |
| 4 - RCU_SINK | Resistance | 1.315E-01 | |
| Primary Area: 3.247E-04 m^2 | | | |
| Secndry Area: 3.120E-03 m^2 | | | |
| 5 - LCU_LCOMP | Resistance | 2.434E-04 | |
| Primary Area: 3.247E-04 m^2 | | | |
| Secndry Area: 2.456E-04 m^2 | | | |
| 6 - RCU_RCOMP | Resistance | 2.434E-04 | |
| Primary Area: 3.247E-04 m^2 | | | |
| Secndry Area: 2.456E-04 m^2 | | | |
| 7 - LPIN | Resistance | 5.000E+00 | |
| Primary Area: 3.663E-05 m^2 | | | |
| Secndry Area: 6.257E-05 m^2 | | | |
| 8 - RPIN | Resistance | 5.000E+00 | |
| Primary Area: 3.663E-05 m^2 | | | |
| Secndry Area: 6.257E-05 m^2 | | | |

Table B1.5 Sensitivity Analysis on Contact Resistance (Screw)

| Number of thermal couplings: | | | 8 |
|------------------------------|------------|-----------|---|
| Thermal Coupling | Type | Value | |
| 1 - LSI_SOLDER | Resistance | 6.220E-02 | |
| Primary Area: 8.000E-05 m^2 | | | |
| Secndry Area: 3.247E-04 m^2 | | | |
| 2 - RSI_SOLDER | Resistance | 6.220E-02 | |
| Primary Area: 8.000E-05 m^2 | | | |
| Secndry Area: 3.247E-04 m^2 | | | |
| 3 - LCU_SINK | Resistance | 1.302E-01 | |
| Primary Area: 3.247E-04 m^2 | | | |
| Secndry Area: 3.120E-03 m^2 | | | |
| 4 - RCU_SINK | Resistance | 1.302E-01 | |
| Primary Area: 3.247E-04 m^2 | | | |
| Secndry Area: 3.120E-03 m^2 | | | |
| 5 - LCU_LCOMP | Resistance | 2.434E-04 | |
| Primary Area: 3.247E-04 m^2 | | | |
| Secndry Area: 2.456E-04 m^2 | | | |
| 6 - RCU_RCOMP | Resistance | 2.434E-04 | |
| Primary Area: 3.247E-04 m^2 | | | |
| Secndry Area: 2.456E-04 m^2 | | | |
| 7 - LPIN | Resistance | 5.050E+00 | |
| Primary Area: 3.663E-05 m^2 | | | |
| Secndry Area: 6.257E-05 m^2 | | | |
| 8 - RPIN | Resistance | 5.050E+00 | |
| Primary Area: 3.663E-05 m^2 | | | |
| Secndry Area: 6.257E-05 m^2 | | | |

B.2 Thermal Simulations of IPEMs

This section lists the ESC simulation files for the thermal analysis and the sensitivity analysis of the IPEM.

Table B2.1 Thermal Analysis of Gen-II.A IPEM

```
I-DEAS Electronics System Cooling
=====
Thermal/Flow Solver Software Copyright (c) 1994
MAYA Heat Transfer Technologies Ltd.

Run directory specified for ESC/TMG analysis:
/home/ypangideas/IDEAS/1-9-existing/

TMG/ESC Version 8.0.0 April 3 12:00:00 EST 2000

ID2ESC - Thermal/flow model file builder
=====
Time: Wed Jan 23 17:59:05 2002

+-----+
|           Model Builder           |
+-----+

Reading model file...
...model file read.

+-----+
|           Model Summary           |
+-----+

Finite Element Model
-----

Model File: /home/ypangideas/IDEAS/ExistingIPEM.mf1

Current FE Study: DEFAULT FE STUDY

Number of nodes in thermal model:          4275
Number of elements in thermal model:        16176

Number of nodes in flow model:              3342
Number of elements in flow model:            13457

Solution Options
-----

Steady-State Analysis
Solution Method:                           Concurrent
Communication Frequency:                  5
Solving Flow
Solving Thermal
Restart from Previous Solution

Ambient Temperature:                      5.000E+01 C
Ambient Pressure:                         1.014E+05 Pa

Fluid buoyancy:                            Off
Gravity Acceleration:                    9.810E+00 m/s^2
Gravity Vector:   X: 0.000E+00  Y: 0.000E+00  Z:-1.000E+00
```

| | | | | |
|---|-----------------------|-------------|-----|-----|
| Flow laminar/turbulent model: | Fixed viscosity | | | |
| Flow solver iteration limit: | 1000 | | | |
| Flow converged when RMS residual less than: | 2.000E-04 | | | |
| Flow solver physical time step: | 2.000E+00 s | | | |
| Flow solver heat imbalance: | 2.000E-02 | | | |
| Thermal Boundary Conditions | | | | |
| ----- | | | | |
| Number of thermal boundary conditions: | 3 | | | |
| Thermal Boundary Condition | Type | Value | FSF | TCP |
| ----- | | | | |
| 1 - THERMAL BOUNDARY CONDIT | Heat Load | 1.200E+01 W | No | Yes |
| 2 - THERMAL BOUNDARY CONDIT | Heat Load | 7.000E+00 W | No | Yes |
| 3 - THERMAL BOUNDARY CONDIT | Heat Load | 1.000E+00 W | No | No |
| ----- | | | | |
| Thermal Couplings | | | | |
| ----- | | | | |
| Number of thermal couplings: | 8 | | | |
| Thermal Coupling | Type | Value | | |
| ----- | | | | |
| 1 - THERMAL COUPLING SI-CU | Resistance | 3.920E-02 | | |
| Primary Area: 1.271E-04 m^2 | | | | |
| Secndry Area: 6.355E-04 m^2 | | | | |
| 2 - THERMAL COUPLING CU TRACE-CE | Resistance | 9.600E-04 | | |
| Primary Area: 7.594E-04 m^2 | | | | |
| Secndry Area: 8.076E-04 m^2 | | | | |
| 3 - THERMAL COUPLING CERAMIC BAS | Resistance | 9.600E-04 | | |
| Primary Area: 8.076E-04 m^2 | | | | |
| Secndry Area: 8.076E-04 m^2 | | | | |
| 4 - THERMAL COUPLING CU BASE-SIN | Resistance | 1.574E-01 | | |
| Primary Area: 8.076E-04 m^2 | | | | |
| Secndry Area: 5.134E-03 m^2 | | | | |
| 5 - THERMAL COUPLING GATE-CERAMI | Resistance | 4.960E-01 | | |
| Primary Area: 1.794E-04 m^2 | | | | |
| Secndry Area: 1.794E-04 m^2 | | | | |
| 6 - THERMAL COUPLING CERAMIC-CU | Resistance | 2.500E-03 | | |
| Primary Area: 5.891E-04 m^2 | | | | |
| Secndry Area: 7.164E-04 m^2 | | | | |
| 7 - THERMAL COUPLING CERAMIC-SI | Resistance | 2.569E+01 | | |
| Primary Area: 5.537E-05 m^2 | | | | |
| Secndry Area: 5.537E-05 m^2 | | | | |
| 8 - THERMAL COUPLING CU TRACE-SI | Resistance | 3.050E-03 | | |
| Primary Area: 1.271E-04 m^2 | | | | |
| Secndry Area: 1.024E-04 m^2 | | | | |
| ----- | | | | |
| Flow Surfaces | | | | |
| ----- | | | | |
| Number of flow surfaces: | 1 | | | |
| Flow Surface | Surface Properties | Elements | | |
| | +ve side -ve side | Surfc Atchd | | |
| ----- | | | | |
| 1 - FLOW SURFACE SINK | SURFACE PR SURFACE PR | 228 0 | | |
| Area: 5.134E-03 m^2 | | | | |
| ----- | | | | |
| Flow Blockages | | | | |
| ----- | | | | |
| Number of flow blockages: | 1 | | | |
| Flow Blockage | Type | Loss Coeff | | |
| ----- | | | | |

```

1 - FLOW BLOCKAGE SINK           Auto-convect 0.000E+00 1/m
Volume: 6.807E-05 m^3
-----
Fans
-----
Number of fans: 1
Fan          Type      Value
-----
1 - Inlet - FAN 1             Vol. Flow   9.440E-03 m^3/s
Area: 2.351E-03 m^2
-----
Vents
-----
Number of vents: 1
Vent          Type
-----
1 - VENT 1                  Ambient
Area: 8.478E-03 m^2
-----
Performing mesh checks...
- interior and warping angle
checks on fluid elements...
...angle checks on fluid
elements completed.

- interior and warping angle
checks on thermal elements...
+-----+
| ID2ESC - WARNING 1205           GRP001 |
+-----+
| Thermal element(s) with interior angles < 1 deg. found. This may
| result convergence problems.
|
| List of element labels:
| 27336  27483  28133  28591  28594  29573  29584  29585
| Number of elements found: 8
+-----+
...angle checks on thermal
elements completed.

- coincident node check
on fluid model...
...node check on fluid
model completed.

- coincident node check
on thermal model...
+-----+
| ID2ESC - WARNING 1214           GRP002 |
+-----+
| Coincident thermal nodes found. If the air mesh was generated
| with the PEX Mesher, you can probably ignore this message. If not
| perform a coincident node check on the model.
|
Pairs of coincident node labels:
  5,      531 /      61,      549 /      62,      548
  63,      547 /      64,      546 /      65,      545
  66,      544 /      67,      543 /      68,      542
  69,      541 /      70,      540 /      71,      539
  72,      538 /      6,       530 /     112,      550

```

```

|      73,      589 /     111,      551 /      74,      588 |
|     110,      552 /      75,      587 /     109,      553 |
|      76,      586 /     108,      554 /      77,      585 |
| ... list too long to display.
| Number of coincident nodes found:   246
+-----+
    ...node check on thermal
    model completed.

    ...mesh checks completed.

Building free face list...
...found    4366 free faces.

Processing flow blockages...
...Blockage 1 done.

Processing fans...

- Building entity face list...
...found      32 entity faces.
...Fan 1 done.

Processing vents...

- Building entity face list...
...found      137 entity faces.
...Vent 1 done.

Processing flow surfaces...

- Building entity face list...
...found      80 entity faces.

+-----+
| ID2ESC - WARNING 1144
+-----+
| Flow Surface 1 - FLOW SURFACE SINK
| More than 15.7% of the flow surface is not in contact with the
| fluid. This may be caused by a mis-alignment of the flow surface
| with the fluid nodes, or by other entities which are overlapping
| the present flow surface.
+-----+

...Flow Surface 1 done,

- Processing flow surfaces
due to convective blockage...
...done.

Flow Model Conditions:
-----

Total Fluid Volume available for Flow: 2.6853E-03 m^3

Estimated Characteristic Velocity: 1.4011E+00 m/s
Estimated Characteristic Length: 1.3895E-01 m
Approximate Reynolds number: 1.2702E+04
Approximate Mach number: 4.0856E-03
Approximate Grashof number: 3.8201E+05

Number of Flow Sub-domains: 1

Writing flow model files...
...done.

Writing thermal model files...
...done.

Executing Coupled Thermal/Flow Solver

```

```

COUPLED - Coupled Flow/Thermal analysis
=====
Time: Wed Jan 23 17:59:38 2002

+-----+
| Preparing Thermal Model - Elapsed Time: 00 min 42 sec |
+-----+

Cpu time=      0.0      MAIN Module
Cpu time=      3.2      DATACH Module
Cpu time=    163.9      ECHOS Module
Cpu time=    212.8      MEREL Module
Cpu time=    339.2      ANP Module

+-----+
| Solving ESC Model - Elapsed Time: 07 min 28 sec |
+-----+

+-----+
| Average Scale Information |
+-----+

Global Length Scale      :      1.390E-01
Density Scale            :      1.089E+00
Dynamic Viscosity Scale :      1.850E-05
Advection Time Scale    :      1.162E-01
Reynolds Number          :      9.785E+03
Velocity Scale           :      1.196E+00
Prandtl Number           :      7.084E-01
Temperature Range        :      7.645E+00
Cp Scale                 :      1.007E+03
Conductivity Scale       :      2.630E-02

+-----+
| Convergence History   |
+-----+

TIME STEP = 1 SIMULATION TIME = 2.00E+00      CPU SECONDS = 6.06E+00
+-----+
| Equation | Rate | RMS Res | Max Res | Location | Linear Solution |
+-----+-----+-----+-----+-----+-----+
| U - Mom | 0.00 | 1.3E-06 | 6.0E-05 | 3966 | 4.7E-03 OK
| V - Mom | 0.00 | 2.5E-07 | 1.4E-05 | 3966 | 1.9E-02 OK
| W - Mom | 0.00 | 1.1E-07 | 2.4E-06 | 3964 | 2.8E-02 OK
| P - Mass | 0.00 | 6.1E-08 | 1.3E-06 | 5135 | 8.8 1.3E-02 OK
+-----+-----+-----+-----+-----+
| H-Energy | 0.00 | 4.1E-06 | 3.3E-05 | 4567 | 14.3 8.1E-03 OK
+-----+-----+-----+-----+-----+

Flow solver - Mass Imbalance      = -3.6112E-05%
Flow solver - X Momentum Imbalance = -9.2317E-05%
Flow solver - Y Momentum Imbalance = -8.1473E-06%
Flow solver - Z Momentum Imbalance = 8.1293E-06%
Flow solver - Energy Imbalance   = 1.8731E-02%

TIME STEP = 2 SIMULATION TIME = 4.00E+00      CPU SECONDS = 1.30E+01
+-----+
| Equation | Rate | RMS Res | Max Res | Location | Linear Solution |
+-----+-----+-----+-----+-----+
| U - Mom | 0.56 | 7.1E-07 | 3.3E-05 | 3966 | 4.6E-03 OK
| V - Mom | 0.59 | 1.5E-07 | 8.1E-06 | 3966 | 1.6E-02 OK
| W - Mom | 0.57 | 6.5E-08 | 1.4E-06 | 6265 | 2.5E-02 OK
| P - Mass | 0.54 | 3.3E-08 | 7.8E-07 | 5135 | 8.8 1.0E-02 OK
+-----+-----+-----+-----+-----+
| H-Energy | 0.26 | 1.1E-06 | 8.4E-06 | 4567 | 14.3 7.4E-03 OK
+-----+

```

```

+-----+-----+-----+-----+-----+
| Flow solver - Mass Imbalance          = -1.8056E-05%
| Flow solver - X Momentum Imbalance   = -9.2317E-05%
| Flow solver - Y Momentum Imbalance   = -4.6803E-06%
| Flow solver - Z Momentum Imbalance   = 3.0601E-06%
| Flow solver - Energy Imbalance        = 4.5112E-03%
+-----+-----+-----+-----+-----+
TIME STEP = 3 SIMULATION TIME = 6.00E+00 CPU SECONDS = 1.98E+01
+-----+-----+-----+-----+-----+
| Equation | Rate | RMS Res | Max Res | Location | Linear Solution |
+-----+-----+-----+-----+-----+
| U - Mom | 0.56 | 3.9E-07 | 1.8E-05 | 3966 | 4.0E-03 OK |
| V - Mom | 0.55 | 8.0E-08 | 4.4E-06 | 3966 | 1.5E-02 OK |
| W - Mom | 0.58 | 3.8E-08 | 8.5E-07 | 6265 | 2.2E-02 OK |
| P - Mass | 0.61 | 2.0E-08 | 4.5E-07 | 5135 | 8.8 7.3E-03 OK |
+-----+-----+-----+-----+-----+
| H-Energy | 1.57 | 1.7E-06 | 1.3E-05 | 4567 | 14.3 8.6E-03 OK |
+-----+-----+-----+-----+-----+
Flow solver - Mass Imbalance          = -1.8056E-05%
Flow solver - X Momentum Imbalance   = -1.2661E-04%
Flow solver - Y Momentum Imbalance   = -9.2472E-07%
Flow solver - Z Momentum Imbalance   = 2.2873E-06%
Flow solver - Energy Imbalance        = 7.6390E-03%
Heat Convected to the Fluid          = 2.00000E+01 ( 1.99999E+01)
Heat Convected from the Fluid        = 0.00000E+00 ( 0.00000E+00)
Convective Heat Residual            = 3.14713E-06
Maximum Solid Temperature Change    = 2.01416E-03
+-----+-----+-----+-----+-----+
| CSOLVER | Minimum | Location | Maximum | Location | Average | Convg |
+-----+-----+-----+-----+-----+
| y+      | 1.65E+00 | 30476 | 2.13E+01 | 31236 | 1.21E+01 ok |
| htc     | 2.02E+00 | 30872 | 5.55E+01 | 5426 | 1.28E+01 |
| T-Solid | 8.11E+01 | 8709 | 9.22E+01 | 9039 | 8.61E+01 OK |
+-----+-----+-----+-----+-----+

```

Execution terminating:
 all RMS residual AND global imbalance
 are below their target criteria.

```

+-----+-----+
| Computed Model Constants           |
+-----+-----+
Turbulence length scale (Turbulence model 1) = 1.9856E-02
Turbulence velocity scale (Turbulence model 1) = 3.9531E+00
Turbulence viscosity (Turbulence Model 1)      = 8.5469E-04
+-----+-----+
| Boundary Mass Flow and Total Source Term Summary |
+-----+-----+
ADIABATIC FACES                      0.0000E+00
CONVECTING FACES                     0.0000E+00
INLET _FAN 1_FAN 1                   1.0316E-02
VENT 1_VENT 1                        -1.0316E-02
OPEN_TETRAHEDRAL_ELEMENTS           0.0000E+00
+-----+-----+
Global Mass Balance:                 -1.8626E-09
Global Imbalance, in %:              0.0000 %
+-----+-----+

```

| Boundary Momentum Flow and Total Source Term Summary | | | | | |
|--|----------------------|---------------|----------------|------------|--|
| ----- | | | | | |
| | X-Comp. | Y-Comp. | Z-Comp. | | |
| ADIABATIC FACES | 2.1959E-02 | -1.5281E-05 | 1.2159E-04 | | |
| CONVECTING FACES | 1.7879E-03 | 2.1449E-05 | -8.3075E-05 | | |
| INLET _FAN 1_FAN 1 | -3.5309E-02 | 3.6888E-06 | 6.4752E-06 | | |
| VENT 1_VENT 1 | 1.1562E-02 | -9.8575E-06 | -4.4991E-05 | | |
| OPEN_TETRAHEDRAL_ELEMENTS | 0.0000E+00 | 0.0000E+00 | 0.0000E+00 | | |
| ----- | | | | | |
| Global Momentum Balance: | -4.4703E-08 | -3.2651E-10 | 8.0763E-10 | | |
| Global Imbalance, in %: | -0.0001 % | 0.0000 % | 0.0000 % | | |
| ----- | | | | | |
| Boundary Energy Flow and Total Source Term Summary | | | | | |
| ----- | | | | | |
| | 0.0000E+00 | | | | |
| ADIABATIC FACES | 0.0000E+00 | | | | |
| CONVECTING FACES | 2.0000E+01 | | | | |
| INLET _FAN 1_FAN 1 | 0.0000E+00 | | | | |
| VENT 1_VENT 1 | -1.9998E+01 | | | | |
| OPEN_TETRAHEDRAL_ELEMENTS | 0.0000E+00 | | | | |
| ----- | | | | | |
| Global Energy Balance: | 1.5278E-03 | | | | |
| Global Imbalance, in %: | 0.0076 % | | | | |
| ----- | | | | | |
| Locations of maximum residuals | | | | | |
| ----- | | | | | |
| Equation | Node # | X | Y | Z | |
| U - Mom | 3966 | 1.625E-01 | 5.924E-02 | -1.914E-02 | |
| V - Mom | 3966 | 1.625E-01 | 5.924E-02 | -1.914E-02 | |
| W - Mom | 6265 | 1.531E-01 | -3.665E-02 | 1.836E-02 | |
| P - Mass | 5135 | 1.625E-01 | -1.429E-03 | -1.854E-02 | |
| H-Energy | 4567 | -1.346E-02 | -5.000E-03 | -1.270E-04 | |
| ----- | | | | | |
| Peak Values of residuals | | | | | |
| ----- | | | | | |
| Equation | Peak occur at loop # | Peak Residual | Final Residual | | |
| U - Mom | 1 | 1.27019E-06 | 3.94043E-07 | | |
| V - Mom | 1 | 2.49579E-07 | 8.03923E-08 | | |
| W - Mom | 1 | 1.14518E-07 | 3.80632E-08 | | |
| P - Mass | 1 | 6.05303E-08 | 1.99115E-08 | | |
| H-Energy | 1 | 4.08344E-06 | 1.65521E-06 | | |
| ----- | | | | | |
| Average Scale Information | | | | | |
| ----- | | | | | |
| Global Length Scale : | | 1.390E-01 | | | |
| Density Scale : | | 1.089E+00 | | | |
| Dynamic Viscosity Scale : | | 1.850E-05 | | | |
| Advection Time Scale : | | 1.162E-01 | | | |
| Reynolds Number : | | 9.785E+03 | | | |
| Velocity Scale : | | 1.196E+00 | | | |
| Prandtl Number : | | 7.084E-01 | | | |
| Temperature Range : | | 7.647E+00 | | | |

| | | |
|--------------------|---|-----------|
| Cp Scale | : | 1.007E+03 |
| Conductivity Scale | : | 2.630E-02 |

| y+ information (min, max, average) | | | |
|------------------------------------|----------|----------|----------|
| Face set name | min y+ | max y+ | ave y+ |
| ADIABATIC FACES | 3.23E+00 | 2.94E+01 | 1.44E+01 |
| CONVECTING FACES | 1.64E+00 | 2.12E+01 | 1.20E+01 |

| CPU Requirements of Numerical Solution | | | |
|--|----------------------------------|-----------------------------------|--|
| Equation Type | Discretization (secs. %total) | Linear Solution (secs. %total) | |
| Momentum-Mass | 1.05E+01 52.5 % | 3.47E+00 17.4 % | |
| Scalars | 3.41E+00 17.1 % | 2.62E+00 13.1 % | |

| Memory Usage Information | |
|--------------------------|--------------|
| Peak Memory Use: | 6677 Kb |
| Shared Workspace: | 687824 words |

| Coupled Solution Summary | |
|--------------------------|--|
|--------------------------|--|

Maximum Temperature: 92.188 at Element 9039
 Minimum Temperature: 81.095 at Element 8709
 Average Temperature: 86.072

Maximum Heat Transfer Coefficient: 0.555E+02
 Minimum Heat Transfer Coefficient: 0.202E+01
 Average Heat Transfer Coefficient: 0.128E+02

Maximum Y+ Value: 0.213E+02
 Minimum Y+ Value: 0.165E+01
 Average Y+ Value: 0.121E+02
 Percent of faces with Y+ < 30: 100.0
 Percent of faces with Y+ < 11.5: 16.5

ESC WARNING: Y+ Values

Mesh correction is ON. The solver will compensate where Y+ values are less than 30. (Although mesh correction is ON, it is recommended to make sure that the mesh is not too fine or that the turbulent model selected is appropriate for the flow regime.)

Heat flow into temperature B.C.s: 0.000E+00
 Heat flow from temperature B.C.s: 0.000E+00
 Heat convected to fluid: 0.200E+02
 Heat convected from fluid: 0.000E+00
 Total heat load on non-fluid elements: 0.200E+02
 Total Heat Imbalance: -0.191E-04
 Percent Heat Imbalance: -0.954E-04 %

Total Number Of Iterations 3
 Maximum Temperature Change: 0.202E-02 at Element 7721

```

Maximum Temperature Change in Coupled Solution: 0.201E-02
Normalized Convective Heat Imbalance in Coupled Solution: 0.315E-05

Coupled Solve complete. Maximum boundary condition change
between iterations is less than target.

Cpu time= 463.9 RSLTPOST Module

ESCRR - Converting analysis results
=====
Time: Wed Jan 23 18:08:59 2002

+-----+
|          Results Recovery          |
+-----+

Recovering Velocity
Recovering Pressure
Recovering Temperature
Recovering Mass Flux

Reading fluid flow results...
Reading thermal results...
Writing results data to escrra.dat...

+-----+
|          Solution Summary          |
+-----+

Results Summary      Maximum      Minimum      Average
-----
Fluid Temperature    5.765E+01    5.000E+01    5.118E+01 C
Fluid Velocity       3.953E+00    8.976E-02    1.147E+00 m/s
Fluid Pressure       6.679E-01   -4.226E+00   -1.196E-01 Pa
Solid Temperature   9.219E+01    8.110E+01    8.607E+01 C
Y+                  2.126E+01    1.646E+00    1.207E+01
Heat Trans. Coef.   5.553E+01    2.025E+00    1.279E+01 W/m^2-C
-----

Volume/Mass Flow Summary
(Values < 0 are outflow)      Volume Flow      Mass Flow
-----
FAN 1                  9.440E-03 m^3/s     1.032E-02 kg/s
VENT 1                 -9.496E-03 m^3/s    -1.032E-02 kg/s
-----

Flow Solver:
Heat Convected To/From Fluid
(Values < 0 are outflows)      Positive Side      Negative Side
-----
FLOW SURFACE SINK        2.354E+00 W      0.000E+00 W
FLOW BLOCKAGE SINK       1.765E+01 W      0.000E+00 W
-----
Total Heat Convected to Fluid      2.000E+01 W

Thermal Solver: Heat Flow
-----
Total heat load on non-fluid elements      2.000E+01 W
Heat flow from temperature B.C.s         0.000E+00 W
Heat flow into temperature B.C.s        0.000E+00 W
Heat convected to fluid                 2.000E+01 W
Heat convected from fluid              0.000E+00 W

```

| | |
|---|------------------|
| Total Heat Imbalance | -1.907E-05 W |
| Solver Convergence | |
| Thermal solver - Maximum temperature change | 2.022E-03 C |
| Flow solver - Momentum imbalance | -0.00013 Percent |
| Flow solver - Mass imbalance | -0.00002 Percent |
| Flow solver - Energy imbalance | 0.00764 Percent |
| Coupled solution - Maximum temperature change | 2.014E-03 C |
| Coupled solution - Normalized Heat Imbalance | 3.147E-06 |
| ----- | |
| +-----+ END +-----+ | |
| Solution elapsed time: 10 min 20 sec | |

Table B2.2 Thermal Analysis of Gen-II.B IPEM

| | |
|--|-------|
| I-DEAS Electronics System Cooling | ===== |
| ===== Thermal/Flow Solver Software Copyright (c) 1994 MAYA Heat Transfer Technologies Ltd. | |
| Run directory specified for ESC/TMG analysis: /home/ypangideas/IDEAS/1-7-25mil/ | |
| TMG/ESC Version 8.0.0 April 3 12:00:00 EST 2000 | |
| ID2ESC - Thermal/flow model file builder | ===== |
| ===== Time: Wed Jan 23 19:51:13 2002 | |
| +-----+ Model Builder +-----+ | |
| Reading model file... ...model file read. | |
| +-----+ Model Summary +-----+ | |
| Finite Element Model | ----- |
| Model File: /home/ypangideas/IDEAS/1design-Ceramics.mf1 | |
| Current FE Study: DEFAULT FE STUDY | |
| Number of nodes in thermal model: | 5237 |
| Number of elements in thermal model: | 20072 |
| Number of nodes in flow model: | 4051 |
| Number of elements in flow model: | 16717 |
| Solution Options | ----- |
| Steady-State Analysis | |

| | | | | |
|--|-----------------|-------------|-----|-----|
| Solution Method: | Concurrent | | | |
| Communication Frequency: | 5 | | | |
| Solving Flow | | | | |
| Solving Thermal | | | | |
| Ambient Temperature: | 5.000E+01 C | | | |
| Ambient Pressure: | 1.014E+05 Pa | | | |
| Fluid buoyancy: | Off | | | |
| Gravity Acceleration: | 9.810E+00 m/s^2 | | | |
| Gravity Vector: X: 0.000E+00 Y: 0.000E+00 Z:-1.000E+00 | | | | |
| Flow laminar/turbulent model: | Fixed viscosity | | | |
| Flow solver iteration limit: | 1000 | | | |
| Flow converged when RMS residual less than: | 2.000E-04 | | | |
| Flow solver physical time step: | 2.000E+00 s | | | |
| Flow solver heat imbalance: | 2.000E-02 | | | |
| Thermal Boundary Conditions | | | | |
| ----- | | | | |
| Number of thermal boundary conditions: | 3 | | | |
| Thermal Boundary Condition | Type | Value | FSF | TCP |
| ----- | | | | |
| 1 - THERMAL BOUNDARY CONDIT | Heat Load | 1.200E+01 W | No | Yes |
| 2 - THERMAL BOUNDARY CONDIT | Heat Load | 7.000E+00 W | No | Yes |
| 3 - THERMAL BOUNDARY CONDIT | Heat Load | 1.000E+00 W | No | No |
| ----- | | | | |
| Thermal Couplings | | | | |
| ----- | | | | |
| Number of thermal couplings: | 9 | | | |
| Thermal Coupling | Type | Value | | |
| ----- | | | | |
| 1 - THERMAL COUPLING SI-CU | Resistance | 3.920E-02 | | |
| Primary Area: 1.271E-04 m^2 | | | | |
| Secndry Area: 2.222E-04 m^2 | | | | |
| 2 - THERMAL COUPLING CU TRACE-CE | Resistance | 1.000E-03 | | |
| Primary Area: 2.751E-04 m^2 | | | | |
| Secndry Area: 7.771E-04 m^2 | | | | |
| 3 - THERMAL COUPLING CERAMIC BAS | Resistance | 1.000E-03 | | |
| Primary Area: 7.771E-04 m^2 | | | | |
| Secndry Area: 7.771E-04 m^2 | | | | |
| 4 - THERMAL COUPLING CU BASE-SIN | Resistance | 1.635E-01 | | |
| Primary Area: 7.771E-04 m^2 | | | | |
| Secndry Area: 5.134E-03 m^2 | | | | |
| 5 - THERMAL COUPLING GATE-CERAMI | Resistance | 4.960E-01 | | |
| Primary Area: 1.794E-04 m^2 | | | | |
| Secndry Area: 5.667E-04 m^2 | | | | |
| 6 - THERMAL COUPLING CERAMIC-GEL | Resistance | 2.500E-03 | | |
| Primary Area: 5.667E-04 m^2 | | | | |
| Secndry Area: 4.705E-04 m^2 | | | | |
| 7 - THERMAL COUPLING GEL-CERAMIC | Resistance | 2.500E-03 | | |
| Primary Area: 4.705E-04 m^2 | | | | |
| Secndry Area: 7.771E-04 m^2 | | | | |
| 8 - THERMAL COUPLING CERAMIC-SI | Resistance | 2.569E+01 | | |
| Primary Area: 5.536E-05 m^2 | | | | |
| Secndry Area: 5.537E-05 m^2 | | | | |
| 9 - THERMAL COUPLING CU TRACE-SI | Resistance | 3.000E-03 | | |
| Primary Area: 1.271E-04 m^2 | | | | |
| Secndry Area: 1.259E-04 m^2 | | | | |
| ----- | | | | |
| Flow Surfaces | | | | |
| ----- | | | | |
| Number of flow surfaces: | 1 | | | |


```

on thermal model...

+-----+
| ID2ESC - WARNING 1214                               GRP002 |
+-----+
| Coincident thermal nodes found. If the air mesh was generated
| with the PEX Mesher, you can probably ignore this message. If not
| perform a coincident node check on the model.

Pairs of coincident node labels:
  2822,      3323 /    2914,      3354 /    2913,      3355
  2912,      3356 /    2911,      3357 /    2910,      3358
  2909,      3359 /    2908,      3360 /    2907,      3361
  2906,      3362 /    2905,      3363 /    2904,      3364
  2903,      3365 /    2902,      3366 /    2823,      3322
  2889,      3379 /    2927,      3341 /    2890,      3378
  2926,      3342 /    2891,      3377 /    2925,      3343
  2892,      3376 /    2924,      3344 /    2893,      3375
... list too long to display.
Number of coincident nodes found: 322
+-----+

...node check on thermal
model completed.

...mesh checks completed.

Building free face list...
...found 4798 free faces.

Processing flow blockages...
...Blockage 1 done.

Processing fans...
- Building entity face list...
...found 54 entity faces.
...Fan 1 done.

Processing vents...
- Building entity face list...
...found 192 entity faces.
...Vent 1 done.

Processing flow surfaces...
- Building entity face list...
...found 82 entity faces.

+-----+
| ID2ESC - WARNING 1144
+-----+
| Flow Surface 1 - FLOW SURFACE 1
| More than 15.1% of the flow surface is not in contact with the
| fluid. This may be caused by a mis-alignment of the flow surface
| with the fluid nodes, or by other entities which are overlapping
| the present flow surface.
+-----+

...Flow Surface 1 done,
- Processing flow surfaces
due to convective blockage...
...done.

Flow Model Conditions:
-----
Total Fluid Volume available for Flow: 2.6851E-03 m^3

```

```

Estimated Characteristic Velocity: 1.3821E+00 m/s
Estimated Characteristic Length: 1.3895E-01 m
Approximate Reynolds number: 1.2529E+04
Approximate Mach number: 4.0301E-03
Approximate Grashof number: 3.8197E+05

Number of Flow Sub-domains: 1

Writing flow model files...
...done.

Writing thermal model files...
...done.

Executing Coupled Thermal/Flow Solver

COUPLED - Coupled Flow/Thermal analysis
=====
Time: Wed Jan 23 19:51:50 2002

+-----+
| Preparing Thermal Model - Elapsed Time: 00 min 44 sec |
+-----+

Cpu time= 0.0 MAIN Module
Cpu time= 2.8 DATACH Module
Cpu time= 36.7 ECHOS Module
Cpu time= 52.4 COND Module
Cpu time= 91.2 VUFAC Module
Cpu time= 174.2 MEREL Module
Cpu time= 322.3 ANP Module

+-----+
| Solving ESC Model - Elapsed Time: 07 min 43 sec |
+-----+

+-----+
| Initialization Information |
+-----+

Pressure-Gradients array not found in FLI file.
Zero initial values will be used.

+-----+
| Average Scale Information |
+-----+

Global Length Scale : 1.390E-01
Density Scale : 1.093E+00
Dynamic Viscosity Scale : 1.850E-05
Velocity Scale : 0.000E+00
Prandtl Number : 7.084E-01
Cp Scale : 1.007E+03
Conductivity Scale : 2.630E-02

+-----+
| Convergence History |
+-----+

TIME STEP = 1 SIMULATION TIME = 2.00E+00 CPU SECONDS = 4.11E+00
-----
| Equation | Rate | RMS Res | Max Res | Location | Linear Solution |
+-----+-----+-----+-----+-----+
| U - Mom | 0.00 | 3.4E-02 | 6.6E-01 | 7262 | 4.6E-02 OK |

```

| |
|---|
| V - Mom 0.00 0.0E+00 0.0E+00 0 0.0E+00 OK |
| W - Mom 0.00 0.0E+00 0.0E+00 0 0.0E+00 OK |
| P - Mass 0.00 3.1E-04 5.8E-03 7278 12.6 8.7E-02 OK |
| +-----+-----+-----+-----+-----+-----+-----+ |
| H-Energy 0.00 0.0E+00 0.0E+00 0 5.5 0.0E+00 OK |
| +-----+-----+-----+-----+-----+-----+-----+ |
| Flow solver - Mass Imbalance = 0.0000E+00% |
| Flow solver - X Momentum Imbalance = 0.0000E+00% |
| Flow solver - Y Momentum Imbalance = 0.0000E+00% |
| Flow solver - Z Momentum Imbalance = 0.0000E+00% |
| Flow solver - Energy Imbalance = 0.0000E+00% |
| TIME STEP = 2 SIMULATION TIME = 4.00E+00 CPU SECONDS = 1.38E+01 |
| +-----+-----+-----+-----+-----+-----+-----+ |
| Equation Rate RMS Res Max Res Location Linear Solution |
| +-----+-----+-----+-----+-----+-----+-----+ |
| U - Mom 1.25 4.2E-02 4.0E-01 6022 6.0E-03 OK |
| V - Mom 0.00 5.8E-03 9.1E-02 7280 2.3E-02 OK |
| W - Mom 0.00 6.2E-03 9.5E-02 7286 2.2E-02 OK |
| P - Mass 54.88 1.7E-02 3.3E-01 7276 8.7 5.0E-02 OK |
| +-----+-----+-----+-----+-----+-----+-----+ |
| H-Energy 0.00 0.0E+00 0.0E+00 0 5.4 0.0E+00 OK |
| +-----+-----+-----+-----+-----+-----+-----+ |
| Flow solver - Mass Imbalance = 9.0736E+00% |
| Flow solver - X Momentum Imbalance = -8.9342E+01% |
| Flow solver - Y Momentum Imbalance = 8.6485E-03% |
| Flow solver - Z Momentum Imbalance = 6.8628E-03% |
| Flow solver - Energy Imbalance = 0.0000E+00% |
| TIME STEP = 3 SIMULATION TIME = 6.00E+00 CPU SECONDS = 2.20E+01 |
| +-----+-----+-----+-----+-----+-----+-----+ |
| Equation Rate RMS Res Max Res Location Linear Solution |
| +-----+-----+-----+-----+-----+-----+-----+ |
| U - Mom 0.37 1.5E-02 1.4E-01 7230 8.1E-03 OK |
| V - Mom 0.43 2.5E-03 3.1E-02 5968 3.0E-02 OK |
| W - Mom 0.52 3.2E-03 3.8E-02 6008 2.1E-02 OK |
| P - Mass 0.36 6.2E-03 8.6E-02 5972 8.6 1.5E-02 OK |
| +-----+-----+-----+-----+-----+-----+-----+ |
| H-Energy 0.00 3.0E-02 3.1E-01 6666 18.6 2.2E-03 OK |
| +-----+-----+-----+-----+-----+-----+-----+ |
| Flow solver - Mass Imbalance = 2.4632E+00% |
| Flow solver - X Momentum Imbalance = -5.2973E+01% |
| Flow solver - Y Momentum Imbalance = 1.0003E-01% |
| Flow solver - Z Momentum Imbalance = -7.0339E-02% |
| Flow solver - Energy Imbalance = 0.0000E+00% |
| Heat Convected to the Fluid = 2.00000E+01 (2.00000E+01) |
| Heat Convected from the Fluid = 0.00000E+00 (0.00000E+00) |
| Convective Heat Residual = 1.90735E-07 |
| Maximum Solid Temperature Change = 8.50536E+01 |
| +-----+-----+-----+-----+-----+-----+-----+ |
| CSOLVER Minimum Location Maximum Location Average Convg |
| +-----+-----+-----+-----+-----+-----+-----+ |
| y+ 1.71E+00 38830 1.45E+01 38565 9.02E+00 LO |
| htc 2.09E+00 38620 6.47E+01 16330 1.23E+01 |
| T-Solid 8.01E+01 19646 9.46E+01 134 8.82E+01 OK |
| +-----+-----+-----+-----+-----+-----+-----+ |
| TIME STEP = 4 SIMULATION TIME = 8.00E+00 CPU SECONDS = 3.14E+01 |
| +-----+-----+-----+-----+-----+-----+-----+ |
| Equation Rate RMS Res Max Res Location Linear Solution |
| +-----+-----+-----+-----+-----+-----+-----+ |
| U - Mom 0.64 9.9E-03 1.2E-01 7242 9.5E-03 OK |
| V - Mom 0.59 1.5E-03 1.9E-02 5990 3.1E-02 OK |
| W - Mom 0.63 2.1E-03 2.5E-02 7212 1.8E-02 OK |
| P - Mass 0.21 1.3E-03 2.0E-02 5974 8.6 2.1E-02 OK |
| +-----+-----+-----+-----+-----+-----+-----+ |

| |
|--|
| H-Energy 0.18 5.4E-03 4.6E-02 6654 18.6 2.3E-03 OK |
| Flow solver - Mass Imbalance = 6.5160E-01% |
| Flow solver - X Momentum Imbalance = -1.5180E+01% |
| Flow solver - Y Momentum Imbalance = -3.2431E-02% |
| Flow solver - Z Momentum Imbalance = -1.8948E-01% |
| Flow solver - Energy Imbalance = 2.5966E+01% |
| TIME STEP = 5 SIMULATION TIME = 1.00E+01 CPU SECONDS = 4.04E+01 |
| ----- |
| Equation Rate RMS Res Max Res Location Linear Solution |
| +-----+-----+-----+-----+-----+-----+ |
| U - Mom 0.49 4.9E-03 6.7E-02 7240 7.7E-03 OK |
| V - Mom 0.51 7.6E-04 1.2E-02 5974 2.2E-02 OK |
| W - Mom 0.46 9.4E-04 1.5E-02 5974 1.9E-02 OK |
| P - Mass 0.47 6.2E-04 1.1E-02 6002 8.7 1.6E-02 OK |
| +-----+-----+-----+-----+-----+-----+ |
| H-Energy 0.23 1.2E-03 7.4E-03 5696 18.7 2.1E-03 OK |
| +-----+-----+-----+-----+-----+-----+ |
| Flow solver - Mass Imbalance = 1.8228E-01% |
| Flow solver - X Momentum Imbalance = -2.8298E+00% |
| Flow solver - Y Momentum Imbalance = -1.8223E-02% |
| Flow solver - Z Momentum Imbalance = -1.2601E-01% |
| Flow solver - Energy Imbalance = 5.7880E+00% |
| TIME STEP = 6 SIMULATION TIME = 1.20E+01 CPU SECONDS = 4.91E+01 |
| ----- |
| Equation Rate RMS Res Max Res Location Linear Solution |
| +-----+-----+-----+-----+-----+-----+ |
| U - Mom 0.49 2.4E-03 3.9E-02 7234 5.1E-03 OK |
| V - Mom 0.45 3.4E-04 7.6E-03 5962 2.1E-02 OK |
| W - Mom 0.43 4.0E-04 7.5E-03 5982 2.3E-02 OK |
| P - Mass 0.44 2.7E-04 3.0E-03 6040 8.7 9.6E-03 OK |
| +-----+-----+-----+-----+-----+-----+ |
| H-Energy 0.28 3.4E-04 2.3E-03 5696 18.6 2.1E-03 OK |
| +-----+-----+-----+-----+-----+-----+ |
| Flow solver - Mass Imbalance = 5.1099E-02% |
| Flow solver - X Momentum Imbalance = 2.5417E-01% |
| Flow solver - Y Momentum Imbalance = 1.8811E-02% |
| Flow solver - Z Momentum Imbalance = -9.6175E-02% |
| Flow solver - Energy Imbalance = 1.3456E+00% |
| TIME STEP = 7 SIMULATION TIME = 1.40E+01 CPU SECONDS = 5.81E+01 |
| ----- |
| Equation Rate RMS Res Max Res Location Linear Solution |
| +-----+-----+-----+-----+-----+-----+ |
| U - Mom 0.52 1.2E-03 2.2E-02 7234 5.0E-03 OK |
| V - Mom 0.46 1.5E-04 4.3E-03 5962 2.1E-02 OK |
| W - Mom 0.50 2.0E-04 3.5E-03 5962 2.2E-02 OK |
| P - Mass 0.64 1.7E-04 2.3E-03 6040 8.7 7.4E-03 OK |
| +-----+-----+-----+-----+-----+-----+ |
| H-Energy 0.33 1.1E-04 8.0E-04 5744 14.2 9.5E-03 OK |
| +-----+-----+-----+-----+-----+-----+ |
| Flow solver - Mass Imbalance = 1.4580E-02% |
| Flow solver - X Momentum Imbalance = 5.5338E-01% |
| Flow solver - Y Momentum Imbalance = 1.0825E-02% |
| Flow solver - Z Momentum Imbalance = -4.5372E-02% |
| Flow solver - Energy Imbalance = 3.3750E-01% |
| TIME STEP = 8 SIMULATION TIME = 1.60E+01 CPU SECONDS = 6.64E+01 |
| ----- |
| Equation Rate RMS Res Max Res Location Linear Solution |
| +-----+-----+-----+-----+-----+-----+ |
| U - Mom 0.52 6.3E-04 1.2E-02 5699 5.9E-03 OK |
| V - Mom 0.50 7.7E-05 1.7E-03 5962 2.3E-02 OK |
| W - Mom 0.55 1.1E-04 1.7E-03 5962 2.6E-02 OK |
| P - Mass 0.59 1.0E-04 1.2E-03 6040 8.7 7.2E-03 OK |

| | | | | | | | |
|----------|-------|---------|---------|------|------|---------|----|
| H-Energy | 15.16 | 1.7E-03 | 1.3E-02 | 5904 | 18.6 | 2.2E-03 | OK |
|----------|-------|---------|---------|------|------|---------|----|

Flow solver - Mass Imbalance = 3.7286E-03%
 Flow solver - X Momentum Imbalance = 2.8729E-01%
 Flow solver - Y Momentum Imbalance = 2.9470E-03%
 Flow solver - Z Momentum Imbalance = -2.1480E-02%
 Flow solver - Energy Imbalance = 8.7687E+00%

Heat Convected to the Fluid = 2.00000E+01 (1.99940E+01)
 Heat Convected from the Fluid = 0.00000E+00 (0.00000E+00)
 Convective Heat Residual = 3.02360E-04
 Maximum Solid Temperature Change = 1.21218E+00

| CSOLVER | Minimum | Location | Maximum | Location | Average | Convg |
|---------|----------|----------|----------|----------|----------|-------|
| y+ | 1.69E+00 | 38127 | 2.01E+01 | 38565 | 1.15E+01 | ok |
| htc | 2.06E+00 | 38620 | 6.33E+01 | 16330 | 1.30E+01 | |
| T-Solid | 8.10E+01 | 19646 | 9.57E+01 | 134 | 8.93E+01 | OK |

TIME STEP = 9 SIMULATION TIME = 1.80E+01 CPU SECONDS = 7.58E+01

| Equation | Rate | RMS Res | Max Res | Location | Linear Solution |
|----------|------|---------|---------|----------|-----------------|
| U - Mom | 0.52 | 3.3E-04 | 7.0E-03 | 5699 | 6.4E-03 OK |
| V - Mom | 0.52 | 4.0E-05 | 4.9E-04 | 6010 | 2.8E-02 OK |
| W - Mom | 0.55 | 6.1E-05 | 1.1E-03 | 5972 | 2.8E-02 OK |
| P - Mass | 0.52 | 5.4E-05 | 5.7E-04 | 7232 | 8.7 7.6E-03 OK |
| H-Energy | 0.25 | 4.3E-04 | 3.3E-03 | 5904 | 14.2 9.8E-03 OK |

Flow solver - Mass Imbalance = 7.4933E-04%
 Flow solver - X Momentum Imbalance = 1.1207E-01%
 Flow solver - Y Momentum Imbalance = 5.2143E-04%
 Flow solver - Z Momentum Imbalance = -1.0555E-02%
 Flow solver - Energy Imbalance = 2.2121E+00%

TIME STEP = 10 SIMULATION TIME = 2.00E+01 CPU SECONDS = 8.44E+01

| Equation | Rate | RMS Res | Max Res | Location | Linear Solution |
|----------|------|---------|---------|----------|-----------------|
| U - Mom | 0.51 | 1.7E-04 | 3.8E-03 | 7234 | 6.7E-03 OK |
| V - Mom | 0.54 | 2.2E-05 | 3.3E-04 | 5996 | 3.0E-02 OK |
| W - Mom | 0.54 | 3.3E-05 | 5.9E-04 | 5972 | 2.9E-02 OK |
| P - Mass | 0.48 | 2.6E-05 | 2.9E-04 | 7232 | 8.7 7.7E-03 OK |
| H-Energy | 0.26 | 1.1E-04 | 8.4E-04 | 5904 | 14.2 9.5E-03 OK |

Flow solver - Mass Imbalance = 1.1737E-04%
 Flow solver - X Momentum Imbalance = 3.5423E-02%
 Flow solver - Y Momentum Imbalance = -6.0248E-04%
 Flow solver - Z Momentum Imbalance = -5.8737E-03%
 Flow solver - Energy Imbalance = 5.3718E-01%

TIME STEP = 11 SIMULATION TIME = 2.20E+01 CPU SECONDS = 9.30E+01

| Equation | Rate | RMS Res | Max Res | Location | Linear Solution |
|----------|------|---------|---------|----------|-----------------|
| U - Mom | 0.52 | 8.8E-05 | 2.2E-03 | 7234 | 7.0E-03 OK |
| V - Mom | 0.55 | 1.2E-05 | 1.7E-04 | 5585 | 3.0E-02 OK |
| W - Mom | 0.52 | 1.7E-05 | 2.9E-04 | 5972 | 3.0E-02 OK |
| P - Mass | 0.46 | 1.2E-05 | 1.4E-04 | 7232 | 8.7 8.2E-03 OK |
| H-Energy | 0.27 | 3.0E-05 | 2.2E-04 | 5840 | 14.2 9.3E-03 OK |

| Flow solver - Mass Imbalance | = | 2.7084E-05% | | | | | | | | | | | | | | | | | | | | | | | | | | | | | | | | | | | | | | | |
|---|----------|----------------------------|----------|----------|-----------------|----------|---------|----------|---------|----------|-----------------|---------|------|----------|---------|----------|------------|----------|------|---------|----------|-------|------------|---------|----------|---------|---------|----------|------------|----------|------|----------|---------|------|----------------|----------|-------|---------|---------|------|-----------------|
| Flow solver - X Momentum Imbalance | = | 1.0656E-02% | | | | | | | | | | | | | | | | | | | | | | | | | | | | | | | | | | | | | | | |
| Flow solver - Y Momentum Imbalance | = | -7.6623E-04% | | | | | | | | | | | | | | | | | | | | | | | | | | | | | | | | | | | | | | | |
| Flow solver - Z Momentum Imbalance | = | -3.1279E-03% | | | | | | | | | | | | | | | | | | | | | | | | | | | | | | | | | | | | | | | |
| Flow solver - Energy Imbalance | = | 1.3345E-01% | | | | | | | | | | | | | | | | | | | | | | | | | | | | | | | | | | | | | | | |
| TIME STEP = 12 SIMULATION TIME = 2.40E+01 CPU SECONDS = 1.01E+02 | | | | | | | | | | | | | | | | | | | | | | | | | | | | | | | | | | | | | | | | | |
| <table border="1"> <thead> <tr><th>Equation</th><th>Rate</th><th>RMS Res</th><th>Max Res</th><th>Location</th><th>Linear Solution</th></tr> </thead> <tbody> <tr><td>U - Mom</td><td>0.54</td><td>4.8E-05</td><td>1.3E-03</td><td>7234</td><td>7.1E-03 OK</td></tr> <tr><td>V - Mom</td><td>0.55</td><td>6.5E-06</td><td>1.5E-04</td><td>5962</td><td>3.1E-02 OK</td></tr> <tr><td>W - Mom</td><td>0.52</td><td>9.0E-06</td><td>1.6E-04</td><td>5725</td><td>3.0E-02 OK</td></tr> <tr><td>P - Mass</td><td>0.46</td><td>5.5E-06</td><td>6.7E-05</td><td>7232</td><td>8.7 8.9E-03 OK</td></tr> <tr><td>H-Energy</td><td>0.28</td><td>8.6E-06</td><td>6.1E-05</td><td>5840</td><td>14.2 9.6E-03 OK</td></tr> </tbody> </table> | | | | | | Equation | Rate | RMS Res | Max Res | Location | Linear Solution | U - Mom | 0.54 | 4.8E-05 | 1.3E-03 | 7234 | 7.1E-03 OK | V - Mom | 0.55 | 6.5E-06 | 1.5E-04 | 5962 | 3.1E-02 OK | W - Mom | 0.52 | 9.0E-06 | 1.6E-04 | 5725 | 3.0E-02 OK | P - Mass | 0.46 | 5.5E-06 | 6.7E-05 | 7232 | 8.7 8.9E-03 OK | H-Energy | 0.28 | 8.6E-06 | 6.1E-05 | 5840 | 14.2 9.6E-03 OK |
| Equation | Rate | RMS Res | Max Res | Location | Linear Solution | | | | | | | | | | | | | | | | | | | | | | | | | | | | | | | | | | | | |
| U - Mom | 0.54 | 4.8E-05 | 1.3E-03 | 7234 | 7.1E-03 OK | | | | | | | | | | | | | | | | | | | | | | | | | | | | | | | | | | | | |
| V - Mom | 0.55 | 6.5E-06 | 1.5E-04 | 5962 | 3.1E-02 OK | | | | | | | | | | | | | | | | | | | | | | | | | | | | | | | | | | | | |
| W - Mom | 0.52 | 9.0E-06 | 1.6E-04 | 5725 | 3.0E-02 OK | | | | | | | | | | | | | | | | | | | | | | | | | | | | | | | | | | | | |
| P - Mass | 0.46 | 5.5E-06 | 6.7E-05 | 7232 | 8.7 8.9E-03 OK | | | | | | | | | | | | | | | | | | | | | | | | | | | | | | | | | | | | |
| H-Energy | 0.28 | 8.6E-06 | 6.1E-05 | 5840 | 14.2 9.6E-03 OK | | | | | | | | | | | | | | | | | | | | | | | | | | | | | | | | | | | | |
| Flow solver - Mass Imbalance | = | 3.6112E-05% | | | | | | | | | | | | | | | | | | | | | | | | | | | | | | | | | | | | | | | |
| Flow solver - X Momentum Imbalance | = | 3.1146E-03% | | | | | | | | | | | | | | | | | | | | | | | | | | | | | | | | | | | | | | | |
| Flow solver - Y Momentum Imbalance | = | -5.7015E-04% | | | | | | | | | | | | | | | | | | | | | | | | | | | | | | | | | | | | | | | |
| Flow solver - Z Momentum Imbalance | = | -1.6537E-03% | | | | | | | | | | | | | | | | | | | | | | | | | | | | | | | | | | | | | | | |
| Flow solver - Energy Imbalance | = | 3.4174E-02% | | | | | | | | | | | | | | | | | | | | | | | | | | | | | | | | | | | | | | | |
| TIME STEP = 13 SIMULATION TIME = 2.60E+01 CPU SECONDS = 1.10E+02 | | | | | | | | | | | | | | | | | | | | | | | | | | | | | | | | | | | | | | | | | |
| <table border="1"> <thead> <tr><th>Equation</th><th>Rate</th><th>RMS Res</th><th>Max Res</th><th>Location</th><th>Linear Solution</th></tr> </thead> <tbody> <tr><td>U - Mom</td><td>0.56</td><td>2.7E-05</td><td>7.5E-04</td><td>7234</td><td>7.0E-03 OK</td></tr> <tr><td>V - Mom</td><td>0.58</td><td>3.8E-06</td><td>1.2E-04</td><td>5962</td><td>3.0E-02 OK</td></tr> <tr><td>W - Mom</td><td>0.52</td><td>4.7E-06</td><td>8.8E-05</td><td>5725</td><td>2.9E-02 OK</td></tr> <tr><td>P - Mass</td><td>0.47</td><td>2.6E-06</td><td>3.3E-05</td><td>7232</td><td>8.7 9.5E-03 OK</td></tr> <tr><td>H-Energy</td><td>19.33</td><td>1.7E-04</td><td>1.5E-03</td><td>6666</td><td>18.7 2.2E-03 OK</td></tr> </tbody> </table> | | | | | | Equation | Rate | RMS Res | Max Res | Location | Linear Solution | U - Mom | 0.56 | 2.7E-05 | 7.5E-04 | 7234 | 7.0E-03 OK | V - Mom | 0.58 | 3.8E-06 | 1.2E-04 | 5962 | 3.0E-02 OK | W - Mom | 0.52 | 4.7E-06 | 8.8E-05 | 5725 | 2.9E-02 OK | P - Mass | 0.47 | 2.6E-06 | 3.3E-05 | 7232 | 8.7 9.5E-03 OK | H-Energy | 19.33 | 1.7E-04 | 1.5E-03 | 6666 | 18.7 2.2E-03 OK |
| Equation | Rate | RMS Res | Max Res | Location | Linear Solution | | | | | | | | | | | | | | | | | | | | | | | | | | | | | | | | | | | | |
| U - Mom | 0.56 | 2.7E-05 | 7.5E-04 | 7234 | 7.0E-03 OK | | | | | | | | | | | | | | | | | | | | | | | | | | | | | | | | | | | | |
| V - Mom | 0.58 | 3.8E-06 | 1.2E-04 | 5962 | 3.0E-02 OK | | | | | | | | | | | | | | | | | | | | | | | | | | | | | | | | | | | | |
| W - Mom | 0.52 | 4.7E-06 | 8.8E-05 | 5725 | 2.9E-02 OK | | | | | | | | | | | | | | | | | | | | | | | | | | | | | | | | | | | | |
| P - Mass | 0.47 | 2.6E-06 | 3.3E-05 | 7232 | 8.7 9.5E-03 OK | | | | | | | | | | | | | | | | | | | | | | | | | | | | | | | | | | | | |
| H-Energy | 19.33 | 1.7E-04 | 1.5E-03 | 6666 | 18.7 2.2E-03 OK | | | | | | | | | | | | | | | | | | | | | | | | | | | | | | | | | | | | |
| Flow solver - Mass Imbalance | = | 9.9309E-05% | | | | | | | | | | | | | | | | | | | | | | | | | | | | | | | | | | | | | | | |
| Flow solver - X Momentum Imbalance | = | 8.9029E-04% | | | | | | | | | | | | | | | | | | | | | | | | | | | | | | | | | | | | | | | |
| Flow solver - Y Momentum Imbalance | = | -3.6152E-04% | | | | | | | | | | | | | | | | | | | | | | | | | | | | | | | | | | | | | | | |
| Flow solver - Z Momentum Imbalance | = | -8.6566E-04% | | | | | | | | | | | | | | | | | | | | | | | | | | | | | | | | | | | | | | | |
| Flow solver - Energy Imbalance | = | 8.5867E-01% | | | | | | | | | | | | | | | | | | | | | | | | | | | | | | | | | | | | | | | |
| Heat Convected to the Fluid | = | 2.00000E+01 (1.99994E+01) | | | | | | | | | | | | | | | | | | | | | | | | | | | | | | | | | | | | | | | |
| Heat Convected from the Fluid | = | 0.00000E+00 (0.00000E+00) | | | | | | | | | | | | | | | | | | | | | | | | | | | | | | | | | | | | | | | |
| Convective Heat Residual | = | 2.77523E-05 | | | | | | | | | | | | | | | | | | | | | | | | | | | | | | | | | | | | | | | |
| Maximum Solid Temperature Change | = | 2.53036E-01 | | | | | | | | | | | | | | | | | | | | | | | | | | | | | | | | | | | | | | | |
| <table border="1"> <thead> <tr><th>CSOLVER</th><th>Minimum</th><th>Location</th><th>Maximum</th><th>Location</th><th>Average</th><th>Convg</th></tr> </thead> <tbody> <tr><td>y+</td><td>1.69E+00</td><td>38020</td><td>2.03E+01</td><td>38565</td><td>1.15E+01</td><td>ok</td></tr> <tr><td>htc</td><td>2.06E+00</td><td>38620</td><td>6.33E+01</td><td>16330</td><td>1.30E+01</td><td></td></tr> <tr><td>T-Solid</td><td>8.13E+01</td><td>19646</td><td>9.59E+01</td><td>134</td><td>8.95E+01</td><td>OK</td></tr> </tbody> </table> | | | | | | CSOLVER | Minimum | Location | Maximum | Location | Average | Convg | y+ | 1.69E+00 | 38020 | 2.03E+01 | 38565 | 1.15E+01 | ok | htc | 2.06E+00 | 38620 | 6.33E+01 | 16330 | 1.30E+01 | | T-Solid | 8.13E+01 | 19646 | 9.59E+01 | 134 | 8.95E+01 | OK | | | | | | | | |
| CSOLVER | Minimum | Location | Maximum | Location | Average | Convg | | | | | | | | | | | | | | | | | | | | | | | | | | | | | | | | | | | |
| y+ | 1.69E+00 | 38020 | 2.03E+01 | 38565 | 1.15E+01 | ok | | | | | | | | | | | | | | | | | | | | | | | | | | | | | | | | | | | |
| htc | 2.06E+00 | 38620 | 6.33E+01 | 16330 | 1.30E+01 | | | | | | | | | | | | | | | | | | | | | | | | | | | | | | | | | | | | |
| T-Solid | 8.13E+01 | 19646 | 9.59E+01 | 134 | 8.95E+01 | OK | | | | | | | | | | | | | | | | | | | | | | | | | | | | | | | | | | | |
| TIME STEP = 14 SIMULATION TIME = 2.80E+01 CPU SECONDS = 1.19E+02 | | | | | | | | | | | | | | | | | | | | | | | | | | | | | | | | | | | | | | | | | |
| <table border="1"> <thead> <tr><th>Equation</th><th>Rate</th><th>RMS Res</th><th>Max Res</th><th>Location</th><th>Linear Solution</th></tr> </thead> <tbody> <tr><td>U - Mom</td><td>0.57</td><td>1.5E-05</td><td>4.6E-04</td><td>5962</td><td>7.1E-03 OK</td></tr> <tr><td>V - Mom</td><td>0.60</td><td>2.3E-06</td><td>9.4E-05</td><td>5962</td><td>3.1E-02 OK</td></tr> <tr><td>W - Mom</td><td>0.52</td><td>2.5E-06</td><td>4.7E-05</td><td>5725</td><td>3.0E-02 OK</td></tr> <tr><td>P - Mass</td><td>0.48</td><td>1.2E-06</td><td>1.6E-05</td><td>7232</td><td>8.7 1.2E-02 OK</td></tr> <tr><td>H-Energy</td><td>0.26</td><td>4.3E-05</td><td>3.7E-04</td><td>6666</td><td>14.2 9.8E-03 OK</td></tr> </tbody> </table> | | | | | | Equation | Rate | RMS Res | Max Res | Location | Linear Solution | U - Mom | 0.57 | 1.5E-05 | 4.6E-04 | 5962 | 7.1E-03 OK | V - Mom | 0.60 | 2.3E-06 | 9.4E-05 | 5962 | 3.1E-02 OK | W - Mom | 0.52 | 2.5E-06 | 4.7E-05 | 5725 | 3.0E-02 OK | P - Mass | 0.48 | 1.2E-06 | 1.6E-05 | 7232 | 8.7 1.2E-02 OK | H-Energy | 0.26 | 4.3E-05 | 3.7E-04 | 6666 | 14.2 9.8E-03 OK |
| Equation | Rate | RMS Res | Max Res | Location | Linear Solution | | | | | | | | | | | | | | | | | | | | | | | | | | | | | | | | | | | | |
| U - Mom | 0.57 | 1.5E-05 | 4.6E-04 | 5962 | 7.1E-03 OK | | | | | | | | | | | | | | | | | | | | | | | | | | | | | | | | | | | | |
| V - Mom | 0.60 | 2.3E-06 | 9.4E-05 | 5962 | 3.1E-02 OK | | | | | | | | | | | | | | | | | | | | | | | | | | | | | | | | | | | | |
| W - Mom | 0.52 | 2.5E-06 | 4.7E-05 | 5725 | 3.0E-02 OK | | | | | | | | | | | | | | | | | | | | | | | | | | | | | | | | | | | | |
| P - Mass | 0.48 | 1.2E-06 | 1.6E-05 | 7232 | 8.7 1.2E-02 OK | | | | | | | | | | | | | | | | | | | | | | | | | | | | | | | | | | | | |
| H-Energy | 0.26 | 4.3E-05 | 3.7E-04 | 6666 | 14.2 9.8E-03 OK | | | | | | | | | | | | | | | | | | | | | | | | | | | | | | | | | | | | |
| Flow solver - Mass Imbalance | = | -1.8056E-05% | | | | | | | | | | | | | | | | | | | | | | | | | | | | | | | | | | | | | | | |
| Flow solver - X Momentum Imbalance | = | 2.0295E-04% | | | | | | | | | | | | | | | | | | | | | | | | | | | | | | | | | | | | | | | |
| Flow solver - Y Momentum Imbalance | = | -2.1624E-04% | | | | | | | | | | | | | | | | | | | | | | | | | | | | | | | | | | | | | | | |
| Flow solver - Z Momentum Imbalance | = | -4.3781E-04% | | | | | | | | | | | | | | | | | | | | | | | | | | | | | | | | | | | | | | | |

| | | | | | | |
|--|-------|---------|---------|----------|-----------------|---------------|
| Flow solver - Energy Imbalance | | | | | | = 2.1519E-01% |
| TIME STEP = 15 SIMULATION TIME = 3.00E+01 CPU SECONDS = 1.28E+02 | | | | | | |
| Equation | Rate | RMS Res | Max Res | Location | Linear Solution | |
| U - Mom | 0.57 | 8.6E-06 | 3.0E-04 | 5962 | 6.5E-03 | OK |
| V - Mom | 0.61 | 1.4E-06 | 6.6E-05 | 5962 | 2.8E-02 | OK |
| W - Mom | 0.53 | 1.3E-06 | 2.4E-05 | 5725 | 2.9E-02 | OK |
| P - Mass | 0.49 | 6.1E-07 | 8.2E-06 | 7232 | 8.7 | 1.1E-02 OK |
| +-----+-----+-----+-----+-----+-----+-----+ | | | | | | |
| H-Energy | 0.26 | 1.1E-05 | 9.4E-05 | 6666 | 14.2 | 9.4E-03 OK |
| +-----+-----+-----+-----+-----+-----+-----+ | | | | | | |
| Flow solver - Mass Imbalance = 6.3197E-05% | | | | | | |
| Flow solver - X Momentum Imbalance = -6.7651E-05% | | | | | | |
| Flow solver - Y Momentum Imbalance = -1.2334E-04% | | | | | | |
| Flow solver - Z Momentum Imbalance = -2.3402E-04% | | | | | | |
| Flow solver - Energy Imbalance = 5.2110E-02% | | | | | | |
| TIME STEP = 16 SIMULATION TIME = 3.20E+01 CPU SECONDS = 1.36E+02 | | | | | | |
| Equation | Rate | RMS Res | Max Res | Location | Linear Solution | |
| U - Mom | 0.57 | 4.9E-06 | 1.9E-04 | 5962 | 5.9E-03 | OK |
| V - Mom | 0.61 | 8.4E-07 | 4.3E-05 | 5962 | 2.6E-02 | OK |
| W - Mom | 0.52 | 6.8E-07 | 1.3E-05 | 5725 | 2.9E-02 | OK |
| P - Mass | 0.50 | 3.0E-07 | 4.2E-06 | 5986 | 8.7 | 1.0E-02 OK |
| +-----+-----+-----+-----+-----+-----+-----+ | | | | | | |
| H-Energy | 0.27 | 2.9E-06 | 2.3E-05 | 6666 | 14.2 | 9.1E-03 OK |
| +-----+-----+-----+-----+-----+-----+-----+ | | | | | | |
| Flow solver - Mass Imbalance = 7.2225E-05% | | | | | | |
| Flow solver - X Momentum Imbalance = -8.3888E-05% | | | | | | |
| Flow solver - Y Momentum Imbalance = -7.7457E-05% | | | | | | |
| Flow solver - Z Momentum Imbalance = -1.0695E-04% | | | | | | |
| Flow solver - Energy Imbalance = 1.2828E-02% | | | | | | |
| TIME STEP = 17 SIMULATION TIME = 3.40E+01 CPU SECONDS = 1.44E+02 | | | | | | |
| Equation | Rate | RMS Res | Max Res | Location | Linear Solution | |
| U - Mom | 0.57 | 2.8E-06 | 1.1E-04 | 5962 | 5.2E-03 | OK |
| V - Mom | 0.60 | 5.0E-07 | 2.7E-05 | 5962 | 2.4E-02 | OK |
| W - Mom | 0.53 | 3.6E-07 | 7.1E-06 | 5984 | 2.9E-02 | OK |
| P - Mass | 0.52 | 1.6E-07 | 2.3E-06 | 5986 | 8.7 | 1.0E-02 OK |
| +-----+-----+-----+-----+-----+-----+-----+ | | | | | | |
| H-Energy | 0.27 | 8.0E-07 | 5.8E-06 | 6666 | 14.2 | 9.1E-03 OK |
| +-----+-----+-----+-----+-----+-----+-----+ | | | | | | |
| Flow solver - Mass Imbalance = 9.0281E-05% | | | | | | |
| Flow solver - X Momentum Imbalance = -7.3063E-05% | | | | | | |
| Flow solver - Y Momentum Imbalance = -4.1464E-05% | | | | | | |
| Flow solver - Z Momentum Imbalance = -4.9322E-05% | | | | | | |
| Flow solver - Energy Imbalance = 3.1878E-03% | | | | | | |
| TIME STEP = 18 SIMULATION TIME = 3.60E+01 CPU SECONDS = 1.53E+02 | | | | | | |
| Equation | Rate | RMS Res | Max Res | Location | Linear Solution | |
| U - Mom | 0.57 | 1.6E-06 | 6.6E-05 | 5962 | 4.6E-03 | OK |
| V - Mom | 0.59 | 3.0E-07 | 1.7E-05 | 5962 | 2.1E-02 | OK |
| W - Mom | 0.53 | 1.9E-07 | 4.2E-06 | 5984 | 2.8E-02 | OK |
| P - Mass | 0.53 | 8.3E-08 | 1.3E-06 | 5986 | 8.7 | 1.0E-02 OK |
| +-----+-----+-----+-----+-----+-----+-----+ | | | | | | |
| H-Energy | 19.85 | 1.6E-05 | 1.5E-04 | 6666 | 18.7 | 2.2E-03 OK |
| +-----+-----+-----+-----+-----+-----+-----+ | | | | | | |
| Flow solver - Mass Imbalance = 6.3197E-05% | | | | | | |
| Flow solver - X Momentum Imbalance = -1.0554E-04% | | | | | | |
| Flow solver - Y Momentum Imbalance = -2.2160E-05% | | | | | | |

| | | |
|------------------------------------|---|----------------------------|
| Flow solver - Z Momentum Imbalance | = | -2.3911E-05% |
| Flow solver - Energy Imbalance | = | 8.1682E-02% |
| Heat Convected to the Fluid | = | 2.00000E+01 (2.00000E+01) |
| Heat Convected from the Fluid | = | 0.00000E+00 (0.00000E+00) |
| Convective Heat Residual | = | 2.38419E-06 |
| Maximum Solid Temperature Change | = | 2.46964E-02 |

| CSOLVER | Minimum | Location | Maximum | Location | Average | Convg |
|---------|----------|----------|----------|----------|----------|-------|
| y+ | 1.69E+00 | 38020 | 2.03E+01 | 38565 | 1.15E+01 | ok |
| htc | 2.06E+00 | 38620 | 6.33E+01 | 16330 | 1.30E+01 | |
| T-Solid | 8.13E+01 | 19646 | 9.59E+01 | 134 | 8.95E+01 | OK |

Execution terminating:
 all RMS residual AND global imbalance
 are below their target criteria.

| | |
|--|--------------|
| Computed Model Constants | |
| Turbulence length scale (Turbulence model 1) | = 1.9856E-02 |
| Turbulence velocity scale (Turbulence model 1) | = 3.8757E+00 |
| Turbulence viscosity (Turbulence Model 1) | = 8.3785E-04 |

| | |
|--|-------------|
| Boundary Mass Flow and Total Source Term Summary | |
| ADIABATIC FACES | 0.0000E+00 |
| CONVECTING FACES | 0.0000E+00 |
| INLET _FAN 1_FAN 1 | 1.0316E-02 |
| VENT 1_VENT 1 | -1.0316E-02 |
| OPEN_TETRAHEDRAL_ELEMENTS | 0.0000E+00 |
| Global Mass Balance: | 6.5193E-09 |
| Global Imbalance, in %: | 0.0001 % |

| | | | |
|--|--------------------|---------------------|---------------------|
| Boundary Momentum Flow and Total Source Term Summary | | | |
| ADIABATIC FACES | X-Comp. 2.1030E-02 | Y-Comp. -4.9326E-06 | Z-Comp. -6.8536E-06 |
| CONVECTING FACES | 1.8226E-03 | 1.2173E-05 | 3.5799E-05 |
| INLET _FAN 1_FAN 1 | -3.4416E-02 | -2.0777E-06 | 1.3107E-05 |
| VENT 1_VENT 1 | 1.1564E-02 | -5.1701E-06 | -4.2060E-05 |
| OPEN_TETRAHEDRAL_ELEMENTS | 0.0000E+00 | 0.0000E+00 | 0.0000E+00 |
| Global Momentum Balance: | -3.6322E-08 | -7.6266E-09 | -8.2291E-09 |
| Global Imbalance, in %: | -0.0001 % | 0.0000 % | 0.0000 % |

| | |
|--|-------------|
| Boundary Energy Flow and Total Source Term Summary | |
| ADIABATIC FACES | 0.0000E+00 |
| CONVECTING FACES | 2.0000E+01 |
| INLET _FAN 1_FAN 1 | 0.0000E+00 |
| VENT 1_VENT 1 | -1.9984E+01 |
| OPEN_TETRAHEDRAL_ELEMENTS | 0.0000E+00 |

```

-----+
Global Energy Balance:           1.6336E-02
Global Imbalance, in %:          0.0817 %

+-----+
|               Locations of maximum residuals
+-----+
| Equation | Node # |   X    |   Y    |   Z    |
+-----+
| U - Mom |      5962 | 1.628E-01 | 5.940E-02 | -1.914E-02
| V - Mom |      5962 | 1.628E-01 | 5.940E-02 | -1.914E-02
| W - Mom |      5984 | 1.628E-01 | 2.853E-02 | -5.114E-02
| P - Mass |      5986 | 1.628E-01 | 3.882E-02 | -5.114E-02
| H-Energy |      6666 | -1.397E-02 | 2.203E-03 | -1.270E-04
+-----+

+-----+
|               Peak Values of residuals
+-----+
| Equation | Peak occur at loop # | Peak Residual | Final Residual |
+-----+
| U - Mom |            2       | 4.22521E-02 | 1.61944E-06
| V - Mom |            2       | 5.82437E-03 | 2.97214E-07
| W - Mom |            2       | 6.24652E-03 | 1.89352E-07
| P - Mass |            2       | 1.71108E-02 | 8.26999E-08
| H-Energy |            3       | 3.02927E-02 | 1.59253E-05
+-----+

+-----+
|               Average Scale Information
+-----+
Global Length Scale      :      1.390E-01
Density Scale           :      1.089E+00
Dynamic Viscosity Scale :      1.850E-05
Advection Time Scale   :      1.140E-01
Reynolds Number         :      9.977E+03
Velocity Scale          :      1.220E+00
Prandtl Number          :      7.084E-01
Temperature Range        :      7.690E+00
Cp Scale                :      1.007E+03
Conductivity Scale      :      2.630E-02

+-----+
|               y+ information (min, max, average)
+-----+
| Face set name        | min y+ | max y+ | ave y+
+-----+
| ADIABATIC FACES     | 2.74E+00 | 2.44E+01 | 1.39E+01
| CONVECTING FACES     | 1.67E+00 | 2.03E+01 | 1.15E+01
+-----+

+-----+
|               CPU Requirements of Numerical Solution
+-----+
Equation Type      Discretization      Linear Solution
                  (secs. %total)      (secs. %total)
+-----+
Momentum-Mass     7.73E+01  50.7 %    2.83E+01  18.5 %
Scalars           2.58E+01  16.9 %    2.12E+01  13.9 %
+-----+

```

```

+-----+
|           Memory Usage Information          |
+-----+
| Peak Memory Use:      8063 Kb
| Shared Workspace:    838760 words
+-----+

+-----+
| Coupled Solution Summary
+-----+

Maximum Temperature:      95.937 at Element      134
Minimum Temperature:      81.296 at Element      19646
Average Temperature:      89.531

Maximum Heat Transfer Coefficient:      0.633E+02
Minimum Heat Transfer Coefficient:      0.206E+01
Average Heat Transfer Coefficient:      0.130E+02

Maximum Y+ Value:            0.203E+02
Minimum Y+ Value:            0.169E+01
Average Y+ Value:            0.115E+02
Percent of faces with Y+ < 30:   100.0
Percent of faces with Y+ < 11.5:  23.3

-----
ESC WARNING: Y+ Values
-----
Mesh correction is ON. The solver will compensate where Y+ values are less than 30. ( Although mesh correction is ON, it is recommended to make sure that the mesh is not too fine or that the turbulent model selected is appropriate for the flow regime.)

Heat flow into temperature B.C.s:      -0.191E-05
Heat flow from temperature B.C.s:      0.000E+00
Heat convected to fluid:                0.200E+02
Heat convected from fluid:              0.000E+00
Total heat load on non-fluid elements: 0.200E+02
Total Heat Imbalance:                 -0.153E-04
Percent Heat Imbalance:                -0.763E-04 %

Total Number Of Iterations           18
Maximum Temperature Change:        0.247E-01 at Element      38828

Maximum Temperature Change in Coupled Solution:      0.247E-01
Normalized Convective Heat Imbalance in Coupled Solution:  0.238E-05

Coupled Solve complete. Maximum boundary condition change between iterations is less than target.

Cpu time=     899.1    RSLTPOST Module

ESCR - Converting analysis results
=====
Time: Wed Jan 23 20:08:45 2002

+-----+
|           Results Recovery          |
+-----+

Recovering Velocity
Recovering Pressure
Recovering Temperature
Recovering Mass Flux

Reading fluid flow results...
Reading thermal results...
Writing results data to escrra.dat...

```

```

+-----+
|           Solution Summary           |
+-----+

Results Summary      Maximum      Minimum      Average
-----
Fluid Temperature    5.769E+01    5.000E+01    5.121E+01 C
Fluid Velocity       3.876E+00    8.299E-02    1.160E+00 m/s
Fluid Pressure       7.591E-01   -4.031E+00   -1.203E-01 Pa
Solid Temperature   9.594E+01    8.130E+01    8.953E+01 C
Y+                  2.028E+01    1.687E+00    1.154E+01
Heat Trans. Coef.   6.332E+01    2.055E+00    1.299E+01 W/m^2-C
-----


Volume/Mass Flow Summary
(Values < 0 are outflow)      Volume Flow      Mass Flow
-----
FAN 1                      9.440E-03 m^3/s    1.032E-02 kg/s
VENT 1                      -9.496E-03 m^3/s   -1.032E-02 kg/s
-----


Flow Solver:
Heat Convected To/From Fluid
(Values < 0 are outflows)      Positive Side      Negative Side
-----
FLOW SURFACE 1              2.232E+00 W      0.000E+00 W
FLOW BLOCKAGE SINK          1.777E+01 W      0.000E+00 W
-----  

Total Heat Convected to Fluid      2.000E+01 W
-----


Thermal Solver: Heat Flow
-----
Total heat load on non-fluid elements      2.000E+01 W
Heat flow from temperature B.C.s        0.000E+00 W
Heat flow into temperature B.C.s        1.907E-06 W
Heat convected to fluid                 2.000E+01 W
Heat convected from fluid               0.000E+00 W
-----  

Total Heat Imbalance                -1.526E-05 W
-----


Solver Convergence
-----
Thermal solver - Maximum temperature change      2.470E-02 C
Flow solver - Momentum imbalance            -0.00011 Percent
Flow solver - Mass imbalance                0.00006 Percent
Flow solver - Energy imbalance             0.08168 Percent
Coupled solution - Maximum temperature change 2.470E-02 C
Coupled solution - Normalized Heat Imbalance 2.384E-06
-----  

+-----+
|           END           |
+-----+


Solution elapsed time: 17 min 57 sec

```

Table B2.3 Thermal Analysis of Modified Gen-II.B IPEM (Case 8)

```

I-DEAS Electronics System Cooling
=====
Thermal/Flow Solver Software Copyright (c) 1994
MAYA Heat Transfer Technologies Ltd.

Run directory specified for ESC/TMG analysis:
/home/ypangideas/IDEAS/1-7-centeredSI/

TMG/ESC Version 8.0.0 April 3 12:00:00 EST 2000

ID2ESC - Thermal/flow model file builder
=====
Time: Wed Jan 23 19:18:04 2002

+-----+
|           Model Builder           |
+-----+

Reading model file...
...model file read.

+-----+
|           Model Summary           |
+-----+

Finite Element Model
-----

Model File: /home/ypangideas/IDEAS/1design-centersI.mf1

Current FE Study: DEFAULT FE STUDY

Number of nodes in thermal model:          8014
Number of elements in thermal model:        34184

Number of nodes in flow model:              3768
Number of elements in flow model:            15241

Solution Options
-----

Steady-State Analysis
Solution Method:                           Concurrent
Communication Frequency:                  5
Solving Flow
Solving Thermal

Ambient Temperature:                      5.000E+01 C
Ambient Pressure:                         1.014E+05 Pa

Fluid buoyancy:                            Off
Gravity Acceleration:                     9.810E+00 m/s^2
Gravity Vector:   X: 0.000E+00  Y: 0.000E+00  Z:-1.000E+00

Flow laminar/turbulent model:             Fixed viscosity

Flow solver iteration limit:               1000
Flow converged when RMS residual less than: 2.000E-04
Flow solver physical time step:          2.000E+00 s
Flow solver heat imbalance:              2.000E-02

Thermal Boundary Conditions

```

Number of thermal boundary conditions: 3

| Thermal Boundary Condition | Type | Value | FSF | TCP |
|-----------------------------|-----------|-------------|-----|-----|
| 1 - THERMAL BOUNDARY CONDIT | Heat Load | 1.200E+01 W | No | Yes |
| 2 - THERMAL BOUNDARY CONDIT | Heat Load | 7.000E+00 W | No | Yes |
| 3 - THERMAL BOUNDARY CONDIT | Heat Load | 1.000E+00 W | No | No |

Thermal Couplings

Number of thermal couplings: 10

| Thermal Coupling | Type | Value |
|-----------------------------------|------------|-----------|
| 1 - THERMAL COUPLING SI-CU | Resistance | 3.920E-02 |
| Primary Area: 1.271E-04 m^2 | | |
| Secndry Area: 2.222E-04 m^2 | | |
| 2 - THERMAL COUPLING CU TRACE-CE | Resistance | 1.000E-03 |
| Primary Area: 2.751E-04 m^2 | | |
| Secndry Area: 7.771E-04 m^2 | | |
| 3 - THERMAL COUPLING CERAMIC BAS | Resistance | 1.000E-03 |
| Primary Area: 7.771E-04 m^2 | | |
| Secndry Area: 7.771E-04 m^2 | | |
| 4 - THERMAL COUPLING CU BASE-HEA | Resistance | 3.200E-03 |
| Primary Area: 7.771E-04 m^2 | | |
| Secndry Area: 1.752E-03 m^2 | | |
| 5 - THERMAL COUPLING HEAT SPREAD | Resistance | 7.100E-02 |
| Primary Area: 1.752E-03 m^2 | | |
| Secndry Area: 5.134E-03 m^2 | | |
| 6 - THERMAL COUPLING GATE-CERAMI | Resistance | 4.960E-01 |
| Primary Area: 1.794E-04 m^2 | | |
| Secndry Area: 5.667E-04 m^2 | | |
| 7 - THERMAL COUPLING CERAMIC-GEL | Resistance | 2.500E-03 |
| Primary Area: 5.667E-04 m^2 | | |
| Secndry Area: 4.705E-04 m^2 | | |
| 8 - THERMAL COUPLING GEL-CERAMIC | Resistance | 2.500E-03 |
| Primary Area: 4.705E-04 m^2 | | |
| Secndry Area: 7.771E-04 m^2 | | |
| 9 - THERMAL COUPLING CERAMIC-SI | Resistance | 2.569E+01 |
| Primary Area: 5.536E-05 m^2 | | |
| Secndry Area: 5.537E-05 m^2 | | |
| 10 - THERMAL COUPLING CU TRACE-SI | Resistance | 3.000E-03 |
| Primary Area: 1.271E-04 m^2 | | |
| Secndry Area: 1.259E-04 m^2 | | |

Flow Surfaces

Number of flow surfaces: 2

| Flow Surface | Surface Properties | | | Elements |
|--------------------------------|--------------------|------------|-------|----------|
| | +ve side | -ve side | Surfc | Atchd |
| 1 - FLOW SURFACE SINK | SURFACE PR | SURFACE PR | 228 | 0 |
| Area: 5.134E-03 m^2 | | | | |
| 2 - FLOW SURFACE HEAT SPREADER | SURFACE PR | SURFACE PR | 1388 | 0 |
| Area: 1.752E-03 m^2 | | | | |

Flow Blockages

Number of flow blockages: 2

| Flow Blockage | Type | Loss Coeff |
|---------------|------|------------|
|---------------|------|------------|

```

1 - FLOW BLOCKAGE SINK           Auto-convect 0.000E+00 1/m
    Volume: 6.807E-05 m^3
2 - FLOW BLOCKAGE HEAT SPREADER Auto-convect 0.000E+00 1/m
    Volume: 8.759E-06 m^3
-----
Fans
-----
Number of fans: 1
Fan          Type      Value
-----
1 - Inlet - FAN 1             Vol. Flow  9.440E-03 m^3/s
    Area: 2.449E-03 m^2
-----
Vents
-----
Number of vents: 1
Vent          Type
-----
1 - VENT 1                  Ambient
    Area: 8.478E-03 m^2
-----
Performing mesh checks...
- interior and warping angle
  checks on fluid elements...
  ...angle checks on fluid
  elements completed.

- interior and warping angle
  checks on thermal elements...

+-----+
| ID2ESC - WARNING 1205           GRP001 |
+-----+
| Thermal element(s) with interior angles < 1 deg. found. This may
| result convergence problems.

| List of element labels:
|   37891  38027
| Number of elements found: 2
+-----+
  ...angle checks on thermal
  elements completed.

- coincident node check
  on fluid model...
  ...node check on fluid
  model completed.

- coincident node check
  on thermal model...

+-----+
| ID2ESC - WARNING 1214           GRP002 |
+-----+
| Coincident thermal nodes found. If the air mesh was generated
| with the PEX Mesher, you can probably ignore this message. If not
| perform a coincident node check on the model.

| Pairs of coincident node labels:
|   9375,     9876 /     9467,     9907 /     9466,     9908
|   9465,     9909 /     9464,     9910 /     9463,     9911
|   9462,     9912 /     9461,     9913 /     9460,     9914

```

```

|      9459,      9915 /      9458,      9916 /      9457,      9917
|      9456,      9918 /      9455,      9919 /      9376,      9875
|      9442,      9932 /      9480,      9894 /      9443,      9931
|      9479,      9895 /      9444,      9930 /      9478,      9896
|      9445,      9929 /      9477,      9897 /      9446,      9928
| ... list too long to display.
| Number of coincident nodes found:      322
+-----+
| ...node check on thermal
|   model completed.

...mesh checks completed.

Building free face list...
...found      4858 free faces.

Processing flow blockages...
...Blockage  1 done,
...Blockage  2 done.

Processing fans...

- Building entity face list...
  ...found      92 entity faces.
...Fan  1 done.

Processing vents...

- Building entity face list...
  ...found      137 entity faces.
...Vent  1 done.

Processing flow surfaces...

- Building entity face list...
  ...found      66 entity faces.
+-----+
| ID2ESC - WARNING 1144
+-----+
| Flow Surface  1 - FLOW SURFACE SINK
| More than 35.1% of the flow surface is not in contact with the
| fluid. This may be caused by a mis-alignment of the flow surface
| with the fluid nodes, or by other entities which are overlapping
| the present flow surface.
+-----+

...Flow Surface  1 done,

- Building entity face list...
  ...found      125 entity faces.
+-----+
| ID2ESC - WARNING 1144
+-----+
| Flow Surface  2 - FLOW SURFACE HEAT SPREADER
| More than 43.9% of the flow surface is not in contact with the
| fluid. This may be caused by a mis-alignment of the flow surface
| with the fluid nodes, or by other entities which are overlapping
| the present flow surface.
+-----+

...Flow Surface  2 done,

- Processing flow surfaces
  due to convective blockage...
  ...done.

Flow Model Conditions:
-----+

```

```

Total Fluid Volume available for Flow: 2.6761E-03 m^3

Estimated Characteristic Velocity:      1.3744E+00 m/s
Estimated Characteristic Length:        1.3879E-01 m
Approximate Reynolds number:           1.2445E+04
Approximate Mach number:              4.0077E-03
Approximate Grashof number:            3.8070E+05

Number of Flow Sub-domains:          1

Writing flow model files...
...done.

Writing thermal model files...
...done.

Executing Coupled Thermal/Flow Solver

COUPLED - Coupled Flow/Thermal analysis
=====
Time: Wed Jan 23 19:19:10 2002

+-----+
| Preparing Thermal Model - Elapsed Time: 01 min 14 sec |
+-----+

Cpu time=      0.0      MAIN Module
Cpu time=      4.0      DATACH Module
Cpu time=     61.5      ECHOS Module
Cpu time=    86.2      COND Module
Cpu time=   165.9      VUFAC Module
Cpu time=   320.8      MEREL Module
Cpu time=   586.9      ANP Module

+-----+
| Solving ESC Model - Elapsed Time: 12 min 37 sec |
+-----+

+-----+
| Initialization Information |
+-----+

Pressure-Gradients array not found in FLI file.
Zero initial values will be used.

+-----+
| Average Scale Information |
+-----+

Global Length Scale      :      1.388E-01
Density Scale            :      1.093E+00
Dynamic Viscosity Scale :      1.850E-05
Velocity Scale           :      0.000E+00
Prandtl Number          :      7.084E-01
Cp Scale                 :      1.007E+03
Conductivity Scale       :      2.630E-02

+-----+
| Convergence History |
+-----+

TIME STEP =    1    SIMULATION TIME = 2.00E+00    CPU SECONDS = 3.93E+00
-----
| Equation | Rate | RMS Res | Max Res | Location | Linear Solution |

```

| Time Step 1: Simulation Time = 0.00E+00 CPU Seconds = 0.00E+00 | | | | | | |
|---|--|--|--|--|--|--|
| U - Mom 0.00 3.8E-02 5.5E-01 2909 2.7E-02 OK | | | | | | |
| V - Mom 0.00 0.0E+00 0.0E+00 0 0.0E+00 OK | | | | | | |
| W - Mom 0.00 0.0E+00 0.0E+00 0 0.0E+00 OK | | | | | | |
| P - Mass 0.00 3.9E-04 5.4E-03 2929 16.5 6.9E-02 OK | | | | | | |
| +-----+-----+-----+-----+-----+-----+-----+ | | | | | | |
| H-Energy 0.00 0.0E+00 0.0E+00 0 5.4 0.0E+00 OK | | | | | | |
| +-----+-----+-----+-----+-----+-----+-----+ | | | | | | |
| Flow solver - Mass Imbalance = 0.0000E+00% | | | | | | |
| Flow solver - X Momentum Imbalance = 0.0000E+00% | | | | | | |
| Flow solver - Y Momentum Imbalance = 0.0000E+00% | | | | | | |
| Flow solver - Z Momentum Imbalance = 0.0000E+00% | | | | | | |
| Flow solver - Energy Imbalance = 0.0000E+00% | | | | | | |
| TIME STEP = 2 SIMULATION TIME = 4.00E+00 CPU SECONDS = 1.26E+01 | | | | | | |
| Time Step 2: Simulation Time = 4.00E+00 CPU Seconds = 1.26E+01 | | | | | | |
| +-----+-----+-----+-----+-----+-----+-----+ | | | | | | |
| Equation Rate RMS Res Max Res Location Linear Solution | | | | | | |
| +-----+-----+-----+-----+-----+-----+-----+ | | | | | | |
| U - Mom 1.24 4.7E-02 3.6E-01 2845 6.3E-03 OK | | | | | | |
| V - Mom 0.00 7.5E-03 1.1E-01 2930 1.9E-02 OK | | | | | | |
| W - Mom 0.00 7.8E-03 1.1E-01 2924 2.3E-02 OK | | | | | | |
| P - Mass 53.25 2.1E-02 3.5E-01 2929 8.7 6.3E-02 OK | | | | | | |
| +-----+-----+-----+-----+-----+-----+-----+ | | | | | | |
| H-Energy 0.00 0.0E+00 0.0E+00 0 5.4 0.0E+00 OK | | | | | | |
| +-----+-----+-----+-----+-----+-----+-----+ | | | | | | |
| Flow solver - Mass Imbalance = 7.5663E+00% | | | | | | |
| Flow solver - X Momentum Imbalance = -8.7736E+01% | | | | | | |
| Flow solver - Y Momentum Imbalance = 2.6818E-02% | | | | | | |
| Flow solver - Z Momentum Imbalance = 1.8953E-02% | | | | | | |
| Flow solver - Energy Imbalance = 0.0000E+00% | | | | | | |
| TIME STEP = 3 SIMULATION TIME = 6.00E+00 CPU SECONDS = 1.99E+01 | | | | | | |
| Time Step 3: Simulation Time = 6.00E+00 CPU Seconds = 1.99E+01 | | | | | | |
| +-----+-----+-----+-----+-----+-----+-----+ | | | | | | |
| Equation Rate RMS Res Max Res Location Linear Solution | | | | | | |
| +-----+-----+-----+-----+-----+-----+-----+ | | | | | | |
| U - Mom 0.36 1.7E-02 1.2E-01 2953 9.2E-03 OK | | | | | | |
| V - Mom 0.40 3.0E-03 3.3E-02 3826 2.5E-02 OK | | | | | | |
| W - Mom 0.55 4.3E-03 4.7E-02 3525 2.1E-02 OK | | | | | | |
| P - Mass 0.35 7.4E-03 1.1E-01 2824 8.8 1.5E-02 OK | | | | | | |
| +-----+-----+-----+-----+-----+-----+-----+ | | | | | | |
| H-Energy 0.00 4.0E-02 5.1E-01 4504 14.2 8.3E-03 OK | | | | | | |
| +-----+-----+-----+-----+-----+-----+-----+ | | | | | | |
| Flow solver - Mass Imbalance = 2.1244E+00% | | | | | | |
| Flow solver - X Momentum Imbalance = -5.1710E+01% | | | | | | |
| Flow solver - Y Momentum Imbalance = 7.5885E-02% | | | | | | |
| Flow solver - Z Momentum Imbalance = -2.9192E-01% | | | | | | |
| Flow solver - Energy Imbalance = 0.0000E+00% | | | | | | |
| Heat Convected to the Fluid = 2.00000E+01 (2.00000E+01) | | | | | | |
| Heat Convected from the Fluid = 0.00000E+00 (0.00000E+00) | | | | | | |
| Convective Heat Residual = 1.90735E-07 | | | | | | |
| Maximum Solid Temperature Change = 8.37871E+01 | | | | | | |
| +-----+-----+-----+-----+-----+-----+-----+ | | | | | | |
| CSOLVER Minimum Location Maximum Location Average Convg | | | | | | |
| +-----+-----+-----+-----+-----+-----+-----+ | | | | | | |
| y+ 2.57E+00 51076 1.63E+01 51522 9.70E+00 LO | | | | | | |
| htc 1.97E+00 51100 1.40E+02 2158 1.31E+01 | | | | | | |
| T-Solid 7.86E+01 48205 8.85E+01 29778 8.33E+01 OK | | | | | | |
| +-----+-----+-----+-----+-----+-----+-----+ | | | | | | |
| TIME STEP = 4 SIMULATION TIME = 8.00E+00 CPU SECONDS = 2.83E+01 | | | | | | |
| Time Step 4: Simulation Time = 8.00E+00 CPU Seconds = 2.83E+01 | | | | | | |
| +-----+-----+-----+-----+-----+-----+-----+ | | | | | | |
| Equation Rate RMS Res Max Res Location Linear Solution | | | | | | |
| +-----+-----+-----+-----+-----+-----+-----+ | | | | | | |
| U - Mom 0.56 9.5E-03 1.0E-01 3838 7.3E-03 OK | | | | | | |
| V - Mom 0.48 1.5E-03 1.7E-02 3836 2.6E-02 OK | | | | | | |
| W - Mom 0.48 2.1E-03 2.0E-02 3730 1.4E-02 OK | | | | | | |

| |
|--|
| P - Mass 0.18 1.3E-03 1.9E-02 3812 8.8 1.7E-02 OK |
| +-----+-----+-----+-----+-----+-----+ |
| H-Energy 0.18 7.1E-03 8.1E-02 4504 14.1 9.3E-03 OK |
| +-----+-----+-----+-----+-----+-----+ |
| Flow solver - Mass Imbalance = 5.6672E-01% |
| Flow solver - X Momentum Imbalance = -1.4087E+01% |
| Flow solver - Y Momentum Imbalance = -1.3452E-03% |
| Flow solver - Z Momentum Imbalance = -2.1685E-01% |
| Flow solver - Energy Imbalance = 2.6145E+01% |
| TIME STEP = 5 SIMULATION TIME = 1.00E+01 CPU SECONDS = 3.64E+01 |
| +-----+-----+-----+-----+-----+-----+ |
| Equation Rate RMS Res Max Res Location Linear Solution |
| +-----+-----+-----+-----+-----+-----+ |
| U - Mom 0.48 4.6E-03 6.9E-02 3838 6.8E-03 OK |
| V - Mom 0.48 7.0E-04 1.7E-02 3836 2.6E-02 OK |
| W - Mom 0.43 8.8E-04 1.2E-02 5031 2.2E-02 OK |
| P - Mass 0.44 5.8E-04 7.7E-03 3513 8.8 1.3E-02 OK |
| +-----+-----+-----+-----+-----+-----+ |
| H-Energy 0.22 1.6E-03 1.4E-02 3123 14.2 9.4E-03 OK |
| +-----+-----+-----+-----+-----+-----+ |
| Flow solver - Mass Imbalance = 1.5542E-01% |
| Flow solver - X Momentum Imbalance = -2.7465E+00% |
| Flow solver - Y Momentum Imbalance = -2.9865E-03% |
| Flow solver - Z Momentum Imbalance = -1.0345E-01% |
| Flow solver - Energy Imbalance = 6.1593E+00% |
| TIME STEP = 6 SIMULATION TIME = 1.20E+01 CPU SECONDS = 4.42E+01 |
| +-----+-----+-----+-----+-----+-----+ |
| Equation Rate RMS Res Max Res Location Linear Solution |
| +-----+-----+-----+-----+-----+-----+ |
| U - Mom 0.47 2.2E-03 3.9E-02 2967 5.5E-03 OK |
| V - Mom 0.41 2.9E-04 5.5E-03 3836 2.8E-02 OK |
| W - Mom 0.38 3.4E-04 3.9E-03 5213 1.7E-02 OK |
| P - Mass 0.56 3.2E-04 4.4E-03 2824 8.7 6.9E-03 OK |
| +-----+-----+-----+-----+-----+-----+ |
| H-Energy 0.26 4.1E-04 2.4E-03 4202 14.2 9.8E-03 OK |
| +-----+-----+-----+-----+-----+-----+ |
| Flow solver - Mass Imbalance = 4.2892E-02% |
| Flow solver - X Momentum Imbalance = -1.8049E-02% |
| Flow solver - Y Momentum Imbalance = 8.6976E-03% |
| Flow solver - Z Momentum Imbalance = -8.0221E-02% |
| Flow solver - Energy Imbalance = 1.5540E+00% |
| TIME STEP = 7 SIMULATION TIME = 1.40E+01 CPU SECONDS = 5.20E+01 |
| +-----+-----+-----+-----+-----+-----+ |
| Equation Rate RMS Res Max Res Location Linear Solution |
| +-----+-----+-----+-----+-----+-----+ |
| U - Mom 0.49 1.1E-03 2.3E-02 2967 6.2E-03 OK |
| V - Mom 0.45 1.3E-04 2.9E-03 3838 2.9E-02 OK |
| W - Mom 0.49 1.6E-04 2.2E-03 3836 2.3E-02 OK |
| P - Mass 0.62 2.0E-04 2.9E-03 2824 8.7 6.9E-03 OK |
| +-----+-----+-----+-----+-----+-----+ |
| H-Energy 0.35 1.4E-04 8.4E-04 4202 14.2 9.5E-03 OK |
| +-----+-----+-----+-----+-----+-----+ |
| Flow solver - Mass Imbalance = 1.1646E-02% |
| Flow solver - X Momentum Imbalance = 2.7818E-01% |
| Flow solver - Y Momentum Imbalance = 1.7667E-03% |
| Flow solver - Z Momentum Imbalance = -3.5969E-02% |
| Flow solver - Energy Imbalance = 4.4868E-01% |
| TIME STEP = 8 SIMULATION TIME = 1.60E+01 CPU SECONDS = 6.01E+01 |
| +-----+-----+-----+-----+-----+-----+ |
| Equation Rate RMS Res Max Res Location Linear Solution |
| +-----+-----+-----+-----+-----+-----+ |
| U - Mom 0.50 5.2E-04 1.3E-02 2967 6.1E-03 OK |
| V - Mom 0.48 6.3E-05 1.1E-03 3838 2.7E-02 OK |

| |
|---|
| W - Mom 0.55 9.1E-05 1.1E-03 3836 2.6E-02 OK |
| P - Mass 0.54 1.1E-04 1.3E-03 2824 8.8 5.3E-03 OK |
| +-----+-----+-----+-----+-----+-----+-----+ |
| H-Energy 14.45 2.0E-03 2.5E-02 3133 14.2 1.0E-02 OK |
| +-----+-----+-----+-----+-----+-----+-----+ |
| Flow solver - Mass Imbalance = 3.1237E-03% |
| Flow solver - X Momentum Imbalance = 1.3735E-01% |
| Flow solver - Y Momentum Imbalance = -2.2433E-03% |
| Flow solver - Z Momentum Imbalance = -1.5451E-02% |
| Flow solver - Energy Imbalance = 8.6999E+00% |
| Heat Convected to the Fluid = 2.00000E+01 (1.99924E+01) |
| Heat Convected from the Fluid = 0.00000E+00 (0.00000E+00) |
| Convective Heat Residual = 3.80684E-04 |
| Maximum Solid Temperature Change = 1.14709E+00 |
| +-----+-----+-----+-----+-----+-----+-----+ |
| CSOLVER Minimum Location Maximum Location Average Convg |
| +-----+-----+-----+-----+-----+-----+-----+ |
| y+ 2.20E+00 51081 2.14E+01 51518 1.22E+01 ok |
| htc 1.96E+00 51100 1.37E+02 2158 1.38E+01 |
| T-Solid 7.95E+01 47218 8.95E+01 29778 8.44E+01 OK |
| +-----+-----+-----+-----+-----+-----+-----+ |
| TIME STEP = 9 SIMULATION TIME = 1.80E+01 CPU SECONDS = 6.84E+01 |
| +-----+-----+-----+-----+-----+-----+-----+ |
| Equation Rate RMS Res Max Res Location Linear Solution |
| +-----+-----+-----+-----+-----+-----+-----+ |
| U - Mom 0.51 2.7E-04 6.7E-03 2967 6.5E-03 OK |
| V - Mom 0.51 3.2E-05 4.9E-04 3840 2.7E-02 OK |
| W - Mom 0.53 4.8E-05 5.6E-04 3822 2.9E-02 OK |
| P - Mass 0.48 5.3E-05 5.5E-04 2828 8.7 6.1E-03 OK |
| +-----+-----+-----+-----+-----+-----+-----+ |
| H-Energy 0.25 5.1E-04 6.1E-03 3133 14.2 1.0E-02 OK |
| +-----+-----+-----+-----+-----+-----+-----+ |
| Flow solver - Mass Imbalance = 5.6877E-04% |
| Flow solver - X Momentum Imbalance = 4.4436E-02% |
| Flow solver - Y Momentum Imbalance = -8.5441E-04% |
| Flow solver - Z Momentum Imbalance = -7.7597E-03% |
| Flow solver - Energy Imbalance = 2.2105E+00% |
| TIME STEP = 10 SIMULATION TIME = 2.00E+01 CPU SECONDS = 7.62E+01 |
| +-----+-----+-----+-----+-----+-----+-----+ |
| Equation Rate RMS Res Max Res Location Linear Solution |
| +-----+-----+-----+-----+-----+-----+-----+ |
| U - Mom 0.52 1.4E-04 3.4E-03 2967 6.7E-03 OK |
| V - Mom 0.53 1.7E-05 2.6E-04 3822 2.5E-02 OK |
| W - Mom 0.52 2.5E-05 3.9E-04 3822 3.0E-02 OK |
| P - Mass 0.45 2.4E-05 2.7E-04 2828 8.7 6.0E-03 OK |
| +-----+-----+-----+-----+-----+-----+-----+ |
| H-Energy 0.26 1.3E-04 1.5E-03 3133 14.2 9.8E-03 OK |
| +-----+-----+-----+-----+-----+-----+-----+ |
| Flow solver - Mass Imbalance = 5.4169E-05% |
| Flow solver - X Momentum Imbalance = 8.3243E-03% |
| Flow solver - Y Momentum Imbalance = 1.0511E-04% |
| Flow solver - Z Momentum Imbalance = -3.6579E-03% |
| Flow solver - Energy Imbalance = 5.4691E-01% |
| TIME STEP = 11 SIMULATION TIME = 2.20E+01 CPU SECONDS = 8.40E+01 |
| +-----+-----+-----+-----+-----+-----+-----+ |
| Equation Rate RMS Res Max Res Location Linear Solution |
| +-----+-----+-----+-----+-----+-----+-----+ |
| U - Mom 0.52 7.3E-05 1.7E-03 2967 6.8E-03 OK |
| V - Mom 0.54 9.2E-06 1.8E-04 3822 2.4E-02 OK |
| W - Mom 0.52 1.3E-05 2.4E-04 3822 2.9E-02 OK |
| P - Mass 0.44 1.0E-05 1.3E-04 2829 8.7 6.4E-03 OK |
| +-----+-----+-----+-----+-----+-----+-----+ |
| H-Energy 0.26 3.4E-05 3.6E-04 3133 14.2 9.5E-03 OK |

| Flow solver - Mass Imbalance | = | -7.2225E-05% | | | | | | | | | | | | | | | | | | | | | | | | | | | | | | | | | | | | | | | |
|---|----------|----------------------------|----------|----------|-----------------|----------|---------|----------|---------|----------|-----------------|---------|----------|---------|----------|-------|-------------|---------|----------|---------|----------|------|------------|---------|----------|---------|----------|-------|-------------|----------|------|---------|---------|------|----------------|----------|-------|---------|---------|------|-----------------|
| Flow solver - X Momentum Imbalance | = | 3.7094E-04% | | | | | | | | | | | | | | | | | | | | | | | | | | | | | | | | | | | | | | | |
| Flow solver - Y Momentum Imbalance | = | 1.3116E-04% | | | | | | | | | | | | | | | | | | | | | | | | | | | | | | | | | | | | | | | |
| Flow solver - Z Momentum Imbalance | = | -1.6271E-03% | | | | | | | | | | | | | | | | | | | | | | | | | | | | | | | | | | | | | | | |
| Flow solver - Energy Imbalance | = | 1.3820E-01% | | | | | | | | | | | | | | | | | | | | | | | | | | | | | | | | | | | | | | | |
| TIME STEP = 12 SIMULATION TIME = 2.40E+01 CPU SECONDS = 9.19E+01 | | | | | | | | | | | | | | | | | | | | | | | | | | | | | | | | | | | | | | | | | |
| <table border="1"> <thead> <tr><th>Equation</th><th>Rate</th><th>RMS Res</th><th>Max Res</th><th>Location</th><th>Linear Solution</th></tr> </thead> <tbody> <tr><td>U - Mom</td><td>0.53</td><td>3.8E-05</td><td>8.2E-04</td><td>2967</td><td>6.9E-03 OK</td></tr> <tr><td>V - Mom</td><td>0.55</td><td>5.0E-06</td><td>1.1E-04</td><td>3822</td><td>2.3E-02 OK</td></tr> <tr><td>W - Mom</td><td>0.53</td><td>7.0E-06</td><td>1.3E-04</td><td>3822</td><td>2.8E-02 OK</td></tr> <tr><td>P - Mass</td><td>0.44</td><td>4.6E-06</td><td>6.3E-05</td><td>2829</td><td>8.7 6.9E-03 OK</td></tr> <tr><td>H-Energy</td><td>0.27</td><td>9.3E-06</td><td>8.4E-05</td><td>3133</td><td>14.2 9.4E-03 OK</td></tr> </tbody> </table> | | | | | | Equation | Rate | RMS Res | Max Res | Location | Linear Solution | U - Mom | 0.53 | 3.8E-05 | 8.2E-04 | 2967 | 6.9E-03 OK | V - Mom | 0.55 | 5.0E-06 | 1.1E-04 | 3822 | 2.3E-02 OK | W - Mom | 0.53 | 7.0E-06 | 1.3E-04 | 3822 | 2.8E-02 OK | P - Mass | 0.44 | 4.6E-06 | 6.3E-05 | 2829 | 8.7 6.9E-03 OK | H-Energy | 0.27 | 9.3E-06 | 8.4E-05 | 3133 | 14.2 9.4E-03 OK |
| Equation | Rate | RMS Res | Max Res | Location | Linear Solution | | | | | | | | | | | | | | | | | | | | | | | | | | | | | | | | | | | | |
| U - Mom | 0.53 | 3.8E-05 | 8.2E-04 | 2967 | 6.9E-03 OK | | | | | | | | | | | | | | | | | | | | | | | | | | | | | | | | | | | | |
| V - Mom | 0.55 | 5.0E-06 | 1.1E-04 | 3822 | 2.3E-02 OK | | | | | | | | | | | | | | | | | | | | | | | | | | | | | | | | | | | | |
| W - Mom | 0.53 | 7.0E-06 | 1.3E-04 | 3822 | 2.8E-02 OK | | | | | | | | | | | | | | | | | | | | | | | | | | | | | | | | | | | | |
| P - Mass | 0.44 | 4.6E-06 | 6.3E-05 | 2829 | 8.7 6.9E-03 OK | | | | | | | | | | | | | | | | | | | | | | | | | | | | | | | | | | | | |
| H-Energy | 0.27 | 9.3E-06 | 8.4E-05 | 3133 | 14.2 9.4E-03 OK | | | | | | | | | | | | | | | | | | | | | | | | | | | | | | | | | | | | |
| Flow solver - Mass Imbalance | = | -9.0281E-05% | | | | | | | | | | | | | | | | | | | | | | | | | | | | | | | | | | | | | | | |
| Flow solver - X Momentum Imbalance | = | -5.9733E-04% | | | | | | | | | | | | | | | | | | | | | | | | | | | | | | | | | | | | | | | |
| Flow solver - Y Momentum Imbalance | = | 1.0660E-04% | | | | | | | | | | | | | | | | | | | | | | | | | | | | | | | | | | | | | | | |
| Flow solver - Z Momentum Imbalance | = | -6.9995E-04% | | | | | | | | | | | | | | | | | | | | | | | | | | | | | | | | | | | | | | | |
| Flow solver - Energy Imbalance | = | 3.6158E-02% | | | | | | | | | | | | | | | | | | | | | | | | | | | | | | | | | | | | | | | |
| TIME STEP = 13 SIMULATION TIME = 2.60E+01 CPU SECONDS = 9.97E+01 | | | | | | | | | | | | | | | | | | | | | | | | | | | | | | | | | | | | | | | | | |
| <table border="1"> <thead> <tr><th>Equation</th><th>Rate</th><th>RMS Res</th><th>Max Res</th><th>Location</th><th>Linear Solution</th></tr> </thead> <tbody> <tr><td>U - Mom</td><td>0.53</td><td>2.0E-05</td><td>4.1E-04</td><td>2967</td><td>7.0E-03 OK</td></tr> <tr><td>V - Mom</td><td>0.55</td><td>2.8E-06</td><td>6.3E-05</td><td>3822</td><td>2.3E-02 OK</td></tr> <tr><td>W - Mom</td><td>0.54</td><td>3.8E-06</td><td>7.8E-05</td><td>2978</td><td>2.7E-02 OK</td></tr> <tr><td>P - Mass</td><td>0.45</td><td>2.1E-06</td><td>3.0E-05</td><td>2829</td><td>8.7 7.7E-03 OK</td></tr> <tr><td>H-Energy</td><td>23.21</td><td>2.1E-04</td><td>2.6E-03</td><td>3131</td><td>14.2 9.7E-03 OK</td></tr> </tbody> </table> | | | | | | Equation | Rate | RMS Res | Max Res | Location | Linear Solution | U - Mom | 0.53 | 2.0E-05 | 4.1E-04 | 2967 | 7.0E-03 OK | V - Mom | 0.55 | 2.8E-06 | 6.3E-05 | 3822 | 2.3E-02 OK | W - Mom | 0.54 | 3.8E-06 | 7.8E-05 | 2978 | 2.7E-02 OK | P - Mass | 0.45 | 2.1E-06 | 3.0E-05 | 2829 | 8.7 7.7E-03 OK | H-Energy | 23.21 | 2.1E-04 | 2.6E-03 | 3131 | 14.2 9.7E-03 OK |
| Equation | Rate | RMS Res | Max Res | Location | Linear Solution | | | | | | | | | | | | | | | | | | | | | | | | | | | | | | | | | | | | |
| U - Mom | 0.53 | 2.0E-05 | 4.1E-04 | 2967 | 7.0E-03 OK | | | | | | | | | | | | | | | | | | | | | | | | | | | | | | | | | | | | |
| V - Mom | 0.55 | 2.8E-06 | 6.3E-05 | 3822 | 2.3E-02 OK | | | | | | | | | | | | | | | | | | | | | | | | | | | | | | | | | | | | |
| W - Mom | 0.54 | 3.8E-06 | 7.8E-05 | 2978 | 2.7E-02 OK | | | | | | | | | | | | | | | | | | | | | | | | | | | | | | | | | | | | |
| P - Mass | 0.45 | 2.1E-06 | 3.0E-05 | 2829 | 8.7 7.7E-03 OK | | | | | | | | | | | | | | | | | | | | | | | | | | | | | | | | | | | | |
| H-Energy | 23.21 | 2.1E-04 | 2.6E-03 | 3131 | 14.2 9.7E-03 OK | | | | | | | | | | | | | | | | | | | | | | | | | | | | | | | | | | | | |
| Flow solver - Mass Imbalance | = | -8.1253E-05% | | | | | | | | | | | | | | | | | | | | | | | | | | | | | | | | | | | | | | | |
| Flow solver - X Momentum Imbalance | = | -3.4640E-04% | | | | | | | | | | | | | | | | | | | | | | | | | | | | | | | | | | | | | | | |
| Flow solver - Y Momentum Imbalance | = | 7.5959E-05% | | | | | | | | | | | | | | | | | | | | | | | | | | | | | | | | | | | | | | | |
| Flow solver - Z Momentum Imbalance | = | -2.8745E-04% | | | | | | | | | | | | | | | | | | | | | | | | | | | | | | | | | | | | | | | |
| Flow solver - Energy Imbalance | = | 8.3833E-01% | | | | | | | | | | | | | | | | | | | | | | | | | | | | | | | | | | | | | | | |
| Heat Convected to the Fluid | = | 2.00000E+01 (1.99995E+01) | | | | | | | | | | | | | | | | | | | | | | | | | | | | | | | | | | | | | | | |
| Heat Convected from the Fluid | = | 0.00000E+00 (0.00000E+00) | | | | | | | | | | | | | | | | | | | | | | | | | | | | | | | | | | | | | | | |
| Convective Heat Residual | = | 2.44144E-05 | | | | | | | | | | | | | | | | | | | | | | | | | | | | | | | | | | | | | | | |
| Maximum Solid Temperature Change | = | 2.36259E-01 | | | | | | | | | | | | | | | | | | | | | | | | | | | | | | | | | | | | | | | |
| <table border="1"> <thead> <tr><th>CSOLVER</th><th>Minimum</th><th>Location</th><th>Maximum</th><th>Location</th><th>Average Convg</th></tr> </thead> <tbody> <tr><td>y+</td><td>2.19E+00</td><td>51447</td><td>2.16E+01</td><td>51518</td><td>1.22E+01 ok</td></tr> <tr><td>htc</td><td>1.96E+00</td><td>51100</td><td>1.37E+02</td><td>2158</td><td>1.38E+01</td></tr> <tr><td>T-Solid</td><td>7.97E+01</td><td>47218</td><td>8.97E+01</td><td>29778</td><td>8.46E+01 OK</td></tr> </tbody> </table> | | | | | | CSOLVER | Minimum | Location | Maximum | Location | Average Convg | y+ | 2.19E+00 | 51447 | 2.16E+01 | 51518 | 1.22E+01 ok | htc | 1.96E+00 | 51100 | 1.37E+02 | 2158 | 1.38E+01 | T-Solid | 7.97E+01 | 47218 | 8.97E+01 | 29778 | 8.46E+01 OK | | | | | | | | | | | | |
| CSOLVER | Minimum | Location | Maximum | Location | Average Convg | | | | | | | | | | | | | | | | | | | | | | | | | | | | | | | | | | | | |
| y+ | 2.19E+00 | 51447 | 2.16E+01 | 51518 | 1.22E+01 ok | | | | | | | | | | | | | | | | | | | | | | | | | | | | | | | | | | | | |
| htc | 1.96E+00 | 51100 | 1.37E+02 | 2158 | 1.38E+01 | | | | | | | | | | | | | | | | | | | | | | | | | | | | | | | | | | | | |
| T-Solid | 7.97E+01 | 47218 | 8.97E+01 | 29778 | 8.46E+01 OK | | | | | | | | | | | | | | | | | | | | | | | | | | | | | | | | | | | | |
| TIME STEP = 14 SIMULATION TIME = 2.80E+01 CPU SECONDS = 1.08E+02 | | | | | | | | | | | | | | | | | | | | | | | | | | | | | | | | | | | | | | | | | |
| <table border="1"> <thead> <tr><th>Equation</th><th>Rate</th><th>RMS Res</th><th>Max Res</th><th>Location</th><th>Linear Solution</th></tr> </thead> <tbody> <tr><td>U - Mom</td><td>0.53</td><td>1.1E-05</td><td>2.1E-04</td><td>4658</td><td>7.9E-03 OK</td></tr> <tr><td>V - Mom</td><td>0.55</td><td>1.5E-06</td><td>3.5E-05</td><td>3822</td><td>2.6E-02 OK</td></tr> <tr><td>W - Mom</td><td>0.54</td><td>2.1E-06</td><td>5.0E-05</td><td>2978</td><td>2.9E-02 OK</td></tr> <tr><td>P - Mass</td><td>0.47</td><td>9.6E-07</td><td>1.5E-05</td><td>2829</td><td>8.7 1.2E-02 OK</td></tr> <tr><td>H-Energy</td><td>0.25</td><td>5.5E-05</td><td>6.7E-04</td><td>3131</td><td>14.2 9.4E-03 OK</td></tr> </tbody> </table> | | | | | | Equation | Rate | RMS Res | Max Res | Location | Linear Solution | U - Mom | 0.53 | 1.1E-05 | 2.1E-04 | 4658 | 7.9E-03 OK | V - Mom | 0.55 | 1.5E-06 | 3.5E-05 | 3822 | 2.6E-02 OK | W - Mom | 0.54 | 2.1E-06 | 5.0E-05 | 2978 | 2.9E-02 OK | P - Mass | 0.47 | 9.6E-07 | 1.5E-05 | 2829 | 8.7 1.2E-02 OK | H-Energy | 0.25 | 5.5E-05 | 6.7E-04 | 3131 | 14.2 9.4E-03 OK |
| Equation | Rate | RMS Res | Max Res | Location | Linear Solution | | | | | | | | | | | | | | | | | | | | | | | | | | | | | | | | | | | | |
| U - Mom | 0.53 | 1.1E-05 | 2.1E-04 | 4658 | 7.9E-03 OK | | | | | | | | | | | | | | | | | | | | | | | | | | | | | | | | | | | | |
| V - Mom | 0.55 | 1.5E-06 | 3.5E-05 | 3822 | 2.6E-02 OK | | | | | | | | | | | | | | | | | | | | | | | | | | | | | | | | | | | | |
| W - Mom | 0.54 | 2.1E-06 | 5.0E-05 | 2978 | 2.9E-02 OK | | | | | | | | | | | | | | | | | | | | | | | | | | | | | | | | | | | | |
| P - Mass | 0.47 | 9.6E-07 | 1.5E-05 | 2829 | 8.7 1.2E-02 OK | | | | | | | | | | | | | | | | | | | | | | | | | | | | | | | | | | | | |
| H-Energy | 0.25 | 5.5E-05 | 6.7E-04 | 3131 | 14.2 9.4E-03 OK | | | | | | | | | | | | | | | | | | | | | | | | | | | | | | | | | | | | |
| Flow solver - Mass Imbalance | = | -1.0834E-04% | | | | | | | | | | | | | | | | | | | | | | | | | | | | | | | | | | | | | | | |
| Flow solver - X Momentum Imbalance | = | -1.9639E-04% | | | | | | | | | | | | | | | | | | | | | | | | | | | | | | | | | | | | | | | |

| | | | | | |
|--|---|--------------|--|--|--|
| Flow solver - Y Momentum Imbalance | = | 4.5996E-05% | | | |
| Flow solver - Z Momentum Imbalance | = | -1.1486E-04% | | | |
| Flow solver - Energy Imbalance | = | 2.1014E-01% | | | |
| TIME STEP = 15 SIMULATION TIME = 3.00E+01 CPU SECONDS = 1.16E+02 | | | | | |
| <hr/> | | | | | |
| Equation Rate RMS Res Max Res Location Linear Solution | | | | | |
| +-----+-----+-----+-----+-----+-----+ | | | | | |
| U - Mom 0.53 5.8E-06 1.2E-04 4658 7.7E-03 OK | | | | | |
| V - Mom 0.54 8.3E-07 1.8E-05 3822 2.3E-02 OK | | | | | |
| W - Mom 0.54 1.1E-06 2.9E-05 2978 2.6E-02 OK | | | | | |
| P - Mass 0.47 4.5E-07 6.9E-06 2829 8.7 9.9E-03 OK | | | | | |
| +-----+-----+-----+-----+-----+-----+ | | | | | |
| H-Energy 0.26 1.4E-05 1.7E-04 3131 14.2 9.0E-03 OK | | | | | |
| +-----+-----+-----+-----+-----+-----+ | | | | | |
| Flow solver - Mass Imbalance | = | -4.5140E-05% | | | |
| Flow solver - X Momentum Imbalance | = | -2.4275E-04% | | | |
| Flow solver - Y Momentum Imbalance | = | 3.3413E-05% | | | |
| Flow solver - Z Momentum Imbalance | = | -5.3827E-05% | | | |
| Flow solver - Energy Imbalance | = | 5.1096E-02% | | | |
| TIME STEP = 16 SIMULATION TIME = 3.20E+01 CPU SECONDS = 1.24E+02 | | | | | |
| <hr/> | | | | | |
| Equation Rate RMS Res Max Res Location Linear Solution | | | | | |
| +-----+-----+-----+-----+-----+-----+ | | | | | |
| U - Mom 0.53 3.1E-06 6.8E-05 4658 7.6E-03 OK | | | | | |
| V - Mom 0.54 4.5E-07 1.0E-05 5952 2.3E-02 OK | | | | | |
| W - Mom 0.53 5.9E-07 1.6E-05 2978 2.5E-02 OK | | | | | |
| P - Mass 0.49 2.2E-07 3.2E-06 2829 8.7 9.8E-03 OK | | | | | |
| +-----+-----+-----+-----+-----+-----+ | | | | | |
| H-Energy 0.26 3.6E-06 4.4E-05 3131 14.2 8.7E-03 OK | | | | | |
| +-----+-----+-----+-----+-----+-----+ | | | | | |
| Flow solver - Mass Imbalance | = | -5.4169E-05% | | | |
| Flow solver - X Momentum Imbalance | = | -4.0914E-05% | | | |
| Flow solver - Y Momentum Imbalance | = | 8.9605E-06% | | | |
| Flow solver - Z Momentum Imbalance | = | -2.1267E-05% | | | |
| Flow solver - Energy Imbalance | = | 1.2617E-02% | | | |
| TIME STEP = 17 SIMULATION TIME = 3.40E+01 CPU SECONDS = 1.31E+02 | | | | | |
| <hr/> | | | | | |
| Equation Rate RMS Res Max Res Location Linear Solution | | | | | |
| +-----+-----+-----+-----+-----+-----+ | | | | | |
| U - Mom 0.53 1.6E-06 3.8E-05 4658 7.7E-03 OK | | | | | |
| V - Mom 0.54 2.4E-07 6.1E-06 5952 2.4E-02 OK | | | | | |
| W - Mom 0.53 3.1E-07 8.4E-06 2978 2.5E-02 OK | | | | | |
| P - Mass 0.50 1.1E-07 1.5E-06 2829 8.7 1.0E-02 OK | | | | | |
| +-----+-----+-----+-----+-----+-----+ | | | | | |
| H-Energy 0.26 9.5E-07 1.1E-05 3131 14.2 8.6E-03 OK | | | | | |
| +-----+-----+-----+-----+-----+-----+ | | | | | |
| Flow solver - Mass Imbalance | = | -5.4169E-05% | | | |
| Flow solver - X Momentum Imbalance | = | 3.0003E-05% | | | |
| Flow solver - Y Momentum Imbalance | = | 4.3684E-06% | | | |
| Flow solver - Z Momentum Imbalance | = | -1.0074E-05% | | | |
| Flow solver - Energy Imbalance | = | 3.2545E-03% | | | |
| TIME STEP = 18 SIMULATION TIME = 3.60E+01 CPU SECONDS = 1.39E+02 | | | | | |
| <hr/> | | | | | |
| Equation Rate RMS Res Max Res Location Linear Solution | | | | | |
| +-----+-----+-----+-----+-----+-----+ | | | | | |
| U - Mom 0.53 8.5E-07 2.1E-05 4658 7.8E-03 OK | | | | | |
| V - Mom 0.54 1.3E-07 3.7E-06 5952 2.6E-02 OK | | | | | |
| W - Mom 0.53 1.6E-07 4.1E-06 2978 2.4E-02 OK | | | | | |
| P - Mass 0.52 5.8E-08 9.2E-07 2824 8.7 1.1E-02 OK | | | | | |
| +-----+-----+-----+-----+-----+-----+ | | | | | |
| H-Energy 20.65 2.0E-05 2.3E-04 3123 14.2 9.8E-03 OK | | | | | |
| +-----+-----+-----+-----+-----+-----+ | | | | | |
| Flow solver - Mass Imbalance | = | -7.2225E-05% | | | |

| | | |
|---|---------------------------------------|----------------------------|
| Flow solver - X Momentum Imbalance | = | 3.0003E-05% |
| Flow solver - Y Momentum Imbalance | = | 4.4376E-06% |
| Flow solver - Z Momentum Imbalance | = | -5.3273E-09% |
| Flow solver - Energy Imbalance | = | 7.6876E-02% |
| Heat Convected to the Fluid | = | 2.00000E+01 (1.99999E+01) |
| Heat Convected from the Fluid | = | 0.00000E+00 (0.00000E+00) |
| Convective Heat Residual | = | 1.90735E-06 |
| Maximum Solid Temperature Change | = | 2.17209E-02 |
| +-----+-----+-----+-----+-----+-----+ | | |
| CSOLVER Minimum Location Maximum Location Average Convg | +-----+-----+-----+-----+-----+-----+ | |
| y+ 2.19E+00 51447 2.16E+01 51518 1.22E+01 ok | +-----+-----+-----+-----+-----+-----+ | |
| htc 1.96E+00 51100 1.37E+02 2158 1.38E+01 | +-----+-----+-----+-----+-----+-----+ | |
| T-Solid 7.97E+01 47218 8.98E+01 29778 8.46E+01 OK | +-----+-----+-----+-----+-----+-----+ | |
| Execution terminating: all RMS residual AND global imbalance are below their target criteria. | | |
| +-----+-----+-----+-----+-----+-----+ | | |
| Computed Model Constants | +-----+-----+-----+-----+-----+-----+ | |
| Turbulence length scale (Turbulence model 1) = 1.9834E-02 | +-----+-----+-----+-----+-----+-----+ | |
| Turbulence velocity scale (Turbulence model 1) = 3.8508E+00 | +-----+-----+-----+-----+-----+-----+ | |
| Turbulence viscosity (Turbulence Model 1) = 8.3166E-04 | +-----+-----+-----+-----+-----+-----+ | |
| +-----+-----+-----+-----+-----+-----+ | | |
| Boundary Mass Flow and Total Source Term Summary | +-----+-----+-----+-----+-----+-----+ | |
| ADIABATIC FACES 0.0000E+00 | +-----+-----+-----+-----+-----+-----+ | |
| CONVECTING FACES 0.0000E+00 | +-----+-----+-----+-----+-----+-----+ | |
| INLET _FAN 1_FAN 1 1.0316E-02 | +-----+-----+-----+-----+-----+-----+ | |
| VENT 1_VENT 1 -1.0316E-02 | +-----+-----+-----+-----+-----+-----+ | |
| OPEN_TETRAHEDRAL_ELEMENTS 0.0000E+00 | +-----+-----+-----+-----+-----+-----+ | |
| Global Mass Balance: -7.4506E-09 | +-----+-----+-----+-----+-----+-----+ | |
| Global Imbalance, in %: -0.0001 % | +-----+-----+-----+-----+-----+-----+ | |
| +-----+-----+-----+-----+-----+-----+ | | |
| Boundary Momentum Flow and Total Source Term Summary | +-----+-----+-----+-----+-----+-----+ | |
| X-Comp. Y-Comp. Z-Comp. | +-----+-----+-----+-----+-----+-----+ | |
| ADIABATIC FACES 2.0599E-02 -1.6679E-05 3.3253E-04 | +-----+-----+-----+-----+-----+-----+ | |
| CONVECTING FACES 1.9847E-03 2.9332E-06 -3.1612E-04 | +-----+-----+-----+-----+-----+-----+ | |
| INLET _FAN 1_FAN 1 -3.4145E-02 1.4788E-06 8.8937E-06 | +-----+-----+-----+-----+-----+-----+ | |
| VENT 1_VENT 1 1.1561E-02 1.2269E-05 -2.5307E-05 | +-----+-----+-----+-----+-----+-----+ | |
| OPEN_TETRAHEDRAL_ELEMENTS 0.0000E+00 0.0000E+00 0.0000E+00 | +-----+-----+-----+-----+-----+-----+ | |
| Global Momentum Balance: 1.0245E-08 1.5152E-09 -1.8190E-12 | +-----+-----+-----+-----+-----+-----+ | |
| Global Imbalance, in %: 0.0000 % 0.0000 % 0.0000 % | +-----+-----+-----+-----+-----+-----+ | |
| +-----+-----+-----+-----+-----+-----+ | | |
| Boundary Energy Flow and Total Source Term Summary | +-----+-----+-----+-----+-----+-----+ | |
| ADIABATIC FACES 0.0000E+00 | +-----+-----+-----+-----+-----+-----+ | |
| CONVECTING FACES 2.0000E+01 | +-----+-----+-----+-----+-----+-----+ | |
| INLET _FAN 1_FAN 1 0.0000E+00 | +-----+-----+-----+-----+-----+-----+ | |
| VENT 1_VENT 1 -1.9985E+01 | +-----+-----+-----+-----+-----+-----+ | |

| | | | | |
|--|----------------------------------|-----------------------------------|----------------|------------|
| OPEN_TETRAHEDRAL_ELEMENTS | 0.0000E+00 | | | |
| ----- | | | | |
| Global Energy Balance: | 1.5375E-02 | | | |
| Global Imbalance, in %: | 0.0769 % | | | |
| ----- | | | | |
| Locations of maximum residuals | | | | |
| ----- | | | | |
| Equation | Node # | X | Y | Z |
| ----- | | | | |
| U - Mom | 4658 | 1.245E-01 | -3.810E-02 | 1.836E-02 |
| V - Mom | 5952 | 1.192E-01 | -2.274E-03 | -5.114E-02 |
| W - Mom | 2978 | 1.628E-01 | -5.820E-03 | -2.088E-02 |
| P - Mass | 2824 | 1.628E-01 | 4.840E-02 | -1.914E-02 |
| H-Energy | 3123 | 1.548E-03 | 1.324E-02 | -5.127E-03 |
| ----- | | | | |
| Peak Values of residuals | | | | |
| ----- | | | | |
| Equation | Peak occur at loop # | Peak Residual | Final Residual | |
| ----- | | | | |
| U - Mom | 2 | 4.74812E-02 | 8.54709E-07 | |
| V - Mom | 2 | 7.46792E-03 | 1.28624E-07 | |
| W - Mom | 2 | 7.76258E-03 | 1.64862E-07 | |
| P - Mass | 2 | 2.07777E-02 | 5.83013E-08 | |
| H-Energy | 3 | 4.00915E-02 | 1.95163E-05 | |
| ----- | | | | |
| Average Scale Information | | | | |
| ----- | | | | |
| Global Length Scale : | 1.388E-01 | | | |
| Density Scale : | 1.089E+00 | | | |
| Dynamic Viscosity Scale : | 1.850E-05 | | | |
| Advection Time Scale : | 1.086E-01 | | | |
| Reynolds Number : | 1.045E+04 | | | |
| Velocity Scale : | 1.279E+00 | | | |
| Prandtl Number : | 7.084E-01 | | | |
| Temperature Range : | 7.202E+00 | | | |
| Cp Scale : | 1.007E+03 | | | |
| Conductivity Scale : | 2.630E-02 | | | |
| ----- | | | | |
| y+ information (min, max, average) | | | | |
| ----- | | | | |
| Face set name | min y+ | max y+ | ave y+ | |
| ----- | | | | |
| ADIABATIC FACES | 2.21E+00 | 2.42E+01 | 1.40E+01 | |
| CONVECTING FACES | 2.17E+00 | 2.16E+01 | 1.21E+01 | |
| ----- | | | | |
| CPU Requirements of Numerical Solution | | | | |
| ----- | | | | |
| Equation Type | Discretization (secs. %total) | Linear Solution (secs. %total) | | |
| ----- | | | | |
| Momentum-Mass | 7.14E+01 51.8 % | 2.63E+01 19.0 % | | |
| Scalars | 2.32E+01 16.9 % | 1.69E+01 12.3 % | | |

```

+-----+
|           Memory Usage Information
+-----+
|   Peak Memory Use:          7534 Kb
|   Shared Workspace:         776640 words
+-----+

+-----+
| Coupled Solution Summary
+-----+

Maximum Temperature:      89.765 at Element    29778
Minimum Temperature:      79.730 at Element    47218
Average Temperature:      84.621

Maximum Heat Transfer Coefficient:      0.137E+03
Minimum Heat Transfer Coefficient:      0.196E+01
Average Heat Transfer Coefficient:      0.138E+02

Maximum Y+ Value:            0.216E+02
Minimum Y+ Value:            0.219E+01
Average Y+ Value:            0.122E+02
Percent of faces with Y+ < 30:    100.0
Percent of faces with Y+ < 11.5:   22.3

-----
ESC WARNING: Y+ Values
-----
Mesh correction is ON. The solver will compensate where Y+ values are less than 30. ( Although mesh correction is ON, it is recommended to make sure that the mesh is not too fine or that the turbulent model selected is appropriate for the flow regime.)

Heat flow into temperature B.C.s:      0.381E-05
Heat flow from temperature B.C.s:      0.000E+00
Heat convected to fluid:                0.200E+02
Heat convected from fluid:              0.000E+00
Total heat load on non-fluid elements: 0.200E+02
Total Heat Imbalance:                  0.134E-04
Percent Heat Imbalance:                 0.668E-04 %

Total Number Of Iterations           18
Maximum Temperature Change:        0.217E-01 at Element    46896

Maximum Temperature Change in Coupled Solution:      0.217E-01
Normalized Convective Heat Imbalance in Coupled Solution: 0.191E-05

Coupled Solve complete. Maximum boundary condition change between iterations is less than target.

Cpu time= 1052.2 RSLTPOST Module

ESCRR - Converting analysis results
=====
Time: Wed Jan 23 19:38:43 2002

+-----+
|           Results Recovery
+-----+

Recovering Velocity
Recovering Pressure
Recovering Temperature
Recovering Mass Flux

Reading fluid flow results...
Reading thermal results...

```

```
Writing results data to escrra.dat...
```

```
+-----+  
|                  Solution Summary          |  
+-----+
```

| Results Summary | Maximum | Minimum | Average |
|-------------------|-----------|------------|-------------------|
| Fluid Temperature | 5.720E+01 | 5.000E+01 | 5.116E+01 C |
| Fluid Velocity | 3.851E+00 | 9.595E-02 | 1.194E+00 m/s |
| Fluid Pressure | 7.289E-01 | -4.129E+00 | -1.722E-01 Pa |
| Solid Temperature | 8.977E+01 | 7.973E+01 | 8.462E+01 C |
| Y+ | 2.157E+01 | 2.189E+00 | 1.219E+01 |
| Heat Trans. Coef. | 1.371E+02 | 1.963E+00 | 1.383E+01 W/m^2-C |

| Volume/Mass Flow Summary (Values < 0 are outflow) | Volume Flow | Mass Flow |
|--|------------------|-----------------|
| FAN 1 | 9.440E-03 m^3/s | 1.032E-02 kg/s |
| VENT 1 | -9.496E-03 m^3/s | -1.032E-02 kg/s |

Flow Solver:

| Heat Convected To/From Fluid (Values < 0 are outflows) | Positive Side | Negative Side |
|---|---------------|---------------|
| FLOW SURFACE SINK | 1.889E+00 W | 0.000E+00 W |
| FLOW SURFACE HEAT SPREADER | 8.095E-01 W | 0.000E+00 W |
| FLOW BLOCKAGE SINK | 1.679E+01 W | 0.000E+00 W |
| FLOW BLOCKAGE HEAT SPREADER | 5.116E-01 W | 0.000E+00 W |
| Total Heat Convected to Fluid | 2.000E+01 W | |

Thermal Solver: Heat Flow

| | |
|---------------------------------------|--------------|
| Total heat load on non-fluid elements | 2.000E+01 W |
| Heat flow from temperature B.C.s | 0.000E+00 W |
| Heat flow into temperature B.C.s | -3.815E-06 W |
| Heat convected to fluid | 2.000E+01 W |
| Heat convected from fluid | 0.000E+00 W |
| Total Heat Imbalance | 1.335E-05 W |

Solver Convergence

| | |
|---|------------------|
| Thermal solver - Maximum temperature change | 2.172E-02 C |
| Flow solver - Momentum imbalance | 0.00003 Percent |
| Flow solver - Mass imbalance | -0.00007 Percent |
| Flow solver - Energy imbalance | 0.07688 Percent |
| Coupled solution - Maximum temperature change | 2.172E-02 C |
| Coupled solution - Normalized Heat Imbalance | 1.907E-06 |

```
+-----+  
|                  END                  |  
+-----+
```

```
Solution elapsed time: 21 min 07 sec
```

Table B2.4 Sensitivity Analysis on Power Loss A

| Number of thermal boundary conditions: | | | | 3 |
|--|-----------|-------------|-----|-----|
| Thermal Boundary Condition | Type | Value | FSF | TCP |
| 1 - THERMAL BOUNDARY CONDIT | Heat Load | 1.212E+01 W | No | Yes |
| 2 - THERMAL BOUNDARY CONDIT | Heat Load | 7.000E+00 W | No | Yes |
| 3 - THERMAL BOUNDARY CONDIT | Heat Load | 1.000E+00 W | No | No |

Table B2.5 Sensitivity Analysis on Power Loss B

| Number of thermal boundary conditions: | | | | 3 |
|--|-----------|-------------|-----|-----|
| Thermal Boundary Condition | Type | Value | FSF | TCP |
| 1 - THERMAL BOUNDARY CONDIT | Heat Load | 1.200E+01 W | No | Yes |
| 2 - THERMAL BOUNDARY CONDIT | Heat Load | 7.070E+00 W | No | Yes |
| 3 - THERMAL BOUNDARY CONDIT | Heat Load | 1.000E+00 W | No | No |

Table B2.6 Sensitivity Analysis on Epoxy A

| Number of thermal couplings: | | | | 10 |
|-----------------------------------|------------|-----------|--|----|
| Thermal Coupling | Type | Value | | |
| 1 - THERMAL COUPLING SI-CU | Resistance | 3.920E-02 | | |
| Primary Area: 1.271E-04 m^2 | | | | |
| Secndry Area: 2.222E-04 m^2 | | | | |
| 2 - THERMAL COUPLING CU TRACE-CE | Resistance | 1.000E-03 | | |
| Primary Area: 2.751E-04 m^2 | | | | |
| Secndry Area: 7.771E-04 m^2 | | | | |
| 3 - THERMAL COUPLING CERAMIC BAS | Resistance | 1.000E-03 | | |
| Primary Area: 7.771E-04 m^2 | | | | |
| Secndry Area: 7.771E-04 m^2 | | | | |
| 4 - THERMAL COUPLING CU BASE-HEA | Resistance | 3.200E-03 | | |
| Primary Area: 7.771E-04 m^2 | | | | |
| Secndry Area: 1.752E-03 m^2 | | | | |
| 5 - THERMAL COUPLING HEAT SPREAD | Resistance | 7.100E-02 | | |
| Primary Area: 1.752E-03 m^2 | | | | |
| Secndry Area: 5.134E-03 m^2 | | | | |
| 6 - THERMAL COUPLING GATE-CERAMI | Resistance | 5.010E-01 | | |
| Primary Area: 1.794E-04 m^2 | | | | |
| Secndry Area: 5.667E-04 m^2 | | | | |
| 7 - THERMAL COUPLING CERAMIC-GEL | Resistance | 2.500E-03 | | |
| Primary Area: 5.667E-04 m^2 | | | | |
| Secndry Area: 4.705E-04 m^2 | | | | |
| 8 - THERMAL COUPLING GEL-CERAMIC | Resistance | 2.500E-03 | | |
| Primary Area: 4.705E-04 m^2 | | | | |
| Secndry Area: 7.771E-04 m^2 | | | | |
| 9 - THERMAL COUPLING CERAMIC-SI | Resistance | 2.569E+01 | | |
| Primary Area: 5.536E-05 m^2 | | | | |
| Secndry Area: 5.537E-05 m^2 | | | | |
| 10 - THERMAL COUPLING CU TRACE-SI | Resistance | 3.000E-03 | | |
| Primary Area: 1.271E-04 m^2 | | | | |
| Secndry Area: 1.259E-04 m^2 | | | | |

Table B2.7 Sensitivity Analysis on Epoxy B

| Number of thermal couplings: | 10 | |
|-----------------------------------|------------|-----------|
| Thermal Coupling | Type | Value |
| 1 - THERMAL COUPLING SI-CU | Resistance | 3.920E-02 |
| Primary Area: 1.271E-04 m^2 | | |
| Secndry Area: 2.222E-04 m^2 | | |
| 2 - THERMAL COUPLING CU TRACE-CE | Resistance | 1.000E-03 |
| Primary Area: 2.751E-04 m^2 | | |
| Secndry Area: 7.771E-04 m^2 | | |
| 3 - THERMAL COUPLING CERAMIC BAS | Resistance | 1.000E-03 |
| Primary Area: 7.771E-04 m^2 | | |
| Secndry Area: 7.771E-04 m^2 | | |
| 4 - THERMAL COUPLING CU BASE-HEA | Resistance | 3.200E-03 |
| Primary Area: 7.771E-04 m^2 | | |
| Secndry Area: 1.752E-03 m^2 | | |
| 5 - THERMAL COUPLING HEAT SPREAD | Resistance | 7.100E-02 |
| Primary Area: 1.752E-03 m^2 | | |
| Secndry Area: 5.134E-03 m^2 | | |
| 6 - THERMAL COUPLING GATE-CERAMI | Resistance | 4.960E-01 |
| Primary Area: 1.794E-04 m^2 | | |
| Secndry Area: 5.667E-04 m^2 | | |
| 7 - THERMAL COUPLING CERAMIC-GEL | Resistance | 2.500E-03 |
| Primary Area: 5.667E-04 m^2 | | |
| Secndry Area: 4.705E-04 m^2 | | |
| 8 - THERMAL COUPLING GEL-CERAMIC | Resistance | 2.500E-03 |
| Primary Area: 4.705E-04 m^2 | | |
| Secndry Area: 7.771E-04 m^2 | | |
| 9 - THERMAL COUPLING CERAMIC-SI | Resistance | 2.695E+01 |
| Primary Area: 5.536E-05 m^2 | | |
| Secndry Area: 5.537E-05 m^2 | | |
| 10 - THERMAL COUPLING CU TRACE-SI | Resistance | 3.000E-03 |
| Primary Area: 1.271E-04 m^2 | | |
| Secndry Area: 1.259E-04 m^2 | | |

Table B2.8 Sensitivity Analysis on Solder A

| Number of thermal couplings: | 10 | |
|----------------------------------|------------|-----------|
| Thermal Coupling | Type | Value |
| 1 - THERMAL COUPLING SI-CU | Resistance | 3.959E-02 |
| Primary Area: 1.271E-04 m^2 | | |
| Secndry Area: 2.222E-04 m^2 | | |
| 2 - THERMAL COUPLING CU TRACE-CE | Resistance | 1.000E-03 |
| Primary Area: 2.751E-04 m^2 | | |
| Secndry Area: 7.771E-04 m^2 | | |
| 3 - THERMAL COUPLING CERAMIC BAS | Resistance | 1.000E-03 |
| Primary Area: 7.771E-04 m^2 | | |
| Secndry Area: 7.771E-04 m^2 | | |
| 4 - THERMAL COUPLING CU BASE-HEA | Resistance | 3.200E-03 |
| Primary Area: 7.771E-04 m^2 | | |
| Secndry Area: 1.752E-03 m^2 | | |
| 5 - THERMAL COUPLING HEAT SPREAD | Resistance | 7.100E-02 |
| Primary Area: 1.752E-03 m^2 | | |
| Secndry Area: 5.134E-03 m^2 | | |
| 6 - THERMAL COUPLING GATE-CERAMI | Resistance | 4.960E-01 |
| Primary Area: 1.794E-04 m^2 | | |
| Secndry Area: 5.667E-04 m^2 | | |
| 7 - THERMAL COUPLING CERAMIC-GEL | Resistance | 2.500E-03 |
| Primary Area: 5.667E-04 m^2 | | |

| | | | |
|------|------------------------------|--------------------------|-----------|
| | Secndry Area: | 4.705E-04 m ² | |
| 8 - | THERMAL COUPLING GEL-CERAMIC | Resistance | 2.500E-03 |
| | Primary Area: | 4.705E-04 m ² | |
| | Secndry Area: | 7.771E-04 m ² | |
| 9 - | THERMAL COUPLING CERAMIC-SI | Resistance | 2.569E+01 |
| | Primary Area: | 5.536E-05 m ² | |
| | Secndry Area: | 5.537E-05 m ² | |
| 10 - | THERMAL COUPLING CU TRACE-SI | Resistance | 3.000E-03 |
| | Primary Area: | 1.271E-04 m ² | |
| | Secndry Area: | 1.259E-04 m ² | |

Table B2.9 Sensitivity Analysis on Solder B

| Number of thermal couplings: | | 10 |
|-----------------------------------|--------------------------|-----------|
| Thermal Coupling | Type | Value |
| 1 - THERMAL COUPLING SI-CU | Resistance | 3.920E-02 |
| Primary Area: | 1.271E-04 m ² | |
| Secndry Area: | 2.222E-04 m ² | |
| 2 - THERMAL COUPLING CU TRACE-CE | Resistance | 1.000E-03 |
| Primary Area: | 2.751E-04 m ² | |
| Secndry Area: | 7.771E-04 m ² | |
| 3 - THERMAL COUPLING CERAMIC BAS | Resistance | 1.000E-03 |
| Primary Area: | 7.771E-04 m ² | |
| Secndry Area: | 7.771E-04 m ² | |
| 4 - THERMAL COUPLING CU BASE-HEA | Resistance | 3.232E-03 |
| Primary Area: | 7.771E-04 m ² | |
| Secndry Area: | 1.752E-03 m ² | |
| 5 - THERMAL COUPLING HEAT SPREAD | Resistance | 7.100E-02 |
| Primary Area: | 1.752E-03 m ² | |
| Secndry Area: | 5.134E-03 m ² | |
| 6 - THERMAL COUPLING GATE-CERAMI | Resistance | 4.960E-01 |
| Primary Area: | 1.794E-04 m ² | |
| Secndry Area: | 5.667E-04 m ² | |
| 7 - THERMAL COUPLING CERAMIC-GEL | Resistance | 2.500E-03 |
| Primary Area: | 5.667E-04 m ² | |
| Secndry Area: | 4.705E-04 m ² | |
| 8 - THERMAL COUPLING GEL-CERAMIC | Resistance | 2.500E-03 |
| Primary Area: | 4.705E-04 m ² | |
| Secndry Area: | 7.771E-04 m ² | |
| 9 - THERMAL COUPLING CERAMIC-SI | Resistance | 2.569E+01 |
| Primary Area: | 5.536E-05 m ² | |
| Secndry Area: | 5.537E-05 m ² | |
| 10 - THERMAL COUPLING CU TRACE-SI | Resistance | 3.000E-03 |
| Primary Area: | 1.271E-04 m ² | |
| Secndry Area: | 1.259E-04 m ² | |

Table B2.10 Sensitivity Analysis on Grease

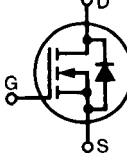
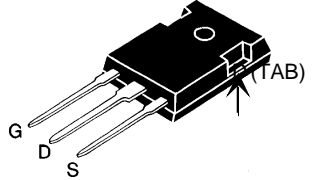
| | | |
|-----------------------------------|------------|-----------|
| Number of thermal couplings: | | 10 |
| Thermal Coupling | Type | Value |
| ----- | | |
| 1 - THERMAL COUPLING SI-CU | Resistance | 3.920E-02 |
| Primary Area: 1.271E-04 m^2 | | |
| Secndry Area: 2.222E-04 m^2 | | |
| 2 - THERMAL COUPLING CU TRACE-CE | Resistance | 1.000E-03 |
| Primary Area: 2.751E-04 m^2 | | |
| Secndry Area: 7.771E-04 m^2 | | |
| 3 - THERMAL COUPLING CERAMIC BAS | Resistance | 1.000E-03 |
| Primary Area: 7.771E-04 m^2 | | |
| Secndry Area: 7.771E-04 m^2 | | |
| 4 - THERMAL COUPLING CU BASE-HEA | Resistance | 3.200E-03 |
| Primary Area: 7.771E-04 m^2 | | |
| Secndry Area: 1.752E-03 m^2 | | |
| 5 - THERMAL COUPLING HEAT SPREAD | Resistance | 7.171E-02 |
| Primary Area: 1.752E-03 m^2 | | |
| Secndry Area: 5.134E-03 m^2 | | |
| 6 - THERMAL COUPLING GATE-CERAMI | Resistance | 4.960E-01 |
| Primary Area: 1.794E-04 m^2 | | |
| Secndry Area: 5.667E-04 m^2 | | |
| 7 - THERMAL COUPLING CERAMIC-GEL | Resistance | 2.500E-03 |
| Primary Area: 5.667E-04 m^2 | | |
| Secndry Area: 4.705E-04 m^2 | | |
| 8 - THERMAL COUPLING GEL-CERAMIC | Resistance | 2.500E-03 |
| Primary Area: 4.705E-04 m^2 | | |
| Secndry Area: 7.771E-04 m^2 | | |
| 9 - THERMAL COUPLING CERAMIC-SI | Resistance | 2.569E+01 |
| Primary Area: 5.536E-05 m^2 | | |
| Secndry Area: 5.537E-05 m^2 | | |
| 10 - THERMAL COUPLING CU TRACE-SI | Resistance | 3.000E-03 |
| Primary Area: 1.271E-04 m^2 | | |
| Secndry Area: 1.259E-04 m^2 | | |
| ----- | | |

Appendix C

Data Sheet for Experiment Equipments

Table C1 shows the manufacturer's data sheet of the TO247 package while Table C2 shows the data sheet for the axial fan used in the experiment discussed in Chapter 3.

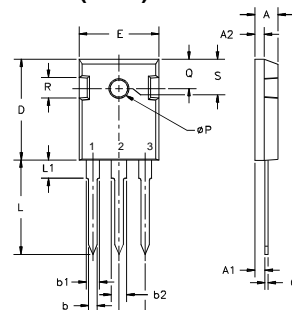
Table C1 Data Sheet for TO247 Package

| IXYS | | | | |
|---|--|--|--|--|
| MegaMOS™FET | | IXTH / IXTM 67N10 IXTH / IXTM 75N10 | V_{DSS} 100 V 100 V | I_{D25} 67 A 75 A |
| | | R_{DS(on)} 25 mΩ 20 mΩ | | |
| N-Channel Enhancement Mode | |  Maximum Ratings |  TO-247 AD (IXTH) | |
| Symbol | Test Conditions | | | |
| V_{DSS} | $T_J = 25^\circ\text{C}$ to 150°C | 100 | V | |
| V_{DGR} | $T_J = 25^\circ\text{C}$ to 150°C ; $R_{GS} = 1 \text{ M}\Omega$ | 100 | V | |
| V_{GS} | Continuous | ±20 | V | |
| V_{GSM} | Transient | ±30 | V | |
| I_{D25} | $T_c = 25^\circ\text{C}$ | 67N10 75N10 | 67 75 | A |
| I_{DM} | $T_c = 25^\circ\text{C}$, pulse width limited by T_{JM} | 67N10 75N10 | 268 300 | A |
| P_D | $T_c = 25^\circ\text{C}$ | 300 | W | |
| T_J | | -55 ... +150 | °C | |
| T_{JM} | | 150 | °C | |
| T_{stg} | | -55 ... +150 | °C | |
| M_d | Mounting torque | 1.13/10 | Nm/lb.in. | |
| Weight | | TO-204 = 18 g, TO-247 = 6 g | | |
| Maximum lead temperature for soldering 1.6 mm (0.062 in.) from case for 10 s | | 300 | °C | |
| Symbol | Test Conditions | Characteristic Values | | |
| | | $(T_J = 25^\circ\text{C}, \text{unless otherwise specified})$ | min. | typ. |
| V_{DSS} | $V_{GS} = 0 \text{ V}$, $I_D = 250 \mu\text{A}$ | 100 | | V |
| V_{GS(th)} | $V_{DS} = V_{GS}$, $I_D = 250 \mu\text{A}$ | 2 | | 4 V |
| I_{GSS} | $V_{GS} = \pm 20 \text{ V}_{DC}$, $V_{DS} = 0$ | | ±100 | nA |
| I_{DSS} | $V_{DS} = 0.8 \cdot V_{DSS}$ $V_{GS} = 0 \text{ V}$ | $T_J = 25^\circ\text{C}$ $T_J = 125^\circ\text{C}$ | 200 1 | μA mA |
| R_{DS(on)} | $V_{GS} = 10 \text{ V}$, $I_D = 0.5 I_{D25}$ | 67N10 75N10 | 0.025 0.020 | Ω |
| | Pulse test, $t \leq 300 \mu\text{s}$, duty cycle $d \leq 2 \%$ | | | |
| 91533E(5/96) | | | | |
| © 2000 IXYS All rights reserved | | | | |
| IXYS reserves the right to change limits, test conditions, and dimensions. | | | | |

| Symbol | Test Conditions | Characteristic Values | | |
|---|---|--|------|------|
| | | ($T_j = 25^\circ\text{C}$, unless otherwise specified) | min. | typ. |
| g_{fs} | $V_{DS} = 10 \text{ V}; I_D = 0.5 I_{D25}$, pulse test | 25 | 30 | S |
| C_{iss} C_{oss} C_{rss} | $V_{GS} = 0 \text{ V}, V_{DS} = 25 \text{ V}, f = 1 \text{ MHz}$ | 4500 | pF | |
| | | 1300 | pF | |
| | | 550 | pF | |
| $t_{d(on)}$ t_r $t_{d(off)}$ t_f | $V_{GS} = 10 \text{ V}, V_{DS} = 0.5 \cdot V_{DSS}, I_D = 0.5 I_{D25}$ $R_G = 2 \Omega$, (External) | 40 | 60 | ns |
| | | 60 | 110 | ns |
| | | 100 | 140 | ns |
| | | 30 | 60 | ns |
| $Q_{g(on)}$ Q_{gs} Q_{gd} | $V_{GS} = 10 \text{ V}, V_{DS} = 0.5 \cdot V_{DSS}, I_D = 0.5 I_{D25}$ | 180 | 260 | nC |
| | | 30 | 70 | nC |
| | | 90 | 160 | nC |
| R_{thJC} | | | 0.42 | K/W |
| R_{thCK} | | | 0.25 | K/W |

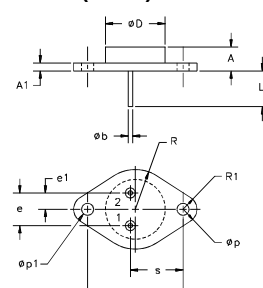
Source-Drain Diode

| Symbol | Test Conditions | Characteristic Values | | |
|----------|---|--|------|----------------|
| | | ($T_j = 25^\circ\text{C}$, unless otherwise specified) | min. | typ. |
| I_s | $V_{GS} = 0 \text{ V}$ | 67N10 75N10 | | 67 A 75 A |
| I_{SM} | Repetitive; pulse width limited by T_{JM} | 67N10 75N10 | | 268 A 300 A |
| V_{SD} | $I_F = I_s, V_{GS} = 0 \text{ V},$ Pulse test, $t \leq 300 \mu\text{s}$, duty cycle $d \leq 2 \%$ | | 1.75 | V |
| t_{rr} | $I_F = I_s, -di/dt = 100 \text{ A}/\mu\text{s}, V_R = 100 \text{ V}$ | 300 | | ns |

TO-247 AD (IXTH) Outline


Terminals: 1 - Gate 2 - Drain 3 - Source Tab - Drain

| Dim. | Millimeter | | Inches | |
|----------------|------------|-------|--------|------|
| | Min. | Max. | Min. | Max. |
| A | 4.7 | 5.3 | .185 | .209 |
| A ₁ | 2.2 | 2.54 | .087 | .102 |
| A ₂ | 2.2 | 2.6 | .059 | .098 |
| b | 1.0 | 1.4 | .040 | .055 |
| b ₁ | 1.65 | 2.13 | .065 | .084 |
| b ₂ | 2.87 | 3.12 | .113 | .123 |
| C | .4 | .8 | .016 | .031 |
| D | 20.80 | 21.46 | .819 | .845 |
| E | 15.75 | 16.26 | .610 | .640 |
| e | 5.20 | 5.72 | .205 | .225 |
| L | 19.81 | 20.32 | .780 | .800 |
| L ₁ | | 4.50 | | .177 |
| ØP | 3.55 | 3.65 | .140 | .144 |
| Q | 5.89 | 6.40 | .232 | .252 |
| R | 4.32 | 5.49 | .170 | .216 |
| S | 6.15 | BSC | 242 | BSC |

TO-204AE (IXTM) Outline

 Pins 1 - Gate 2 - Source
Case - Drain

| Dim. | Millimeter | | Inches | |
|-----------------|------------|-------|--------|------|
| | Min. | Max. | Min. | Max. |
| A | 6.4 | 11.4 | .250 | .450 |
| A ₁ | 1.53 | 3.42 | .060 | .135 |
| Øb | 1.45 | 1.60 | .057 | .063 |
| ØD | | 22.22 | | .875 |
| e | 10.67 | 11.17 | .420 | .440 |
| e ₁ | 5.21 | 5.71 | .205 | .225 |
| L | 11.18 | 12.19 | .440 | .480 |
| Øp | 3.84 | 4.19 | .151 | .165 |
| Øp ₁ | 3.84 | 4.19 | .151 | .165 |
| q | 30.15 | BSC | 1.187 | BSC |
| R | 12.58 | 13.33 | .495 | .525 |
| R ₁ | 3.33 | 4.77 | .131 | .188 |
| s | 16.64 | 17.14 | .655 | .675 |

Fig. 1 Output Characteristics

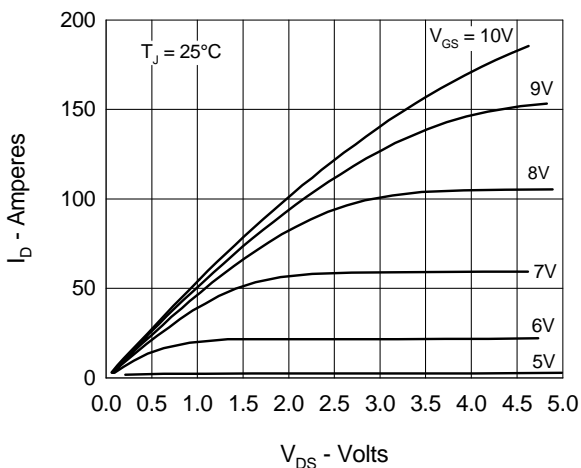


Fig. 2 Input Admittance

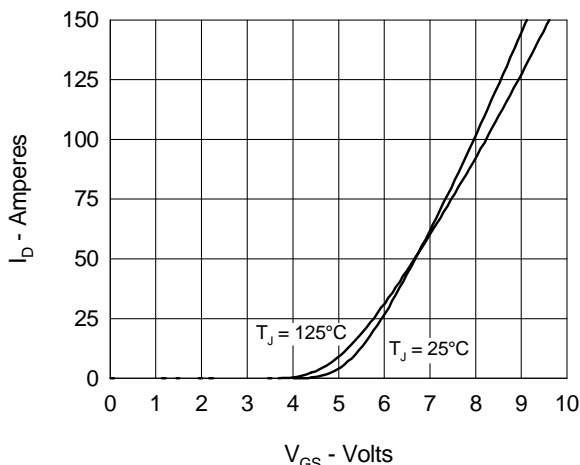


Fig. 3 $R_{DS(on)}$ vs. Drain Current

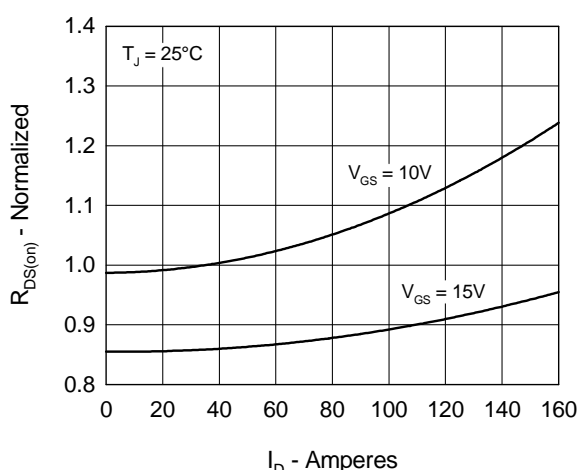


Fig. 4 Temperature Dependence of Drain to Source Resistance

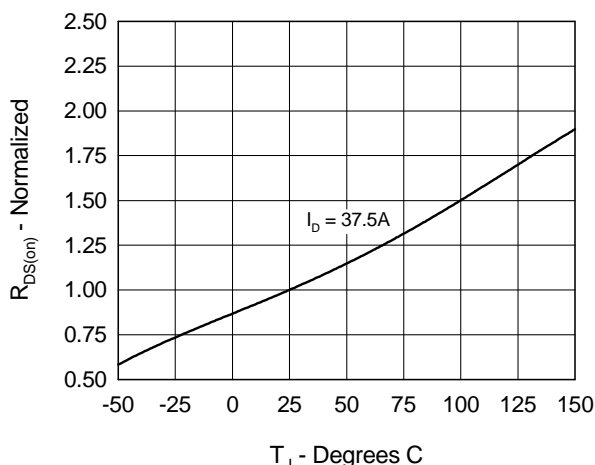


Fig. 5 Drain Current vs. Case Temperature

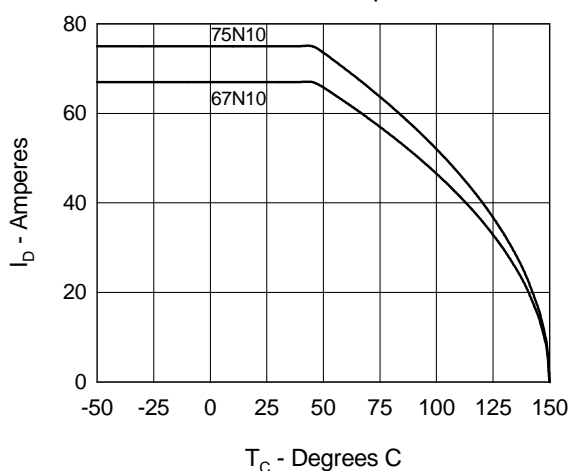


Fig. 6 Temperature Dependence of Breakdown and Threshold Voltage

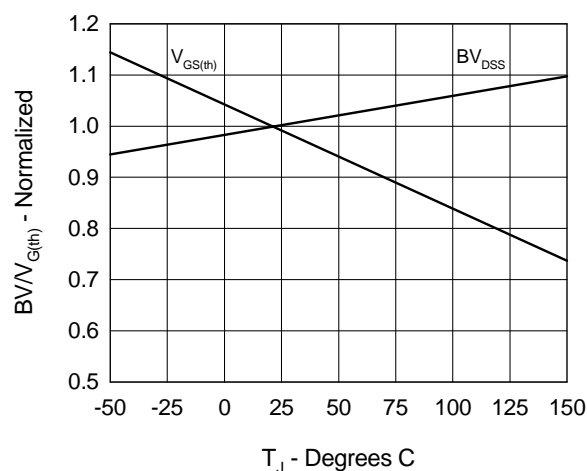


Fig.7 Gate Charge Characteristic Curve

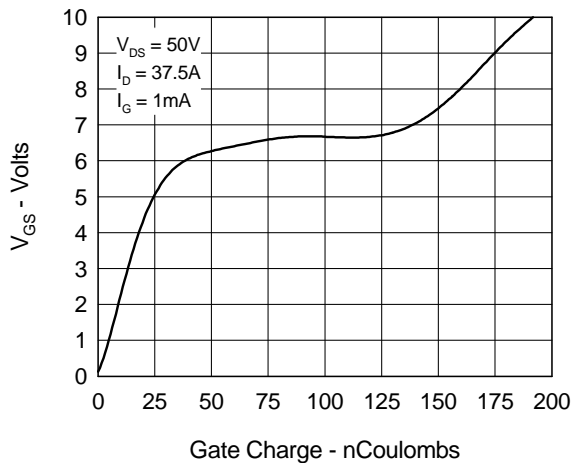


Fig.9 Capacitance Curves

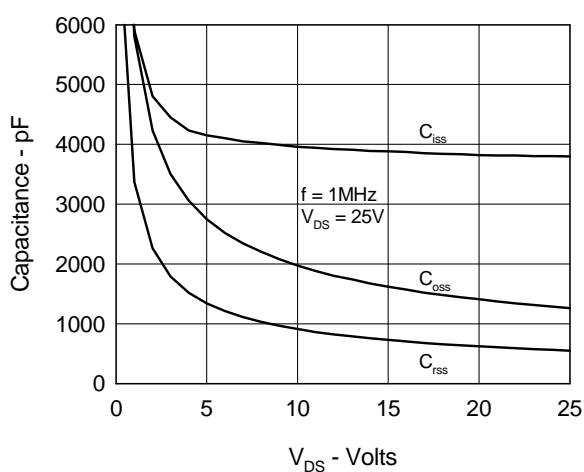


Fig.11 Transient Thermal Impedance

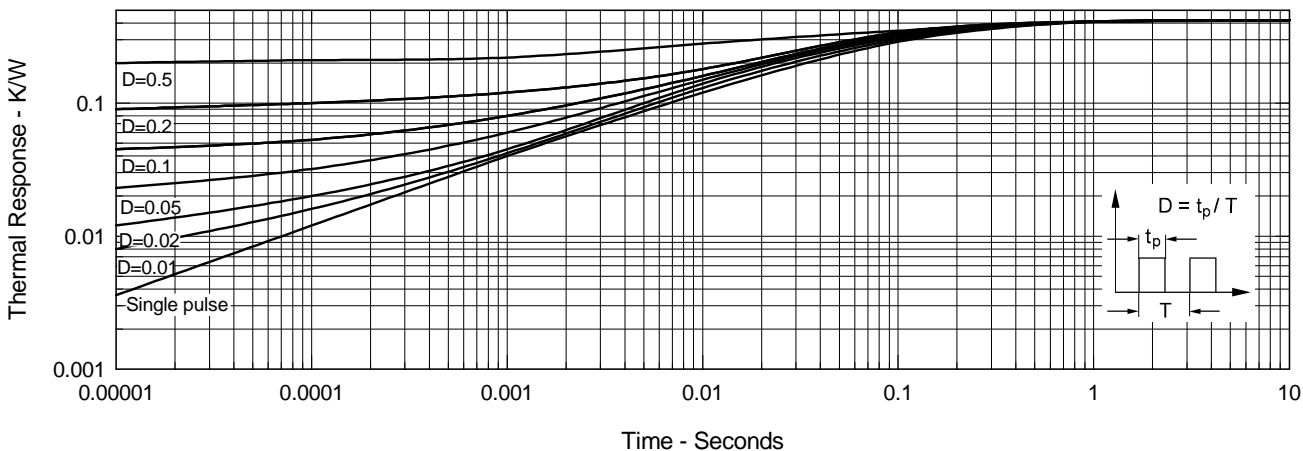


Fig.8 Forward Bias Safe Operating Area

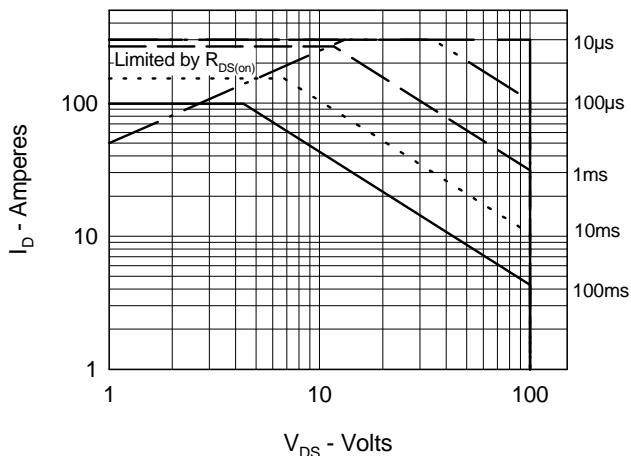


Fig.10 Source Current vs. Source to Drain Voltage

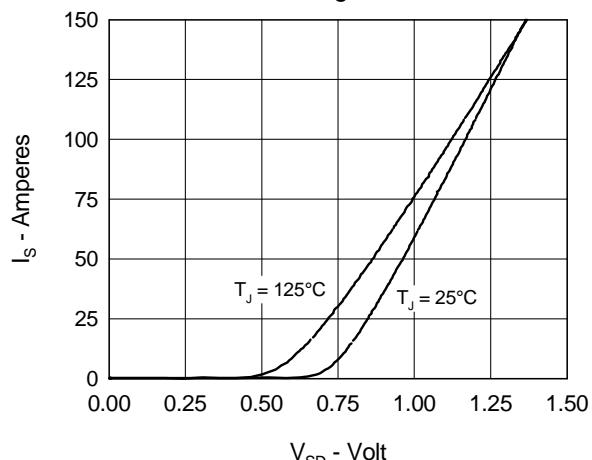
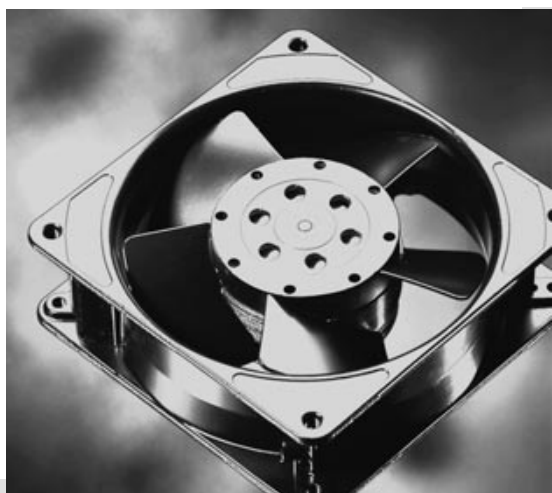


Table C2 Data Sheet for Papst-Motoren Axial Fan



PAPST

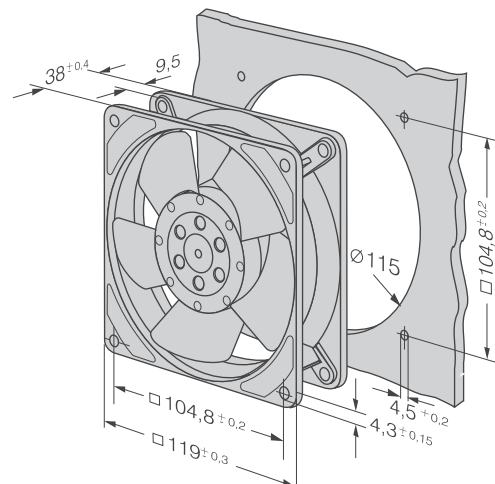
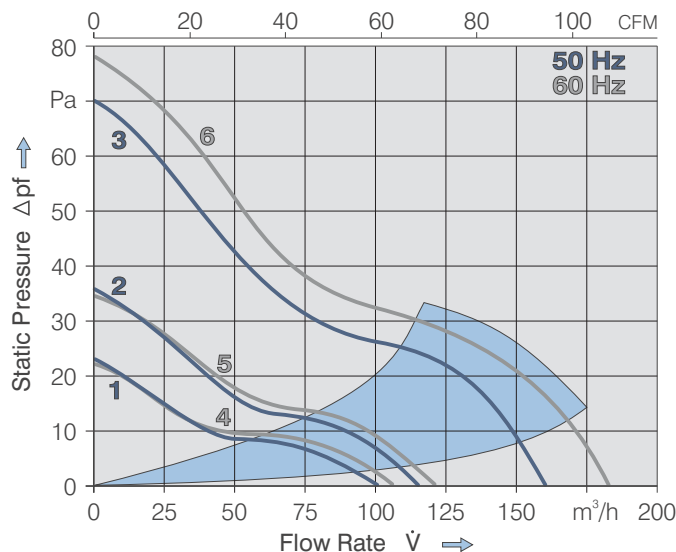
- AC fans with external rotor shaded pole motor. Impedance protected against overloading.
- Metal fan housing and impeller
- Air exhaust over struts. Rotational direction CW looking at rotor.
- Electrical connection via 2 flat pins 2.8 x 0.5 mm.
- Fan housing with ground lug and screw M4x8 (TORX).
- Mass 540 g.

S e r i e s 4 0 0 0 Z 119 x 119 x 38 mm

| Air Flow m³/h | Air Flow CFM | Nominal Voltage V | Nominal Frequency Hz | Noise dB(A) | bels | Sinter-Sleeve Bearings Ball Bearings | Power Input Watt | Nominal Speed min⁻¹ | Temperature Range °C | Service Life L ₁₀ at 40 °C at t _{max} | Curve | Type |
|------------------|-----------------|----------------------|-------------------------|----------------|------|---|---------------------|------------------------|-------------------------|---|-------|--------|
| 100 | 58.9 | 230 | 50 | 26 | 4.0 | ■ | 13 | 1700 | -10...+65 | 50000 / 27500 | 1 | 4850 Z |
| 115 | 67.7 | 230 | 50 | 30 | 4.3 | ■ | 13 | 1900 | -10...+65 | 50000 / 27500 | 2 | 4580 Z |
| 160 | 94.2 | 230 | 50 | 40 | 5.3 | ■ | 19 | 2650 | -10...+50 | 37500 / 30000 | 3 | 4650 Z |
| 160 | 94.2 | 230 | 50 | 40 | 5.3 | ■ | 19 | 2650 | -40...+75 | 37500 / 17500 | 3 | 4656 Z |
| 105 | 61.8 | 115 | 60 | 28 | 4.1 | ■ | 12 | 1800 | -10...+70 | 52500 / 25000 | 4 | 4800 Z |
| 120 | 70.6 | 115 | 60 | 32 | 4.4 | ■ | 12 | 2000 | -10...+70 | 52500 / 25000 | 5 | 4530 Z |
| 180 | 105.9 | 115 | 60 | 45 | 5.6 | ■ | 18 | 3100 | -10...+60 | 40000 / 25000 | 6 | 4600 Z |
| 180 | 105.9 | 115 | 60 | 45 | 5.6 | ■ | 18 | 3100 | -40...+85 | 40000 / 15000 | 6 | 4606 Z |

Available on request:

- Electrical connection via 2 single leads 310 mm long.



Appendix D

Quotation for DBC Ceramic

To:
 Virginia Technical University
 Att: Yingfeng Pang
 Blacksburg, Virginia

3770 Realty Road
 Addison, Texas 75001-4311
 Phone: 214.615.1533
 Fax: 214.615.1540



From: Andreas Utz-Kistner
 Phone: 214.615.3770
 e-mail: akistner@curamikusa.com

Dear Yingfeng:

Thank you for your Request for Quote, dated 10th of July 2002.
 We are glad to submit you the following offer in accordance with the curamik electronics DBC specifications which we mailed to you, together with some interesting literature today to your attention.

Our reference number for this budgetary offer is **D02/111** for an estimated part resulting 6 single pieces per 7" x 5" master card in different material configurations. Please note this number on every inquiry in regards to the offered materials and prices.

| Pos. | Description | Volume Cards 7" x 5" | Price in US\$ per mastercard (6 up) |
|------|--|--------------------------------|--|
| 1. | DBC substrate Size: 2.30" x 2.20" Copper: .08" both sides Ceramic: .015" CurSTD 96 % alumina Surface: electroless nickel and emersion gold flash Delivery: as single pieces | 10 50 100 500 1000 | 42.10 36.78 22.12 18.99 18.52 |
| 2. | DBC substrate Size: 2.30" x 2.20" Copper: .12" both sides Ceramic: .025" CurSTD 96 % alumina Surface: electroless nickel and emersion gold flash Delivery: as single pieces | 10 50 100 500 1000 | 40.08 24.89 20.60 17.71 17.26 |

| | | | |
|----|--|--------------------------------|--|
| 3. | DBC substrate Size: 2.30" x 2.20" Copper: .12" both sides Ceramic: .040" CurSTD 96 % alumina Surface: electroless nickel and emersion gold flash Delivery: as single pieces | 10 50 100 500 1000 | 47.23 29.09 23.96 20.56 20.05 |
| 4. | DBC substrate Size: 2.30" x 2.20" Copper: .08" both sides Ceramic: .015" AlN 170 W/mK Surface: electroless nickel and emersion gold flash Delivery: as single pieces | 10 50 100 500 1000 | 98.22 91.24 91.15 84.22 80.86 |
| 5. | DBC substrate Size: 2.30" x 2.20" Copper: .12" both sides Ceramic: .025" AlN 170 W/mK Surface: electroless nickel and emersion gold flash Delivery: as single pieces | 10 50 100 500 1000 | 74.82 69.71 69.62 64.57 62.14 |
| 6. | DBC substrate Size: 2.30" x 2.20" Copper: .12" both sides Ceramic: .040" AlN 170 W/mK Surface: electroless nickel and emersion gold flash Delivery: as single pieces | 10 50 100 500 1000 | 167.52 167.09 167.00 143.95 140.62 |
| 7. | NRE tooling | | 960.00 |

Delivery:

Samples (10 cards) 5 to 6 weeks, volume 9 to 10 weeks after receipt of the order, start of production after total technical clarification, drawing hard copy and dxf- or dwg-file required, design done by Curamik Electronics, Inc. will add US\$ 293.00 engineering charge.

Terms:

Prices are FOB Dallas, TX.,

Prices are subject to change according to changes in material and labor cost or changes of the currencies.

Payment 30 days net.

Due to customer manufacturing the number of shipped parts might vary by +/- 10%.

The minimum factory order is US\$ 1500.00

All quoted prices are guaranteed for 60 days from date of quote.

If PO is awarded, please reference quote number

Our standard terms and conditions are available via fax upon request.

If you require any further information, please do not hesitate to contact us in our Dallas office.

Best regards,

Andreas Utz-Kistner

Vita

Ying-Feng Pang was born in Segamat, Johor, Malaysia. In May 1998, she received her degree in Bachelor of Science in Mechanical Engineering at Michigan Technological University, Houghton, Michigan. She started working as a mechanical engineer in WeBlast Sdn Bhd, Kuala Lumpur, Malaysia from August 1998 to July 2000. During these two years, her work involved shot blasting machine design, material planning and purchasing, production planning, and product information management. In August 2000, she started her M.S. program in Virginia Tech, Blacksburg, Virginia. She joined CPES in January 2001 and conducted her master's research in heat transfer in power electronics under Dr. Elaine Scott's supervision as well as Dr. Karen Thole's guidance. She received her Master of Science in Mechanical Engineering in Fall 2002. Ying-Feng is currently pursuing her doctorate degree in mechanical engineering at Virginia Tech.